

https://dspace.org/

The Effect of Quinoline Heterocyclic Derivatives on the Malaria Parasite and Anopheles Vector

Lala, Sahil

2024
University of the Witwatersrand, Johannesburg
https://hdl.handle.net/10539/47053

Lala, Sahil. (2024). The Effect of Quinoline Heterocyclic Derivatives on the Malaria Parasite and Anopheles Vector [Master`s dissertation, University of the Witwatersrand, Johannesburg]. WIReDSpace. https://hdl.handle.net/10539/47053

Downloaded from a DSpace repository. https://dspace.org/

The Effect of Quinoline Heterocyclic Derivatives on the Malaria Parasite and *Anopheles* Vector

Sahil Lala



A dissertation submitted to the Faculty of Health Sciences,

University of the Witwatersrand,

in fulfilment of the requirements for the degree

of

Master of Science in Medicine (Clinical and Experimental Pharmacology)

Johannesburg,

2024

DECLARATION

I Sahil Lala declare that this dissertation is my own, unaided work. It is being submitted for the Degree of Master of Science in Medicine at the University of the Witwatersrand, Johannesburg. It has not been submitted before for any degree or examination at any other University.



24 October 2024 at Parktown

DEDICATIONS

I would like to dedicate this dissertation to all those who encouraged me and provided support throughout the years.

"The only *true wisdom* is in knowing you know nothing."

Socrates

ACKNOWLEDGEMENTS

I would like to acknowledge and thank my supervisor Prof. Robyn L van Zyl, for her supervision, advice, wealth of knowledge and all the time and effort that she dedicated to this study.

Thank you to Dr Shune Oliver their guidance with the larvicidal/ovicidal studies and for providing the larvae/ovum for this study.

I would like to acknowledge and thank Mr Chien-Teng Chen his technical expertise and support in the laboratory.

I would like to thank Mr J. Mahlangu, Miss P. Thabana and Miss N Rooplal for their support in the laboratory and interesting discussions.

Sincerest thanks to all the staff of the Department of Pharmacy and Pharmacology and the WITS Research Institute for Malaria for all their advice, help and support.

Sincerest thanks to the University of Witwatersrand, the National Research Foundation, the German Academic Exchange Service (DAAD) and Faculty Research Committee for providing financial support.

ABSTRACT

The World Health Organization estimated that in 2022 there were 249 million cases of malaria with 608,000 fatalities worldwide. The development of drug resistance by the *Plasmodium* parasite, as well as insecticide resistance in the *Anopheles* vector, has necessitated intense research to identify lead compounds. Quinoline derivatives have been used to generate a range of important antimalarial derivatives with promising activity. As such forty-two quinoline heterocyclic derivatives were designed, synthesised, purified and structures verified before being evaluated for *in vitro* antimalarial and insecticidal properties, in conjunction with a preliminary toxicological profile. The antimalarial activity was evaluated against chloroquine-sensitive (NF54) *P. falciparum* using the *Plasmodium* lactate dehydrogenase assay, with the insecticidal activity determined against *Anopheles arabiensis* (KWAG) larvae in accordance with the WHO insecticide testing guidelines. The toxicity of the derivatives was evaluated against *Artemia franciscana*, human kidney endothelial (HEK293) and human red blood cells. Of the forty-two heterocyclic derivatives, twenty-six possessed promising antimalarial activity (>50% growth inhibition) at 50µM. All derivatives had a direct effect on the intra-erythrocytic parasite, where there was minimal lysis of the red blood cell host. One Dihydroquinoline-Carbothioamide (**DC14**) (100%) and one Quinoline-3-Carboxamide (**Q3C11)** (89.15%) derivative displayed activity with IC_{50} values of 7.23 ± 1.17 and 7.99 ± 0.31 µM that were 85-fold less active than quinine. In combination with quinine, a synergistic and additive interaction were observed with compound **DC14** and **Q3C11**, respectively. Both derivatives were found to possess negligible insecticidal activity at 0.05µM against the *An. arabiensis 3rd* instar larvae (**DC14**: 6.67%; **Q3C11**: 11.67%) and eggs (**DC14**: 16.25%; **Q3C11**: 8.13%) compared to 0.05µM DDT (100%) and 1% formalin (100%). In comparison, compounds **DC14** and **Q3C11** were 14.4- and 7.5-fold more toxic against *Ar. Franciscana,* with LC_{50} values of 2.678 µM and 7.83 µM, respectively. The derivatives were minimally toxic to the HEK293 cells, such that there was a selectivity index towards the malaria parasite of 11.13 and 7.55 for compounds **DC14** and **Q3C11**, respectively. Although there was favourable antimalarial activity, pharmacokinetics and safety index for the quinoline heterocyclic compound **DC14**, further derivatisation is needed before this lead compound could be further considered for development as an antimalarial agent.

LIST OF PUBLICATIONS AND CONFERENCE ATTENDANCE

Publications:

Manuscripts in preparation

Lala, S., Govender, H., Oliver, S., Koorbanally, N., van Zyl, R.L. The antimalarial and insecticidal activity of Quinoline heterocyclic derivatives.

Conference attendance:

Lala, S., Govender, H., Oliver, S., Koorbanally, N., van Zyl, R.L.

The effect of Dihydroquinoline-carbothioamide derivatives on the *Plasmodium* parasite and *Anopheles* vector. 4th Southern Africa Malaria Research Conference. National Institute of Communicable Diseases, Johannesburg, South Africa. 30 July-1 August 2018 (Poster presentation)

Lala, S., Govender, H., Oliver, S., Koorbanally, N., van Zyl, R.L.

The antimalarial and insecticidal activity of 2-phenylhydrazono-[1,5-a]quinoline derivatives. WITS Faculty of Health Sciences Research Day and Postgraduate Expo 2018. Parktown, South Africa. 6 September 2018 (Poster presentation)

Lala, S., Govender, H., Oliver, S., Koorbanally, N., van Zyl, R.L.

The antimalarial and insecticidal activity Quinoline-3-carboxamide derivatives. Conference of Biomedical and Natural Sciences and Therapeutics (CoBNest). Stellenbosch, South Africa. 7-10 October 2018 (Poster presentation).

Lala, S., Govender, H., Oliver, S., Koorbanally, N., van Zyl, R.L.

The antimalarial and insecticidal activity Quinoline-3-carboxamide derivatives. 5th Southern Africa Malaria Research Conference. University of Pretoria, Future Africa Campus, Pretoria, South Africa. 31 July 2019 (Poster presentation)

Lala, S., Govender, H., Oliver, S., Koorbanally, N., van Zyl, R.L.

The antimalarial and insecticidal activity Quinoline-3-carboxamide derivatives. WITS Faculty of Health Sciences School of Therapeutic Sciences Biennial Research Day 2019. Parktown, South Africa. 10 September 2019 (Poster presentation)

Lala, S., Govender, H., Oliver, S., Koorbanally, N., van Zyl, R.L.

The antimalarial and insecticidal activity Quinoline-3-carboxamide derivatives. WITS Faculty of Health Sciences School, WRIM World Malaria Day. Parktown, South Africa. 25 April 2023 (Poster presentation)

TABLE OF CONTENTS

Declaration i

Dedication ii

Acknowledgements iii

Abstract iv

Publications and conference attendance v

Table of Contents vii

List of Figures xii

List of Tables xiv

List of Equations xvii

List of Abbreviations xviii

CHAPTER ONE – INTRODUCTION

1.1. Malaria Etiology 1

1.2. *Plasmodium* Life Cycle 3

1.3. *Anopheles Vector* 6

1.3.1. *Anopheles* in South Africa 6

1.3.2. *Anopheles* Life Cycle 7

1.4. Malaria Symptoms and Diagnosis 9

1.5. Malaria Prophylaxis and Treatment in South Africa 11

1.6. Antimalarial drug resistance in South Africa 20

1.7. Insecticide resistance in South Africa 21

1.8. Novel drug compounds 23

1.8.1. Hybrid compounds 23

1.8.2. Quinoline 24

1.8.3. Dihydroquinoline-carbothioamide 25
1.8.4. Phenylhydrazone 25
1.8.5. Quinoline-3-Carboxamide 26
1.8.6. Rationale of the heterocyclic derivative study 26
1.9. Rationale, Aims & Objectives..... 27
1.9.1 Rationale 27
1.9.2 Aim..... 27
1.9.3 Objectives..... 27

CHAPTER TWO – METHODS AND MATERIALS

2.1. Compounds and Reagents 29
2.1.1. Test and Control compounds 29
2.1.2. Preparation of test compounds and control drugs 29
2.1.3. Analysis of test compounds and positive controls..... 32
2.2. Antimalarial assay..... 35
2.2.1. Malaria parasite culture maintenance 35
2.2.1.1. Parasite culture reagents and solutions..... 35
2.2.2. Collection and preparation of uninfected red blood cells 36
2.2.3. Parasite culture maintenance 37
2.2.4. Giemsa staining..... 37
2.2.5. Parasite culture syncronization..... 38
2.2.6. Parasite culture cryopreservation..... 39
2.2.7. Parasite culture initiation from frozen cryovials..... 39
2.2.8. *Plasmodium* lactate dehydrogenase drug sensitivity assay..... 40
2.2.8.1. Solutions and reagents..... 41
2.2.8.2. *pLDH* assay protocol..... 41
2.3. Antimalarial combination studies 43
2.3.1. Antimalarial combination 43

2.3.2. Parasite morphology and stage determination 45

2.4. Vector studies 46

2.4.1. *Anopheles* mosquitoes 46

2.4.2. Larvicidal assay 47

2.4.2.1. Larvicidal lethality assay 47

2.4.2.2. Morphological effects 49

2.4.3. Ovicidal assay 49

2.4.3.1. Ovicidal lethality assay 49

2.5. Toxicological assays 50

2.5.1. Haemolysis assay 50

2.6. Cytotoxicity studies 51

2.6.1. Cytotoxicity assay 51

2.6.2. Cytotoxicity assay cells 52

2.6.2.1. Cell culture reagents and solutions 52

2.6.2.1.1. Incomplete and complete cell line culture medium 52

2.6.2.1.2. Foetal bovine serum 53

2.6.2.1.3. MTT 53

2.6.2.1.4. Cell line cryopreservation solution 53

2.6.2.2. Maintenance of cell culture 53

2.6.2.2.1. HEK293 cell line 54

2.6.2.2.2. K562 cell line 54

2.6.2.3. Cryopreservation of cell lines 55

2.6.3. MTT cellular viability protocol 55

2.6.4. Cellular viability combination studies 57

2.6.5. Safety index 58

2.7. *Artemia* toxicity study 58

2.8. Artemia lethality assay protocol 59

2.8.1. Hatching *Artemia* eggs 59

2.8.2. *Artemia* lethality assay 59

2.9. Free radical-induced oxidative stress and Iron chelation 60

2.9.1. Preparation of test compounds and control drugs for iron chelation and free radical scavenging assays..... 61

2.9.2. Free radical scavenging assay 61

2.9.2.1. Free radical scavenging assay protocol 61

2.9.3. Iron chelation assay 63

2.9.3.1. Iron chelation assay protocol.....64

2.10. Computational analysis 65

2.11. Statistical analysis 66

CHAPTER THREE – RESULTS

3.1. Antimalarial activity 67

3.2. Antimalarial combination studies 69

3.3. Morphological and stage specific effects..... 70

3.4. Vector Studies..... 75

3.4.1. Larvicidal Activity 75

3.4.2. Morphological effects of the test compounds on the *An. arabiensis* larvae ... 77

3.4.3. Ovicidal Activity 79

3.5. Cytotoxicity Studies..... 80

3.5.1. Haemolysis..... 80

3.5.2. MTT cytotoxic activity 80

3.6. Cytotoxic combination studies..... 84

3.7. Safety and selectivity Index 84

3.8. *Artemia* lethality assay..... 85

3.8.1. *Artemia* lethality studies 85

3.8.2. Morphological effects of the test compounds on the *Ar. franciscana* nauplii . 86

3.9. Anti-Oxidant and Iron Chelating Activity..... 91

3.9.1. Free Radical Scavenging 91

3.9.2. Iron Chelation 91
3.10. Computational Analysis 91
3.10.1 Drug-likeness predictions 91

CHAPTER FOUR – DISCUSSION

4.1. Discussion 98
4.1.1. Phenyl-hydrazono derivatives 99
4.1.2. Dihydroquinoline-carbothioamide derivatives 100
4.1.3. Quinoline-3-carboxamide derivatives 103
4.1.4. Lead Compounds DC14 and Q3C11 103
4.1.5. Possible mechanism of action of the quinoline derivatives 105
4.2. Insecticidal Activity 110
4.3. Toxicity profile 112

CHAPTER FIVE – CONCLUSIONS, LIMITATIONS AND RECOMMENDATIONS FOR FURTHER RESEARCH

5.1 Conclusions 117
5.2 Limitations and Future study recommendations 119

References 120

Appendices

Appendix A: Ethics documents **144**

Appendix B: Antimalarial activity **150**

Appendix C: Larvicidal activity **155**

Appendix D: Ovicidal activity **159**

Appendix E: Haemolysis statistical analysis **161**

Appendix F: 24 hour nauplii mortality **164**

Appendix G: The summary of the activity for test compounds Q3C8 ..... **165**

LIST OF FIGURES

Figure 1.1: The global distribution of countries with indigenous cases of malaria and the 2023 status of recent malaria cases.	2
Figure 1.2: Life cycle of the *Plasmodium* parasite in both its human and *Anopheles* hosts.	5
Figure 1.3: The resting/feeding stance of the female *Anopheles* species (A), which differentiates them from other non-malaria transmitting vectors, such as *Aedes aegypti* (B).	7
Figure 1.4: The *Anopheles* mosquito life cycle including eggs, larva, pupae and adult mosquito.	8
Figure 1.5: The quinoline core structure which served as a scaffold for the hybrid test compounds under investigation in this study.	24
Figure 2.1: Structural formulas of the positive controls listed in Table 2.4 that were used in various assays.	34
Figure 2.2: The Malstat™ assay for the detection of the *Plasmodium* lactate dehydrogenase enzyme.	40
Figure 2.3: Layout for the *p*LDH drug sensitivity assay.	42
Figure 2.4: Isobologram depicting three possible pharmacological interactions between compound X and compound Y.	45
Figure 2.5: Conversion of MTT (yellow colour) to the formazan (purple colour) product by succinate dehydrogenase which indicates cellular viability.	52
Figure 2.6: Plate layout of the MTT cell viability assay.	56
Figure 2.7: The interaction between DPPH free radical and an anti-oxidant and the observed colour changes.	62
Figure 2.8: Plate layout of the free radical scavenging assay.	63
Figure 3.1: Dose dependent antimalarial inhibitory effect of the most active compounds, DC14 and Q3C11 against the *in vitro* asexual blood stages of *P. falciparum* in comparison to standard antimalarial drug, quinine using the *p*LDH assay	67
Figure 3.2: The antimalarial IC_{50} values of the most active dihydroquinoline-carbothioamide (DC), and quinoline-3-carboxamide (Q3C) compounds on the *P. falciparum* NF54 parasite compared to the standard antimalarial drugs, quinine and chloroquine using the *p*LDH assay.	69
Figure 3.3: Isobolograms displaying the drug interactions between test compound DC14 (A,C) or Q3C11 (B,D) in combination with the standard antimalarial drug, quinine using the *p*LDH assay. (n=4). A synergistic drug interaction were observed between	70

quinine and compound DC14, compared to an antagonist interaction between quinine and Q3C11.	
Figure 3.4: The % gametocytes observed over 48 hours in the untreated parasites control, compared to compounds DC14 (7.23 µM), Q3C11 (7.99 µM) and quinine (0.09 µM) treated parasites control.	71
Figure 3.5: The comparison of the % parasitaemia over 48 hours of the ring (A), trophozoite (B), schizont (C) stages and the total % parasitaemia (D) of the untreated parasites control compared to compound DC14 (7.23 µM), Q3C11 (7.99 µM) and the quinine (0.09 µM) treated parasites.	73
Figure 3.6: Development of a gametocyte in the treated NF54 *P. falciparum* parasite flask after 24 hours of exposure to test compound Q3C11.	74
Figure 3.7: Dose-dependent cytotoxic effect of the most active compounds, DC12 and **Q3C8** against chronic myelogenous leukaemia K562 cell line in comparison to cytotoxic control cisplatin using the MTT assay.	83
Figure 3.8: The cytotoxic effect of dihydroquinoline-carbothioamide (DC), phenyl-hydrazono (PHYD) and quinoline-3-carboxamide (Q3C) compound groups on human K562 cells compared to cisplatin (positive control).	83
Figure 3.9: Isobolograms displaying the drug interactions between test compound DC12 (A) and Q3C8 (B) in combination with cisplatin against the human chronic myelogenous leukaemia K562 cell line using the MTT assay.	84
Figure 4.1: The summary of the activity for test compound DC14. The activity of DC14 across this study divided into its antimalarial, antioxidant and iron chelating, and toxicity properties.	101
Figure 4.2: The summary of the activity for test compound Q3C11. The activity of Q3C11 across this study divided into its antimalarial, antioxidant and iron chelating, and toxicity properties.	102
Figure 4.3: Overview of the effect of antimalarials, chloroquine (CQ) and artemisinin (ART) on the haemozoin pathway in the digestive vacuole (DV) of *P. falciparum* lifecycle.	106
Figure 4.4: The *Plasmodium* asexual intraerythrocytic cycle.	107
Figure 4.5: Quinoline drugs complex with ferriprotoporphyrin IX (FPIX) and form a complex which inhibits further sequestration of free haem into the haemozoin crystalline polymer.	108
Figure 4.6: The summary of the activity for test compound **DC12**.	115
Figure C1: Larvicidal DDT EC50 Analysis Screenshot	158
Figure G1: The summary of the activity for test compound **Q3C8**.	165

LIST OF TABLES

Table 1.1: The chemotherapeutic preventative prophylaxis of malaria.	12
Table 1.2: Clinical and laboratory indicators of uncomplicated and severe malaria.	16
Table 1.3: Standard antimalarials used for treatment, their mechanism of action, adverse effects and contra-indications.	18
Table 2.1: The International Union of Pure and Applied Chemistry (IUPAC) name of the novel dihydroquinoline-carbothioamide hybrid compounds and their corresponding molecular formulas and molecular weights (MW).	30
Table 2.2: The IUPAC name of the novel test quinoline-phenylhydrazono hybrid compounds and their corresponding molecular formulas and molecular weights (MW).	31
Table 2.3: The IUPAC name of the novel test quinoline-3-carboxamide hybrid compounds and their corresponding structural formulas and molecular weights (MW).	32
Table 2.4: Properties of the positive controls used in the various assays and their corresponding structures in Figure 2.1.	33
Table 2.5: Combined concentration ratios of compounds X and Y. Where X and Y were mixed in 1:1 volume ratio.	44
Table 3.1: The IC_{50} values of test compound and controls as determined by the *p*LDH assay in micromolar (µM) concentration against the *P. falciparum* NF54 parasite.	68
Table 3.2: The effect of test compounds DC14, Q3C11 and Quinine at the IC_{50} value concentrations on the parasitic stages and morphology over a 48 hour period in comparison to untreated NF54 *P. falciparum* parasites.	74
Table 3.3: The percentage larval mortality at 72 hours for each of the test compounds in comparison with positive control DDT at 0.5 µM.	76
Table 3.4: The morphological effects of compounds DC3, DC7 and DC11 on 3rd instar *An. arabiensis* larvae after a 72 hour period in comparison to the positive control DDT and untreated negative control.	77
Table 3.5: The percentage cell viability of the human embryonic kidney (HEK-293) and chronic myelogenous leukaemia K562 cell lines after treatment with 50 µM test compound and controls as determined by the MTT cytotoxicity assay	81
Table 3.6: The IC_{50} values of test compound and controls tested against the human chronic myelogenous leukaemia (K562) cell line as determined by the MTT assay.	82
Table 3.7: The selectivity index (or safety profile) of the test compounds corresponding to their respective antimalarial and cytotoxic activity at the screening concentration of 50 µM.	85
Table 3.8: The percentage *Ar. franciscana* nauplii mortality at 48 and 72 hours for each of the test compounds (0.5 µM) in comparison with positive control potassium dichromate at 50 µM.	87

Table 3.9: The LC_{50} values of the active test compounds and controls as determined by the *Artemia* lethality assay in comparison to positive control, potassium dichromate.	88
Table 3.10: The morphological effects of the two most active compounds from each compound group on the *Ar. franciscana* nauplii after a 72 hour period in comparison to positive control potassium dichromate and untreated negative control.	89
Table 3.11: The predicted molecular properties of the dihydroquinoline-carbothioamide and phenyl-hydrazono hybrids screened against *P. falciparum* based on Lipinski's Rule of Five	92
Table 3.12: The predicted pharmacokinetic properties of the dihydroquinoline-carbothioamide test compounds screened against *P. falciparum* using SwissADME and Chemicalize web-based software and ToxTree Version 3.1.0-1851.	94
Table 3.13: The predicted pharmacokinetic properties of the phenyl-hydrazono test compounds screened against *P. falciparum* using SwissADME and Chemicalize web-based software and ToxTree Version 3.1.0-1851.	95
Table 3.14: The predicted pharmacokinetic properties of the quinoline-3-carboxamide test compounds screened against *P. falciparum* using SwissADME and Chemicalize web-based software and ToxTree Version 3.1.0-1851.	96
Table 3.15: The predicted pKa values and percentage ionisation of the test compounds compared to quinine at physiological pH (7.4) of the human plasma and red blood cell compared to the acidic food vacuole pH (5) of the *P. falciparum* parasite.	97
Table B1: The percentage parasite viability for each of the test compounds in comparison with positive control Quinine at 50 µM.	150
Table B2: Ordinary one-way ANOVA statistical analysis multiple comparisons table for the pLDH assay IC_{50} values obtained	151
Table C1: The percentage larval mortality at 24 hours for each of the test compounds in comparison with positive control DDT at 0.5 µM.	155
Table C2: The percentage larval mortality at 48 hours for each of the test compounds in comparison with positive control DDT at 0.5 µM.	156
Table C3: The percentage pupae formation at 24, 48 and 72 hours for each of the test compounds in comparison with positive control DDT at 0.5 µM	158
Table D1: The percentage of unhatched eggs after being exposed to the test compounds at 0.5 µM for 72 hours in comparison with positive control formalin (1% v/v).	159
Table D2: Ordinary one-way ANOVA statistical analysis multiple comparisons table for the most active ovicidal test compounds obtained at 0.5 µM after 72 hours of exposure.	160
Table E1: Ordinary one-way ANOVA statistical analysis multiple comparisons table for the Haemolysis values obtained at 50 µM	161
Table F1: The percentage *Ar. franciscana* nauplii mortality at 24 hours for each of the test compounds (0.5 µM) in comparison with positive control potassium dichromate at 50 µM.	164

LIST OF EQUATIONS

Equation 2.1: Equation used to calculate the percentage parasitaemia.	38
Equation 2.2: The equation used to calculate the percentage parasite growth taking both the test and reference wavelengths into account.	43
Equation 2.3: Relative concentration ratios of X:Y or ΣFIC value. Ratios were calculated using the IC_{50} values of combined ratios of X and Y over the individual IC_{50} values of X and Y, respectively.	45
Equation 2.4 The equation used to calculate the percentage survival of the larvae after incubation with test compound after a 24-hour period.	48
Equation 2.5 The equation used to calculate the percentage mortality of the larvae after incubation with test compound after a 24-hour period.	49
Equation 2.6 The equation used to calculate the percentage mortality of the eggs after incubation with test compound after a 24-hour period.	50
Equation 2.7 The equation used to calculate the percentage haemolysis.	51
Equation 2.8: Determination of cells in cell suspension when counted using a haemocytometer at 100x magnification.	55
Equation 2.9: The equation used to calculate the percentage cell viability taking both the test and reference wavelengths into account.	57
Equation 2.10: The equation used to calculate the safety index for *P. falciparum* compared to human kidney epithelial (HEK293) cells.	58
Equation 2.11: The equation used to calculate the selectivity index for human leukemic K562 compared to human kidney epithelial (HEK293) cells.	58
Equation 2.12 The equation used to calculate the percentage mortality of the *Artemia* nauplii after incubation with test compound after a 24-hour period.	60
Equation 2.13 The equation used to calculate the percentage decolourisation of the $DPPH^{\bullet}$ by the test compounds and controls.	63
Equation 2.14 The equation used to calculate the percentage iron chelation of the ferrous-ferrozine complex by the test compounds.	64
Equation 2.15 The equation used to calculate the percentage Ionisation of the test compounds.	65

LIST OF ABBREVIATIONS

APAD	3-Acetylpyridine adenine dinucleotide
APAD+	3-Acetylpyridine adenine dinucleotide (oxidised form)
ACD-B	Acid citrate dextrose solution B
ACT	Artemisinin-based combination therapy
CDC	Centers for Disease Control and Prevention
°C	Degrees Celsius
DC	Dihydroquinoline-carbothioamide
DDT	Dichlorodiphenyltrichloroethane
DMEM	Dulbecco's Modified Eagle's Medium
DMSO	Dimethyl sulfoxide
DPPH	2,2-Diphenyl-1-picrylhydrazyl
DPPH$^{\bullet}$	2,2-Diphenyl-1-picrylhydrazyl free radical
EDTA	Ethylenediaminetetraacetic acid
et al,.	et alia
FBS	Foetal Bovine Serum
ΣFIC	Fractional inhibitory concentration
FPIX	Ferriprotoporphyrin IX
g	Gram
g	Gravitational force / G-force
g/L	Grams per Litre
g/mol	Grams per mole
GIT	Gastro Intestinal Tract
G6PD	Glucose-6-Phosphate Dehydrogenase
HBA	Hydrogen Bond Acceptor
HBD	Hydrogen Bond Donor
HEPES	N-2-Hydroxyelthlypiperazine-N'-2-ethane-sulfonic acid

IC_{50}	Concentration required to inhibit 50% parasite/cell growth. Inhibitory Concentration
IRS	Indoor Residual Spraying
Ham-F12	Ham's Nutrient Mixture F12
HPLC	High-Performance Liquid Chromatography
HEK293	Human Embryonic Kidney epithelial cell
IBM SPSS®	International Business Machines Corporation Statistical Product and Service Solutions
IRAC	Insecticide Resistance Action Committee
ITN	insecticide treated mosquito net
IUPAC	International Union of Pure and Applied Chemistry
IV	Intravenous
K562	Chronic myelogenous leukemia K562 cell
Kg/cm2	Kilograms per centimeter squared
L	Litre
LC_{50}	Concentration required to kill 50% larvae/eggs/nauplii
LDH	Lactate dehydrogenase
LLIN	Long Lasting Insecticidal Net
LogP	Logarithm of the partition coefficient of a solute between octanol and water
LogD	Logarithm of the distribution coefficient of a solute between octanol and water
MMV	Medicines for Malaria Venture
m	Metre
mg	Milligram
mL	millilitre
mM	Millimolar
µM	Micromolar
µL	Microlitre
M	Molar

mol	Mole
MTT	3-(4,5-Dimethylthiazol-2-yl)-2,5-diphenyltetrazolium bromide
MW	Molecular Weight
NAD	Nicotinamide adenine dinucleotide
NAD+	Nicotinamide adenine dinucleotide (oxidised form)
NADH	Nicotinamide adenine dinucleotide phosphate (reduced form)
NBT	Nitroblue Tetrazolium
n.d	Not determined
n.s	Not significant
%	Percentage
PBS	Phosphate Buffered Saline
PES	Phenazine ethosulfate
pH	Potential of Hydrogen
PHYD	Phenyl-hydrazono
pKa	Ionisation constants
*p*LDH	*Plasmodium* Lactate Dehydrogenase
Q3C	Quinoline-3-carboxamide
QN	Quinine
RBC	Human Red Blood Cells
RDT	Rapid Diagnostic Test
Ro5	Rule of Five (5)
ROS	Reactive Oxidative Species
rpm	Revolutions per minute
RPMI-1640	Roswell Park Memorial Institute 1640
RTS,S/AS01	R:specifies central repeat units; T: T-cell epitopes; S: surface antigen of Hepatitis B (#1), S: surface antigen of Hepatitis B (#2); AS01: Adjuvant system 01
SA-DOH	South African Department of Health
s.d	Standard deviation

S.I	Selectivity Index (or Safety Index)
SI-HEK293/*Pf*	Selectivity Index HEK293 versus *P. falciparum*
SI-HEK293/K562	Selectivity Index HEK293 versus K562
UV-vis	Ultraviolet-visible
WHO	World Health Organization
WRIM	WITS Research Institute for Malaria

CHAPTER 1 - INTRODUCTION

1.1 Malaria Etiology

According to the World Malaria Report 2023, it is estimated by the World Health Organization (WHO) that globally there were 249 million cases of malaria in 85 malaria endemic countries, with 608,000 deaths in 2022 (WHO, 2023a). Malaria is caused by the protozoan *Plasmodium* parasite that is transmitted through the bite of an infected female *Anopheles* mosquito (WHO, 2023a). The 2023 World Malaria Report states that significant progress has been achieved in reducing the total number of malaria deaths worldwide in comparison to 2000's statistical data. The total estimated number of malaria deaths in 2000 worldwide was estimated at 864,000 and this declined steadily to an estimated 586,000 in 2015. The malaria mortality rate halved between 2000 and 2015 from an estimated 29 per 100 000 population at risk to 15.0 per 100,000 and continued to decline worldwide reaching an estimated 14.3 per 100,000 in 2022 (WHO, 2023a).

However, despite the decrease in total malaria deaths worldwide, the mortality reduction rate has slowed since 2000 in the WHO Africa region. The malaria mortality rate decreased by 60% between 2000 and 2019, from 143 to 57 deaths per 100,000 population at risk before rising to 61 in 2020 and decreasing again to 56 in 2022 in the Africa region (WHO, 2023a). Most of the fatal cases of malaria which are predominantly related to *P. falciparum* infections are due to severe anaemia or cerebral malaria (Autino *et al.,* 2012). Different clinical manifestations also exist and vary in their severity and outcomes depending on the parasite species, affected organs and the access to available care (Autino *et al.,* 2012).

Several malaria endemic countries worldwide have reported zero cases for more than 3 years, and multiple countries have been certified malaria free (Figure 1.1) (WHO, 2023a). Most malaria cases in 2022 were in the WHO African Region (93.6%) followed by the WHO South-East Asia Region (2%) and the WHO Eastern Mediterranean Region (3%). The WHO African Region accounted for 95.4% of all malaria deaths in 2022 and malaria deaths continue to be concentrated within this region. Nigeria accounted for 31.1% of all global malaria deaths

followed by the Democratic Republic of Congo (11.6%), Niger (5.6%), United Republic of Tanzania (4.4%) and Mozambique (3.5%) (WHO, 2023a).

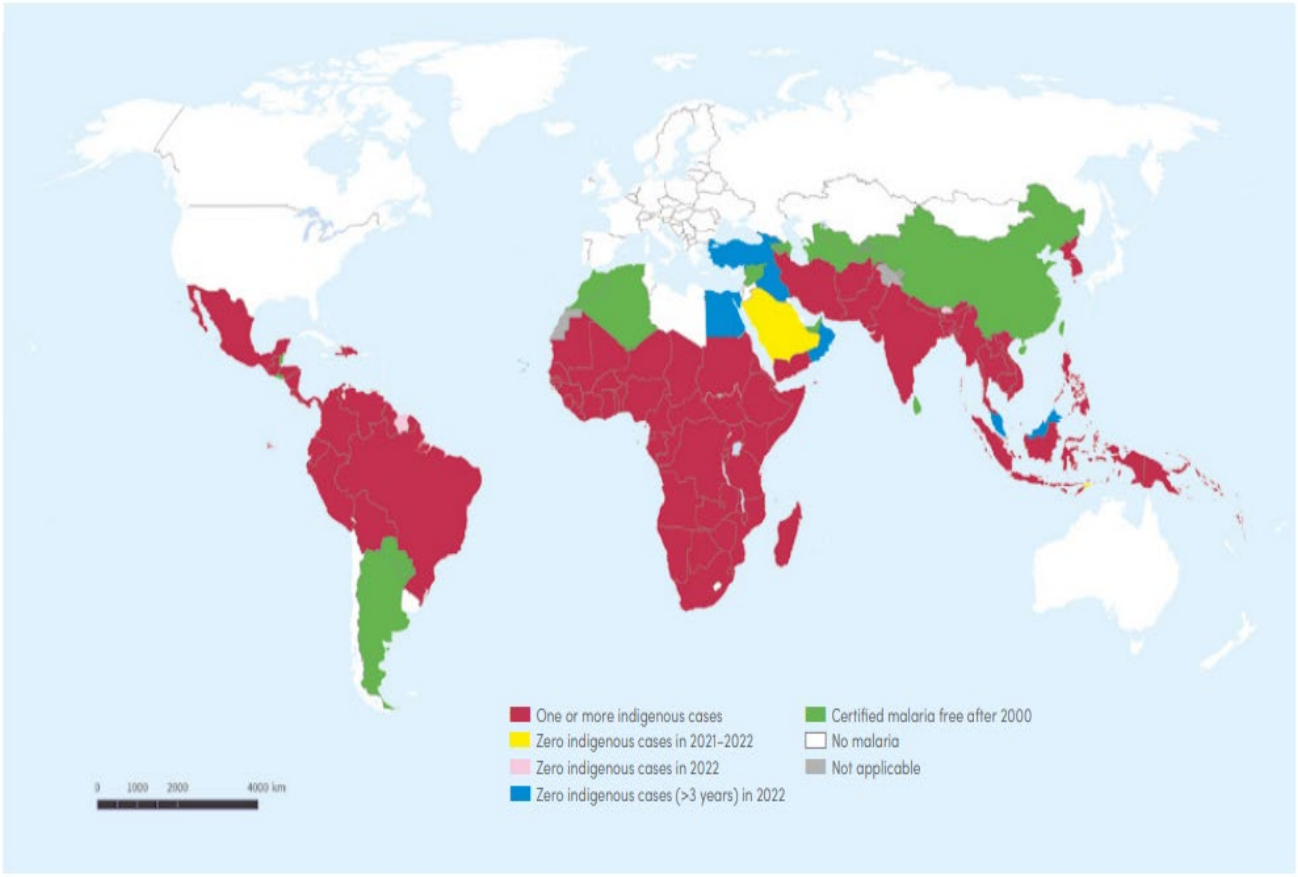


Figure 1.1: The global distribution of countries with indigenous cases of malaria and the 2023 status of recent malaria cases (WHO, 2023a).

Immunosuppressed individuals, pregnant women, young children and frequent travellers are at high risk of contracting malaria (WHO, 2023a). For pregnant women in particular, malaria infection can cause severe disease and death. There is an increased risk of death both before and after childbirth and malaria is an important contributor to stillbirth and preterm birth. Malaria is a major risk factor in perinatal, neonatal and infant (<1 year old) mortality (WHO, 2023a).

Malaria has an incubation period of 7 to 30 days post infection before the onset of symptoms occurs. According to the Centers for Disease Control and Prevention (CDC) there are shorter time

periods before symptoms can be observed. This occurs more frequently with *P. falciparum* infections than with other species of malaria parasite following the bite of an infected *Anopheles* mosquito vector (CDC, 2022). The South African Department of Health (SA-DOH) states that the initial symptoms of a malaria infection include presenting with an acute febrile illness with fever, chills, perspiration, rigors (cold shivers/hot sweats), headache, muscle/joint aches and malaise (SA-DOH, 2019a). Whilst severe malaria clinically presents itself as a medical emergency with numerous symptoms such as severe anaemia, acute respiratory distress syndrome, cardiovascular collapse, metabolic acidosis, fever, chills, headache, shivering, fatigue, nausea, vomiting, sweating, weakness and general malaise (SA-DOH, 2019a). In young children, high fevers are often associated with regurgitation of medication and seizures. Generalised seizures are more common in children with *P. falciparum* malaria than in those with malaria due to other species. Seizures are a prodrome of cerebral malaria and patients who have more than two seizures within a 24 hour period should be treated for severe malaria (WHO, 2023a).

*1.*2 *Plasmodium* Life Cycle

Malaria is caused by obligate intraerythrocytic protozoa of the genus *Plasmodium* as reviewed by Trampuz *et al.,* (2003). There are five known species of *Plasmodium* that can cause malaria in humans, these being, *P. falciparum, P. vivax, P. malariae, P. ovale* and *P. knowlesi* (Trampuz *et al.,* 2003; WHO, 2013; Lee *et al.,* 2022). *Plasmodium falciparum* is the deadliest of the five malaria parasites that are known to infect humans and is the most prevalent malaria parasite in the WHO African Region accounting for almost all (99%) malaria cases and deaths (WHO, 2023a). *Plasmodium vivax* accounted for 0.5% of malaria cases in the WHO African Region and mixed infections accounting for the remainder (WHO, 2023a). *Plasmodium knowlesi* has been reported in forested regions of Southeast Asia but not yet in sub-Saharan Africa (SA-DOH, 2019a).

Malaria in humans involves the cyclical infection of two hosts, namely, humans and the female *Anopheles* mosquito (Figure 1.2). Malaria is transmitted by all female *Anopheles* species in South Africa and rate of infection is dependent on climatic and environmental conditions, such as rainfall patterns, temperature, larval breeding sites, proximity to human settlement and humidity that may affect the number and survival of mosquitoes (Sinka *et al.,* 2010).

During a blood meal, the female *Anopheles* mosquito carrying the parasite inoculates sporozoites into the human host (Figure 1.2. #1). Sporozoites infect liver cells (Figure 1.2. #2) and mature into schizonts #3, which will eventually rupture and release merozoites #4 into the blood stream (CDC, 2022). After this initial replication in the liver (exo-erythrocytic schizogony), the parasites undergo asexual multiplication in the erythrocytes (erythrocytic schizogony). The merozoites released from the schizonts then further infect red blood cells #5. The ring stage parasites in the red blood cells mature into larger trophozoites and eventually form into schizonts, which then rupture #6 and release 16-32 daughter merozoites and thereby repeats the intra-erythrocytic life cycle of the parasite. The lysis of the red blood cells is responsible for the clinical manifestations of malaria in an infected individual (CDC, 2022). Humans that have been infected with malaria often develop fever, chills, headache and other flu-like symptoms which if left untreated can result in severe health complications and ultimately death (CDC, 2022). Uncomplicated malaria can rapidly progress to severe forms of the disease especially in people with no or low immunity, and early diagnosis combined with effective treatment within 24-48 hours of the onset of malaria symptoms is recommended (WHO, 2023a).

Some parasites differentiate into sexual erythrocytic stages and form gametocytes #7. When an *Anopheles* mosquito takes a blood meal, both male (microgametocytes) and female (macrogametocytes), are ingested #8. While in the mosquito's stomach, the microgametes fuse with the macrogametes and generate zygotes #9. These zygotes in turn become motile and elongated (ookinetes) #10 and invade the midgut wall of the mosquito where they will eventually develop into oocysts #11. The oocysts rupture #12 to release sporozoites, which then travel to the mosquito's salivary glands. The parasite multiplication in the mosquito is known as the sporogonic cycle. Inoculation of the sporozoites into a new human host perpetuates the life cycle of the malaria parasite (CDC, 2022).

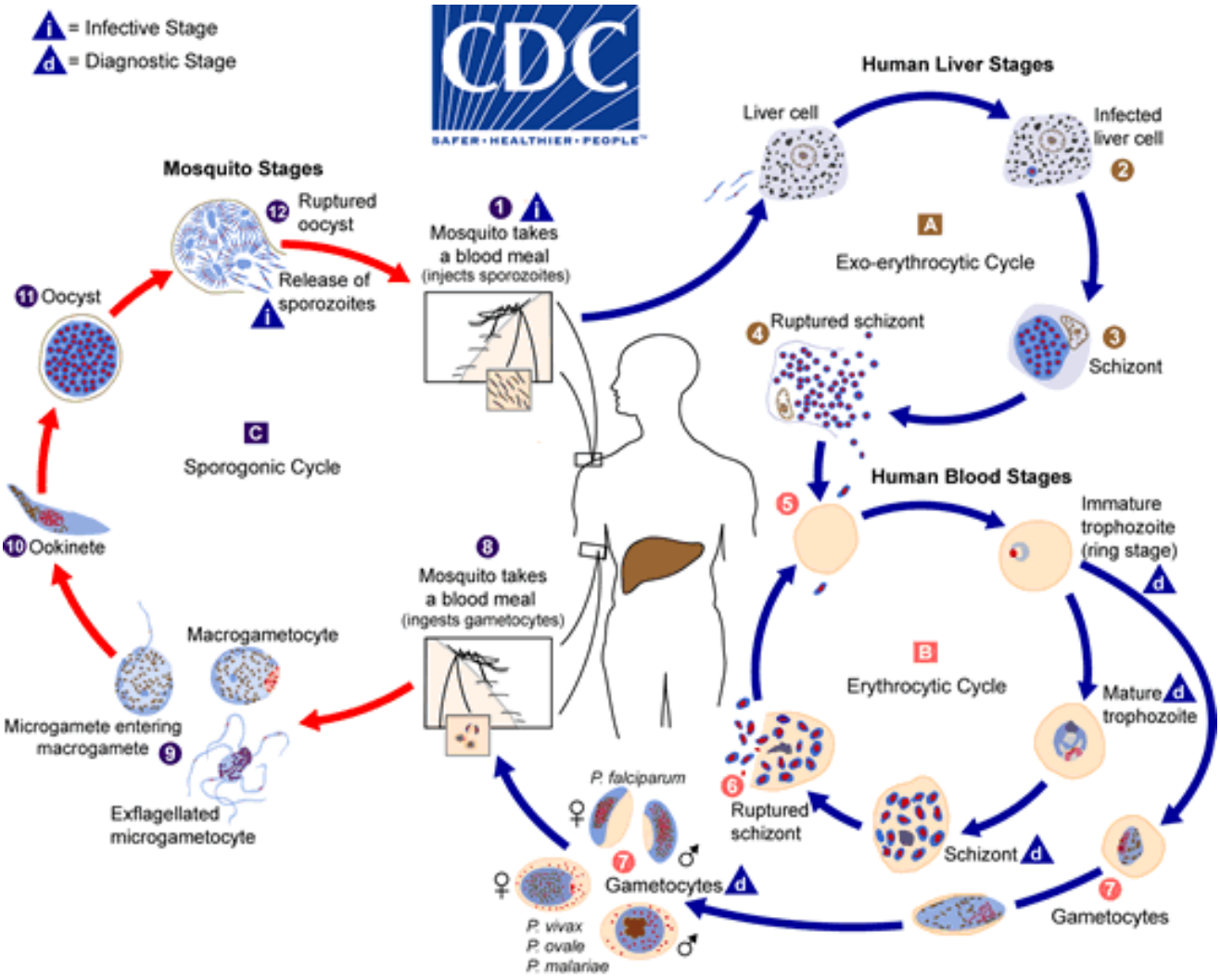


Figure 1.2: Life cycle of the *Plasmodium* parasite in both its human and *Anopheles* hosts (CDC, 2022). The exo-eyrthocytic cycle (A) represents the stages of the malaria parasite life cycle that takes place within the human liver where freshly inoculated sporozoites from an *Anopheles* mosquito enter liver cells, form a schizont and release daughter merozoites which travel to the bloodstream and infect human red blood cells starting the erythrocytic cycle (B) of the parasite's life cycle. After parasite maturation in the red blood cells the erythrocytic cycle repeats or gametocytes are formed which are then ingested by another female *Anopheles* vector when it takes a fresh blood meal. Ingestion of gametocytes by a female *Anopheles* vector starts the sporogonic cycle (C) of the malaria parasite's life cycle within the mosquito vector whereby microgametes and macrogametes form ookinetes. These ookinetes develop into oocysts that release sporozoites that invade the mosquito's salivary glands, ready to be inoculated into a new human host when the female *Anopheles* vector takes another blood meal (CDC, 2022).

1.3 Anopheles Vector

Mosquitoes belong to the phylum of Arthropoda and class of Insecta, order Diptera (WHO, 2013). Many insect vectors are members of species complexes composed of sibling species which are often morphologically identical but differ in their behaviour and ecology (Hill and Crampton, 1994). There are over 400 *Anopheles* mosquito species in nature and around 40 have been identified as major malaria vectors of importance (WHO, 2023b). In nature, adult female *Anopheles* mosquitoes are estimated to live between 1 to 2 weeks. In captivity they have been shown to live up to a month or longer (CDC, 2022). Climatic and environmental conditions play an important role in the mosquito life cycle with temperature, rainfall and humidity influencing larval development, parasite development within the mosquito, mosquito survival and vector competence (WHO, 2023a).

1.3.1 *Anopheles* in South Africa

In South Africa, *P. falciparum* is transmitted by two species groups of *Anopheles* mosquitoes, *Anopheles funestus* and *Anopheles arabiensis* (Brooke *et al.*, 2013; Dandalo *et al.,* 2017). *Anopheles funestus* however has been reduced to a point where it is almost entirely undetectable using a range of surveillance methods (Burke *et al., 2019)*, while *An. arabiensis* remains implicated in low-level seasonal transmission in malaria affected regions in South Africa (Burke *et al.,* 2019). Members of the *An. funestus* group of mosquitoes are suspected to be implicated in residual transmission include *An. vaneedeni (*Burke *et al.,* 2017) and *An. parensis* (Burke *et al.,* 2019). In South Africa, malaria has been limited to the north-eastern region of the country including Kwa-Zulu Natal, Mpumalanga and Limpopo (SA-DOH, 2019b). The areas bordering Zimbabwe, Mozambique and Swaziland have been identified as moderate to high-risk regions for contracting the disease (SA-DOH, 2019b).

Anopheles arabiensis occurs in all three of South Africa's malaria affected provinces (Braack *et al.,* 2020) and prefers dry, savannah environments while generally breeding in small, sunlit, temporary, freshwater pools (Sinka *et al.*, 2010). *Anopheles funestus* are strongly anthropophilic (prefer to feed on humans) while *An. arabiensis* are zoophilic, exophilic opportunistic feeders

(They feed on both humans and animals in cosmopolitan settings) however both species are efficient malaria vectors in Africa (Gillies and de Meillon, 1968; Sinka *et al.*, 2010).

The *Anopheles* vector is identifiable by the presence of palps that are as long as their proboscis (Figure 1.3) and by the presence of discrete blocks of black and white scales on the wings (Gillies and de Meillon, 1968; Gillies and Coetzee, 1987). Additionally, *Anopheles* are identifiable based on their resting position (Figure 1.3), which involves a raised abdomen protruding into the air as opposed to other mosquito species that rest with their abdomen parallel to the surface (CDC, 2022).

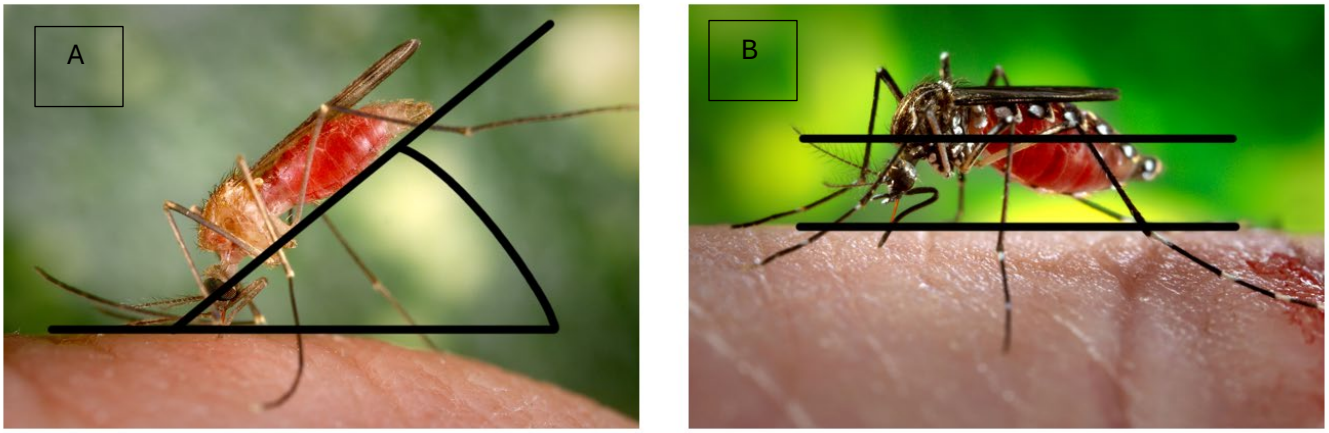


Figure 1.3: The resting/feeding stance of the female *Anopheles* species (A), which differentiates them from other non-malaria transmitting vectors, such as *Aedes aegypti* (B) (Van Zyl, 2016).

1.3.2 *Anopheles* Life Cycle

Anopheles mosquitoes, like all mosquitoes, go through four stages in their life cycle, namely the egg, larva, pupa and adult stages (CDC, 2022). Water is an essential part of the mosquito life cycle. Different mosquito species may lay their eggs separately or attached together as rafts floating on the water surface. *Anopheles* mosquitos lay 50 to 200 eggs per oviposition as single eggs on the water surface (CDC, 2022). Most of the eggs laid will hatch into larvae (Figure 1.4) within 48-72 hours. The larval stage of their life cycle involves 4 phases or “instars” with a moult occurring between each phase to allow for growth (CDC, 2022). Larvae mature into comma-shaped pupae that remain close to or parallel to the water’s surface to take in oxygen through a

breathing opening. In the water environment, the mosquito larvae will feed on microorganisms and organic matter (CDC, 2022).

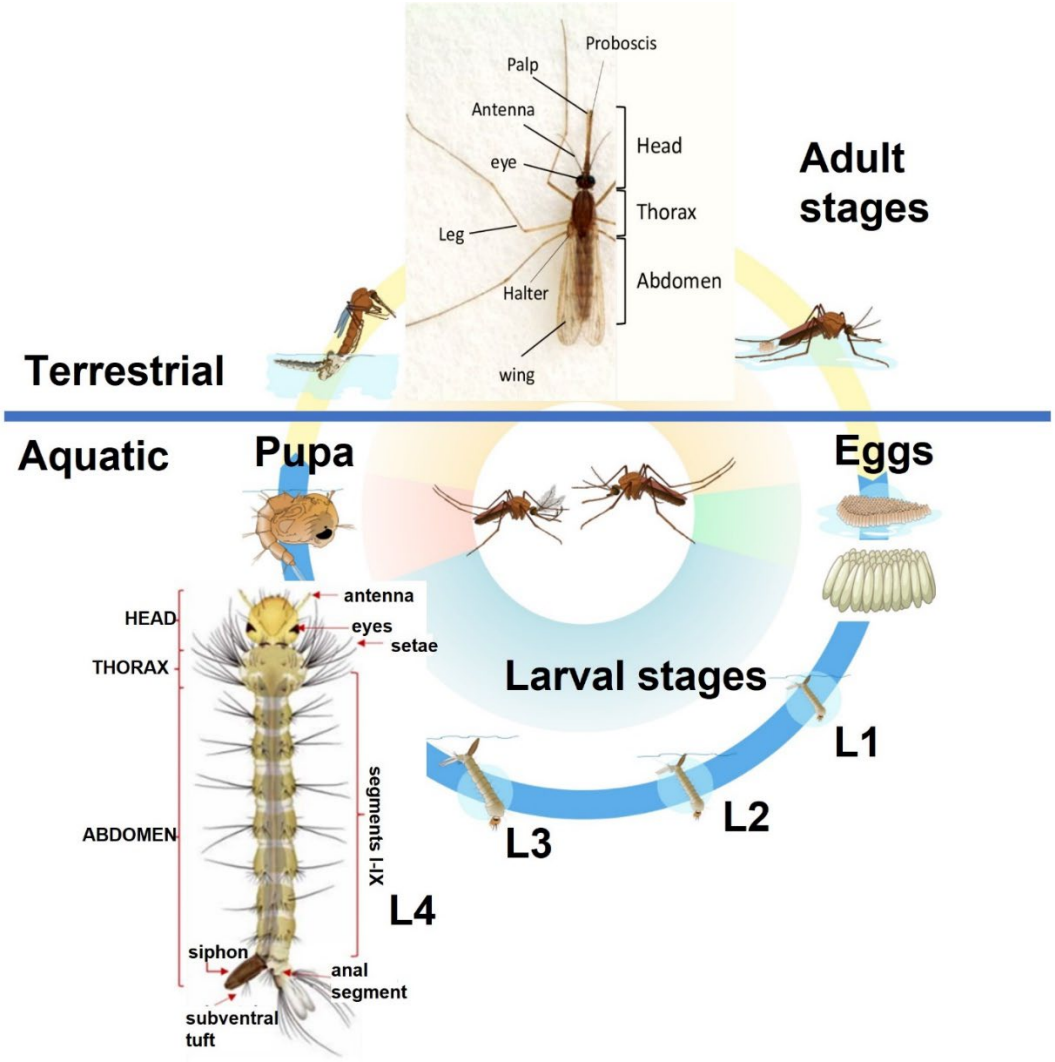


Figure 1.4: The typical mosquito life cycle including eggs, larva, pupae and adult mosquito (Adapted from Rueda, 2004; Williams and Pinto, 2012; Vector Disease Control International, 2018).

After a series of 4 moults, the larvae will form pupae. The pupal stage of development is a resting stage during which no feeding occurs. The pupae are however motile and respond to changes in light and may dive deeper into the water using their tail for mobility. Within 3 days the pupa will split along the dorsal surface of the cephalothorax and the adult *Anopheles* mosquito will emerge (CDC, 2022). The emergent mosquito will rest on the water surface while it waits for its body

parts to dry and harden (American Mosquito Control Association, 2022). The adult mosquito will typically mate within two to seven days of emerging from the pupal stage (Fereda, 2022). Female mosquitos will seek a blood meal and rest after feeding. While the blood digests within the female mosquito, new eggs are developed (CDC, 2022).

1.4 Malaria Symptoms and Diagnosis

The onset of malaria signs and symptoms may present as early as seven days, with a usual range of 10 to 30 days, before symptoms appear after being bitten by an infected vector mosquito (CDC, 2022, SA-DOH, 2019a). Once in the human red blood cell stage of malaria parasite infection, the signs and symptoms of malaria infection occur. Malaria features a range of signs and symptoms that are non-specific and require a high index of suspicion for proper diagnosis to be made according to the South African Department of Health (SA-DOH, 2019a). Any individual that presents with an acute febrile illness and any symptoms that include fever, chills, perspiration, rigors, headache, muscle/joint aches, malaise, lethargy, lassitude, fatigue, loss of appetite, abdominal discomfort, diarrhoea, nausea, vomiting, cough and splenomegaly should be referred for a laboratory diagnosis (SA-DOH, 2019a).

Malaria has an incubation period of 7 to 30 days and the possibility of infection is considered any time between 7 days to 3 months after the first possible exposure. If not treated within 24 hours of the onset of symptoms, *P. falciparum* malaria can rapidly progress to severe illness, often leading to death (WHO, 2023b). *Plasmodium. vivax*, *P. ovale* or *P. malariae* can take up to 12 months to first manifest clinically, with relapses occurring months or even years later, if primaquine is not taken to ensure radical cure (SA-DOH, 2019a). Presentation of *P. falciparum* malaria is very variable and may mimic many other diseases (and vice versa) including influenza, viral hepatitis, meningitis, encephalitis, septicaemia, typhoid fever, tick bite fever, gastroenteritis, viral haemorrhagic fever, trypanosomiasis, HIV seroconversion illness, urinary tract infection and relapsing fever (SA-DOH, 2019a). *Plasmodium. vivax*, *P. ovale* or *P. malariae* infection generally causes milder uncomplicated malaria in comparison to *P. falciparum* (SA-DOH, 2019a).

To optimise the management of malaria, the general public and healthcare workers should be encouraged to seek early treatment within 24 hours of symptoms developing, and ensure proper diagnostic testing if malaria is presumed. Individuals who test positive for malaria should have disease severity assessed and treatment should be initiated immediately. Malaria is a notifiable disease and each and every case including all imported cases in non-endemic areas should be reported (SA-DOH, 2019a).

A suspected malaria infected patient blood sample should be examined immediately using a malaria antigen rapid diagnostic test (RDT) or microscopy of thick and thin blood smears to confirm or exclude the diagnosis. A negative RDT or smear may not exclude diagnosis should the patient continue to exhibit symptoms and no other diagnosis has been determined. Further RDT or blood films should be examined at 6 to 12 hour intervals and repeat testing should continue until a diagnosis has been confirmed. Correctly stained blood smears will reveal malaria parasites if infection has occurred and the patient can then be treated at the primary health care level in accordance with treatment guidelines or given pre-referral treatment and transferred to the nearest hospital as an emergency case where severe malaria is confirmed (SA-DOH, 2019a).

The examination of peripheral blood smears will give an indication of the parasite density as well as the species of parasite present in the infected individual. High levels of parasitaemia (more than 4% asexual parasitized red blood cells/µL of peripheral blood) should be treated as severe malaria (SA-DOH, 2019a). Conversely however, severe disease symptoms may present themselves with low parasitaemia in the peripheral blood and as such the interpretation of a low parasite count must always be considered in conjunction with the patient's clinical condition and other laboratory results (SA-DOH, 2019a).

Commercially available RDT kits detect parasite antigens, namely, the histidine-rich protein 2 (or parasite lactate dehydrogenase or aldolase). Most RDTs will only detect *P. falciparum*, however some can detect other species such as *P. vivax* but are less sensitive for those. The use of a RDT kit may lead to false negatives early in the disease progression and false positives are encountered occasionally. RDTs should only be used for diagnosis of acute malaria infections and

not for follow-up as they may remain positive for several weeks even after successful treatment of malaria infection (SA-DOH, 2019a).

In all settings, suspected malaria should be confirmed with a parasitological test however where parasitological diagnosis is not possible, a decision to provide antimalarial treatment must be based on the probability that the illness is malaria (WHO, 2023b). Diagnosis with either microscopy or RDTs is expected to reduce the overuse of antimalarial medicines by ensuring that treatment is given only to patients with confirmed malaria infection as opposed to treating all patients that present with a fever (WHO, 2023b)

1.5 Malaria Prophylaxis and Treatment in South Africa

More than 90% of human malaria infections in Sub-Saharan Africa are due to *P. falciparum* while the remainder of infections are attributed to *P. vivax, P. ovale* or *P. malariae.* As mentioned in Section 1.4, the signs and symptoms of *P. falciparum* malaria are very variable and may present as early as 7 days after being bitten by an infected vector mosquito. The usual incubation range before symptoms develop is between 10 to 30 days, however longer incubation periods may occur in individuals who have failed chemoprophylaxis or have been on selected antibiotics that have known anti-malarial activity such as cotrimoxazole, tetracycline, macrolides, chloramphenicol and quinolones (SA-DOH, 2019a).

Malaria prophylaxis in South Africa involves the use of various chemoprophylactic agents such as mefloquine, atovaquone-proguanil or doxycycline (Table 1.1) (SA-DOH, 2019b). The WHO recommends that if a patient has taken chemoprophylaxis, the same medicine should not be used for treatment (WHO, 2023b). Chemoprophylaxis needs to be implemented in addition to personal protection measures to prevent malaria transmission and blanket recommendations are not advised (SA-DOH, 2019b). The choice of prophylaxis should be tailored to the individual with additional non-drug measures being implemented such as mosquito avoidance and the use of insect repellents (SA-DOH, 2019b).

Table 1.1: The chemotherapeutic preventative prophylaxis of malaria (Blumberg, 2015; Van Zyl, 2016; SA-DOH,2019; SA-DOH,2019b; WHO, 2023b).

Prophylaxis	Parasite Species	Dosing	Mechanism of Action	Adverse Effects	Contra Indications	Notable Info
Atovaquone and Proguanil	*P. falciparum*	250mg atovaquone plus 100mg proguanil. Should be taken one day before exposure, continued daily during exposure and for seven days after the last possible exposure to malaria.	Inhibitor of parasitic pyrimidine synthesis in the schizont stage. Selective inhibition of malaria cytochrome bc1 complex which leads to disassembling mitochondrial membrane potential. Proguanil inhibits parasitic dihydrofolate reductase resulting in folate synthesis inhibition.	Headache and abdominal pain (GIT symptoms). Proguanil can cause mouth ulcers, vomiting, nausea and diarrhoea.	Severe renal impairment, Children < 11kg, pregnancy/ lactation due to lack of data.	Atovaquone and proguanil always used in combination. Taken with milk or food for better absorption

* GIT: Gastro-Intestinal Tract

Table 1.1 (Continued): The chemotherapeutic preventative prophylaxis of malaria (Blumberg, 2015; Van Zyl, 2016; SA-DOH,2019; SA-DOH,2019b; WHO, 2023b).

Prophylaxis	Parasite Species	Dosing	Mechanism of Action	Adverse Effects	Contra Indications	Notable Info
Doxycycline	Multi-drug resistant strain *P. falciparum*	100mg once daily starting one day before entering the area, continuing daily while in the area, and daily for four weeks after leaving the area.	Protein synthesis at the apicoplast	Photosensitivity, nausea, dizziness, headache, abdominal pain (GIT symptoms), candidiasis	Pregnancy/lactation, children < 8 years	Antibiotic. Must be taken with enough fluid to prevent oesophageal ulceration. Avoid excessive UV exposure and do not lie down for at least one hour after ingestion.
Mefloquine	*P. falciparum* and *P. vivax*	250mg (one tablet) weekly, starting one week before entering the area, once weekly while in the area, and once weekly for four weeks after leaving the area	Schizonticidal in the red blood cell phase of the parasite life cycle	Headache, rash, nausea, vomiting, dizziness, insomnia, mood changes	Patients with a history of epilepsy or psychiatric illness, children < 5kg, severe hepatic or renal impairment. Prior history of severe reactions	Widely used in malaria endemic regions. Prophylaxis of choice during pregnancy. Safe in lactation. Taken after a meal with plenty of fluid

* GIT: Gastro-Intestinal Tract

In 2021, the WHO recommended the use of the RTS,S/AS01 malaria vaccine as a part of a comprehensive malaria control strategy (WHO, 2023a). The RTS,S/AS01 malaria vaccine is composed of combining genes from repeat ('R') and T-cell epitope ('T') of the pre-erythrocytic circumsporozoite protein (CSP) of the *Plasmodium falciparum* malaria parasite together with a viral surface antigen ('S') of the hepatitis B virus (HBsAg). This is mixed with another hepatitis B surface antigen (HBsAg) to improve purification ('S') before all is added to an adjuvant system, AS01 (Laurens, 2020),

In October 2023, the WHO recommended a second malaria vaccine, R21, and suggested that a two-vaccine market will make broad vaccine scale-up possible across Africa possible (WHO, 2023a). Due to the constrained supply of the RTS,S/AS01 vaccine and the need for R21 to complete ongoing WHO prequalification, the full benefits of the malaria vaccines are yet to be determined in highly malaria endemic regions (WHO, 2023a). The R21 vaccine has shown promising results in trials with an efficacy of more than 75% in preventing malaria (Ngou et al., 2024), while the RTS,S/AS01 showed less efficacy (less than 50%) in a randomised phase 2b control trial in Ghana and Kenya depending on the number of doses administered (Samuels et al., 2022).

Treatment of malaria is dependent on the severity of the illness and the pattern of drug resistance of the parasite in the geographical region where infection took place (SA-DOH, 2019a). In managing uncomplicated malaria, individuals may be treated at the primary healthcare level. Effective treatment should be started as soon as malaria is diagnosed at the clinic or hospital level. Delays in treatment initiation led to an increase in morbidity and mortality (SA-DOH, 2019a). In South Africa, the recommended treatment for patients with uncomplicated malaria is the fixed dose artemisinin-based combination therapy (ACT), artemether-lumefantrine (Blumberg, 2015; SA-DOH, 2019a). The WHO recommends ACTs as the best treatment for uncomplicated *P. falciparum* malaria as ACTs are associated with rapid clinical and parasitological response (SA-DOH, 2019a).

ACTs recommended by the WHO can include one of the following combinations: Artemether and lumefantrine, artesunate and amodiaquine, artesunate and mefloquine, dihydroartemisinin and

piperaquine and artesunate and sulfadoxine-pyrimethamine (WHO, 2023a). In South Africa, chloroquine and sulfadoxine-pyrimethamine are not recommended given the high-level of resistance present (SA-DOH, 2019a).

Depending on whether the malaria infection is uncomplicated or not (Table 1.2), the recommended treatment for patients will differ. For patients diagnosed with uncomplicated malaria, a short treatment course of artemether-lumefantrine consisting of 6 doses over 3 days shows good tolerability and is used (SA-DOH, 2019a). Artemether-lumefantrine can be administered safely to pregnant women with uncomplicated malaria and should be used in the second and third trimester and may be considered as an alternative to quinine plus clindamycin during the first trimester of pregnancy (SA-DOH, 2019a).

Severe cases of *P. falciparum* malaria infection are treated with intravenous (IV) artesunate or IV quinine. A minimum of three IV doses of artesunate should be administered for severe malaria at 0, 12 and 24 hours after diagnosis, followed by a full course of six artemether-lumefantrine oral doses (SA-DOH, 2019a). A combination of oral quinine and doxycycline or clindamycin can be used in place of artemether-lumefantrine if the latter is unavailable or contra-indicated in a patient. Doxycycline is contraindicated in pregnancy and children under the age of 8 years old and clindamycin should be used for these patients instead (SA-DOH, 2019a). Quinine is intravenously dosed in a slow, rate-controlled manner and never by rapid injection. A loading dose of quinine is given by a slow infusion and a maintenance dose is infused over 2 to 4 hours every 8 hours for 48 hours or until the patient can tolerate oral medication (SA-DOH, 2019a).

The choice of chemotherapy for malaria is based upon the species of parasite identified. Initial treatment should be the same as the above depending on the severity of the infection however a 14-day primaquine course is necessary for the radical cure of *P. ovale* and *P. vivax*. Primaquine is contraindicated in pregnancy, children under six months of age and women breastfeeding children under six months of age (SA-DOH, 2019a). Primaquine is also contraindicated in severe glucose-6-phosphate dehydrogenase (G-6-PD) deficiency (SA-DOH, 2019a). In South Africa, Primaquine is currently not registered for use and must be obtained on a named patient basis.

Table 1.2: Clinical and laboratory indicators of uncomplicated and severe malaria (Blumberg, 2015; Lalloo *et al.,* 2016; Van Zyl, 2016; SAMF, 2020; WHO, 2023b)

Common presenting symptoms	Physical findings	Laboratory findings: uncomplicated malaria	Symptoms of severe malaria	Laboratory findings: severe malaria
• Headache • Fatigue • Abdominal discomfort • Myalgia • Fever • Chills • Perspiration • Anorexia • Nausea/Vomiting • General malaise	• Elevated temperatures (≥37.5°C) • Rigors • Weakness • Splenomegaly • Mild jaundice • Hepatomegaly • Increased respiratory rate	• Microscopic confirmation of malaria/species differentiation • Mild anaemia • Mild thrombocytopenia • Elevated bilirubin • Elevated Aminotransferase	• Fever • Impaired consciousness • Multiple seizures • Prostration • Respiratory distress/ pulmonary oedema • Jaundice • Spontaneous or abnormal bleeding • Anuria	• Parasite density >4% • Haemoglobin <7g/dL • Metabolic acidosis (pH<7.3; plasma bicarbonate < 15 mmol/L, serum lactate >5 mmol/L) • Hypoglycaemia (< 2.2 mmol/L) • Renal impairment (oliguria <0.4 ml/kg bodyweight/hour; serum creatinine >265 µmol/L) • Thrombocytopenia (<50,000/µL) • Liver transaminase • Pulmonary oedema

Severe cases of *P. falciparum* malaria infection are treated with intravenous (IV) artesunate or IV quinine. A minimum of three IV doses of artesunate should be administered for severe malaria at 0, 12 and 24 hours after diagnosis, followed by a full course of six artemether-lumefantrine oral doses (SA-DOH, 2019a). A combination of oral quinine and doxycycline or clindamycin can be used in place of artemether-lumefantrine if the latter is unavailable or contra-indicated in a patient. Doxycycline is contraindicated in pregnancy and children under the age of 8 years old and clindamycin should be used for these patients instead (SA-DOH, 2019a). Quinine is intravenously dosed in a slow, rate-controlled manner and never by rapid injection. A loading dose of quinine is given by a slow infusion and a maintenance dose is infused over 2 to 4 hours every 8 hours for 48 hours or until the patient can tolerate oral medication (SA-DOH, 2019a).

The choice of chemotherapy for malaria is based upon the species of parasite identified. Initial treatment should be the same as the above depending on the severity of the infection however a 14-day primaquine course is necessary for the radical cure of *P. ovale* and *P. vivax*. Primaquine is contraindicated in pregnancy, children under six months of age and women breastfeeding children under six months of age (SA-DOH, 2019a). Primaquine is also contraindicated in severe glucose-6-phosphate dehydrogenase (G-6-PD) deficiency (SA-DOH, 2019a). In South Africa, Primaquine is currently not registered for use and must be obtained on a named patient basis under Section 21 of the Medicines and Related Substances Act, 1965 (Act 101 of 1965) following authorisation by the Medicines Control Council (SA-DOH, 2019a).

Antimalarial chemotherapy is therefore based on the type of *Plasmodium* species and the severity of the disease considering patient demographics such as age, pregnancy, co-morbidities as well as the availability of medication and resources (SA-DOH, 2019a). Allergies and concomitant medications also need to be considered when treatment is initiated (SA-DOH, 2019a). Antimalarial drugs are broadly classified into tissue schizonticides, blood schizonticides or gametocides based on the parasite life cycle stage that they target (Rosenthal, 2023). There are several antimalarial combinations in use globally and in South Africa (Table 1.3) with artemisinin combinations being strongly recommended by the WHO (SA-DOH, 2019a; WHO, 2023b).

Table 1.3: Standard antimalarials used for treatment, their mechanism of action, adverse effects and contra-indications (Braga *et al.,* 2015; SA-DOH, 2019; Camarda *et al.*, 2019; WHO, 2023b).

Treatment Drug	Parasite species targeted	Mechanism of action	Adverse Effects	Contra Indications
Artemether and Lumefantrine	All species of *Plasmodium* that cause malaria.	• Artemether affects plasmodial transport proteins, interferes with mitochondrial electron transport and produces free radicals creating reactive oxygen species (ROS). • Lumefantrine inhibits haemozoin formation.	• Artemether: Nausea, vomiting, diarrhoea, allergic reactions. • Lumefantrine: Inhibits cytochrome CYP3A4. • Combination: Sleep disturbances, headache, dizziness, abdominal pain, fatigue.	First trimester of pregnancy (Evidence however suggests it may be safe), congenital prolonged QT syndrome
Artesunate	*P. falciparum* (Severe or complicated malaria)	• Artesunate targets the blood schizont stage of the parasite and works in a similar manner to Artemether	• Generally safe and tolerable. Common adverse effects are nausea, vomiting, rash, dizziness and gastro-intestinal disturbance.	Hypersensitivity to artemisinin

Table 1.3 (Continued): Standard antimalarials used for treatment, their mechanism of action, adverse effects and contra-indications (Braga *et al.,* 2015; SA-DOH, 2019; Camarda *et al.*, 2019; WHO, 2023b).

Treatment Drug	Parasite species targeted	Mechanism of action	Adverse Effects	Contra Indications
Quinine and Doxycycline/ Clindamycin	*P. falciparum*. Can be used for other species if artemether lumefantrine or artesunate is unavailable	Quinine interferes with haemoglobin digestion in the blood stage of the parasite life cycle. Doxycycline and clindamycin inhibit protein synthesis at the apicoplast.	Well tolerated in combination with quinine. Vomiting, diarrhoea, fever, chills, nausea, cinchonism, hypoglycaemia and headache.	Hypersensitivity to quinine. Prolonged QT interval, patients with glucose-6-phosphate dehydrogenase (G-6-PD) deficiency. Doxycycline: Pregnancy and children <8 years old.
Primaquine	*P. vivax* and *P. ovale* Can be used to eliminate *P. falciparum* gametocytes	Primaquine metabolites generate reactive oxygen species and hydrogen peroxide causing liver stage parasite death.	Nause, dizziness, vomiting, abdominal pain and choluria	Severe G-6-PD deficiency. Pregnancy. Women who are breastfeeding a child under months of age. Children <6 months. Elimination of the hepatic stage of the parasite must be delayed until after delivery in pregnant women.

Upon the administration of drugs for uncomplicated malaria infection treatment, patients must be observed for at least an hour since vomiting may occur. Vomiting is one of the most common reasons for treatment failure. Malaria is easily underestimated, and complications may arise despite apparent appropriate chemotherapy. Patients should be carefully assessed and closely monitored for the duration of their treatment. Treatment failure after completing a full course of either artemether-lumefantrine or quinine plus doxycycline or clindamycin is rare considering that both sets of treatment have high cure rates (SA-DOH, 2019a). Primaquine is effective against *P. falciparum* gametocytes in non-contraindicated patients and the WHO recommends adding a single low dose in addition to full artemether-lumefantrine treatment to further reduce malaria transmission (SA-DOH, 2019a; WHO, 2023b).

1.6 Antimalarial drug resistance in South Africa

The WHO states that "historically, the emergence of chloroquine resistance in the 1970s and 1980s in Africa was associated with increased hospital admissions and mortality at the community level" (WHO, 2015). In South Africa, resistant *P. falciparum* strains are found against chloroquine and sulfadoxine-pyrimethamine (Cui *et al.*, 2015; SA-DOH, 2019; CDC, 2022). Artemisinin resistance has been confirmed to be spreading in Southeast Asia, however this has not been confirmed in Africa or South Africa (SA-DOH, 2019a). There have been some reports of the emergence of resistance in Africa, particular in Uganda and Kenya however the evidence should be treated with caution due to deviations from the WHO standard protocol (WHO, 2023a). Selective pressure and genetic polymorphisms within parasite species play a role in drug resistance (Cui *et al.*, 2015).

The WHO currently recommends fix ACT formulations for the treatment of uncomplicated falciparum malaria worldwide (WHO, 2023b). Artemisinin quickly and radically reduces the majority of malaria parasites present in a patient, while the partner drug in the combination therapy clears the remaining parasites (WHO, 2023b). It is widely accepted that protecting the efficacy of ACTs for the treatment of malaria is of utmost importance in the fight against malaria. The future efficacy of ACTs is at risk due to the emergence of resistance to both artemisinin itself as well as to the partner drugs used in combination therapy (WHO, 2023a).

Antimalarial drug resistance has influenced antimalarial chemotherapy for decades and has had a significant impact on the cost of global malaria control (Leroy, 2017; WHO, 2023a). New drugs have to be developed to replace those that have become ineffective but there are grounds for guarded optimism moving forward (Leroy, 2017; WHO, 2023a). Resistance to artemisinin is only partial and reflects a capacity of mutant parasites to survive short-lived drug pressure but not to replicate in the presence of drug (Blasco *et al.*, 2017). Fast acting antimalarials are less prone to yield resistance *in vitro* (Corey *et al.*, 2016) and longer lasting drugs with a similar mode of action to artemisinin might prove superior at reducing the risk of resistance (Blasco *et al.*, 2017). Various strategies exist and targeting more than one parasite life stage would be advantageous (Blasco *et al.*, 2017).

In South Africa, the combination treatment regimen recommended by the SA-DOH involving the deployment of artemisinin-based treatments for uncomplicated malaria (artemether-lumefantrine) and severe malaria (IV artesunate) have played a key role in decreasing the burden of malaria (SA-DOH, 2019a). Monotherapies, chloroquine and sulfadoxine-pyrimethamine are not recommended due to the high-level of resistance recorded in parts of the world, including South Africa (SA-DOH, 2019a).

1.7 Insecticide Resistance in South Africa

Malaria vector control is primarily achieved by means of insecticides (Brooke *et al.*, 2013). Indoor residual spraying (IRS) and the use of long-lasting insecticide treated nets (LLIN) are the mainstay of malaria vector control in preventing parasite transmission to human hosts (Brooke *et al.*, 2013; WHO, 2019; SA-DOH, 2019b). The WHO currently recommends twenty-seven different insecticides from five chemical classes for IRS, namely carbamates, neonicotinoids, organophosphates, organochlorines and pyrethroids (WHO, 2023b). Pyrethroids resistance has been exhibited in over three quarters of the countries that are actively monitoring pyrethroid resistance in malaria vectors (WHO, 2023a).

The Insecticide Resistance Action Committee (IRAC), a specialist technical industry group, defines insecticide resistance as “a heritable change in the sensitivity of a pest population that is reflected in the repeated failure of a product to achieve the expected level of control when used according to the label recommendation for that pest species” (IRAC, 2024). The

WHO states that from 2010 to 2020, of the 88 malaria endemic countries that provided standard monitoring data, resistance was detected in 78 countries to at least one insecticide in one malaria vector from one collection site (WHO, 2023a). The percentage resistance detected to each insecticide class from each of the countries reporting was listed as 82% for organochlorines, 87% for pyrethroids, 69% for carbamates and 60% for organophosphates (WHO, 2023a).

In 2023, the WHO issued new recommendations on vector control involving the use of insecticide treated mosquito nets (ITNs) with different modes of action. The WHO issued a strong recommendation for the deployment of pyrethroid-chlorfenapyr ITNs versus pyrethroid only nets to prevent malaria in adults and children in areas where mosquitos have become resistant to pyrethroids (WHO, 2023a).

In South Africa, vector resistance to permethrin and propoxur, a pyrethroid and carbamate respectively, have been reported in the *An. funestes* and *An. arabiensis* species (Mouatcho *et al.,* 2009; Brooke *et al.*, 2013). Samples of vector species from different malaria risk areas in South Africa displayed varying levels of insecticide resistance (Brooke *et al.*, 2013). Dichlorodiphenyltrichloroethane (DDT), which is banned worldwide with an exception for malaria vector control, is widely used in South Africa in areas where there is resistance to pyrethroids and organophosphates and remains effective against malaria vectors, although some resistance has been reported in localised vector populations (Brooke *et al.*, 2013, Maharaj *et al.,* 2024). A critical need for efficacious as well as affordable alternatives to DDT as an insecticide in malaria control programmes exists across Africa (Maharaj *et al.,* 2024).

Insecticide resistance in malaria vectors signifies a need for new tools in managing insecticide resistance. New insecticide classes such as neonicotinoids and pyrroles should be further monitored for resistance and their usefulness ascertained in controlling vector populations (Agumba *et al.,* 2019; WHO, 2023b,). The WHO indicates that an accelerated research and development response for tools such as longer lasting insecticides and other vector control agents is essential to achieving malaria eradication (WHO, 2023a).

1.8 Novel drug compounds

Due to malaria parasite drug resistance, as well as insecticide resistance in the vectors, there is an increased need for novel drug compound research to be performed (Cui *et al.*, 2015; WHO, 2019; WHO, 2023a). The Medicines for Malaria Venture (MMV) state in their 2022 annual report that there is a "continuing need" for chemoprevention and new antimalarials to combat the burden of drug resistance (MMV, 2022). The MMV emphasises the development of highly active compounds as well as potent combination medicines that are safe, effective and affordable (MMV, 2022). The development of novel drug compounds and their assessment for their toxicological profile thus forms an essential part of the drug development pipeline in treating or preventing malaria. In this study, novel quinoline heterocyclic hybrid compounds with either a carboxamide, thiosemicarbazone, phenylhydrazone group were synthesized and tested for their *in vitro* antimalarial and insecticidal activity as part of identifying new antimalarial and larvicidal agents.

1.8.1 Hybrid compounds

The hybridisation of chemical compounds is a concept that involves the artificial assembly of two or more pharmacophores that can be categorised under a recognised agent known for triggering the desired activity (Alkhzem *et al.*, 2022). Hybrid compounds are created by covalently binding various biologically active agents with the aim of retaining the pharmacological actions of each of the separate parts (Alkhzem *et al.*, 2022). A molecular linker is employed to attach the constituents through a covalent bond that is either cleavable or non-cleavable. A cleavable bond results in a hybrid pro-drug strategy where two useful drugs can be delivered to the site of action. A non-cleavable linker results in a hybrid drug strategy where two pharmacophores bound together may result in combination therapy where effectiveness is retained in combating pathogens that may be resistant to individual drug components (Alkhzem *et al.*, 2022).

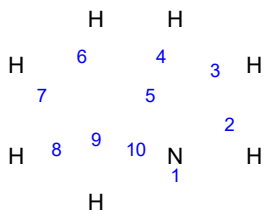
Hybridisation may also introduce supplementary physiochemical properties which may change the pharmacological spectrum of the hybrid such as introducing a novel antibacterial action to the resultant hybrid (Alkhzem *et al.*, 2022). Hybridisation also has the potential to

significantly increase the activity of a drug (Pokrovskaya *et al.*, 2009) or improve its safety and decrease toxicity towards normal healthy cells (Moiseeva *et al.,* 2019).

1.8.2 Quinoline

Quinoline is a privileged scaffold (Figure 1.5) in many natural and synthetic compounds (Yadav & Shah, 2021). Quinoline and its derivatives have been shown to possess numerous pharmacological properties such as antimalarial, antibacterial, antituberculosis, anti-HIV, antiplasmodial, antitumor, anti-inflammatory and anticonvulsant activity (Kumar *et al.*, 2009; Marella *et al.*, 2013; Hu *et al.,* 2017). Quinoline and its derivatives have emerged as an important class of bioactive heterocyclic compounds in the field of pharmaceuticals (Hu *et al.,* 2017). The quinoline ring system exists in a range of natural products, especially in alkaloids and the quinoline skeleton often serves as a lead molecule for the development of newer more potent molecules that showcase pharmacological activity (Kumar *et al.*, 2009; Marella *et al.*, 2013).

Quinoline compounds have been used to generate a range of important antimalarial drug derivatives such as chloroquine, mefloquine and primaquine (Kumar *et al.*, 2009; Parhizgar and Tahghighi, 2017). Various derivatives of quinoline have been evaluated *in vitro* and *in vivo* against resistant strains of the malaria parasite (Kumar *et al.*, 2009; Marella *et al.*, 2013; Parhizgar and Tahghighi, 2017). Additionally, quinoline derivatives have shown notable anticancer activity (Kumar *et al.*, 2009; Marella *et al.*, 2013; Afzal *et al.,* 2015). As such the quinoline group was the core structure on which the three groups of test compounds were designed, to generate the dihydroquinoline-carbothioamide (Section 1.8.3), phenylhydrazone (Section 1.8.4) and quinoline-3-carboxyamide (Section 1.8.5) derivatives.



Quinoline

Figure 1.5: The quinoline core structure which served as a scaffold for the hybrid test compounds under investigation in this study (National Center for Biotechnology Information, 2024a).

1.8.3 Dihydroquinoline-carbothioamide

The dihydroquinoline-carbothioamide group of derivatives consists of a quinolone analogue with a thiosemicarbazone moiety attached. Derivatives with a similar structure were shown to have antituberculosis and cytotoxic properties (Kumar *et al.,* 2018). A similar group of dihydroquinoline derivatives developed from ethyl 2-(1,3-benzodioxol-5-yl)-7-methoxy-4-oxo-1,4-dihydroquinoline-3-carboxylate (TDR42098) were potently active against both chloroquine-sensitive (3D7) (2-fold) and -resistant (K1) (16-fold) strains of *P. falciparum* compared to chloroquine (Zhang *et al.,* 2010). The introduction of a thiosemicarbazone group to the quinoline structure has showcased promising inhibitory activity against acetylcholinesterase in Alzheimer's disease, where the inhibitory IC_{50} values ranged from 0.12 – 60.9 µM compared to the positive standard, galantamine, 0.62 µM (Zaib *et al.,* 2021). Further research is warranted to examine those compounds with minimal inhibitory activity on human acetylcholinesterase against *Anopheles* acetylcholinesterase (Rants'o *et al.,* 2022). There is potential as an insecticide as there is a 40% difference between Human and Anopheles acetylcholinesterase where targeted inhibition can result in selective Anopheles insecticidal activity (Rants'o *et al.,* 2022). The thiosemicarbazone group has shown promising bioactivities such as antioxidant (Priyadarshini *et al.,* 2016), antibacterial (Alam *et al.,* 2023), anticancer (Ćurčić *et al.,* 2024) and antitumour (Zou *et al.,* 2017) properties. Govender *et al.* (2019) showed that quinoline thiosemicarbazones had moderate antibacterial activity against Gram positive and Gram-negative bacteria compared to their respective positive control antibiotics.

1.8.4 Phenylhydrazone

Phenylhydrazone derivatives have reported to possess a wide range of pharmacological activities where hydrazones possess an azometine -NHN=CH- proton constitute that is an important class of compounds for new drug development. Using this scaffold, numerous derivatives have been synthesised. Of the phenylhydrazone derivatives, several have been found to possess antimalarial activity and proposed to target PfATP6 (calcium ATPase) and PfDHFR (dihydrofolate reductase) using *in silico* molecular modelling (Rollas and Küçükgüzel, 2007; Amengor *et al*., 2024). Other antimicrobial properties that have been reported include antibacterial and antifungal (Khan *et al.,* 2014; Abhishek *et al.,* 2014; Wang *et al.,* 2017),

antituberculosis (Savini *et al.,* 2002; Nayyar and Jain, 2008), as well as in vitro anticancer properties against human neuroblastoma (SH-SY5Y) and breast adenocarcinoma (MDA-MB-231 and MCF-7) cell lines (Bingul *et al.,* 2016) and *in vivo* anti-inflammatory activity (Abhishek *et al.,* 2014). Phenylhydrazone derivatives containing a pyridine amide moiety have displayed insecticidal activity against several targets including *Culex pipiens*, where 5-bromo-N-(2-(2-(2,4-dichlorobenzylidene)hydrazinecarbonyl)-5-chloro-3-methylphenyl)pyridine amide had similar activity to the positive controls, tebufenozide and chlorpyrifos at 2.5 mg/ml (Yang *et al.,* 2016). It is always important when investigating a novel insecticide that parallel toxicity assays are undertaken against human cell lines as well as aquatic organisms such as Artemia or Zebrafish (due to their similar morphology and physiology of their nervous, cardiovascular and digestive systems to humans) to ensure safety when used clinically or introduced to the environment (Yu & Lu, 2018; Modarresi Chahardehi et al., 2020). This principle was undertaken in this study when evaluating the pharmacological properties of the novel compounds.

1.8.5 Quinoline-3-Carboxamide

Quinoline-3-carboxamide derivatives such as laquinimod, tasquinimod, or pasquinimod are researched for their immunomodulatory, antitumor, and anti-angiogenic effects in pre-clinical animal models (Li *et al.,* 2012; Fransén Pettersson *et al.,* 2018; Ott *et al.,* 2019; Yao *et al.,* 2019). Whilst quinoline-3-carboxyamide derivatives with alkyl groups showed good to moderate activity against several Gram-positive and Gram-negative bacteria (Wang *et al.,* 2016; Govender *et al*., 2018). Various quinoline-3-carboxamide derivatives have shown varying potency as antimalarial compounds *in vitro* and *in vivo* that are proposed to target the malaria parasite haemoglobin degradation pathway (Singh *et al.,* 2021).

1.8.6 Rationale of the heterocyclic derivative study

With the current antimalarial trend of combination therapy being advocated by the WHO and the ongoing need for additional safe and effective agents to combat the biological threat of drug resistance and insecticide resistance (WHO, 2023a), the hybridisation of known compounds is a key component of drug design and development. The rationale of the combination of a quinoline scaffold pharmacophore with linkers to carboxamide,

thiosemicarbazone and phenylhydrazone groups was to determine if the resultant compounds could act in a complementary manner to inhibit malaria parasite growth or cause lethality to *Anopheles* vector eggs and larvae. Despite the emergence of resistance to the quinoline containing chloroquine (Foley & Tilley, 1997; Sidhu *et al.,* 2002; Jones *et al.,* 2015; WHO, 2023a), this pharmacophore displays unique antimalarial abilities and low host cell toxicity, which warrants its inclusion into new hybrid drugs that may circumvent drug resistance while causing minimal toxicity to the host cell and non-target organisms. Additionally, the hybrid drugs may possess potential insecticidal activity against mosquito larvae and eggs which can help contribute to combating insecticidal resistance while causing minimal toxicity to the environment and non-target organisms.

1.9 Rationale, Aims & Objectives

1.9.1 Rationale:

The ongoing threat of malaria and the development of malaria parasite drug resistance and vector insecticide resistance requires the continued investigation into new compounds for use in combating the disease and its eradication.

1.9.2 Aims:

The aims of this research dissertation were to investigate the effects of the novel quinoline heterocyclic derivatives against *P. falciparum* and *An. arabiensis* vector and determine a preliminary toxicological profile.

1.9.3 Objectives:

To achieve the aim, the objectives of the study were to:

- Evaluate the *in vitro* antimalarial activity and morphologically induced changes by the novel quinoline heterocyclic derivative test compounds (Dihydroquinoline-carbothioamide, Phenylhydrazone and Quinoline-3-Carboxamide derivatives) against a chloroquine-sensitive (NF54) strain of *P. falciparum*.

- Determine the interaction between the most active novel dihydroquinoline-carbothioamide, phenylhydrazone and quinoline-3-carboxamide derivative test compounds and standard antimalarial control drug.
- Evaluate the ovicidal and larvicidal effects of the novel dihydroquinoline-carbothioamide, phenylhydrazone and quinoline-3-carboxamide derivative test compounds against the malaria vector, *An. arabiensis*.
- Evaluate the toxicological profile of the novel dihydroquinoline-carbothioamide, phenylhydrazone and quinoline-3-carboxamide derivative test compounds against human red blood cells, human cell lines (human epithelial kidney cells - HEK293 and human myelogenous leukaemia - K562) and *Artemia franciscana* nauplii.
- Assess the morphological changes exhibited by the *An. arabiensis* vector ovum and larvae and *Ar. franciscana* nauplii after exposure to novel dihydroquinoline-carbothioamide, phenylhydrazone and quinoline-3-carboxamide derivative test compounds and control compounds.
- Evaluate the pharmacokinetic properties of the novel dihydroquinoline-carbothioamide, phenylhydrazone and quinoline-3-carboxamide derivative test compounds compared to standard antimalarial control drugs.
- Evaluate the toxicity hazard profile of the novel dihydroquinoline-carbothioamide, phenylhydrazone and quinoline-3-carboxamide derivative test compounds using a predictive software tool (Toxtree).

CHAPTER 2 – METHODS AND MATERIALS

2.1 Compounds and Reagents

All solutions, buffers and culture media were prepared with MilliQ™ (Millipore®) deionised water and solutions sterile filtered through Sterivex™-GS 0.22 µm filters (Sigma-Aldrich®) and/or autoclaved (121°C at 1.2 kg/cm^2 for 20 minutes) where necessary to prevent contamination. All media and solutions were brought to room temperature or warmed to 37°C before use in the various assays and aseptic techniques were employed when working with the solutions and culturing parasites/cells to prevent contamination.

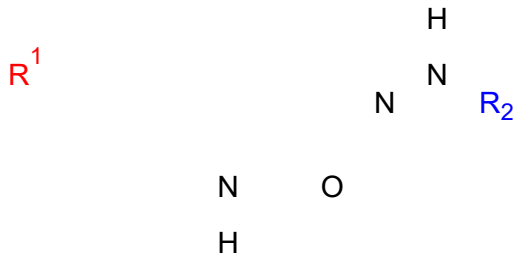
2.1.1 Test and Control compounds

Forty-two novel compounds were obtained from Prof N. Koorbanally (School of Chemistry and Physics, University of KwaZulu-Natal). The test compound structures were verified by nuclear magnetic resonance and mass spectroscopy and the compounds were determined to be of highest purity (≥99%) (Govender, 2018). These compounds were split into three groups based on their chemical structures, namely the dihydroquinoline-carbothioamide (Table 2.1), phenyl-hydrazono (Table 2.2) and quinoline-3-carboxamide (Table 2.3) hybrid groups. Controls used in the various assays are listed in Table 2.4 with their corresponding structures in Figure 2.2. The highest quality or high-performance liquid chromatography (HPLC) grade reagents and control compounds were purchased from reputable commercial companies, including Fluka (Buchs, Switzerland), Sigma-Aldrich® (Merck, Darmstadt, Germany; New Jersey, USA) and Thermo Fisher Scientific (Oxford, UK).

2.1.2 Preparation of test compounds and control drugs

A 10 mM stock solution for each compound was prepared by dissolving each respective compound in dimethyl sulfoxide (DMSO) (Sigma-Aldrich®). Aliquots of each stock were stored at -80°C until required. A screening concentration of 50 µM was prepared for each compound, taking the dilution factor of the respective assays into account. Based on the assay, the 10 mM stock solution was diluted with either incomplete parasite culture medium (Section 2.2.1.1), cell culture medium (Section 2.6.2.1), DMSO or autoclaved MilliQ™ deionised water. Similarly, a 10 mM stock solution of the positive controls (Table 2.4) were prepared to be used for the positive control compounds across the respective assays at various concentrations.

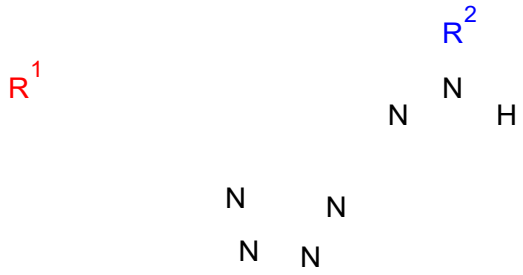
Table 2.1: The International Union of Pure and Applied Chemistry (IUPAC) name of the novel dihydroquinoline-carbothioamide hybrid compounds and their corresponding molecular formulas and molecular weights (MW).



2.1bb	Molecular Formula	R1	R2	IUPAC Name	MW (g/mol)
DC1	$C_{11}H_{10}N_4OS$	H	TSC	(E)-2-((2-oxo-1,2-dihydroquinolin-3-yl) methylene) hydrazine-1-carbothioamide	246.3
DC2	$C_{12}H_{12}N_4OS$	CH_3	TSC	(E)-2-((6-methyl-2-oxo-1,2-dihydroquinolin-3-yl)methylene)hydrazine-1-carbothioamide	260.3
DC3	$C_{11}H_9BrN_4OS$	Br	TSC	(E)-2-((6-bromo-2-oxo-1,2-dihydroquinolin-3-yl)methylene)hydrazine-1-carbothioamide	325.2
DC4	$C_{11}H_9ClN_4OS$	Cl	TSC	(E)-2-((6-chloro-2-oxo-1,2-dihydroquinolin-3-yl)methylene)hydrazine-1-carbothioamide	280.5
DC5	$C_{11}H_9FN_4OS$	F	TSC	(E)-2-((6-fluoro-2-oxo-1,2-dihydroquinolin-3-yl)methylene)hydrazine-1-carbothioamide	264.0
DC6	$C_{12}H_{12}N_4OS$	H	NMTSC	(E)-N-methyl-2-((2-oxo-1,2-dihydroquinolin-3-yl)methylene)hydrazine-1-carbothioamide	260.3
DC7	$C_{13}H_{14}N_4OS$	CH_3	NMTSC	(E)-N-methyl-2-((6-methyl-2-oxo-1,2-dihydro-quinolin-3-yl)methylene)hydrazine-1-carbothioamide	274.3
DC8	$C_{12}H_{11}BrN_4OS$	Br	NMTSC	(E)-2-((6-bromo-2-oxo-1,2-dihydroquinolin-3-yl)methylene)-N-methylhydrazine-1-carbothioamide	339.2
DC9	$C_{12}H_{11}ClN_4OS$	Cl	NMTSC	(E)-2-((6-chloro-2-oxo-1,2-dihydroquinolin-3-yl)methylene)-N-methylhydrazine-1-carbothioamide	294.8
DC10	$C_{12}H_{11}FN_4OS$	F	NMTSC	(E)-2-((6-fluoro-2-oxo-1,2-dihydroquinolin-3-yl)methylene)-N-methylhydrazine-1-carbothioamideamide	278.3
DC11	$C_{17}H_{14}N_4OS$	H	PHTSC	(E)-2-((2-oxo-1,2-dihydroquinolin-3-yl)meth ylene)-N-phenylhydrazine-1-carbothioamide	322.4
DC12	$C_{18}H_{16}N_4OS$	CH_3	PHTSC	(E)-2-((6-methyl-2-oxo-1,2-dihydroquinolin-3-yl)methylene)-N-phenylhydrazine-1-carbothioamide	336.4
DC13	$C_{17}H_{13}BrN_4OS$	Br	PHTSC	(E)-2-((6-bromo-2-oxo-1,2-dihydroquinolin-3-yl)methylene)-N-phenylhydrazine-1-carbothioamide	401.3
DC14	$C_{17}H_{13}ClN_4OS$	Cl	PHTSC	(E)-2-((6-chloro-2-oxo-1,2-dihydroquinolin-3-yl)methylene)-N-phenylhydrazine-1-carbothioamide	356.4
DC15	$C_{17}H_{13}FN_4OS$	F	PHTSC	(E)-2-((6-fluoro-2-oxo-1,2-dihydroquinolin-3-yl)methylene)-N-phenylhydrazine-1-carbothioamide	340.4

NOTE: TSC*: Thiosemicarbazone ;* NMTSC*: N-methylthiosemicarbazone* ; PHTSC*: Phenylthiosemicarbazone*

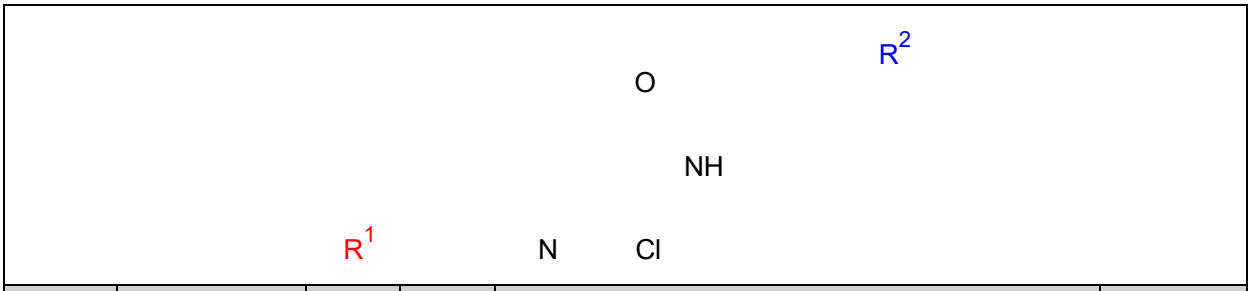
Table 2.2: The IUPAC name of the novel test quinoline-phenylhydrazono hybrid compounds and their corresponding molecular formulas and molecular weights (MW).



Code	Molecular Formula	R1	R2	IUPAC Name	MW (g/mol)
PHYD1	$C_{16}H_{12}N_6$	H	PHYD	(E)-4-((2-phenylhydrazono)methyl)tetrazolo[1,5-a]quinoline	288.3
PHYD2	$C_{17}H_{14}N_6$	CH_3	PHYD	(E)-7-methyl-4-((2-phenylhydrazono)methyl)-tetrazolo[1,5-a]quinoline	302.3
PHYD3	$C_{16}H_{11}BrN_6$	Br	PHYD	(E)-7-bromo-4-((2-phenylhydrazono)methyl)-tetrazolo[1,5-a]quinoline	367.2
PHYD4	$C_{16}H_{11}ClN_6$	Cl	PHYD	(E)-7-chloro-4-((2-phenylhydrazono)methyl)-tetrazolo[1,5-a]quinoline	322.8
PHYD5	$C_{16}H_{11}FN_6$	F	PHYD	(E)-7-fluoro-4-((2-phenylhydrazono)methyl) - tetrazolo[1,5-a]quinoline	306.3
PHYD6	$C_{16}H_{11}FN_6$	H	2F-PHYD	(E)-4-((2-(2-fluorophenyl)hydrazono)methyl)-tetrazolo[1,5-a]quinoline	306.3
PHYD7	$C_{17}H_{13}FN_6$	CH_3	2F-PHYD	(E)-4-((2-(2-fluorophenyl)hydrazono)methyl)-7-methyltetrazolo[1,5-a]quinoline	320.3
PHYD8	$C_{16}H_{10}BrFN_6$	Br	2F-PHYD	(E)-7-bromo-4-((2-(2-fluorophenyl)hydrazono)-methyl)tetrazolo[1,5-a]quinoline	385.2
PHYD9	$C_{16}H_{10}ClFN_6$	Cl	2F-PHYD	(E)-7-chloro-4-((2-(2-fluorophenyl)hydrazono)-methyl)tetrazolo[1,5-a]quinoline	340.8
PHYD10	$C_{16}H_{10}F_2N_6$	F	2F-PHYD	(E)-7-fluoro-4-((2-(2-fluorophenyl)hydrazono)-methyl)tetrazolo[1,5-a]quinoline	324.3
PHYD11	$C_{16}H_{11}FN_6$	H	4F-PHYD	(E)-4-((2-(4-fluorophenyl)hydrazono)methyl)-tetrazolo[1,5-a]quinoline	306.3
PHYD12	$C_{17}H_{13}FN_6$	CH_3	4F-PHYD	(E)-4-((2-(4-fluorophenyl)hydrazono)methyl)-7-methyltetrazolo[1,5-a]quinoline	320.3
PHYD13	$C_{16}H_{10}BrFN_6$	Br	4F-PHYD	(E)-7-bromo-4-((2-(4-fluorophenyl)hydrazono)-methyl)-tetrazolo[1,5-a]quinoline	385.2
PHYD14	$C_{16}H_{10}ClFN_6$	Cl	4F-PHYD	(E)-7-chloro-4-((2-(4-fluorophenyl)hydrazono)-methyl)tetrazolo[1,5-a]quinoline	340.8
PHYD15	$C_{16}H_{10}F_2N_6$	F	4F-PHYD	(E)-7-fluoro-4-((2-(4-fluorophenyl)hydrazono)-methyl)tetrazolo[1,5-a]quinoline	324.3

NOTE: PHYD: *phenylhydrazone*; 2F-PHYD: *2-fluorophenyl)hydrazone*; 4F-PHYD: *4-fluorophenyl)hydrazone*

Table 2.3: The IUPAC name of the novel test quinoline-3-carboxamide hybrid compounds and their corresponding structural formulas and molecular weights (MW).



Code	Molecular Formula	R1	R2	IUPAC Name	MW (g/mol)
Q3C1	$C_{16}H_{11}ClN_2O$	H	H	2-chloro-N-phenylquinoline-3-carboxamide	282.7
Q3C2	$C_{17}H_{13}ClN_2O$	CH_3	H	2-chloro-N-p-tolylquinoline-3-carboxamide	296.8
Q3C3	$C_{16}H_{10}ClFN_2O$	Cl	H	2-chloro-N-(4-fluorophenyl)quinoline-3-carboxamide	300.7
Q3C4	$C_{16}H_{10}ClFN_2O$	F	H	2-Chloro-6-fluoro-N-phenylquinoline-3-carboxamide	300.7
Q3C5	$C_{18}H_{15}ClN_2O$	H	CH_3	2-chloro-6-methyl-N-p-tolylquinoline-3-carboxamide	310.2
Q3C6	$C_{17}H_{12}ClFN_2O$	CH_3	CH_3	2-chloro-N-(4-fluorophenyl)-6-methylquinoline-3-carboxamide	314.7
Q3C7	$C_{16}H_{10}Cl_2N_2O$	Cl	CH_3	2,6-dichloro-N-phenylquinoline-3-carboxamide	317.2
Q3C8	$C_{17}H_{12}ClFN_2O$	F	CH_3	2-Chloro-6-fluoro-N-4-tolylquinoline-3-carboxamide	314.7
Q3C9	$C_{16}H_9Cl_2FN_2O$	H	F	2,6-dichloro-N-(4-fluorophenyl)quinoline-3-carboxamide	335.2
Q3C10	$C_{16}H_{10}ClFN_2O$	CH_3	F	2-Chloro-N-(4-fluorophenyl)-6-methylquinoline-3-carboxamide	300.7
Q3C11	$C_{17}H_{12}ClFN_2O$	Cl	F	2-chloro-6-fluoro-N-p-tolylquinoline-3-carboxamide	314.7
Q3C12	$C_{16}H_9ClF_2N_2O$	F	F	2-chloro-6-fluoro-N-(4-fluorophenyl)-quinoline-3-carboxamide	318.7

2.1.3 Analysis of test compounds and positive controls

Each test compound and control were evaluated in replicate wells and each experiment assay repeated at least in triplicate (biological replicates) to ensure a reproducible mean ± standard deviation (s.d.) was obtained. All compounds were screened and for those that displayed more than 60% activity, serial dilutions were prepared to determine the concentration that

inhibited 50% of activity, i.e. the IC_{50} value. For compounds displaying less than 60% activity, the percentage effect was reported. The GraphPad Prism® version 5.02 Software package (GraphPad Software, Inc, USA) was used to generate log sigmoidal dose response curves for test compounds/controls displaying more than 60% activity in the various experimental assays performed.

Table 2.4: Properties of the positive controls used in the various assays and their corresponding structures in Figure 2.1 (National Center for Biotechnology Information, 2024b-l).

Compound	Molecular Formula	Density	MW (g/mol)
Ascorbic acid[b]	$C_6H_8O_6$	1.69	176.12
Camptothecin[c]	$C_{20}H_{16}N_2O_4$	-	348.36
Chloroquine diphosphate[d]	$C_{18}H_{26}ClN_3 \cdot 2H_3PO_4$	-	515.86
Cisplatin[e]	$H_6Cl_2N_2Pt$	-	300.05
Dichlorodiphenyltrichloroethane (DDT)[f]	$C_{14}H_9Cl_5$	1.56	354.49
Dihydroartemisinin[g]	$C_{15}H_{24}O_5$	-	284.35
Ethylenediaminetetraacetic acid (EDTA)[h]	$C_{10}H_{14}N_2Na_2O_8\ 2H_2O$	0.86	372.24
Formaldehyde[i]	CH_2O	1.09	30.03
Potassium dichromate[j]	$K_2Cr_2O_7$	2.68	294.18
Quinine hydrochloride Dihydrate[k]	$C_{20}H_{24}N_2O_2 \cdot HCl\ 2H_2O$	-	396.91
Triton™ X-100[l]	$C_{14}H_{22}O(C_2H_4O)_n$)	1.07	647

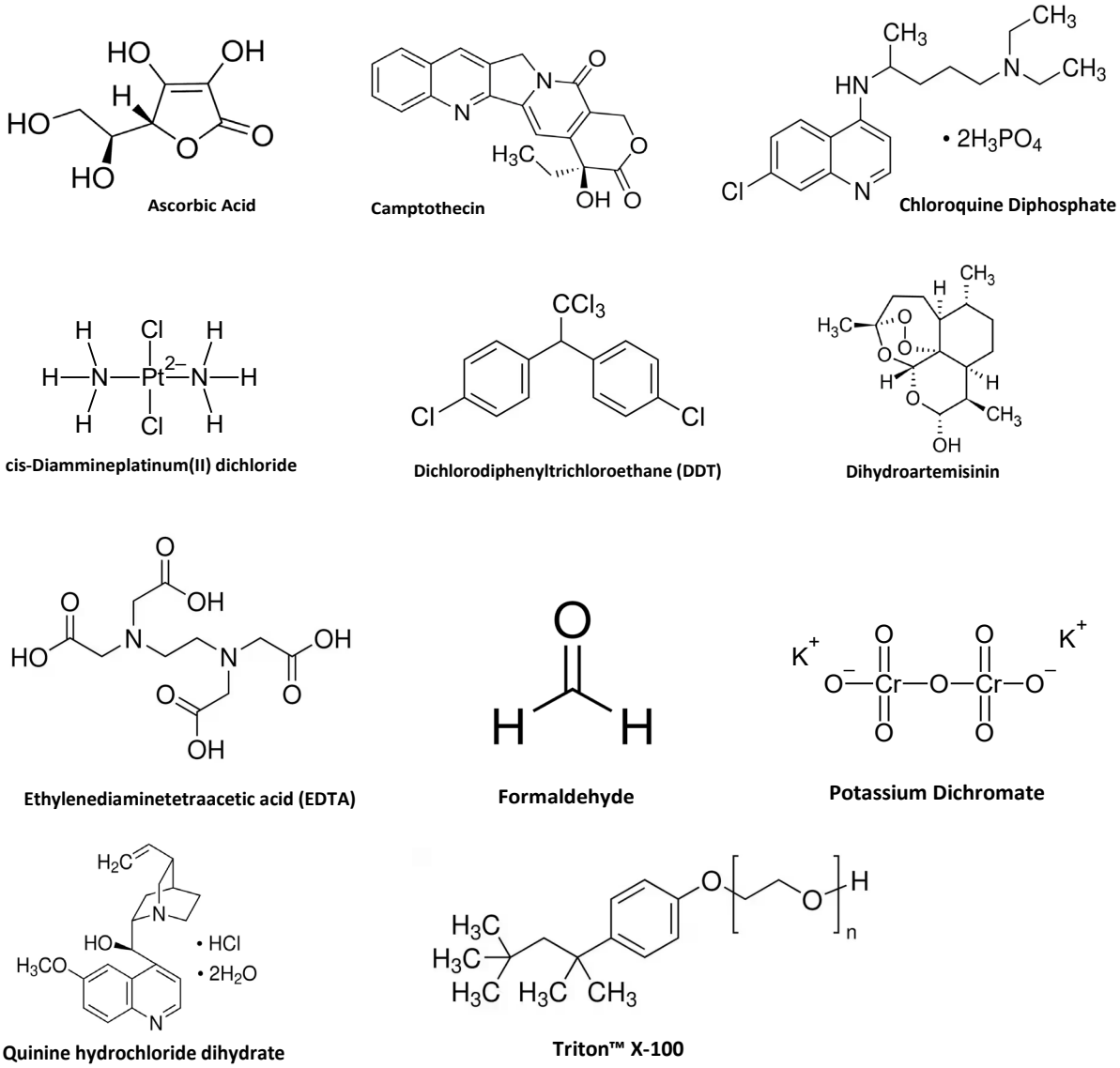


Figure 2.1: Structural formulas of the positive controls listed in Table 2.4 that were used in various assays (National Center for Biotechnology Information, 2024b-l).

2.2 Antimalarial assay

To evaluate the efficacy of the test compounds in comparison to the standard antimalarial drugs, the *Plasmodium* parasite was maintained in complete parasite culture medium (Section 2.2.1 to 2.2.7) to be used in the drug sensitivity assay (Section 2.2.8).

2.2.1 NF54 Malaria parasite culture

The chloroquine-sensitive strain of *P. falciparum* (NF54) was obtained from the Department of Molecular Medicine and Haemotology, University of the Witwatersrand, South Africa and was maintained *in vitro* according to the methods described by Trager and Jansen (1977), Freese *et al.* (1988) and standard departmental protocols (Van Zyl *et al.*, 2010). *Plasmodium falciparum* was used as it is the most pathogenic species of malaria found in to infect humans (Klein, 2013) and the most prevalent in the WHO African region accounting for 96% of estimated malaria cases in 2022 (WHO, 2023a). Biosafety Ethics clearance (Protocol number: 20180101; Appendix A) was obtained from the Biosafety Committee of the University of the Witwatersrand which allowed for the *in vitro* culturing and experimentation of the malaria parasite in a biosafety level 2 laboratory. A human ethics clearance was also obtained from the University of the Witwatersrand Human Research Committee for the use of human red blood cells (RBCs)(HREC M190579) and human plasma (Waiver certificate number: W-CBP-221107-01)(Appendix A). Aseptic culturing techniques, including biosafety level two laminar flow units with 70% ethanol to sterilise containers and work surfaces, were used. All media and solutions were warmed to 37°C before being used to culture the malaria parasites.

2.2.1.1 Parasite culture reagents and solutions

- **Incomplete parasite culture media**

The incomplete parasite culture medium was prepared with 10.4 g Roswell Park Memorial Institution (RPMI)-1640 (Sigma-Aldrich®), 5.9 g N-2-hydroxyethylpiperazine-N‘-2-ethanesulfonic acid (HEPES; 24.76 mM) buffer (Sigma-Aldrich®), 4 g D-glucose monohydrate (Merck; 21.15 mM), 44 mg hypoxanthine (Sigma-Aldrich®; 323.27 µM) and 50 mg/ml gentamicin (Sigma-Aldrich®; 0.1 mM) dissolved in 1 L autoclaved Milli-Q® deionised water. The incomplete culture medium was sterilised through a 0.22 µm Sterivex™-GS filter, before

being stored at 4°C until required. The incomplete parasite culture media to be used for the various experimental assays was prepared as above with the omission of gentamicin and stored at 4°C.

- **Albumax™ II**

A 5% (w/v) solution stock concentration of lipid-rich bovine serum albumin was prepared with Albumax™ II (Gibco™, Thermo Fisher Scientific) in incomplete parasite culture media and stirred vigorously for at least 2 hours at 37°C. The solution was sterilised using a 0.22 µm Sterivex™ filter and stored at -20˚C until required.

- **Complete parasite culture media**

For the preparation of complete parasite culture medium for culturing purposes, the incomplete parasite culture medium was supplemented with 10% (v/v) lipid-rich bovine serum Albumax™ II and 4.2 mL of 5% (w/v) solution (595 mM) sodium bicarbonate per 100 mL. The sodium bicarbonate was prepared in Milli-Q® water and sterilised through a 0.22 µm Sterivex™GS filter and stored at 4°C. The complete parasite culture medium was prepared under aseptic conditions and stored at 4°C when required. The complete parasite culture medium was warmed to 37˚C before being used in parasite culture.

- **Phosphate buffered saline**

A stock concentration of phosphate buffered saline (PBS) was prepared with 136.89 mM sodium chloride (Merck), 4.1 mM di-sodium hydrogen phosphate dihydrate (Sigma-Aldrich®), 4.02 mM potassium chloride (Sigma-Aldrich®), and 1.47 mM potassium dihydrogen phosphate (Fluka) in Milli-Q® deionised water. The pH of the PBS solution was adjusted to 7.4 with sodium hydroxide before being autoclaved and stored at 4°C until required.

2.2.2 Collection and preparation of uninfected red blood cells

Human ethics approval was obtained from the University of the Witwatersrand Human Research Ethics committee (clearance certificate number: M140669) to draw blood from healthy volunteers. Whole blood was collected by a professional phlebotomist in 6 mL blood vial tubes containing acid citrate dextrose solution B (ACD-B) anticoagulant (Lasec, South Africa). Volunteers were screened beforehand to ensure that they matched the inclusion

criteria (healthy donors, age 20-40) and were not taking antimicrobials, anticoagulants, antimalarials or any other medication that could affect the malaria parasite growth or compromise the volunteer (exclusion criteria).

The fresh whole blood was washed by centrifugation at 252 x *g* for 5 min to remove the white blood cells, plasma and platelets. The supernatant was discarded and RBCs washed three times with PBS (pH 7.4). An equal volume of PBS or incomplete experimental medium was added to the RBCs to maintain a 50% haematocrit and the resulting suspension stored at 4˚C for a maximum of 10 days before being discarded in the biohazard waste containers.

2.2.3 Parasite culture maintenance

The malaria parasites were maintained in 75 cm^3 tissue culture flasks (Corning®, Sigma-Aldrich®) in complete parasite culture media (Section 2.2.1.1) supplemented with RBCs (Section 2.2.2) at a 5% haematocrit. Thin blood smears were prepared daily (Section 2.2.4) and based on the microscopic examination of the malaria culture at 1000x magnification under oil immersion, the culture was treated accordingly. To maintain the parasitaemia between 5-10% in the flask, freshly washed RBCs and complete culture media were added when the parasitaemia was >5% trophozoites/schizonts. If the parasitaemia of the flask was <5%, only complete culture media was added to the flask. To ensure the parasites were synchronous, to optimise growth and use in experiments, the culture underwent sorbitol treatment when in the early ring stage (Section 2.2.5). The spent culture media was replaced daily with complete culture medium before being infused with a mixture of 3% oxygen, 4% carbon dioxide and 93% nitrogen gas (Afrox). The culture was incubated at 37˚C in a static position (Jensen and Trager, 1977).

2.2.4 Giemsa staining

Thin blood smears were prepared daily from the malaria culture to monitor % parasitaemia, stage development and the presence of contamination. The thin blood smears were prepared on glass microscope slides that were cleaned with ethanol and air dried in a level two biosafety cabinet. The Rapi-Diff stain kit (Clinical Sciences Diagnostics) was used to stain the

parasites in the RBCs. The slide was immersed once for 5 seconds into solution 1 (thiazine dye in methanol) to fix the RBCs on the slide and then immersed five times for 1 second each into solution 2 (eosin Y dye in phosphate buffer) to stain the RBCs. After being rinsed in tap water and dried, the slide was immersed ten times into solution 3 (methylene blue in phosphate buffer) to stain the parasites before finally being rinsed with tap water and air dried. The slides were microscopically examined at 1000x magnification under oil immersion using an Olympus® CX23 microscope (Olympus®, Japan).

The stage, morphology of the parasite and the percentage parasitaemia (Equation 2.1) were determined after viewing and counting of at least 10 fields across the whole of the thin blood smear. Depending on the percentage parasitaemia and the specific life cycle stage of the parasite culture, the appropriate action was taken for either the maintenance of the parasite or for use of the parasites in the *Plasmodium* lactate dehydrogenase (*pLDH*) drug sensitivity assay (Section 2.2.8) or time dependent parasite morphology and stage determination assessment (Section 2.3.2).

$$\% \text{ Parasitaemia} = \frac{\text{Total number of parasitised RBCs x } 100}{\text{Total number of uninfected RBCs} + \text{parasitised RBCs}}$$

Equation 2.1: Equation used to calculate the percentage parasitaemia.

2.2.5 Parasite culture syncronization

The parasite cultures were synchronised when primarily in the early ring stage with 5% (w/v) D-sorbitol to lyse the trophozoites and schizonts (Lambros *et al.,* 1979). The D-sorbitol kills the more mature stage by osmotic lysis as it permeates into the later stages of *Plasmodium* infected RBCs more easily than the uninfected RBCs and early ring infected RBCs (Lambros *et al.,* 1979). The uninfected RBCs and early ring parasites remain unaffected by the D-sorbitol. The D-sorbitol solution (274.47 mM, Sigma-Aldrich®) was prepared in Milli-Q® deionised water, filtered with a 0.22 µm Sterivex™GS filter and stored at 4°C until needed. The D-sorbitol was warmed to 37°C before use.

Briefly, the parasite culture was transferred to a sterile 50 mL tube and centrifuged at 252 x *g* using a Thermo Scientific Heraeus™ Megafuge™ 40 centrifuge (Thermo Fisher Scientific,

United Kingdom) for 5 minutes before discarding the supernatant and resuspending the resultant pellet with 10 mL of 5% (w/v) D-sorbitol and incubated for 10 minutes at 37˚C. The suspension was then centrifuged at 252 x *g* for 5 minutes and the supernatant discarded. The remaining pellet was washed twice with PBS (pH 7.4) before the addition of complete culture media for re-incubation or used for experiments. If the pellet was not all used in the assays, it was returned to the flask with complete culture media and was gas infused (Section 2.2.3) before being re-incubated.

2.2.6 Parasite culture cryopreservation

To maintain a frozen stock of NF54 parasites to ensure continuity of research, cultures consisting of mainly early ring-infected RBCs (parasitaemia ~5%) were cryopreserved in a freezing solution according to the methodology of Freese *et al.* (1988). The freezing solution was prepared by diluting glycerol (Merck) in PBS (pH 7.4) to obtain a 28% (v/v) solution and was filtered with a 0.22 µm Sterivex™GS filter and stored at 4°C until necessary. The freezing solution was warmed to 37°C before use in the cryopreservation of parasite cultures.

Briefly, a predominantly early ring staged parasite culture was transferred to a sterile 50 mL tube and centrifuged at 252 x *g* for 5 minutes at room temperature and the supernatant discarded. The resultant pellet was then resuspended with an equal volume of freezing solution by gently adding the freezing solution dropwise into the tube while gently swirling. The suspension containing infected RBCs was then aliquoted into sterile cryovials (Corning®, Sigma-Aldrich®) and immediately stored in liquid nitrogen until required.

2.2.7 Parasite culture initiation from frozen cryovials

Thawing of frozen parasite culture stocks required the preparation of two thawing solutions that were prepared with Milli-Q® water, filtered with a 0.22 µm Sterivex™GS filter and stored at 4°C until needed. The thawing solutions were warmed to 37°C before being used to reinitiate the cryopreserved parasites.

The frozen cryovial was submerged into a 37°C water bath for 2-3 minutes rapidly thawing the parasite suspension within. The outside of the cryovial was sprayed with ethanol to ensure sterility before the two thawing solutions were added in sequence. Firstly, 0.1 volume of 0.2

M NaCl (Merck) was added dropwise to the thawed parasite suspension. The latter suspension was then transferred to a sterile 50 mL tube containing 9 volumes of 0.027 M NaCl and centrifuged at 252 x *g* for 5 minutes. The supernatant was discarded and 5 ml incomplete parasite culture medium was added to the pellet. The suspension was then centrifuged at 252 x *g* for 5 minutes and the supernatant discarded. The resultant pellet was resuspended in complete parasite culture medium (Section 2.2.1.1) with RBCs to achieve a 5% haematocrit solution. This was then transferred to a sterile 25 cm^2 tissue culture flask (Corning®, Sigma-Aldrich®) and infused with a mixture of 3% oxygen, 4% carbon dioxide and 93% nitrogen gas and maintained as described in Section 2.2.3.

2.2.8 *Plasmodium* lactate dehydrogenase drug sensitivity assay

The *pLDH* assay is based on the detection of the lactate dehydrogenase (LDH) enzyme that is found in the *P. falciparum* parasite. The *p*LDH assay detects the *Plasmodium* parasitaemia as a measure of the amount of *p*LDH present (Makler *et al.*, 1993). Parasite survival percentages were determined by measuring the conversion of nitro blue tetrazolium (NBT) to a blue or purple formazan end-product (Figure 2.2). To disrupt the RBC membranes and expose the *p*LDH to the NBT/phenazine ethosulfate (PES) solution for the reaction to occur, the haemolytic properties of Triton™ X100 in the Malstat™ reagent (Section 2.2.8.1) was used.

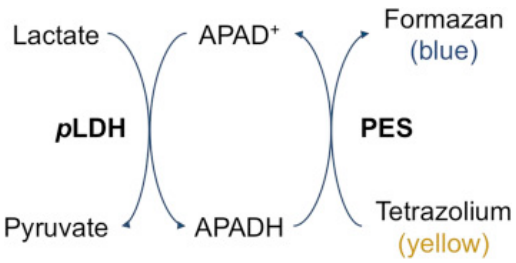


Figure 2.2: The Malstat™ assay for the detection of the *Plasmodium* lactate dehydrogenase enzyme (Markwalter *et al.*, 2016). Lactate dehydrogenase is an essential metabolic enzyme that catalyses the dehydrogenation of lactate and produces pyruvate with nicotinamide adenine dinucleotide (NAD) as a co-enzyme. The assay distinguishes parasites LDH from the host LDH by using acetylpyridine adenine dinucleotide (APAD) as an analogue of NAD. The *p*LDH in lysed infected blood oxidises lactate to pyruvate, while converting $APAD^+$ to APADH which in turn reduces yellow nitro blue tetrazolium (NBT) to blue formazan salts in the presence of phenazine ethosulfate (PES) (Makler *et al.*, 1993).

2.2.8.1 Solutions and reagents

- Malstat™ was prepared by dissolving 40 µL Triton™ X-100 (Sigma-Aldrich®), 91.65 mM calcium L-lactate (Sigma-Aldrich®), and 0.38 mM APAD (Sigma-Aldrich®) into 10 mL of 54.48 mM Tris base solution (Sigma-Aldrich®). The 54.48 mM Tris base solution (Sigma-Aldrich®) was prepared in autoclaved MilliQ® deionised water and the pH was adjusted to 9.1 with NaOH before being filtered through a Sterivex™ GS 0.22 µm filter. The solution was stored at 4°C until required.
- On the day of the experiment, the NBT/PES solution consisting of 0.299 mM PES (Sigma-Aldrich®) and 2.45 mM NBT (Sigma-Aldrich®) was freshly prepared in autoclaved MilliQ® deionised water and filtered through a Sterivex™ GS 0.22 µm filter. This was stored in 15 mL tubes wrapped in foil and stored at 4°C in a dark container to prevent exposure to light, until required.

2.2.8.2 *pLDH* assay protocol

When evaluating the test and control compounds, the malaria parasite culture (Section 2.2.3) was pelleted by centrifugation at 252 x *g* for 5 minutes, sorbitol synchronised (Section 2.2.5) and washed twice with PBS before the resultant pellet was used to make a thin blood smear to determine the percentage parasitaemia of the pellet (Section 2.2.4). The parasitaemia of the pellet was adjusted to 2% with the addition of washed uninfected RBCs (Section 2.2.2) and adjusted to a final 2% haematocrit with complete parasite culture media (Section 2.2.1.1).

A sterile 96 well microtitre plate was used for the *p*LDH assay with only the inner 60 wells used to prevent false positive results due to increased risk of dehydration in the outer wells (Figure 2.3). Autoclaved distilled water or PBS was added to the outer wells to try and overcome this effect and to optimise conditions for the experiment. The *p*LDH plate was prepared by adding 100 µL parasitised RBCs in complete parasite culture media into each of the 58 wells. To the remaining two wells, 100 µL of 2% haematocrit suspension of untreated uninfected RBCs in complete parasite culture media was plated to serve as the blank (B10-B11) to account for background LDH activity in the RBCs. The prepared untreated plate was placed into a sterile candle jar containing autoclaved MilliQ® deionised water to ensure that a humidified atmosphere was maintained while being incubated at 37°C for 24 hours. The

burning of a candle within the candle jar ensured that the approximate micro-anaerobic conditions of 3% oxygen, 4% carbon dioxide and 93% nitrogen gas were obtained (Trager and Jensen, 1977).

After the initial 24 hour incubation period, 12.5 µl test compound or positive control, quinine was prepared in incomplete parasite culture medium, with a 9 fold dilution factor taken into account, were plated into the drug wells (Figure 2.3). Additionally, 12.5 µl incomplete culture medium was added to the untreated uninfected RBC wells and the infected RBC wells to adjust the volume to 112.5 µL. The plates were returned to the candle jar and re-incubated for 24 hours at 37˚C at which time the candles in the candle jar were re-lit, while taking care to maintain sterility.

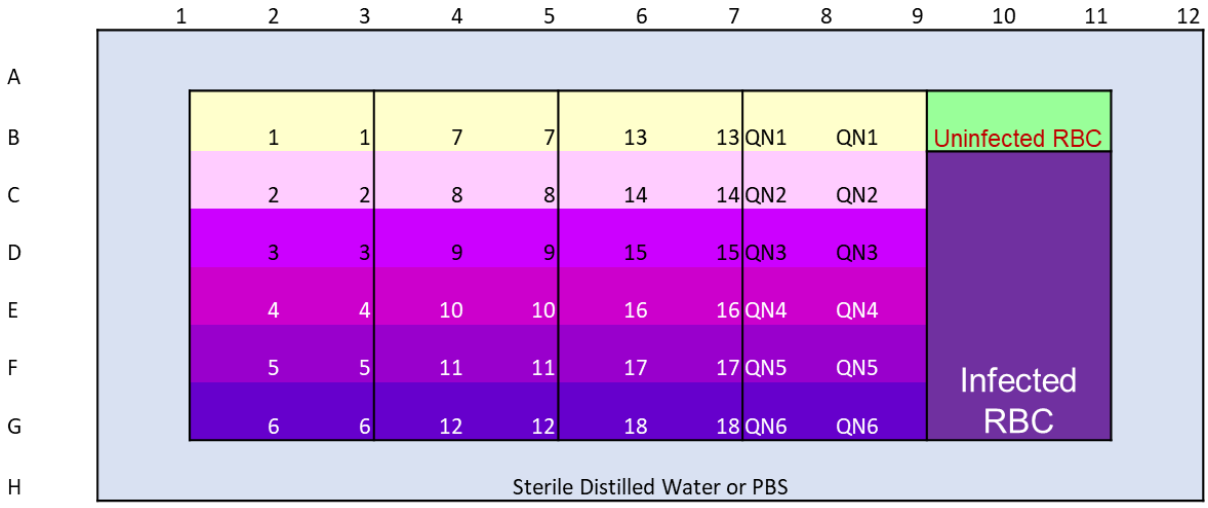


Figure 2.3: Layout for the *p*LDH drug sensitivity assay. The outer wells filled with sterile distilled water or PBS (blue) provided a humidified environment for the optimal environment for parasite growth to assess the inhibitory activity of the test (1-18) compounds and standard antimalarial control drug, quinine (QN), with the uninfected RBC (light green) and untreated infected RBC (dark purple) controls taken into account.

After 48 hours, the 96 well plate was removed from the candle jar, covered with a plate seal (Bio-Rad®), wrapped in parafilm (Sigma-Aldrich®) and frozen at -70°C for 1 hour. The plate was then thawed for 30 minutes at 37°C and shaken at 161 x *g* for 5 minutes with an orbital shaker (MRC Thermo-Shaker™ MB100-4P). A total of 25 µl lysate from each well was

correspondingly transferred to another sterile plate and 100 µl Malstat™ added to each well. The NBT/PES (1:1) solution was prepared (Section 2.2.8.1) and 20 µl added to each well before sealing the plate and shaking it at 161 x *g* with an orbital shaker for 1 minute. Thereafter the 96 well plate was incubated at 37˚C for 40 minutes to allow the reaction to proceed. Fifty microliters of 5% (v/v) (0.833 mM) acetic acid was added to each well to stop the reaction and air bubbles were removed to prevent inaccurate absorbance readings. The 96 well plate was read at an absorbance wavelength of 620 nm using a Lab Systems Multiskan iEMS plate reader and Ascent™ software version 2.6. The percentage parasite growth was calculated using Equation 2.2 in Microsoft Excel® taking the relevant controls into account. For those compounds displaying more than 60% parasite growth inhibition, a set of serial dilutions (0.001 - 200 µM) were prepared to determine the IC_{50} values. The IC_{50} values were calculated from log sigmoid dose response curves generated by GraphPad Prism® 5.02 (GraphPad Software, Inc., USA). IC_{50} values that were less than 1 µM were considered highly active, >1-10 µM had promising activity; >10-50 µM as moderate activity; >50-100 as low activity and >100 µM not active (Clarkson *et al.,* 2004).

$$\% \text{ Parasite Growth} = \frac{[(\text{Average absorbance of compounds} - \text{Average absorbance of RBC control})] \times 100}{[(\text{Average absorbance of parasite control} - \text{Average absorbance of RBC blank})]}$$

Equation 2.2: The equation used to calculate the percentage parasite growth taking both the test and reference wavelengths into account (Van Zyl *et al.,* 2010).

2.3. Antimalarial combination studies

2.3.1 Antimalarial combination

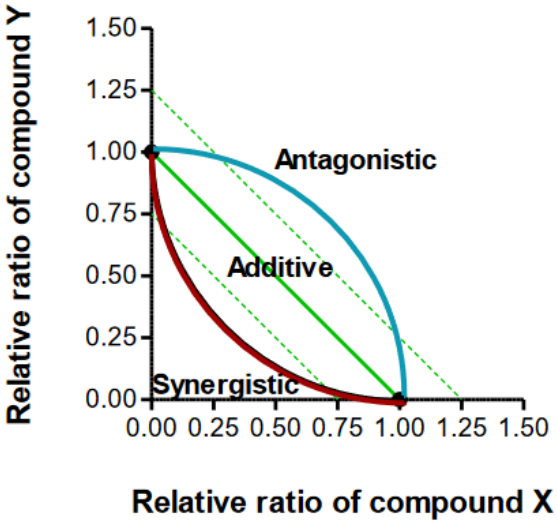
Due to the increase in antimalarial drug resistance in most parts of the world, new antimalarial drug treatment regimens are to include the use of two or more drugs (WHO, 2023b). The use of combinational drug strategies has often been used to enhance the therapeutic effect or delay drug resistance (Yin *et al.,* 2018). The *p*LDH assay (Section 2.2.8) was used with a slight modification where an additional two-fold dilution factor was taken into account when the two compounds were combined (Van Zyl *et al.,* 2010). Two of the most

active test compounds were selected to be combined with the standard antimalarial drug, quinine. Based on the individual IC_{50} values of the test compounds and quinine, the test compound and quinine were combined in different ratios (Table 2.5). Once these initial 1:1 combinations were prepared, serial dilutions were prepared from each combinations ratio and plated out into a sterile 96 well plates and the drug sensitivity assay conducted and analysed as described in Section 2.2.8.2.

Table 2.5: Combined concentration ratios of compounds **X** and **Y**. Where **X** and **Y** were mixed in 1:1 volume ratio.

Concentration (µM)	**A**	**B**	**C**	**D**	**E**	**F**	**G**	**H**
X	50	40	20	15	5	0.5	0.05	0
Y	0	0.075	0.75	7.5	50	100	150	200

To determine the interaction between the two compounds, an isobologram (Figure 2.4) was plotted from X- and Y-axis points generated using Equation 2.3 and the sum of the fractional inhibitory concentration (ΣFIC) was used to quantitate the type of interaction observed on the isobologram. The active test compounds in combination with quinine would either have yielded one of three possible interactions (Figure 2.4). Namely an additive interaction which is defined as the sum of the effects of each compound produced seperately. A synergistic interaction which would result in an effect greater than the sum of the separate compound effects and lastly an antagonistic interaction where the resulting effect would be less than the sum of the separate compound effects (Berenbaum, 1978).



.

Figure 2.4: Isobologram depicting three possible pharmacological interactions between compound **X** and compound **Y**. Where antagonistic (>1.25), additive (0.75-1.25) and synergistic (<0.75) interactions affected the overall therapeutic effect (Berenbaum, 1978; van Zyl *et al.*, 2010).

The ΣFIC reflected the combined interactions of compound **X** and compound **Y** according to Equation 2.3 and this determined the strength of the interaction. The calculation and interpretation of the ΣFIC value in this study was based on the following: ΣFIC values <0.75 was synergistic, 0.75-1.25 was additive and >1.25 was antagonistic (Van Zyl *et al.,* 2010).

$$\Sigma\text{FIC} = \frac{\text{IC50 of } \mathbf{X} \text{ in Combination}}{\text{IC50 of } \mathbf{X} \text{ alone}} : \frac{\text{IC50 of } \mathbf{Y} \text{ in Combination}}{\text{IC50 of } \mathbf{Y} \text{ alone}}$$

Equation 2.3: Relative concentration ratios of **X**:**Y** or ΣFIC value. Ratios were calculated using the IC_{50} values of combined ratios of **X** and **Y** over the individual IC_{50} values of **X** and **Y**, respectively (van Zyl *et al.*, 2010).

2.3.2 Parasite morphology and stage determination

In order to determine the specific effects of the two most active test compounds on the asexual parasitic stages, a 48 hour observational study was conducted (Moseley, 2012). Based on the IC_{50} values of the two most active compounds as determined in the *p*LDH drug sensitivity assay (Section 2.2.4.2), working solutions of these active compounds were

prepared in complete experimental culture media taking a dilution factor of 10 into account to ensure the IC_{50} value was maintained in the total volume of the parasite suspension in the 25 cm^3 tissue culture flasks (Sigma Aldrich®). The parasite suspension was prepared by synchronising the early ring staged culture (Section 2.2.5) and adjusted to a 2% parasitaemia and 2% haematocrit in complete culture media. The synchronised parasites (5400 μL) and 600 μL of each test compound or quinine was added to its respective flask. An appropriate control was prepared, namely an untreated parasite control with a 2% parasitaemia and a 2% haematocrit in complete parasite culture media. The parasite cultures were all gassed with a mixture of 3% oxygen, 4% carbon dioxide and 93% nitrogen for 30 seconds, sealed and placed in an incubator at 37°C in a static position. Every 8 hours, a thin blood smear was prepared for microscopic assessment (Section 2.2.4) and the flask re-gassed and returned to its 37°C environment. The blood smears were analysed microscopically at 1000x magnification using an Olympus® CX23 microscope and CellSens version 1.5 software (Olympus®, Japan) to determine total percentage parasitaemia and percentage of each parasite stage at each time interval. Any morphological changes to the parasites and infected RBCs were noted for each time interval over the 48 hours period.

2.4 Vector studies

To determine if the test compounds possessed any larvicidal activity in comparison to standard insecticides such as DDT, mosquito larvae and eggs were incubated in the presence of these compounds. An animal ethics waiver was obtained for the use of *Anopheles* mosquitoes from the University of the Witwatersrand Animal Research Ethics Committee (Waiver number: 07-11-2017-O, Appendix A).

2.4.1 *Anopheles* mosquitoes

The *Anopheles arabiensis* (KWAG) mosquito larvae and eggs for vector susceptibility assays were sourced from the Botha de Meillon Insectary at the National Institute for Communicable Diseases (NICD), Sandringham, Johannesburg, South Africa. This species was first colonized in

2005 in Kwa-Zulu Natal, South Africa, and possesses a pyrethroid resistance profile (Mouatcho *et al*, 2009).

Third instar mosquito larvae were collected in containers with fresh distilled water at room temperature and used for the vector studies on the day of collection. The temperature in the laboratory test environment was maintained at 25-28°C with a simulated day/night cycle, including a dawn to dusk transition phase, that was established by switching the laboratory lights off after 12 hours and then switching them on again after another 12 hours have elapsed. A 50 minute long dawn and dusk transition phase was implemented by dimming or brightening the lights to simulate sunrise and sunset lighting conditions in the simulated day/night cycle (Hunt *et al*., 2005; Venter, 2023). The average humidity in the laboratory test environment was maintained at 80% by using a humidifier and a hygrometer. Standard larval food for feeding the mosquito larvae was obtained from Prof Koekemoer (WITS Research Institute for Malaria; WRIM) and was prepared by combining 300 g dog biscuits (West's Beeno™, BM & Co) and 100 g Brewer's yeast (MP Biomedicals LLC). The combination was crushed into a fine powder consistency before being allocated into plastic tubes and sealed for storage until necessary (Hunt *et al*., 2005; Venter, 2023).

Mosquito eggs were harvested in accordance with the MR4 Methods in *Anopheles* Research guidelines (MR4, 2014) by placing a filter paper lined cup with clean water inside the mosquito colony cage for oviposition. The freshly laid (<6 hours old) eggs would accumulate on the filter paper and were washed off into a plastic bowl with distilled water at room temperature. The harvested eggs were immediately used for the ovicidal assay on the day of collection.

2.4.2 Larvicidal assay

In accordance with the WHO protocol for insecticide testing (WHO, 2005), all test compounds were screened against *Anopheles arabiensis* (KWAG) mosquito larvae to determine their potential insecticidal activity.

2.4.2.1 Larvicidal lethality assay

The test compounds and the positive control, DDT (50 µM) were prepared taking a dilution factor of 100 into account (WHO, 2005). Clear plastic test cups (173.2 cm^3) were appropriately

labelled and a total of 25 mL distilled water was aliquoted into each test cup. From each of these test cups except for the blank control, a total of 250 µL distilled water was removed and discarded. Batches of twenty 3rd instar larvae were gently introduced to the cups. To each test cup, 250 µL test compound or control was added. DMSO served as the negative solvent control, while autoclaved MilliQ® deionised water served as the blank negative control.

Standard larval food (Section 2.4.1) was added to all cups with enough powdered food to be evenly distributed to lightly cover the water surface in the cups. The cups were then incubated for 24 hours at 25-28 °C (T_{24}), after which larval mortality was recorded. The larvae were gently prodded with a plastic stirring stick and if non-responsive and moribund (lacking energy or vitality), the larvae were recorded as dead. The plastic test cups were covered with a net and secured in place and incubated for a further 24 hours, thereafter the counting process repeated (T_{48}). The latter process was repeated at 72 hours taking care not to release any mosquitoes that may have emerged at this time interval (T_{72}). Pupae were recorded to calculate percentage pupation at each time interval (T_{24}, T_{48} and T_{72}). Percentage survival was calculated according to Equation 2.4 and percentage mortality was calculated according to Equation 2.5. The larvicidal lethality assay was repeated five times such that a minimum of 100 larvae were evaluated per concentration to ensure compliance with the WHO larvicidal assay protocol (WHO, 2005).

Those compounds showing significant mortality of larvae (≥60%) at the screening concentrations were further serially diluted and the percentage mortality were analysed using Probit analysis as described by Finney (1971) with IBM SPSS® statistics version 29 software. From each Probit analysis, the lethal concentration of 50% of the larvae (LC_{50} value) for the positive controls and active test compounds were determined. For the purposes of generating a graph, GraphPad® Prism version 5.02 was used and verified to produce the same LC_{50} value as the Probit analysis (IBM SPSS® Statistics version 29).

$$\% \text{ Survival} = \frac{[(\text{Number of larvae alive} + \text{number of pupae})]\text{x } 100}{\text{Total number of larvae in the cup at time zero (including moribund)}}$$

Equation 2.4 The equation used to calculate the percentage survival of the larvae after incubation with test compound after a 24-hour period (WHO, 2005).

$$\% \text{ Mortality} = \frac{[(\%\text{Survival in untreated control T24 }) - (\%\text{ survival in treated cup T24})]\text{x } 100}{\%\text{ survival in untreated control T24}}$$

Equation 2.5 The equation used to calculate the percentage mortality of the larvae after incubation with test compound after a 24-hour period (WHO, 2005).

2.4.2.2 Morphological effects

Larvae were microscopically assessed for morphological changes by examining them under a BestScope compound microscope (Lasec, South Africa) with TCapture version 3.9.0.602 software at 10x magnification and photographs taken at each time interval (T_{24},T_{48} and T_{72}). Test compound treated larvae were assessed in comparison to an untreated control larvae and changes noted.

2.4.3 Ovicidal assay

A successful integrated mosquito control strategy includes several tactics to eliminate mosquitoes from their habitat, including killing mosquito eggs, i.e. larval source management (WHO, 2019). As such, all test compounds were screened against *An. arabiensis* (KWAG) eggs to determine their potential ovicidal activity and potential use as an ovicide in larval source management. The ovicidal assay was conducted using a modified method adapted from the WHO guidelines for insecticide testing (WHO, 2005).

2.4.3.1 Ovicidal lethality assay

Test compounds (0.5 µM) and positive controls, 3.45 mM formalin (1% w/v) and 0.5 µM DDT were prepared with a dilution factor of 100 taken into account. Freshly laid *An. arabiensis* (KWAG) mosquito eggs were carefully transferred to a small 350ml container filled with fresh distilled water. Ten microliters of the test compound were added to duplicate wells, with DMSO or autoclaved MilliQ® deionised water added to the negative control wells and formalin added to the positive control wells to ensure 100% ovicidal activity. A total of 20 to

40 eggs were carefully added along with 990 µL autoclaved distilled water to each well in the 24 well plate. The plate was incubated at room temperature (25-28°C) for 24 hours, after which the number of hatched eggs were counted.

After a 24 hour incubation period (T_{24}), the plate was microscopically examined under 10x total magnification using a BestScope compound microscope (Lasec, South Africa) with TCapture version 3.9.0.602 software and the number of hatched larvae in each well counted and recorded. The plate was then incubated for a further 24 hours and the counting process repeated at 48 and 72 hours (T_{48}, T_{72})). The percentage ovicidal activity (% mortality) at each time interval (T_{24}, T_{48} and T_{72}) was calculated according to Equation 2.6.

$$\% \text{ Mortality} = \frac{[\text{Unhatched eggs at T24}]\text{x } 100}{\text{Total eggs at T0}}$$

Equation 2.6 The equation used to calculate the percentage mortality of the eggs after incubation with test compound after a 24-hour period (WHO, 2005).

The ovicidal lethality assay was repeated five times such that a minimum of 100 eggs were evaluated per concentration to ensure consistency with the larvicidal assay. Compounds showing significant mortality of eggs (>60%) were further evaluated using serial dilutions and the % mortality at each concentration was analysed by Probit analysis using IBM SPSS® statistics version 29 software (Finney, 1971). The log sigmoid dose response curve generated by GraphPad® Prism version 5.02 was used to verify the LC_{50} value from the Probit analysis (IBM SPSS® Statistics version 29).

2.5 Toxicological assays

A range of assays to assess compound toxicity were performed as described in the following sections (2.5.1-2.10).

2.5.1 Haemolysis assay

The haemolysis assay was performed to ensure that test compounds did not disrupt the RBCs membrane before directly affecting the malaria parasite, thereby resulting in a false positive

result that would have incorrectly indicated antimalarial activity as determined by the *p*LDH assay (Section 2.2.8). The assay determined the extent of RBC lysis by detecting the release of haemoglobin into the culture media (Hayat *et al*., 2011). The haemolytic assay was carried out using aseptic techniques on freshly obtained RBCs from healthy volunteers that were pre-screened prior to their blood being collected for use in the assay (Section 2.2.2).

The test compounds and antimalarial drug control, quinine were screened at 50 µM (with a 10x dilution factor taken into account). The latter (20 µl) were asepticaly added to triplicate wells along with 180 µl of a 2% haematocrit suspension of freshly washed RBCs (Section 2.2.2). Appropriate controls were prepared where the positive control (100% haemolysis) consisted of Triton™-X 100 (0.003 M, 0.2% v/v) (Sigma Aldrich®) and RBC suspension; whilst the negative control consisted of complete experimental media and RBC suspension.

The plates were incubated in a humidified candle jar at 37˚C for 48 hours. Thereafter, the plates were shaken using an orbital shaker (MRC Thermo-Shaker™ MB100-4P) at 161 x *g* for 2 minutes and centrifgued at 252 x *g* for 5 minutes. The resulting supernatant (50 µl) along with 150 µl autoclaved Milli-Q® water were transferred to a second corresponding non-sterile 96 well-plate. The absorbances obtained at the wavelength of 414 nm using the Lab Systems Multiskan iEMS plate reader and Ascent™ software version 2.6 were analysed using Microsoft Excel® and Equation 2.7 used to determine the percentage haemolysis induced by the test/control compounds.

$$\%\ \text{Haemolysis} = \frac{[(\text{Absorbance of compounds} - \text{Average absorbance of 0\% lysis RBC control})]\text{x } 100}{[(\text{Average absorbance of 100\% lysis} - \text{0\% lysis})]}$$

Equation 2.7 The equation used to calculate the percentage haemolysis (Mosely, 2012).

2.6 Cytotoxicity studies

2.6.1 Cytotoxicity assay

In order to determine if the test compounds possessed selective antimalarial properties or caused general cell damage or cell death to mammalian cells, the tetrazolium cytotoxicity assay was undertaken. The 3-(4,5-dimethylthiazol-2-yl)-2,5-diphenyltetrazolium bromide

(MTT) assay is a quantitative colorimetric assay that involves the cleavage of the yellow MTT by succinate dehydrogenase found in the mitochondria of living cells (Figure 2.5). After the tetrazolium ring is cleaved, this produced water-insoluble purple formazan crystal (Mosmann, 1983).

2.6.2 Cytotoxicity assay cells

The MTT method as described by Mosmann (1983) and Van Zyl *et al.* (2010) was performed on the human embryonic kidney epithelial cell (HEK293; Graham) and chronic myelogenous leukaemia cell (K562) lines.

2.6.2.1 Cell culture reagents and solutions

2.6.2.1.1 Incomplete and complete cell line culture medium

The incomplete culture medium was prepared by combining an equal volume of Dulbecco's Modified Eagle's Medium (DMEM) and Ham's Nutrient Mixture F12 (Ham F12) sterile liquid culture medium (Sigma-Aldrich®). Each cell line was maintained separately in incomplete culture medium that was supplemented with 10% (v/v) heat inactivated foetal bovine serum (FBS) (Gibco™, Thermo Fisher Scientific; Section 2.6.2.1.2). This complete cell culture medium was sterile filtered through a 0.22 µm Sterivex™-GS filter before use and all solutions were stored at 4°C until required.

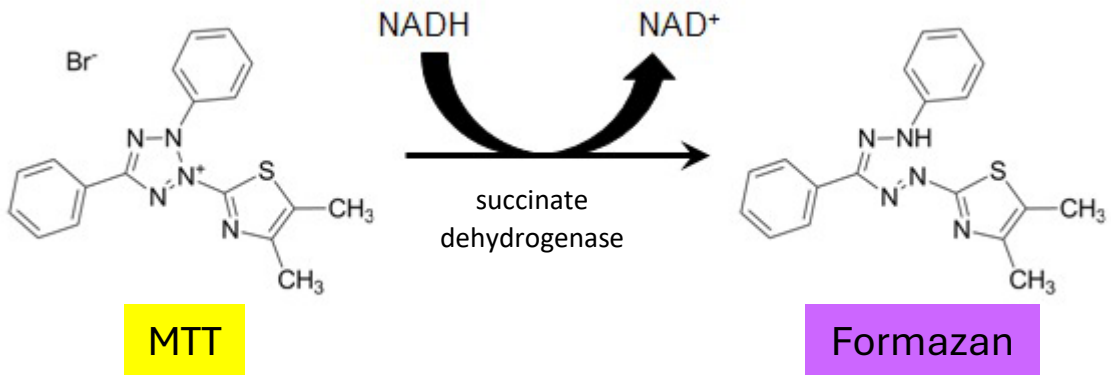


Figure 2.5: Conversion of MTT (yellow colour) to the formazan (purple colour) product by succinate dehydrogenase which indicates cellular viability. This cellular reduction involves the pyridine nucleotide co-factors, Nicotinamide adenine dinucleotide (reduced form) (NADH) and Nicotinamide adenine dinucleotide (oxidised form) (NAD+) (Mosmann, 1983; Riss *et al.,* 2016).

2.6.2.1.2 Foetal bovine serum

The FBS was thawed at 4°C and heat inactivated in a water bath at 56°C for 45 minutes before being aliquoted into 50 mL sterile plastic tubes and stored at -20°C until required. The FBS was thawed at 37°C, centrifuged at 252 x *g* and sterile filtered through a 0.22 µm Sterivex™-GS filter before use.

2.6.2.1.3 MTT

A stock solution of MTT (5 mg/ml, 12 mM) was prepared by dissolving MTT powder in PBS (pH 7.4) and sterile filtered through a 0.22 µm Sterivex™-GS filter before being stored in a light protected container at 4°C until required.

2.6.2.1.4 Cell line cryopreservation solution

The cryopreservation solution consisted of 20% FBS, 10% DMSO and 70% complete cell culture media was sterile filtered through a 0.22 µm Sterivex™-GS filter before being stored at 4°C until required**.** Cell culture grade DMSO (Merck) was used for cryopreservation.

2.6.2.2 Maintenance of cell culture

Human kidney epithelial cells (HEK293) and chronic myelogenous leukaemia cells (K562) were cultured *in vitro*. Cells were monitored daily with an Olympus® CKX41 inverted phase contrast microscope (Olympus®, Japan) at 40X magnification to evaluate growth and to check for microbial contamination.

The K562 and HEK293 cells were grown and maintained aseptically in a 20 mL DMEM-Ham F12 complete culture medium (Section 2.6.2.1.1). The cell culture medium was replaced as necessary based on the confluency or cell density of the cell growth. Cells were cultured in 75 cm^3 cell culture flasks in a 37°C humidified environment with 5% CO_2 (Thermo Fisher Scientific, Forma™ series II Water-Jacketed CO_2 Incubator, UK). The cell culture flask lids were fractionally opened to allow for gaseous exchange to occur with the humidified atmosphere

in the incubator. The cells were used to initiate a new subculture (Section 2.6.2.2.1 and 2.6.2.2.2), cryopreservation (Section 2.2.5) or for cytotoxicity assays (Section 2.6.3).

2.6.2.2.1 HEK293 cell line

The adherent HEK293 cells were trypsinised when cell growth reached levels above 80% cell growth/confluency in the culture flask as microscopically determined at 40x magnification. Trypsin is an enzyme used to dissociate adherent cells from the surface of the cell culture flask and to break up clusters of cells to form single cell suspensions (Thermo Fisher, 2020). The process of trypsinisation involved discarding the spent cell culture medium, rinsing the adherent cells twice with 10 mL PBS (pH 7.4), and adding 5 mL of 0.2% (v/v) trypsin versene-EDTA (Sigma-Aldrich®) to the flask for 3 minutes. Thereafter to inactivate the trypsin, an equal volume of complete cell culture media was added. The cell suspension was transferred to a 50 mL sterile tube, and the cells pelleted by centrifugation at 252 x *g* for 5 minutes. The cell pellet was resuspended in 20 mL complete cell culture media (Section 2.6.2.1.1) to seed another flask or the cells were cryopreserved (Section 2.6.2.1) or used in a cytotoxicity assay (Section 2.6.3).

2.6.2.2.2 K562 cell line

Before the cell density of the K562 suspension cells reached its maximum limit in the cell culture flask, the cells were-sub-cultured to ensure optimal growth of the cells and to prevent them from dying due to nutrient depletion. Subculturing of the K562 cells involved gently agitating the cell culture flask to dislodge a

ny cells that may have settled onto the flask's surface. The resultant cell suspension was transferred into a 50 mL sterile tube, which was centrifuged at 252 x *g* for 5 minutes to pellet the cells and the resulting supernatant discarded. The cell pellet was resuspended in 20 mL of complete cell culture media (Section 2.6.2.1.1) and the suspension placed back into the cell culture flask and incubated, cryopreserved (Section 2.6.2.3) or used in a cytotoxicity assay (Section 2.6.3).

2.6.2.3 Cryopreservation of cell lines

Excess cell suspension of either the HEK293 or K562 cell lines were cryopreserved for either short-term storage at -80°C or long-term storage in liquid nitrogen. The cell suspension was transferred to a 50 ml tube and centrifuged for 5 minutes at 252 x *g* to produce a cell pellet which was resuspended in 10 mL cryopreservation solution (Section 2.6.2.1.4). After resuspension to a single cell suspension, 1.8 mL of the cell suspension was aliquoted into 2 mL cryotubes (Greiner Bio-One®) and placed into a cryobox that was frozen at -80°C freezer for 72 hours. The cryobox allowed for controlled freezing at a rate of 1°C/min that allowed the cells to retain structural integrity and allow for optimal cell viability when thawed (Thermo Fisher, 2020). After 72 hours, the cryotubes were transferred to a liquid nitrogen storage vessel for long term storage at -196°C.

2.6.3 MTT cellular viability protocol

For the cytotoxicity assays, the cells suspension was prepared as described in Sections 2.6.2.2.1 and 2.6.2.2.2. The cell suspensions were pelleted by centrifugation at 252 x *g* and resuspended in 10 mL complete culture media. The cell density was determined by staining the cell suspension in a 1:1 ratio with a trypan blue solution (Section 2.6.2.1.5) and the cell density of 40 µL of this suspension was quantitated microscopically using a haemocytometer at 100x magnification. The number of viable clear or transparent cells were counted whilst the dead or unhealthy cells were stained blue as the trypan blue stain was able to cross into the cell through the compromised cell membrane (Strober, 1997). A minimum of 95% cell viability was required for the cells to be used in this assay. The cell density of the cell suspension was determined using Equation 2.8.

$$\%\ Density = \frac{Cells}{mL} = \left(\frac{\text{Number of viable cells}}{4} \right) \text{x } 2\ (\text{Dilution Factor})$$

Equation 2.8: Determination of cells in cell suspension when counted using a haemocytometer at 100x magnification (Strober, 1997).

The cell density of the cell suspension was adjusted to 10,000 cells per 180 µL of complete experimental culture medium (Section 2.6.2.1.1) and 180 µL added to each well except for the three cell-free control wells, which contained 200 µL of complete culture media (Figure 2.6). A screening concentration of 50 µM was prepared with a 10x dilution factor taken into account for each test compound (Section 2.1.2) and 20 µL was plated out in triplicate wells in a sterile 96 well plate. Whilst 20 µL complete experimental culture media was added to the nine drug-free control wells containing the cell suspension contained. The positive controls, camptothecin and cisplatin (Sigma-Aldrich®) were also screened at 50 µM.

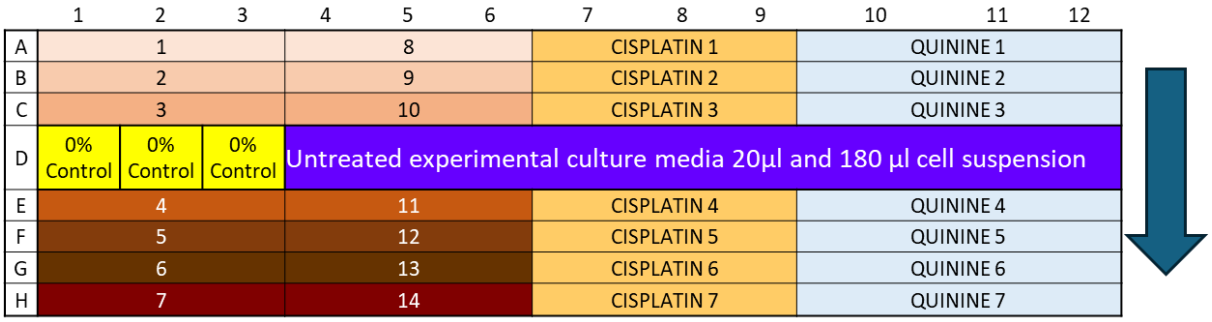


Figure 2.6: Plate layout of the MTT cell viability assay. Compounds were plated in triplicate wells with 180 µL cell suspension to assess their inhibitory activity on cell growth. Untreated experimental cell culture media and cell suspension were added to wells D4-D12 (purple) to serve as the 100% cell growth control. Wells D1-D3 (yellow) contained 200 µL of complete experimental cell culture media to serve as the 0% cell growth control. Positive controls, quinine (light blue) and cisplatin (orange) were plated in decreasing concentrations in row A-C and E-H.

The prepared 96 well plate was incubated for 48 hours under humidified conditions (90-95%) at 37°C with 5% CO_2 in a partially sealed container; after which a volume of 40 µL MTT (Section 2.6.2.1.3) was added to each well and the plate incubated for a further 4 hours. The 4.2 mM trypan blue stock solution (0.4% w/v) (Sigma-Aldrich®) was prepared in PBS (pH 7.4) and sterile filtered through a 0.22 µm Sterivex™-GS filter before being stored at 4°C until required.

Thereafter, the plate was sealed with an adhesive plate seal and centrifuged at 252 x *g* for 5 minutes before 180 µL supernatant was replaced with 200 µL DMSO in all wells. The plate was shaken on an orbital shaker (MRC Thermo-Shaker™ MB100-4P, UK) at 161 x *g* for 5 minutes to ensure cell lysis and dissolution of the formazan crystals. The absorbance was measured using the Lab Systems Multiskan iEMS plate reader at a test wavelength of 540 nm to detect the formazan and a reference wavelength of 690 nm to detect the unreacted MTT.

Using Equation 2.9, the percentage cell viability was determined per well taking the appropriate controls into account. For the test compounds that inhibited more than 60% cell growth, the IC_{50} values were obtained by exposing the cells to a range of concentrations (0.001 - 200 µM). The IC_{50} values were calculated from log sigmoid dose response curves generated by GraphPad Prism® 5.02 (GraphPad Software, Inc., USA).

$$\%\ Cell\ Viability = \frac{[absorbance\ of\ drug\ treated\ well\ (540\ nm) -\ absorbance\ of\ drug\ treated\ well\ (690\ nm)]\ x\ 100}{mean\ absorbance\ of\ drug\ free\ control\ (540\ nm) - Mean\ absorbance\ of\ drug\ free\ control\ (690\ nm)}$$

Equation 2.9: The equation used to calculate the percentage cell viability taking both the test and reference wavelengths into account (van Zyl *et al.,* 2010).

2.6.4 Cellular viability combination studies

Drug combinations have the benefit of improved clinical efficacy when treating cancer and have been shown to delay drug resistance, with synergistic drugs being the most desired (Yin *et al.*, 2018). Ideal combinations have complementary mechanisms of actions to improve the inhibitory effects (Tallarida and Raffa, 2010). The possible mechanistic information and interaction between compounds have clinical relevance if there is an additive or synergistic effect, which can allow for a reduced dose to be administered along with the reduction of potential drug related side effects, while still achieving the required effectiveness (Tallarida and Raffa, 2010). Cisplatin has been shown to display synergistic behaviour in combination with other drugs against the K562 cell line (Li *et al.,* 1997; Wei *et al.,* 2015). As such the two most effective novel test compounds in this study were combined with cisplatin at various drug concentration ratios to determine the combined effects against the K562 cancer cells.

Combination studies were performed using the MTT assay as described in Section 2.6.3 with slight modifications to accommodate the addition of the combined drugs (van Zyl *et al.,* 2010). Based on the initial IC_{50} values obtained for the individual compounds, various drug concentration ratios were prepared taking a 20 times dilution factor into account (10 times dilution factor for the MTT assay and 2 times dilution factor for the 1:1 combination of compound **X** and compound **Y**) (Table 2.5). After the initial combinations were prepared, serial dilutions were plated out into the 96 well plates to determine the interaction between

the two compounds and construct an isobologram (Figure 2.4) plotting X- and Y-axis points (Equation 2.3).

2.6.5 Safety index

The safety index (SI) was determined for each test compound and control to assess the efficacy of the compounds in comparison to the safety/toxicity against human cell lines (HEK293) (Equation 2.10). This ratio was also indicative of the selectivity of the compounds to the malaria parasite over the human host cells which would be preferred to reduce the risk of adverse effects and increase the clearance rate of the parasite. All compounds with SI values >10 are normally regarded as non-toxic (Pink *et al.,* 2005; Bhat *et al.,* 2008). The SI for quinine has been reported to be >1000, as such a SI >100 was considered non-toxic in this study (Chen, 2015). Whilst the selective activity (SeI) of the compounds against the HEK293 cell line compared to their cytotoxicity against the leukemic K562 cell line was determined by calculating the SeI as per Equation 2.11 derived from modifying Equation 2.6 to compare percentage growth inhibition.

$$\text{Safety Index} = \frac{\text{Cytotoxicity HEK293 (50 µm)}}{\text{Antimalarial activity (50 µm)}}$$

Equation 2.10: The equation used to calculate the safety index for *P. falciparum* compared to human kidney epithelial (HEK293) cells (Chen, 2015).

$$\text{Selectivity Index (SeI)} = \frac{\text{Cytotoxicity HEK293 (50 µm)}}{\text{Cytotoxicity K562 (50 µm)}}$$

Equation 2.11: The equation used to calculate the selectivity index for human leukemic K562 compared to human kidney epithelial (HEK293) cells (Chen, 2015).

2.7 *Artemia* toxicity study

The toxicological properties of the test compounds were determined using the *Artemia* lethality assay. The *Artemia* lethality assay is a toxicity test first proposed by Michael *et al.* (1956) and further developed by several other research groups (Van Walbeek *et al*., 1971; Vanhaecke *et al.,* 1981). The *Artemia* lethality assay was carried out in order to determine the

toxicity of the test compounds against a whole organism in comparison to human cell lines and the method described by Ruebhart *et al.* (2009) was adapted for use with *Artemia franciscana* nauplii (brine shrimp).

2.8 *Artemia* lethality assay protocol

2.8.1 Hatching *Artemia* eggs

Animal ethics approval was obtained for the experimental use of *Artemia* from the University of the Witwatersrand Animal Research Ethics Committee (Clearance certificate: 07-11-2017-O, Appendix A).

Artemia franciscana nauplii eggs (0.5 g; Ocean Nutrition™) were placed in a plastic container containing 500 mL sea water (32 g/L Tropic Marine® sea salt in distilled water). A plastic tube connected to an aquarium rotary pump was placed into the water to allow for adequate aeration and dispersion of eggs throughout the container. A desk lamp with a standard 60-watt incandescent lightbulb was placed next to the container for 24 hours to provide a source of heat and light to optimise hatching of the eggs. After 24 hours, the freshly hatched nauplii were placed into a rectangular plastic container and the desk lamp focused over a particular area of the container, with the rest of the container void of light. Over the next 15 minutes the mobile nauplii concentrated into the brightly lit region of the container as they were attracted to light. The nauplii were then plated into a sterile 48 well plate for use in the bioassay.

2.8.2 *Artemia* lethality assay

An average of 20-40 nauplii were plated (50 µL) into each well of a sterile 48 well plate. Salt water (32 g/L; 197.5 µL) was added to each well and lastly, 2.5 µL of 50 µM test compound or positive control, potassium dichromate (dilution factor of 100 taken into account) were added in triplicate. All drugs were prepared in DMSO and further diluted with autoclaved MilliQ™ deionised water to their final concentration to be added to the plate. Salt water (2.5 µL) was plated out to serve as the drug-free/untreated negative control.

Upon adding the nauplii, test compounds and controls into the sterile 48 well plate, each individual well was examined microscopically (10x magnification; Olympus®, Japan) to record

any dead nauplii before incubation (dead at T_0). The plate was then incubated for 24 hours at 25°C, at which time the number of dead nauplii in each well was again recorded (dead at T_{24}) and the plate returned for incubation for a further 24 hours at 25°C. The process was repeated and the total dead at T_{48} and T_{72} recorded. Photographs were taken at 40x total magnification using an Olympus® CKX53 microscope using CellSens™ software at each respective time interval (T_{24}, T_{48} and T_{72}) for morphological assessment (Olympus®, Japan).

In order to determine the total number of nauplii in each well, 100 µL of acetic acid (50% v/v, 8.33 M) was added to each well after T_{72} to kill all nauplii and the total number of dead nauplii microscopically counted under 10x magnification. The percentage mortality was calculated as per Equation 2.12.

$$\%\ Mortality = \frac{[(Dead\ nauplii\ at\ T24, T48\ or\ T72 - Dead\ nauplii\ at\ T0)]x\ 100}{Total\ Nauplii\ - Dead\ nauplii\ at\ T0}$$

Equation 2.12 The equation used to calculate the percentage mortality of the *Artemia* nauplii after incubation with test compound after a 24, 48 or 72-hour period (Kathrada, 2017).

Each compound's morphological effects on the nauplii were noted based on microscopic visual assessment together with the photographs taken at each time interval during the screening process. The assay was repeated three times. Compounds showing significant mortality of *Artemia* (60%) were analysed using Probit analysis using IBM SPSS® statistics version 29 software (Finney, 1971). For the purposes of generating a graph, GraphPad® Prism version 5.02 was used and verified to produce the same LC_{50} as Probit analysis (IBM SPSS® Statistics version 29).

2.9 Free radical-induced oxidative stress and Iron chelation

The iron chelation and free radical scavenging assay were used to determine the ability of the test compounds to chelate iron or to act as an anti-oxidant respectively. Various microbial pathogens require transition metals for structural, catalytic and signaling functions (Niles, 2012) and many diseases such as cancer, diabetes and neurodegeneration are associated with metal ion imbalance (Maret and Wedd, 2014). A balance between free radicals and antioxidants is also necessary for proper physiological functioning (Lobo *et al.,* 2010).

2.9.1 Preparation of test compounds and control drugs for iron chelation and free radical scavenging assays

A 1 mL stock solution of 10 mM was prepared from each test compound by taking into account the respective molecular weight of each compound. The stock solutions were prepared by dissolving the solid test compounds in DMSO and storing them at -80 °C until required. A screening concentration of of each test compound was prepared, taking the dilution factor of 7.5 into account for the iron chelation assay and the dilution factor of 5 for the free radical scavenging assay by diluting the stock solutions with DMSO. Stock solutions of the respective positive controls, EDTA and ascorbic acid were prepared as in Section 2.1.2 for use as control compounds.

2.9.2 Free radical scavenging assay

Free radicals and oxidants play an important dual role as both beneficial and toxic compounds since they can either be harmful or helpful to the body (Pham-Huy *et al.,* 2008). The implication of oxidative stress in the aetiology of several diseases suggests that antioxidant therapy represents a promising avenue for treatment. (Pham-Huy *et al.,* 2008). In severe malaria, highly reactive chemicals formed from oxygen, water and hydrogen peroxide known as reactive oxygen species are generated by parasite haemoglobin metabolism in RBCs. Oxidative stress in RBCs could offer some compensatory benefits to a patient with severe malaria (Ackerman, 2009), while antioxidant supplements can reverse or minimize the oxidative damage to hosts caused by the use of antimalarial drugs, such as primaquine and chloroquine (Percário *et al.,* 2012; Ashley *et al.,* 2014).

2.9.2.1 Free radical scavenging assay protocol

The 2,2-diphenyl-1-picrylhydrazyl free radical (DPPH$^{\bullet}$) scavenging assay is one of the few stable and commercially available organic nitrogen radicals (Hunsaker and Schenk, 1983). According to Huang *et al*. (2005), the colour of the solution of DPPH when combined with an anti-oxidant, fades upon reduction of the anti-oxidant in proportion to the concentration of

the anti-oxidant (Figure 2.7). The DPPH• scavenging assay measured the ability of anti-oxidants to scavenge the stable free radical of DPPH, such that the violet colour changes to yellow-clear when the anti-oxidant compound donates an electron to the DPPH radical. The degree of decolourisation is stoichiometrically correlated to the number of electrons seized by DPPH (Huang *et al.,* 2005).

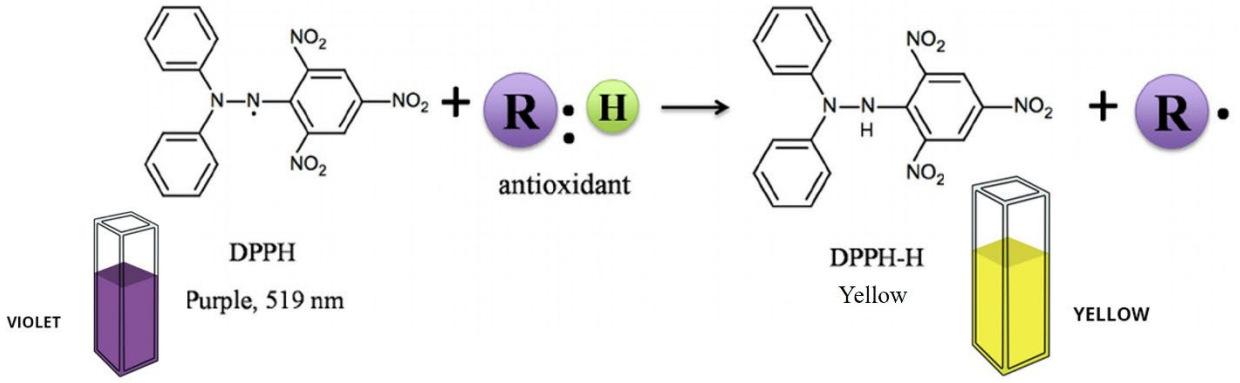


Figure 2.7: The interaction between DPPH free radical and an anti-oxidant and the observed colour changes (Liang & Kitts, 2014).

The modified method of Gülcin *et al*. (2004) and Chen *et al*. (2006) was used to prepare a 96.2 µM DPPH (Sigma Aldrich®) solution in HPLC grade methanol (Sigma Aldrich®). The freshly prepared solution was allowed to stand at 4˚C in the dark for 24 hours before use. To a sterile 96 well plate, 50 µL of each test compound (50 µM; 5 times dilution factor) or control (50 µM; 5 times dilution factor) was aliquoted into triplicate wells (Figure 2.8). DMSO was used in the nine untreated control wells, while L-ascorbic acid was used as the positive control in three wells. HPLC grade methanol (200 µL) was used instead of DPPH in the colour control wells when coloured test compounds or control were tested where the colours absorbance could interfere with the quantification of the reaction. DPPH• (200 µL) was added to the test and untreated control wells and the plate was gently agitated before being incubated at room temperature in the dark for 30 minutes. The degree of decolourisation of the DPPH• was spectrophotmetrically determined at 540 nm using the Lab Systems Multiskan iEMS plate reader and Ascent™ software version 2.6 and the percentage free radical scavenging determined using Equation 2.13 in Microsoft Excel®. For those test compounds and controls that possessed >60% percentage free radical scavenging, serial dilutions were prepared to

determine the IC_{50} values from log sigmoid dose response curves generated by GraphPad Prism® 5.02 (GraphPad Software, Inc., USA)

	1	2	3	4	5	6	7	8	9	10	11	12
A	1			8			15			22		
B	2			9			16			23		
C	3			10			17			24		
D	4			11			18			25		
E	5			12			19			26		
F	6			13			20			27		
G	7			14			21			28		
H	DMSO + DPPH	DMSO + DPPH	DMSO + DPPH	DMSO + DPPH	DMSO + DPPH	DMSO + DPPH	DMSO + Methanol	DMSO + Methanol	DMSO + Methanol	L-Ascorbic Acid	L-Ascorbic Acid	L-Ascorbic Acid

Figure 2.8: Plate layout of the free radical scavenging assay. Test compounds were plated in triplicate wells with 200 µL DPPH• to assess the free radical scavenging activity of the compounds. HPLC grade methanol (200 µL) was used instead of DPPH• in the colour control wells (H7-H9). Wells H1-H6 (dark purple) contained 200 µL of DPPH and 50 µL DMSO to serve as the 0% scavenging control. Positive control compound ascorbic acid (grey) was plated in triplicate in wells H10-H12 to serve as the 100% scavenging control.

$$\% \text{ Free radical scavenging} = \frac{[(\text{Absorbance of compounds} - \text{Average absorbance of colour control})]\text{x } 100}{[(\text{Average absorbance of untreated control} - \text{Average absorbance of colour control})]}$$

Equation 2.13 The equation used to calculate the percentage decolourisation of the DPPH• by the test compounds and controls (Chen, 2015).

2.9.3 Iron chelation assay

Iron is important in the metabolic processes of intra-erythrocytic parasites and if it is withheld by means of iron chelators, the metabolism of the parasite will be disrupted (Mabeza *et al.*, 1999). The method described by Dinis *et al*. (1994) was used to quantify the ability of the test and control compounds to chelate ferrous iron (Fe^{2+}). Iron chelating agents disrupt the formation of this complex by chelating the ferrous ions before ferrozine, reducing the intensity of the purple colour of the complex formed.

2.9.3.1 Iron chelation assay protocol

Briefly, a 0.48 mM $FeCl_2$ solution was prepared in 5% (w/v, 0.64 M) ammonium acetate (Fluka) in autoclaved Milli-Q® deionised water. In a sterile 96 well plate, 20 µL of each 50 µM test compound was aliquoted into triplicate wells and 30 µL of $FeCl_2$ was added to all wells on the plate. The positive control, EDTA was screened at 50 µM and the IC_{50} value determined. DMSO (20 µL) was added to the untreated wells which contained $FeCl_2$ and served as the 100% Fe^{2+}-ferrozine complex formation control. The blank colour control wells consisted of water or DMSO (20 µL). The plate was gently agitated to ensure proper mixing of reagents before being incubated in the dark for 5 mins at room temperature. Thereafter, 100 µL ferrozine was added to all wells except for the six blank colour control wells. The plate was futher incubated for 30 minutes at room temperature in the dark. Following which, the absorbances of each well were read at 540 nm and the percentage ferrous ion chelation was calculated using Equation 2.14. The IC_{50} values were calculated from log sigmoid dose response curves generated by GraphPad Prism® 5.02 (GraphPad Software, Inc., USA).

$$\%\ \text{Ferrous ion chelation} = \frac{[(\text{Absorbance of compound} - \text{Average absorbance of colour control})]\text{x } 100}{[(\text{Average absorbance of untreated control} - \text{Average absorbance of colour control})]}$$

Equation 2.14 The equation used to calculate the percentage iron chelation of the ferrous-ferrozine complex by the test compounds (Chen, 2015).

The absorbances obtained from reading the plate at the wavelength of 540 nm using the Lab Systems Multiskan iEMS plate reader (Thermo Fisher Scientific, United Kingdom) and Ascent™ software version 2.6 were analysed in Microsoft Excel® using Equation 2.14 to determine the percentage iron chelation capacity of the test compounds. For those test compounds and controls that possessed >60% percentage free radical scavenging, serial dilutions were prepared to determine the IC_{50} values from log sigmoid dose response curves generated by GraphPad Prism® 5.02 (GraphPad Software, Inc., USA).

2.10 Computational analysis

The drug-likeness of the test compounds were measured using the physical and chemical properties of the test compounds in comparison to known antimalarial drugs, quinine and chloroquine. Drug-likeness refers to the drug-like permeability properties for the purpose of this investigation (Bhal *et al*., 2007). The Lipinski's "Rule of Five" (Ro5) is a rule to evaluate drug-likeness or determine if a chemical compound with a certain pharmacological or biological activity has properties that would make it a likely drug that would be orally bioactive in humans (Lipinski *et al*., 1997). In this study, the partition coefficient was used as a predictor of the lipid solubility of the tests. The Lipinski's Ro5 concept was applied as outlined by Lipinski *et al*. (1997), such that drugs with a molecular weight less than 500, a partition coefficient (Log P) less than 5, possessing less than 5 H-bonds and less than 10-H bond acceptors were considered to have drug-like properties.

For the drug-likeness to be evaluated, 2-dimensional structures of the test compounds were constructed using ChemSketch® (ACD Labs, Version 2022.2.2). The pharmacokinetics of the test compounds and controls were determined using SwissADME (Molecular Modelling Group of the SIB, Swiss Institute of Bioinformatics. http://www.swissadme.ch) and ChemAxon Chemicalize® (https://chemicalize.com) web-based software. Test compounds that violated more than one of the Ro5 parameters were considered non-drug-like have poor pharmacokinetic properties.

In addition to the Ro5 parameters, the ionisation constants (pKa values) as predicted by the SwissADME and Chemicalize® software were used to determine the degree of ionisation of the test compounds at physiological pH 7.4 (RBC cytosol) and pH 5 (parasite digestive food vacuole) using the Henderson-Hasselbalch equation (Equation 2.15).

$$\% \text{ Ionisation} = \frac{100}{1 + \text{antilog}\,(\text{pKa} - \text{pH})}$$

Equation 2.15 The equation used to calculate the percentage Ionisation of the test compounds (Henderson, 1908; Hasselbalch, 1917).

A toxicological hazard profile was generated using ToxTree (Version 3.1) (https://toxtree.sourceforge.net/) based on the revised Cramer decision tree (Cramer et al., 1978; EFSA Scientific Committee *et al.,* 2019) and test compounds were compared to known antimalarial drugs, quinine and chloroquine. Parameters investigated included whether a compound is heterocyclic, has reactive groups and or possessed other structural features suggestive of toxicity as proposed by Cramer *et al* (1978). Using SwissADME (http://www.swissadme.ch/), properties of the compound such as their ability to cross the blood brain barrier or be absorbed through the gastro-intestinal tract were also noted.

2.11 Statistical analysis

All experiments were carried out in at least triplicate to produce a mean ± standard deviation (s.d.) and each experiment independently repeated three times (biological repeats). For the assays which required IC_{50} value determination (*p*LDH, MTT, free radical scavenging and iron chelation), the values were calculated from log sigmoid dose response curves generated by GraphPad Prism® 5.02 (GraphPad Software, Inc., USA).

The absorbances of the plates in the *p*LDH, haemolysis, and MTT assays were read at their respective wavelengths using an ultraviolet-visible (UV-Vis) spectrophotometer (Labsystems iEMS Reader MF) Ascent™ software version 2.6. For the assay which required LC_{50} values (*Artemia* lethality, larvicidal and ovicidal assay), Probit analysis was conducted using the IBM SPSS Statistical 29 Software Package (IBM Corp., USA).

To determine if there was a statistically significant difference between a test compound and control, a one-way ANOVA (and non-parametric or mixed) was performed using GraphPad® Prism Version 5.02 software with a Dunnett's multiple comparison post test, with a p-value of less than 0.05 considered to be significant.

CHAPTER 3 – RESULTS

3.1 Antimalarial activity

The three sets of novel test compounds possessed varying *in vitro* antimalarial activity when screened at 50 µM against the intra-erythrocytic *P. falciparum* NF54 parasite using the *p*LDH assay (Appendix B, Table B1). All fifteen of the dihydroquinoline-carbothioamide group (**DC1-DC15**) compounds exhibited antimalarial activity resulting in parasite viability within the range of 0.01% - 41.58% The phenyl-hydrazono group (**PHYD1-PHYD15**) compounds exhibited antimalarial activity resulting in parasite viability within the range of 20.92% to 79.44% The quinoline-3-carboxamide group (**Q3C1-Q3C12**) compounds exhibited antimalarial activity resulting in parasite viability within the range of 10.10% to 89.62%.

A dose-dependent response was observed for the active compounds (Figure 3.1), where test compounds, **DC14** and test compound **Q3C11** displayed the lowest IC_{50} values of the test compounds (Table 3.1). Compound **DC14** showed the most antimalarial activity in the dihydroquinoline-carbothioamide group, compound **PHYD1** showed the most antimalarial activity in the phenyl-hydrazono group and compound **Q3C11** showed the most antimalarial activity in the quinoline-3-carboxamide group of compounds (Table 3.1).

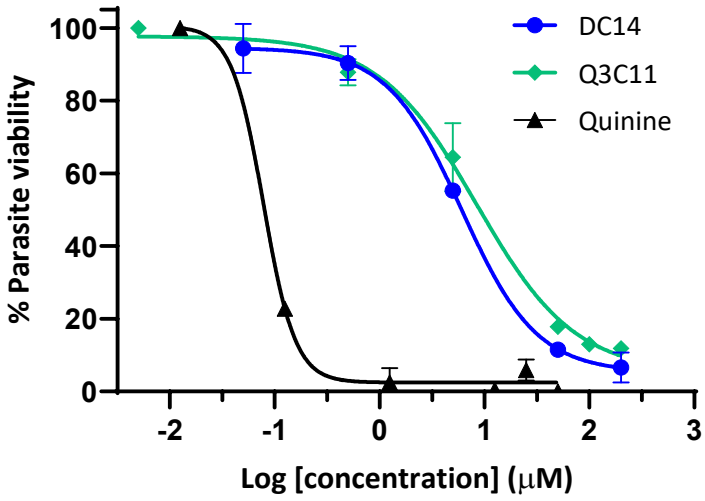


Figure 3.1: Dose dependent antimalarial inhibitory effect of the most active compounds, **DC14** and **Q3C11** against the *in vitro* asexual blood stages of *P. falciparum* in comparison to standard antimalarial drug, quinine using the *p*LDH assay.

Table 3.1: The IC_{50} values of test compound and controls as determined by the *p*LDH assay in micromolar (µM) concentration against the *P. falciparum* NF54 parasite. (n= 3-5). For those compounds where no IC_{50} value was determined, the % inhibitory activity are reported in [ ]. Statistical differences were the determined by comparing the test compound to Quinine. Where *n.d. – IC_{50} value not determined; n.s. = Not significant

Compound	Antimalarial activity (IC_{50} ± s.d; µM) [%]	Statistical differences	Compound	Antimalarial activity (IC_{50} ± s.d; µM) [%]	Statistical differences	Compound	Antimalarial activity (IC_{50} ± s.d; µM) [%]	Statistical differences
DC1	157.15 ± 4.05	Yes (P <0.0001)	**PHYD1**	127.75 ± 3.85	Yes (P <0.0001)	**Q3C1**	n.d. [59.11 ± 13.46]	n.d.
DC2	72.71 ± 8.09	Yes (P <0.0001)	**PHYD2**	142.25 ± 7.35	Yes (P <0.0001)	**Q3C2**	n.d. [68.34 ± 27.21]	n.d.
DC3	66.70 ± 1.51	Yes (P = 0.0009)	**PHYD3**	155.40 ± 19.30	Yes (P <0.0001)	**Q3C3**	21.27 ± 1.74	ns (P = 0.7622)
DC4	40.05 ± 17.98	*ns (P = 0.0871)	**PHYD4**	n.d. [65.12 ± 14.86]	n.d.	**Q3C4**	n.d. [89.62 ± 7.96]	n.d.
DC5	n.d. [33.60 ± 1.60]	n.d.	**PHYD5**	n.d. [58.70 ± 30.05]	n.d.	**Q3C5**	n.d. [84.13 ± 1.7]	n.d.
DC6	76.22 ± 2.06	Yes (P = 0.0002)	**PHYD6**	n.d. [76.98 ± 5.11]	n.d.	**Q3C6**	n.d. [55.67 ± 20.98]	n.d.
DC7	n.d. [38.72 ± 14.79]	n.d.	**PHYD7**	n.d. [75.27 ± 22.63]	n.d.	**Q3C7**	17.34 ± 1.94	*ns (P = 0.9222)
DC8	147.6 ± 2.50	Yes (P <0.0001)	**PHYD8**	n.d. [79.76 ± 20.35]	n.d.	**Q3C8**	85.18 ± 12.73	Yes (P <0.0001)
DC9	93.45 ± 10.55	Yes (P <0.0001)	**PHYD9**	160.4 ± 4.80	Yes (P <0.0001)	**Q3C9**	160.1 ± 9.1	Yes (P <0.0001)
DC10	n.d. [18.38 ± 32.93]	n.d.	**PHYD10**	n.d. [60.96 ± 5.41]	n.d.	**Q3C10**	73.38 ±3.41	Yes (P =0.0003)
DC11	14.56 ± 0.28	*ns (P = 0.9798)	**PHYD11**	n.d. [79.44 ± 20.77]	n.d.	**Q3C11**	7.99 ± 0.31	*ns (P = 0.9992)
DC12	13.5 ± 2.55	*ns (P = 0.9880)	**PHYD12**	n.d. [76.53 ± 20.26]	n.d.	**Q3C12**	160.9 ± 2.1	Yes (P <0.0001)
DC13	105.18 ± 12.52	Yes (P <0.0001)	**PHYD13**	n.d. [77.12 ± 20.54]	n.d.			
DC14	7.23 ± 1.17	*ns (P = 0.9993)	**PHYD14**	n.d. [72.95 ± 28.52]	n.d.	**Quinine**	0.09 ± 0.005	-
DC15	57.14 ± 11.29	Yes (P =0.0050)	**PHYD15**	n.d. [66.85 ± 16.18]	n.d.	**Chloroquine**	0.01005 ± 0.000175	*ns (P >0.9999)

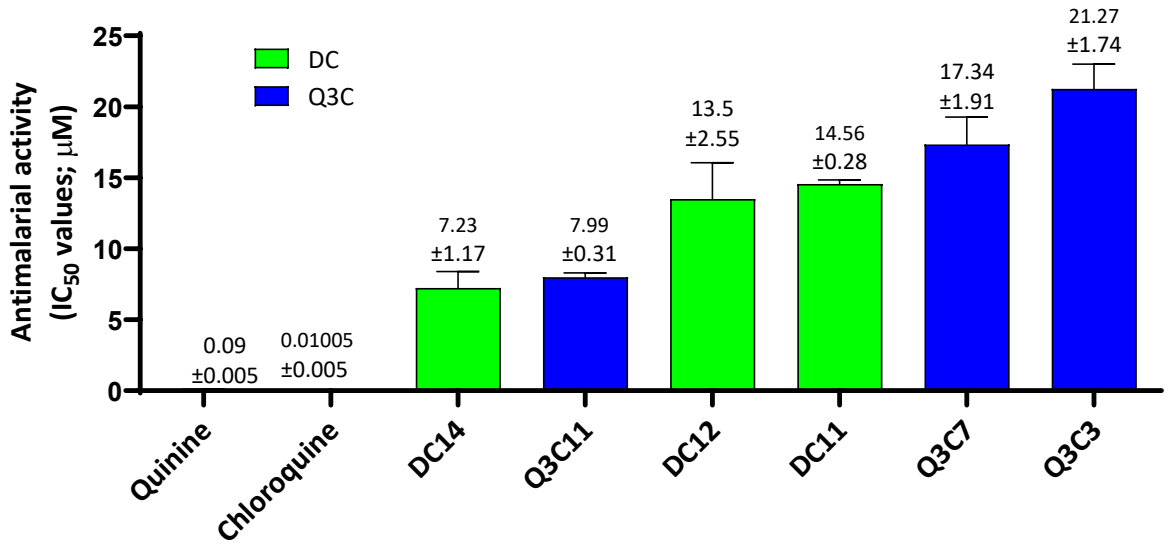


Figure 3.2: The antimalarial IC_{50} values of the most active dihydroquinoline-carbothioamide (**DC**), and quinoline-3-carboxamide (**Q3C**) compounds with IC_{50} values less than 22 µM on the *P. falciparum* NF54 parasite compared to the standard antimalarial drugs, quinine and chloroquine using the *p*LDH assay (n=3).

Compound **DC14** exhibited the highest antimalarial activity across all three groups of compounds with an IC_{50} value of 7.23 ± 1.17 µM. The IC_{50} value of compound **DC14** represented an 80.3-fold lower activity compared to standard antimalarial drug, quinine (0.09 ± 0.005 µM)(*p* value: 0.9993) (Appendix B, Table B2). Compound **Q3C11** displayed the second highest activity with an IC_{50} value of 7.99 µM ± 0.31, which was 88.7-fold lower in activity compared to quinine (*p* value: 0.9992).

3.2 Antimalarial combination studies

Test compounds **DC14** and **Q3C11** were found to be the most active of all the test compounds (Table 3.1); as such were selected to be combined with quinine to evaluate the drug interaction against the malaria parasite using the *p*LDH assay. The combination of **DC14** with quinine demonstrated a synergistic effect with an average ΣFIC value of 0.58 as verified by the points below the synergistic line in the isobologram (Figure 3.3). The combination of **Q3C11** and quinine demonstrated an antagonistic effect with an average ΣFIC value of 1.70. Notably, test compound **Q3C11** displayed an additive interaction at concentration ratios

when lower concentrations of quinine were combined with compound **Q3C11**. With the exclusion of the higher quinine concentration ratios, an additional isobologram was generated to display the additive effects where a ΣFIC value of 0.91 was obtained (Figure 3.4).

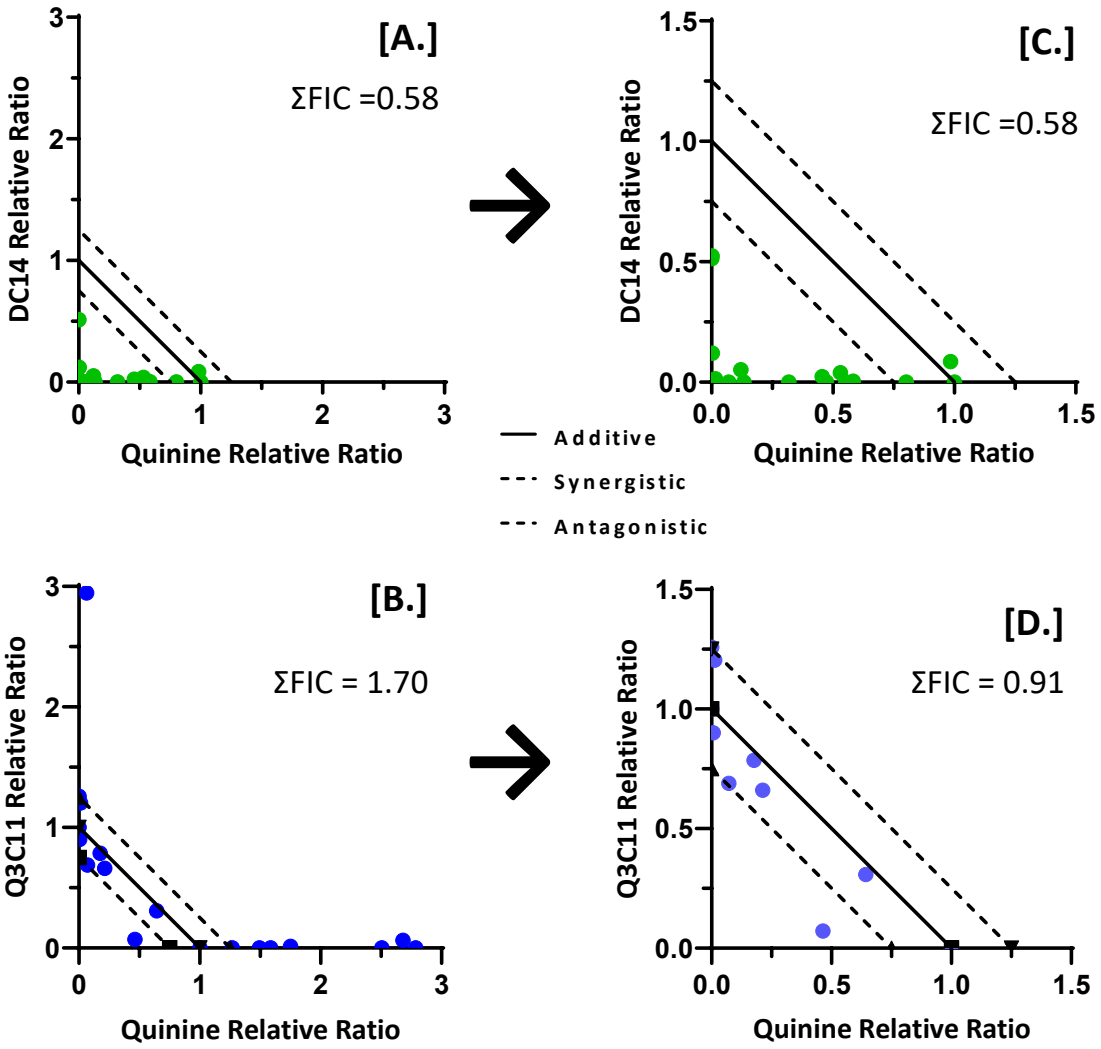


Figure 3.3: Isobolograms displaying the drug interactions between test compound **DC14** (A,C) or **Q3C11** (B,D) in combination with the standard antimalarial drug, quinine using the *p*LDH assay. (n=4). A synergistic drug interaction was observed between quinine and compound **DC14**, compared to an antagonist interaction between quinine and **Q3C11**. Additive effects were observed at lower concentrations of compound **Q3C11** and quinine (D). (n=4).

3.3 Morphological and stage specific effects

Compound **DC14** and **Q3C11** were incubated with synchronised *P. falciparum* NF-54 parasites at their respective IC_{50} concentrations in comparison to standard antimalarial drug quinine for

48 hours (Section 2.3.2). The parasite stages proceeded with a lag phase that developed between the test compound treated parasite and the untreated control. The % parasitaemia for each growth stage was noted (Figure 3.5) and a decline in the total parasitaemia over the 48 hour period was observed in the treated parasites. The presence of gametocytes (Figure 3.6) in the treated parasites is indicative of stressful environmental conditions (Omorou *et al.,* 2022).

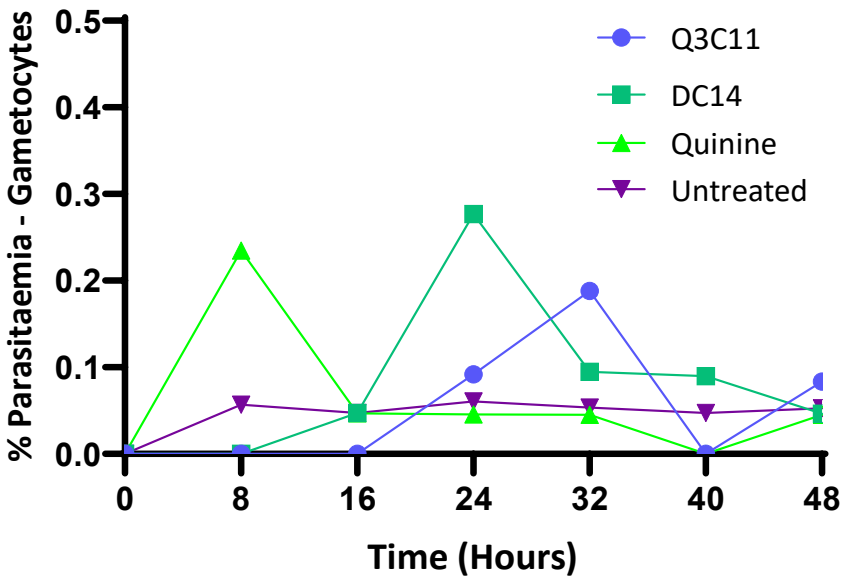


Figure 3.4: The % gametocytes observed over 48 hours in the untreated parasites control, compared to compounds **DC14** (7.23 µM), **Q3C11** (7.99 µM) and quinine (0.09 µM) treated parasites control.

In Figure 3.4, Figure 3.5 and Table 3.2, the following were observed at the different timepoints:

- *0-8 hours:* No significant changes in the morphology of the parasites were observed at this time point. Ring stage parasites were present at a 2% parasitaemia total in the treated and untreated parasites (Figure 3.5.A).
- *8-16 hours:* No changes in the morphology were observed when comparing compounds **DC14**, **Q3C11** and quinine at the 8 hour interval. A higher % of trophozoites were observed in the untreated control (Figure 3.5.B).
- *16-24 hours:* At the 16 hour interval, quinine had less observable trophozoites in comparison to compounds **DC14**, **Q3C11** and the untreated control. An approximate 1%

decrease in total parasitaemia was observed with quinine (Figure 3.5.B). The parasite digestive food vacuole was seen in a trophozoite in the untreated control (Table 3.2.A).

- *24-32 hours:* Gametocytes were observed in the compounds **DC14-** and **Q3C11**-treated flasks (Table 3.2). The gametocytes observed with compounds **DC14** and **Q3C11** were identified as male due to the crescent shape and nucleus with freely scattered chromatin (Table 3.2). The total parasitaemia in the untreated control peaked at the 24 hour interval (Figure 3.5.D). The total % schizonts increased rapidly between 24 and 32 hours in the untreated control in comparison to compounds **DC14**, **Q3C11** and quinine (Figure 3.5.C). The total % trophozoites in the untreated control decreased with the development of the schizonts between these time intervals. The development of schizonts were slower for compounds **DC14**, **Q3C11** and quinine and lagged behind the untreated control indicating an altered growth pattern.
- *32-40 hours:* A slight decline in the total % schizonts in the untreated control was observed which corresponded with an increase in the total % of ring stage parasites in the second generation. The total % schizonts increased slowly with compounds **DC14** and **Q3C11**. Quinine had the lowest number of schizonts indicating an alteration in the stage progression (Figure 3.5.C).
- *40-48 hours:* An increase in the formation of new ring staged parasites were observed in the untreated control while there was a decline of observable schizonts. Few trophozoite and schizont parasites were observed with quinine with no new rings visible. The % parasitaemia remained the same for compound **Q3C11** and declined slightly for compound **DC14**. A few new rings were observed with compound **Q3C11** while compound **DC14** showed no new rings (Figure 3.5. A).
- *48 hours:* Quinine displayed the lowest total % parasitaemia followed by compounds **DC14** and **Q3C11**. No new rings were observed with quinine and compound **DC14,** while very few new rings were observed with compound **Q3C11** (Table 3.2.B). The untreated control displayed an increase in new ring stage parasites and the complete decline in observable schizonts corresponding with the parasite's life cycle. The total % parasitaemia increased for the untreated control in comparison to the decrease observed for compounds **DC14**, **Q3C11** and quinine (Figure 3.5.D).

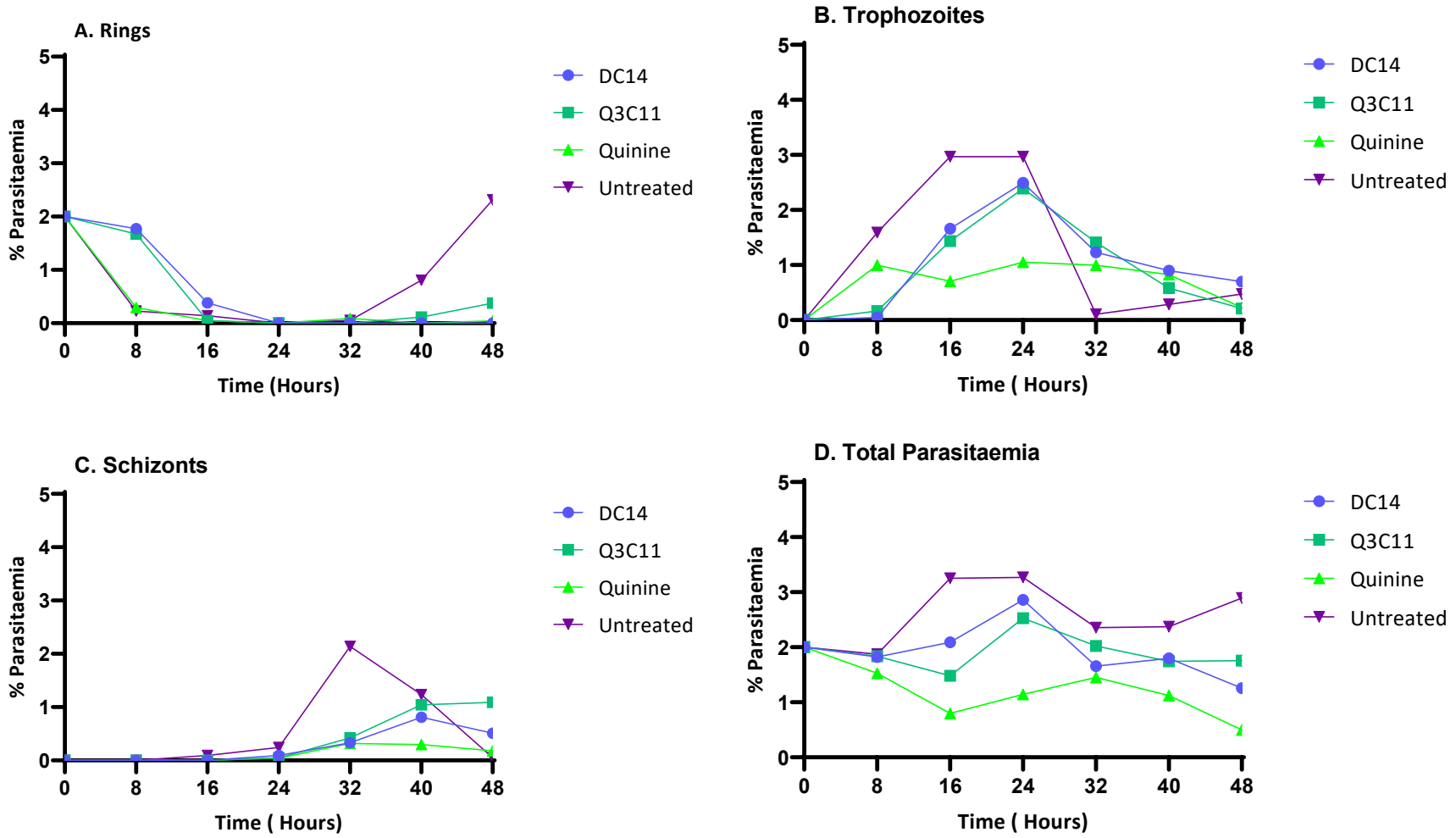


Figure 3.5: The comparison of the % parasitaemia over 48 hours of the ring (**A**), trophozoite (**B**), schizont (**C**) stages and the total % parasitaemia (**D**) of the untreated parasites control compared to compound **DC14** (7.23 µM), **Q3C11** (7.99 µM) and the quinine (0.09 µM) treated parasites.

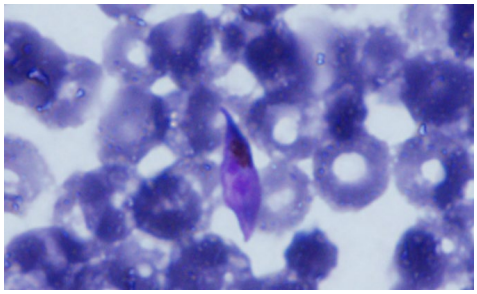


Figure 3.6: Development of a gametocyte in the treated NF54 *P. falciparum* parasite flask after 24 hours of exposure to test compound **Q3C11**.

Table 3.2: The effect of test compounds **DC14**, **Q3C11** and Quinine at the IC_{50} value concentrations on the parasitic stages and morphology over a 48 hour period in comparison to untreated NF54 *P. falciparum* parasites.

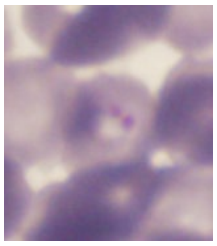
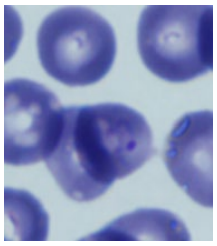
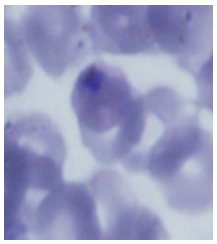
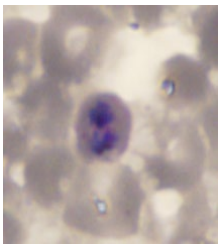
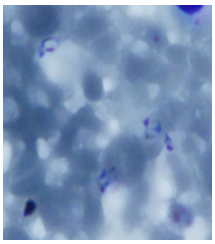
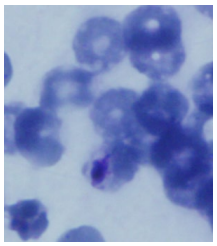
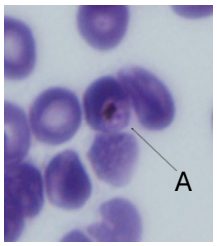
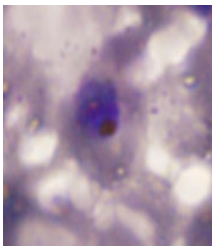
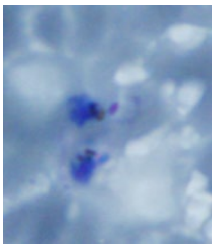
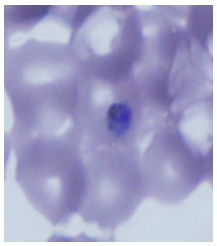
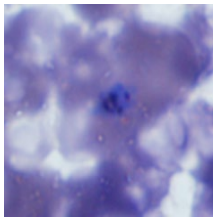
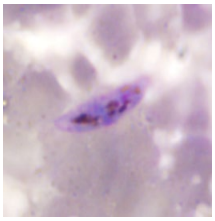
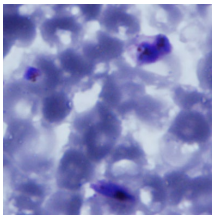
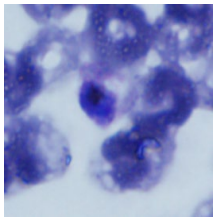
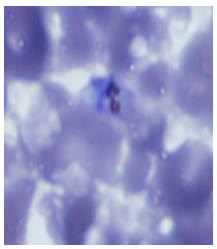
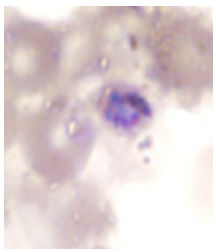
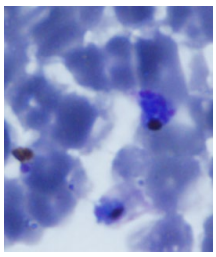
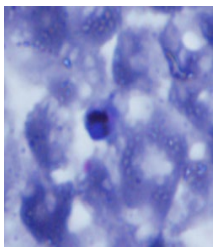
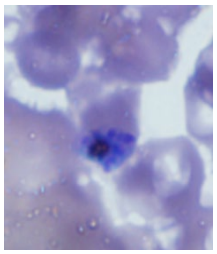
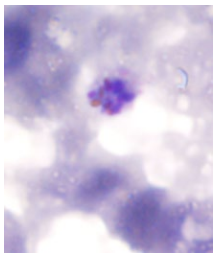
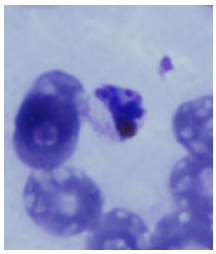
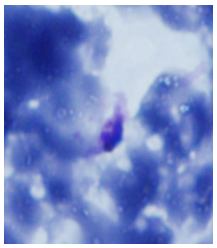
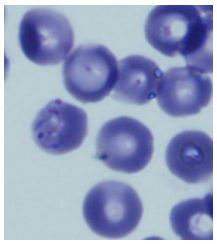
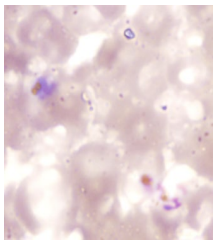
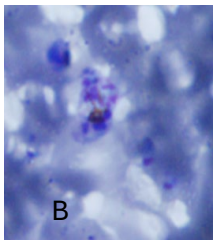
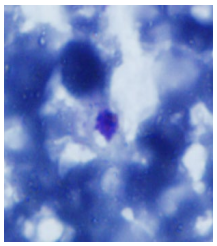
Time (Hours)	**Untreated Control**	**DC14**	**Q3C11**	**Quinine**
0-8 Ring Stage				
8-16 Late Rings – Early trophozoite stage				
16-24 Mid-Trophozoite – Late trophozoite stage				
24-32 Early schizont stage – mid schizont stage		 Gametocyte	 Gametocyte	

Table 3.2 (Continued): The effect of test compounds **DC14**, **Q3C11** and Quinine at the IC_{50} value concentrations on the parasitic stages and morphology over a 48 hour period in comparison to untreated NF54 *P. falciparum* parasites.

Time (Hours)	Untreated Control	DC14	Q3C11	Quinine
32-40 Mid to late Schizont – early new ring stage				
40-48 Late schizont – early new ring stage				
48 New ring stage 10 µm				

3.4 Vector Studies

3.4.1 Larvicidal Activity

The three sets of novel test compounds displayed little to no larvicidal activity compared to DDT (100% death) at 0.5 µM in a time dependant manner (Table 3.3). All three test compound groups displayed larval mortality up to 5% (range: 0-5%) after 48 hours (Appendix C, Table C1 and C2). The three groups of test compound displayed higher larval mortality at the 72 hour time period.

The **DC** group test compounds displayed larval mortality up to 18.3% (range: 2.5-18.3%) after 72 hours with compounds **DC3** (16.6%), **DC7** (18.3%) and **DC12** (16.6%) being the most active

from this group. The **PHYD** group test compounds displayed larval mortality up to 10% (range: 1.6-10%) after 72 hours with compounds **PHYD11**, **PHYD13** and **PHYD14** all causing 10% mortality. Lastly the **Q3C** group test compounds displayed larval mortality up to 15% (range: 5-15%) after 72 hours with compound **Q3C1** (15%), **Q3C9** (13.3%) and **Q3C11** (11.6%) being the most active (Table 3.3) in this group. The larval mortality percentages for 24 hours and 48 hours are reported in Appendix C, Table C1 and Table C2.

Table 3.3: The percentage larval mortality after being exposed for 72 hours to each of the test compounds in comparison with positive control DDT at 0.5 µM.

Compound	% Larval Mortality at 72 hours	Compound	% Larval Mortality at 72 hours	Compound	% Larval Mortality at 72 hours
DC1	5.00	**PHYD1**	5.00	**Q3C1**	15.00
DC2	2.50	**PHYD2**	5.00	**Q3C2**	6.67
DC3	16.67	**PHYD3**	5.00	**Q3C3**	5.00
DC4	10.00	**PHYD4**	6.67	**Q3C4**	8.33
DC5	3.33	**PHYD5**	3.33	**Q3C5**	5.00
DC6	8.33	**PHYD6**	3.33	**Q3C6**	10.00
DC7	18.33	**PHYD7**	6.67	**Q3C7**	10.00
DC8	11.67	**PHYD8**	8.33	**Q3C8**	7.50
DC9	11.67	**PHYD9**	6.67	**Q3C9**	13.33
DC10	11.67	**PHYD10**	5.00	**Q3C10**	6.67
DC11	10.00	**PHYD11**	10.00	**Q3C11**	11.67
DC12	16.67	**PHYD12**	8.33	**Q3C12**	6.67
DC13	6.67	**PHYD13**	10.00		
DC14	6.67	**PHYD14**	10.00	**DDT**	100.00
DC15	10.00	**PHYD15**	1.67		

No mortality was observed in the untreated control over the 72 hour period. The positive control, DDT exhibited 96% larval mortality after 24 hours and 100% larval mortality after 48 and 72 hours at 0.05 µM (Table 3.3). The LC_{50} concentration of DDT was calculated to be 0.3801 ± 0.13 µM after 24 hours, 0.0481 ± 0.001 µM after 48 hours and 0.0057 ± 0.000004 µM after 72 hours (Appendix C, Figure C1). After 72 hours pupae formation above 5% was noted with test compound**s DC5** (7.5% pupation), **DC10** (12.5%), **PHYD9** (7.5%) and **Q3C11** (7.5%), as well as in the untreated control (7%) (Appendix C, Table C3). In contrast, there was no pupae formation in the DDT treated larvae.

3.4.2 Morphological effects of the test compounds on the *An. arabiensis* larvae

The untreated larvae served as the negative control and displayed normal morphological features which contrasted with the altered features of the larvae treated with the positive control DDT (Table 3.4) (Kathrada, 2017). From the three most active larvicidal test compounds, **DC3** displayed a notable morphological change after 72 hours in the few dead larvae present, while compounds **DC7** and **DC12** showed no significant morphological changes to the larvae after 72 hours.

Table 3.4: The morphological effects of compounds **DC3**, **DC7** and **DC11** on 3rd instar *An. arabiensis* larvae after a 72 hour period in comparison to the positive control DDT and untreated negative control. Images were captured using a BestScope compound microscope (Lasec, South Africa) with TCapture version 3.9.0.602 software at 10x total magnification.

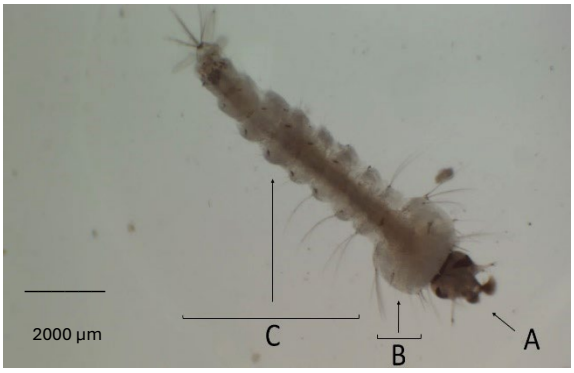
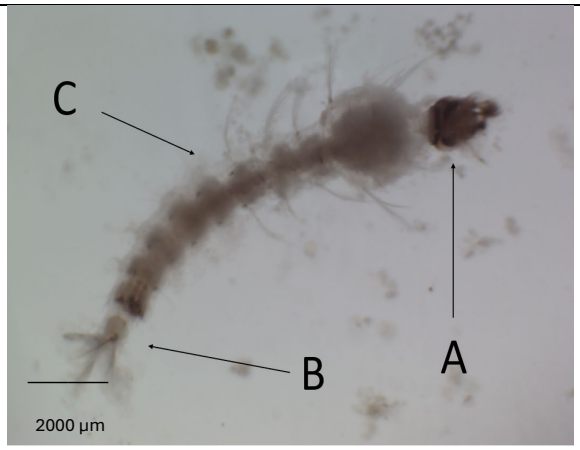
Compound	Larvae	Description
Untreated (Negative control)		**A** - Normal larvae head. **B** - Elliptical shaped thorax. This is wider than the head and has 3 rows of setae. **C** - Elongated abdomen. Ten segments with abdominal and palmate hairs present. Segments I-VII are uniform in shape and size. The final segment is the anal segment with anal brush and gills visible.
DDT		**A** – Head is slightly elongated and appears loosely attached to thorax **B** - Less distinguishable anal brush and gills. Anal segment reduced in size. **C** - Segments are shriveled with narrowing of the abdomen visible

Table 3.4 (continued): The morphological effects of compounds **DC3**, **DC7** and **DC11** on 3rd instar *An. arabiensis* larvae after a 72 hour period in comparison to the positive control DDT and untreated negative control.

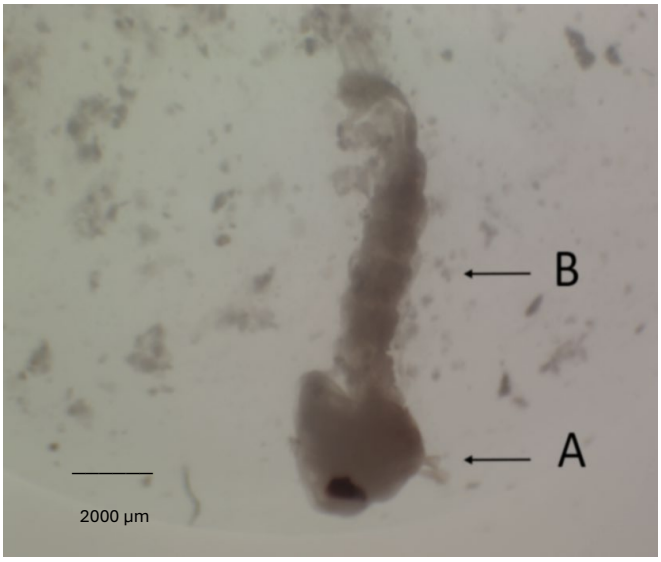
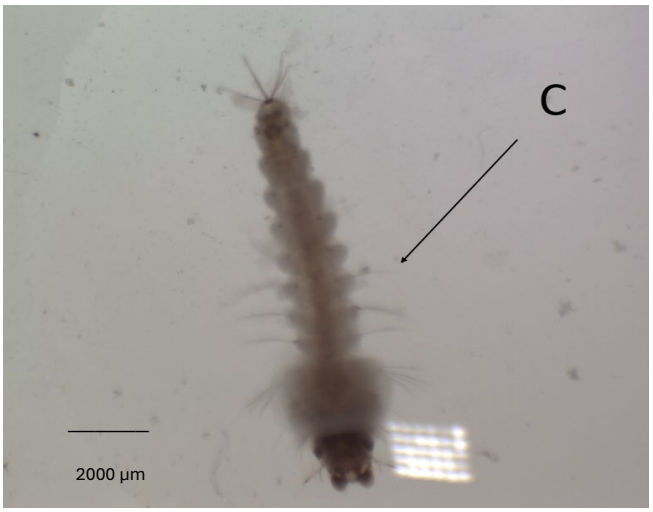
Compound	Larvae	Description
DC3	Dead larva  Live larvae 	A – Dead larva. Head is distorted and thoracic segment enlarged. B- No palmate hairs and total larval size reduced. C- Live larva in comparison with the dead larva displays a thoracic segment that is slightly enlarged. Palmate hairs are present.
DC7		**A** – No morphological changes. All segments intact. Abdominal and palmate hairs present. Anal brush and gills clearly visible

Table 3.4 (continued): The morphological effects of compounds **DC3**, **DC7** and **DC11** on 3rd instar *An. arabiensis* larvae after a 72 hour period in comparison to the positive control DDT and untreated negative control.

Compound	Larvae	Description
DC12		**A** – No morphological changes. Abdominal and palmate hairs present. Anal brush and gills clearly visible

3.4.3 Ovicidal Activity

All three groups of novel test compounds displayed minimal ovicidal activity at the screening concentration of 0.5 µM on the *An. arabiensis* eggs after 72 hours, with average hatch rates ranging from 72% to 100% (Appendix D, Table D1 and D2). In comparison, the untreated controls (DMSO and distilled water) displayed an average hatch rate of 82% to 100% after the 72 hour time period. One compound (**PHYD12**) from the **PHYD** group of test compounds displayed slightly higher ovicidal activity (28%) after 72 hours. The positive control, formalin resulted in 100% ovicidal activity at 48 and 72 hours. The LC_{50} value of formalin was determined to be 6.2 µM by using Probit analysis in the IBM SPSS® Statistics version 29 software package. Eggs treated with DDT (0.5 µM) resulted in an average hatch rate of 60% after 72 hours.

3.5 Cytotoxicity Studies

3.5.1 Haemolysis

The red blood cell toxicity assay was used to determine the haemolytic effect of the test compounds at a concentration of 50 µM. Test compounds with a percentage haemolysis greater than 30% are considered highly haemolytic and therefore have an unfavourable toxicological profile (Hayat *et al.*, 2011; Sæbø *et al.,* 2023). From the three groups of test compounds, none showed significant haemolysis and demonstrated a percentage haemolysis of less than 3.5% (Appendix E, Table E1). The test compounds had negligible haemolysis; the **DC** series (range: 0.1-3.41% lysis), **PHYD** series (range: 0.1-1.79% lysis) and **Q3C** series (range: 0.1-1.4% lysis). Quinine displayed 0.45% haemolysis, in contrast to chloroquine that caused 2.97% haemolysis and the positive control, Triton™ X-100 resulted in 100% haemolysis.

3.5.2 MTT cytotoxic activity

The MTT assay was performed on both human embryonic kidney cell (HEK-293) and chronic myelogenous leukaemia (K562) cell lines. Test compounds from all three groups exhibited varying cytotoxicity against the K562 cell line with the **PHYD** group of test compounds displaying up to 79% cell viability inhibition when screened at 50 µM (Table 3.5). In contrast to the K562 cell line, all three groups of test compounds exhibited low cytotoxicity towards the HEK293 cell line. Test compounds from the dihydroquinoline-carbothioamide group (**DC1-DC15**) exhibited low cytotoxicity with percentage viability ranging from 58.28% to 88.79%; while similarly those from the phenyl-hydrazono group (**PHYD1-PHYD15**) exhibited low cytotoxicity with percentage viability ranging from 57.92% to 90.53%. Test compounds from the quinoline-3-carboxamide group (**Q3C1-Q3C12**) exhibited low cytotoxicity with percentage viability ranging from 55.66% to 100% (Table 3.5).The IC_{50} values for the test compounds demonstrated cytotoxic properties where the lower the IC_{50} value, the more cytotoxic the compound towards the K562 cell line (Table 3.6). Compound **Q3C8** was 20.5-fold more cytotoxic compared to the positive control cisplatin (73.74 ± 7.76 µM) (p value < 0.0001). Whilst compound **DC12** (8.86 ± 1.15 µM) was only 8.3-fold more cytotoxic than cisplatin (p value <0.0001). Figure 3.7 displays the dose-dependent cytotoxic inhibitory effect of the two most active test compounds in comparison with cisplatin.

Table 3.5: The percentage cell viability of the human embryonic kidney (HEK-293) and chronic myelogenous leukaemia K562 cell lines after treatment with 50 µM test compound and controls as determined by the MTT cytotoxicity assay (n= 3). Where n.d.: not determined.

Compound	HEK-293 (% cell growth)	K562 (% cell growth)	Compound	HEK-293 (% cell growth)	K562 (% cell growth)	Compound	HEK-293 (% cell growth)	K562 (% cell growth)
DC1	74.80 ± 3.05	86.4 ± 13.98	**PHYD1**	66.98 ± 7.87	96.60 ± 10.66	**Q3C1**	83.39 ± 12.92	100 ± 26.78
DC2	82.81 ± 4.97	91.67 ± 12.63	**PHYD2**	62.89 ± 5.93	90.06 ± 12.10	**Q3C2**	89.64 ± 5.43	100 ± 13.77
DC3	84.24 ± 2.01	96.19 ± 11.76	**PHYD3**	63.26 ± 8.49	54.95 ± 5.34	**Q3C3**	59.58 ± 5.46	66.85 ± 16.62
DC4	62.28 ± 6.14	85.70 ± 14.58	**PHYD4**	59.59 ± 8.81	64.38 ± 9.11	**Q3C4**	80.04 ± 2.96	93.43 ± 9.75
DC5	70.13 ± 4.82	98.82 ± 14.73	**PHYD5**	71.48 ± 6.58	100 ± 17.21	**Q3C5**	101.08 ± 9.55	65.98 ± 14.46
DC6	64.51 ± 0.92	98.63 ± 12.56	**PHYD6**	57.92 ± 9.05	42.94 ± 9.96	**Q3C6**	64.70 ± 3.81	76.29 ± 2.30
DC7	65.08 ± 12.76	100.00 ± 8.46	**PHYD7**	61.83 ± 14.47	97.42 ± 11.71	**Q3C7**	80.77 ± 13.50	41.15 ± 6.10
DC8	63.94 ± 3.34	100.00 ± 7.73	**PHYD8**	73.97 ± 18.61	20.94 ± 4.79	**Q3C8**	62.24 ± 11.08	32.75 ± 6.29
DC9	61.06 ± 11.10	85.30 ± 14.22	**PHYD9**	65.72 ± 10.00	48.51 ± 5.49	**Q3C9**	55.66 ± 3.78	46.32 ± 7.59
DC10	79.78 ± 5.21	100.00 ± 3.68	**PHYD10**	60.13 ± 3.57	100.00 ± 7.97	**Q3C10**	81.52 ± 6.28	95.98 ± 27.89
DC11	88.79 ± 7.66	100.00 ± 2.68	**PHYD11**	64.31 ± 9.56	94.54 ± 23.51	**Q3C11**	81.84 ± 12.62	48.91 ± 8.24
DC12	80.65 ± 16.05	49.01 ± 1.35	**PHYD12**	75.05 ± 15.18	28.15 ± 5.45	**Q3C12**	88.84 ± 5.12	89.96 ± 23.55
DC13	58.28 ± 4.68	53.53 ± 8.71	**PHYD13**	72.62 ± 16.92	48.96 ± 21.70	**Camptothecin**	30.00 ± 2.36	n.d.
DC14	61.53 ± 10.74	52.94 ± 9.88	**PHYD14**	76.21 ± 2.86	46.46 ± 14.97	**Cisplatin**	55.64 ± 15.82	49.27 ± 16.40
DC15	68.52 ± 5.02	100.00 ± 8.65	**PHYD15**	90.53 ± 4.57	34.18 ± 9.09	**Quinine**	87.4 ± 1.75	100 ± 13.45

Table 3.6: The IC_{50} values of test compound and controls tested against the human chronic myelogenous leukaemia (K562) cell line as determined by the MTT assay. (n= 3). Test compound **DC12**, test compound **PHYD8** and test compound **Q3C8** displayed the lowest IC_{50} values in their respective compound groups. Statistical differences were the determined by comparing the test compound to cisplatin. Where *n.d. – IC_{50} value not determined; n.s. = Not significant

Compound	K562 (IC_{50} ± s.d, µM)	Statistical differences	Compound	K562 (IC_{50} ± s.d, µM)	Statistical differences	Compound	K562 (IC_{50} ± s.d, µM)	Statistical differences
DC1	n.d.	n.d.	**PHYD1**	n.d.	n.d.	**Q3C1**	n.d.	n.d.
DC2	n.d.	n.d.	**PHYD2**	n.d.	n.d.	**Q3C2**	n.d.	n.d.
DC3	n.d.	n.d.	**PHYD3**	61.99 ± 5.65	*ns (P = 0.6064)	**Q3C3**	n.d.	n.d.
DC4	n.d.	n.d.	**PHYD4**	32.40 ± 3.93	Yes (P <0.0001)	**Q3C4**	n.d.	n.d.
DC5	n.d.	n.d.	**PHYD5**	n.d.	n.d.	**Q3C5**	n.d.	n.d.
DC6	n.d.	n.d.	**PHYD6**	33.80 ± 1.40	Yes (P <0.0001)	**Q3C6**	n.d.	n.d.
DC7	n.d.	n.d.	**PHYD7**	n.d.	n.d.	**Q3C7**	37.80 ± 5.02	Yes (P <0.0001)
DC8	n.d.	n.d.	**PHYD8**	18.12 ± 2.87	Yes (P <0.0001)	**Q3C8**	3.58 ± 0.42	Yes (P <0.0001)
DC9	n.d.	n.d.	**PHYD9**	18.21 ± 0.05	Yes (P <0.0001)	**Q3C9**	24.2 ± 4.62	Yes (P <0.0001)
DC10	n.d.	n.d.	**PHYD10**	n.d.	n.d.	**Q3C10**	n.d.	n.d.
DC11	n.d.	n.d.	**PHYD11**	n.d.	n.d.	**Q3C11**	31.16 ± 1.79	Yes (P <0.0001)
DC12	8.86 ± 1.15	Yes (P <0.0001)	**PHYD12**	20.91 ± 1.98	Yes (P <0.0001)	**Q3C12**	n.d.	n.d.
DC13	39.59 ± 6.51	Yes (P = 0.0002)	**PHYD13**	37.64 ± 7.2	Yes (P <0.0001)			
DC14	57.35 ± 5.23	ns (P = 0.1995)	**PHYD14**	130.03 ± 23.01	Yes (P <0.0001)	**Cisplatin**	73.74 ± 7.76	-
DC15	n.d.	n.d.	**PHYD15**	28.51 ± 2.76	Yes (P <0.0001)	**Quinine**	93.85 ± 19.13	n.s. (P = 0.0606)

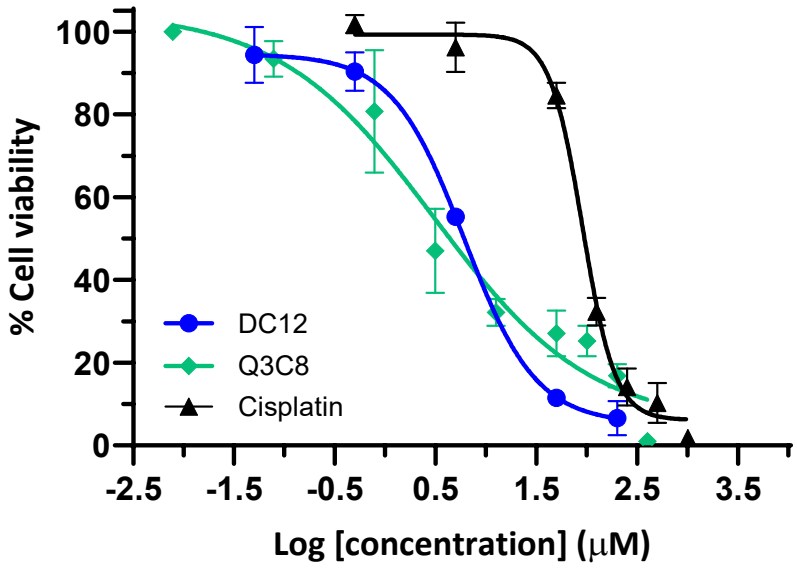


Figure 3.7: Dose-dependent cytotoxic effect of the most active compounds, **DC12** and **Q3C8** against chronic myelogenous leukaemia K562 cell line in comparison to cytotoxic control cisplatin using the MTT assay.

Compounds **DC12, PHYD8** and **Q3C8** were the most cytotoxic in their respective dihydroquinoline-carbothioamide, phenyl-hydrazono group and quinoline-3-carboxamide groups. Compound **Q3C8** was the most cytotoxic compound across all three groups of compounds with an IC_{50} value of 3.58 ± 0.42 μM (Figure 3.8).

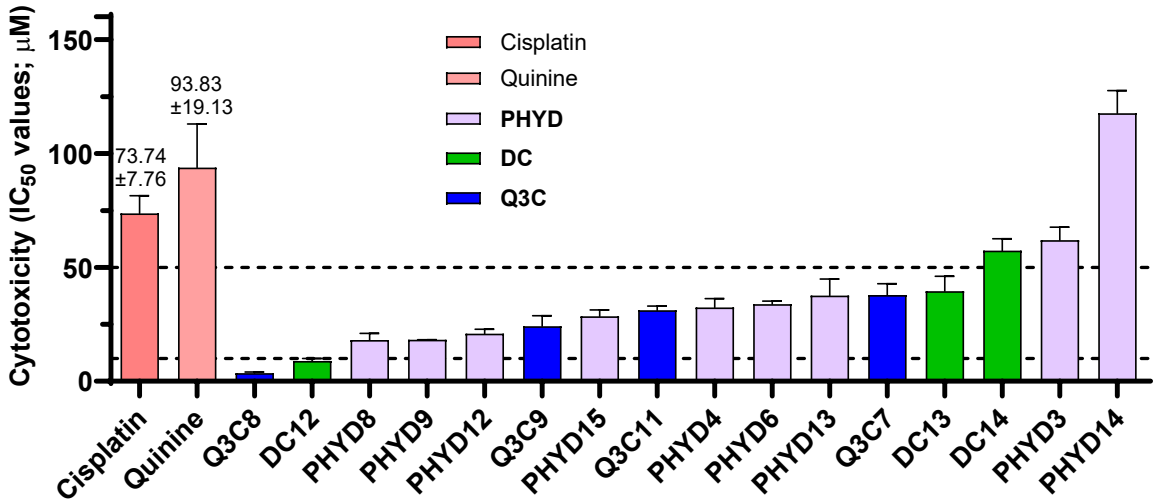


Figure 3.8: The cytotoxic effect of dihydroquinoline-carbothioamide (**DC**), phenyl-hydrazono (**PHYD**) and quinoline-3-carboxamide (**Q3C**) compound groups on human K562 cells compared to cisplatin (positive control) (n=3).

3.6 Cytotoxic combination studies

Test compounds **DC12** and **Q3C8** demonstrated the most cytotoxic activity of all the test compounds with IC_{50} values of 8.86 µM and 3.58 µM, respectively (Table 3.6) against the human chronic myelogenous leukaemia cell line. These compounds were thus selected for further investigation in combination with cisplatin against the K562 cell line using the MTT assay. The combination of **DC12** with cisplatin demonstrated primarily a synergistic effect with an average ΣFIC value of 0.59 as verified by the points below the synergistic line in the isobologram (Figure 3.9.A). The presence of points above the synergistic line in the isobologram indicated that there was an additive effect at higher concentration ratios of **DC12**. The combination of **Q3C8** demonstrated a predominantly synergistic effect with an average ΣFIC value of 0.53. As with compound **DC12**, the presence of points above the synergistic line in the isobologram (Figure 3.9.B) indicated that there was an additive effect at higher concentration ratios of **Q3C8**.

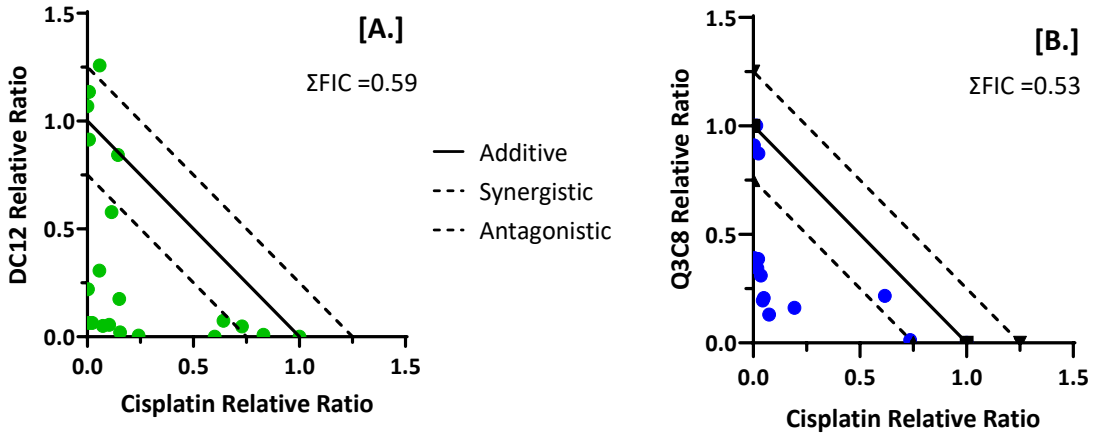


Figure 3.9: Isobolograms displaying the drug interactions between test compound **DC12** (A) and **Q3C8** (B) in combination with cisplatin against the human chronic myelogenous leukaemia K562 cell line using the MTT assay.

3.7 Safety and selectivity Index

The safety index of each of the test compounds were calculated to determine selectivity of the compounds towards the human epithelial kidney (HEK293) cells or NF54 *P. falciparum* intra-erythrocytic parasites. The selectivity index of each of the test compounds were also

calculated to determine selectivity towards the HEK293 cells or the chronic myelogenous leukaemia cells (K562) (Table 3.7). The safety or selectivity indices were calculated using the viability of the respective cell line or parasite viability at the screening concentration of 50 µM. Test compound **DC14**, **PHYD3** and **Q3C7** displayed higher selectivity towards the malaria parasite with values ranging from 7.99-11.13.

Table 3.7: The selectivity index (or safety profile) of the test compounds corresponding to their respective antimalarial and cytotoxic activity at the screening concentration of 50 µM. Where SI-HEK293/*Pf* represents the safety index of HEK293 vs NF54 parasite; SI-HEK293/K562 represents the safety index of HEK293 vs NF54 parasite; values <1 indicate higher activity towards HEK 293, and n.d: not determined; CQ: Chloroquine and QN: Quinine.

Com-pound	SI - HEK293:*Pf*	SI – HEK293:K562	Com-pound	SI - HEK293:*Pf*	SI - HEK293:K562	Com-pound	SI - HEK293:*Pf*	SI - HEK293:K562
DC1	2.26	0.87	**PHYD1**	2.78	0.69	**Q3C1**	1.41	0.81
DC2	1.99	0.90	**PHYD2**	3.01	0.70	**Q3C2**	1.31	0.86
DC3	4.11	0.88	**PHYD3**	9.11	1.15	**Q3C3**	2.17	0.89
DC4	6.03	0.73	**PHYD4**	0.92	0.93	**Q3C4**	0.89	0.86
DC5	2.09	0.71	**PHYD5**	1.22	0.70	**Q3C5**	1.19	1.53
DC6	4.44	0.65	**PHYD6**	0.75	1.35	**Q3C6**	1.16	0.85
DC7	1.68	0.63	**PHYD7**	0.82	0.63	**Q3C7**	7.99	1.96
DC8	6.05	0.60	**PHYD8**	0.93	3.53	**Q3C8**	1.05	1.90
DC9	7.04	0.72	**PHYD9**	1.31	1.35	**Q3C9**	1.00	1.20
DC10	4.34	0.76	**PHYD10**	0.99	0.59	**Q3C10**	1.61	0.85
DC11	5.32	0.87	**PHYD11**	0.81	0.68	**Q3C11**	7.55	1.67
DC12	1.96	1.65	**PHYD12**	0.98	2.67	**Q3C12**	2.30	0.99
DC13	4.41	1.09	**PHYD13**	0.94	1.48	**CQ**	6414.04	2.62
DC14	11.13	1.16	**PHYD14**	1.04	1.64	**QN**	11.98	0.87
DC15	1.16	0.63	**PHYD15**	1.35	2.65	**Cisplatin**	n.d	1.17

3.8 *Artemia* lethality

3.8.1 *Artemia* lethality studies

The test compounds were screened at 50 µM against *Ar. franciscana* nauplii over 72 hours as described in Section 2.8.2. From the DC group of test compounds, four compounds possessed time dependent toxicity towards the *Ar. franciscana* nauplii. From the **PHYD** group of test

compounds, five compounds displayed toxicity. Lastly from the **Q3C** group of test compounds, three were toxic towards the nauplii.

The three sets of novel test compounds displayed moderate to high activity in comparison with positive control potassium dichromate at 50 µM (100% mortality after 72 hours) in a time dependant manner. All three groups had compounds that displayed *Ar. franciscana* nauplii mortality up to 87% (range: 0-87%) after 48 hours. The three groups of test compounds displayed higher *Ar. franciscana* mortality at the 72 hour time period (Table 3.8).

The DC group test compounds displayed *Ar. franciscana* mortality up to 96.86% (range: 20.87-96.86%) after 72 hours with compounds DC12 (86.48%), DC13 (70.05%) and **DC14** (96.86%) being the most active from this group. The PHYD group test compounds displayed mortality up to 98.21% (range: 19.23-98.21%) after 72 hours with compounds PHYD1 (89.05%), PHYD2 (98.21%) and PHYD3 (76.44%) being the most active. Lastly the Q3C group test compounds displayed mortality up to 87.50% (range: 22.09-87.50%) after 72 hours with compound Q3C3 (71.49%), Q3C7 (83.52%) and **Q3C11** (87.50%) being the most active in this group (Table 3.8).

The test compounds from each group that displayed higher than 50% mortality at 48 hours and 72 hours were investigated further to determine LC_{50} values. The LC_{50} values for these compounds demonstrated toxicity, where the lower the LC_{50} values the more toxic the compound (Table 3.9). Test compound **PHYD1** and test compound **PHYD2** displayed the highest toxicity with the lowest IC_{50} values of the test compounds.

3.8.2 Morphological effects of the test compounds on the *Ar. franciscana* nauplii

The untreated nauplii served as the negative control and displayed normal morphological features which contrasted with the altered features of the nauplii treated with the positive control potassium dichromate (Table 3.10). Compounds **DC12**, **DC14**, **PHYD1**, **PHYD2**, **Q3C3** and **Q3C11** have their morphological features after 72 hours described in Table 3.10 in comparison with positive control potassium dichromate and the untreated negative control.

Table 3.8: The percentage *Ar. franciscana* nauplii mortality at 48 and 72 hours for each of the test compounds (0.5 µM) in comparison with positive control potassium dichromate at 50 µM. Data for mortality after 24 hours is in Appendix F, Table F1.

Compound	% Nauplii Mortality at 48 hours	% Nauplii Mortality at 72 hours	Compound	% Nauplii Mortality at 48 hours	% Nauplii Mortality at 72 hours	Compound	% Nauplii Mortality at 48 hours	% Nauplii Mortality at 72 hours
DC1	0.43	20.87	**PHYD1**	77.36	89.06	**Q3C1**	14.18	24.63
DC2	1.71	41.30	**PHYD2**	87.00	98.21	**Q3C2**	16.22	28.83
DC3	8.50	59.80	**PHYD3**	51.44	76.44	**Q3C3**	22.90	71.50
DC4	3.53	32.16	**PHYD4**	22.73	33.77	**Q3C4**	16.46	30.04
DC5	0.66	21.26	**PHYD5**	40.76	56.69	**Q3C5**	11.04	42.86
DC6	3.46	26.64	**PHYD6**	26.09	39.86	**Q3C6**	9.94	22.10
DC7	0.47	22.27	**PHYD7**	25.19	38.93	**Q3C7**	31.87	83.52
DC8	4.71	30.89	**PHYD8**	17.80	23.73	**Q3C8**	5.68	25.00
DC9	4.21	36.78	**PHYD9**	12.12	22.73	**Q3C9**	6.42	37.43
DC10	1.14	22.43	**PHYD10**	12.31	19.23	**Q3C10**	14.07	41.48
DC11	5.86	39.19	**PHYD11**	33.87	52.42	**Q3C11**	20.45	87.50
DC12	58.72	86.48	**PHYD12**	23.58	34.15	**Q3C12**	3.11	31.09
DC13	52.79	70.05	**PHYD13**	17.59	22.22	**K2Cr2O7 (0.5um)**	2.82	5.73
DC14	81.15	96.86	**PHYD14**	13.33	23.81	**K2Cr2O7 (50uM)**	28.76	100.00
DC15	10.56	39.13	**PHYD15**	18.58	35.40	**DDT**	28.93	100.00

Table 3.9: The LC_{50} values of the active test compounds and controls as determined by the *Artemia* lethality assay in comparison to positive control, potassium dichromate.

Compound	*Ar. franciscana* (LC_{50}; µM)	Significant difference to the LC_{50} value of Potassium Dichromate control
DC3	60.45	Yes (P <0.0001)
DC12	7.95	Yes (P <0.0001)
DC13	18.65	Yes (P <0.0001)
DC14	2.68	Yes (P <0.0001)
PHYD1	0.55	Yes (P <0.0001)
PHYD2	1.36	Yes (P <0.0001)
PHYD3	9.36	Yes (P <0.0001)
PHYD5	15.62	Yes (P <0.0001)
PHYD11	9.36	Yes (P <0.0001)
Q3C3	6.50	Yes (P <0.0001)
Q3C7	21.64	Yes (P <0.0001)
Q3C11	7.83	Yes (P <0.0001)
DDT	0.366	Yes (P <0.0001)
Potassium dichromate	31.72	Yes (P <0.0001)

Table 3.10: The morphological effects of the two most active compounds from each compound group on the *Ar. franciscana* nauplii after a 72 hour period in comparison to positive control potassium dichromate and untreated negative control. Images were captured using an Olympus® CKX53 microscope using CellSens™ software at 40x total magnification.

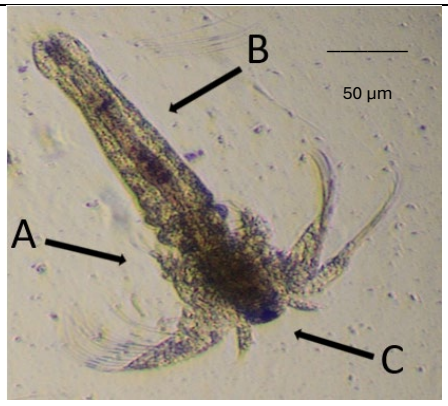
Compound	***Ar. franciscana* nauplii**	**Description**
Untreated (Negative) control		A – Fully developed and swimming appendages present. B – Clear body colour. Intestine visible. C- Eye visible.

Table 3.10 continued: The morphological effects of the two most active compounds from each compound group on the *Ar. franciscana* nauplii after a 72 hour period in comparison to positive control potassium dichromate and untreated negative control. Images were captured using an Olympus® CKX53 microscope using CellSens™ software at 40x total magnification.

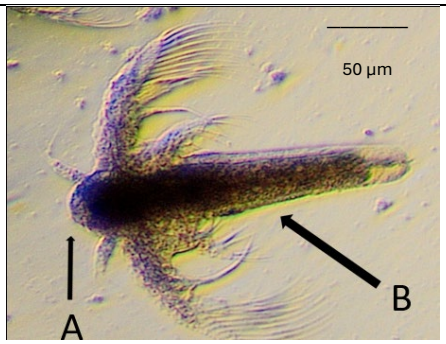
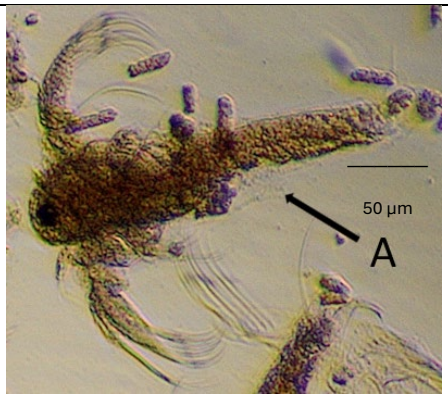
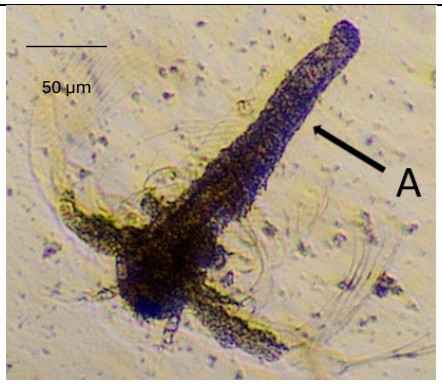
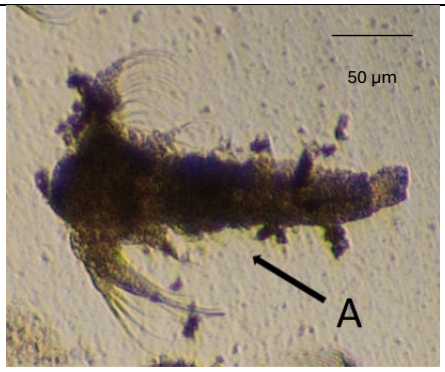
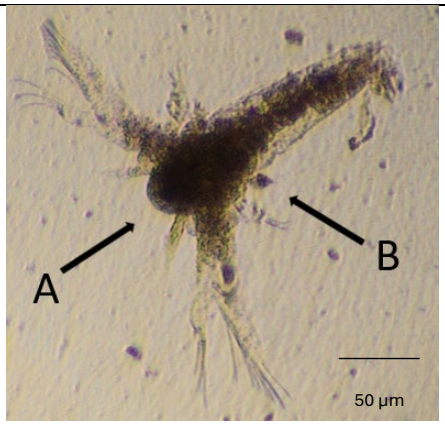
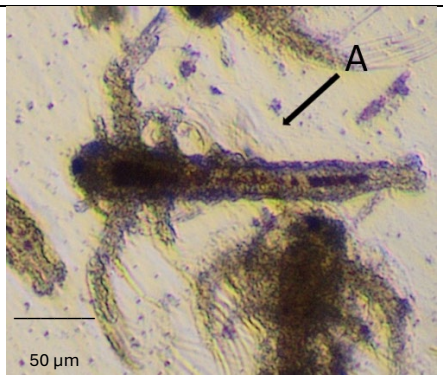
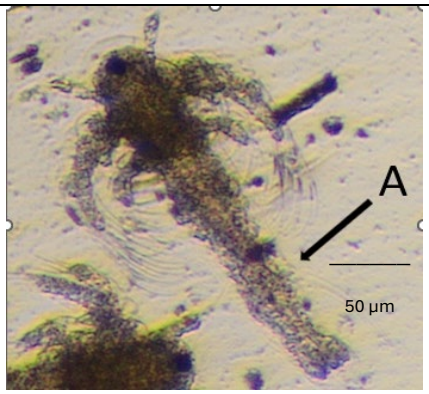
Potassium Dichromate		A – Eye not visible. B – Darkened body, reduced size and stunted growth.
DC12		A – Body is distorted and appears disfigured.
DC14		A – Body is elongated and darkened. Swimming appendages are not fully developed.
PHYD1		A – Body is shrivelled and darkened throughout. No antenna present. Eye not visible

Table 3.10 continued: The morphological effects of the two most active compounds from each compound group on the *Ar. franciscana* nauplii after a 72 hour period in comparison to positive control potassium dichromate and untreated negative control. Images were captured using an Olympus® CKX41 microscope using CellSens™ software at 10x total magnification.

PHYD2		A – Head region darkened. Eye not visible B – Total body size reduced
Q3C3		A – Body is elongated and swimming appendages appear under-developed
Q3C11		A – Body appears shrunken and abdominal region elongated

3.9 Anti-Oxidant and Iron Chelating Activity

3.9.1 Free Radical Scavenging

The IC_{50} value of Trolox and ascorbic acid were 14.73 ± 1.2 µM and 22.56 ± 2.25 µM, respectively as determined by the $DPPH^{\bullet}$ free radical scavenging assay (Section 2.9.2.1). The test compounds displayed minimal free radical scavenging activity at 50 µM ranging from 0.01% to 28.75%, with compound **DC15** the most active compound.

3.9.2 Iron Chelation

The iron chelation assay was used to determine the ferrous iron binding affinity of the test compounds in comparison to the positive control EDTA (IC_{50}: 2.56 ± 0.37 µM). All three groups of test compounds possessed a low binding affinity for Fe^{2+} at 50 µM where the percentage iron chelation ranged between 0.01% to 25.87% in comparison to EDTA which had 100% chelation. The most active compound was **Q3C5** with 25.87 ± 5.57 ferrous iron chelating activity at 50 µM.

3.10 Computational Analysis

3.10.1 Drug-likeness predictions

All three groups of test compounds were analysed for their drug-likeness properties in accordance with Lipinski's rule of five (Table 3.11). The predicted pharmacokinetic properties of each group of test compounds are listed in Table 3.12, Table 3.13 and Table 3.14, respectively; with the pKa, ionisation and absorption properties displayed in Table 3.15.

Table 3.11: The predicted molecular properties of the dihydroquinoline-carbothioamide and phenyl-hydrazono hybrids screened against *P. falciparum* based on Lipinski's Rule of Five (Lipinski *et al*., 1997). Where MW: molecular weight; Log $P_{o/w}$: Log P Octanol/Water; HBD: Hydrogen Bond Donor; HBA: Hydrogen Bond Acceptor.

Compound code	MW (<500 g/mol)	Log $P_{o/w}$ (<4.15)	HBD (<5)	HBA (<10)	Rule of 5 violation
Dihydroquinoline-carbothioamide hybrids					
DC1	246.29	1.34	3	2	No
DC2	260.32	1.68	3	2	No
DC3	325.18	1.97	3	2	No
DC4	280.73	1.87	3	2	No
DC5	264.28	1.65	3	3	No
DC6	260.31	1.67	3	2	No
DC7	274.34	1.95	3	2	No
DC8	339.21	2.31	3	2	No
DC9	294.76	2.21	3	2	No
DC10	278.31	1.99	3	3	No
DC11	322.38	2.95	3	2	No
DC12	336.41	3.21	3	2	No
DC13	401.28	3.56	3	2	No
DC14	356.83	3.47	3	2	No
DC15	340.37	3.24	3	3	No
Phenyl-hydrazono hybrids					
PHYD1	288.31	2.75	1	4	No
PHYD2	302.33	2.99	1	4	No
PHYD3	367.2	3.36	1	4	No
PHYD4	322.75	3.26	1	4	No
PHYD5	306.30	3.04	1	5	No
PHYD6	306.30	3.09	1	5	No
PHYD7	320.32	3.43	1	5	No
PHYD8	385.19	3.70	1	5	No
PHYD9	340.74	3.62	1	5	No
PHYD10	324.29	3.39	1	6	No
PHYD11	306.30	2.98	1	5	No
PHYD12	320.32	3.31	1	5	No
PHYD13	385.19	3.68	1	5	No
PHYD14	340.74	3.49	1	5	No
PHYD15	324.29	3.27	1	6	No

Table 3.11 continued: The predicted molecular properties of the dihydroquinoline-carbothioamide and phenyl-hydrazono hybrids screened against *P. falciparum* based on Lipinski's Rule of Five (Lipinski *et al*., 1997). Where MW: molecular weight; Log $P_{o/w:}$; HBD: ; HBA: .

Compound	MW (<500 g/mol)	Log $P_{o/w}$ (<4.15)	HBD (<5)	HBA (<10)	Rule of 5 violation
Quinoline-3-carboxamide hybrids					
Q3C1	282.72	3.45	1	2	No
Q3C2	296.75	3.77	1	2	No
Q3C3	300.71	3.75	1	3	No
Q3C4	300.71	3.77	1	3	No
Q3C5	310.78	4.12	1	2	No
Q3C6	314.74	4.08	1	3	No
Q3C7	317.17	3.99	1	2	No
Q3C8	314.74	4.08	1	3	No
Q3C9	335.16	4.29	1	3	No
Q3C10	314.74	4.08	1	3	No
Q3C11	335.16	4.29	1	3	No
Q3C12	318.71	4.07	1	4	No
Control					
Quinine	324.42	2.81	1	4	No

Table 3.12: The predicted pharmacokinetic properties of the dihydroquinoline-carbothioamide test compounds screened against *P. falciparum* using SwissADME and Chemicalize web-based software and ToxTree Version 3.1.0-1851. Where GI: Gastro Intestinal ; BBB: Blood Brain Barrier ; Log K_p: Skin Permeability Coefficient ; P-gp: P-Glycoprotein

	Pharmacokinetic predictions					Cytochrome P450 metabolism		Cramer's Rule
Compound	**GI absorption**	**Bioavailability score**	**BBB permeability**	**Log Kp-Skin permeation (cm/s)**	**P-gp substrate**	**Primary site of metabolism**	**CYP3A4 Inhibitor**	**Toxic Hazard**
DC1	High	0.55	No	-7.21	No	Aromatic Hydroxylation	No	High (Class III)
DC2	High	0.55	No	-7.04	No	Aliphatic Hydroxylation	No	High (Class III)
DC3	High	0.55	No	-7.21	No	N-Oxidation	No	High (Class III)
DC4	High	0.55	No	-6.98	No	N-Oxidation	No	High (Class III)
DC5	High	0.55	No	-7.26	No	N-Oxidation	No	High (Class III)
DC6	High	0.55	No	-7.02	No	N-Dealkylation	No	High (Class III)
DC7	High	0.55	No	-6.84	No	N-Dealkylation	No	High (Class III)
DC8	High	0.55	No	-7.01	No	N-Dealkylation	Yes	High (Class III)
DC9	High	0.55	No	-6.78	No	N-Dealkylation	No	High (Class III)
DC10	High	0.55	No	-7.06	No	N-Dealkylation	No	High (Class III)
DC11	High	0.55	No	-6.29	No	Aromatic Hydroxylation	Yes	High (Class III)
DC12	High	0.55	No	-6.12	No	Aliphatic Hydroxylation	Yes	High (Class III)
DC13	High	0.55	No	-6.28	No	Aromatic Hydroxylation	Yes	High (Class III)
DC14	High	0.55	No	-6.06	No	Aromatic Hydroxylation	Yes	High (Class III)
DC15	High	0.55	No	-6.33	No	Aromatic Hydroxylation	Yes	High (Class III)
Reference antimalarial								
Quinine	High	0.55	Yes	-6.23	No	N-Oxidation	No	High (Class III)

Table 3.13: The predicted pharmacokinetic properties of the phenyl-hydrazono test compounds screened against *P. falciparum* using SwissADME and Chemicalize web-based software and ToxTree Version 3.1.0-1851. Where GI: Gastro Intestinal ; BBB: Blood Brain Barrier ; Log K_p: Skin Permeability Coefficient ; P-gp: P-Glycoprotein

Compound	Pharmacokinetic predictions					Cytochrome P450 metabolism		Cramer's Rule
	GI absorption	Bioavailability score	BBB permeability	Log Kp-Skin permeation (cm/s)	P-gp substrate	Primary site of metabolism	CYP3A4 Inhibitor	Toxic Hazard
PHYD1	High	0.55	Yes	-5.74	No	Amine Hydroxylation	No	High (Class III)
PHYD2	High	0.55	Yes	-5.57	No	Amine Hydroxylation	No	High (Class III)
PHYD3	High	0.55	Yes	-5.74	No	Amine Hydroxylation	No	High (Class III)
PHYD4	High	0.55	Yes	-5.51	No	Amine Hydroxylation	No	High (Class III)
PHYD5	High	0.55	Yes	-5.78	No	Amine Hydroxylation	No	High (Class III)
PHYD6	High	0.55	Yes	-5.78	No	Amine Hydroxylation	No	High (Class III)
PHYD7	High	0.55	Yes	-5.61	No	Amine Hydroxylation	No	High (Class III)
PHYD8	High	0.55	Yes	-5.77	No	Amine Hydroxylation	No	High (Class III)
PHYD9	High	0.55	Yes	-5.55	No	Amine Hydroxylation	No	High (Class III)
PHYD10	High	0.55	Yes	-5.82	No	Amine Hydroxylation	No	High (Class III)
PHYD11	High	0.55	Yes	-5.78	No	Amine Hydroxylation	No	High (Class III)
PHYD12	High	0.55	Yes	-5.61	No	Amine Hydroxylation	No	High (Class III)
PHYD13	High	0.55	Yes	-5.77	No	Amine Hydroxylation	No	High (Class III)
PHYD14	High	0.55	Yes	-5.55	No	Amine Hydroxylation	No	High (Class III)
PHYD15	High	0.55	Yes	-5.82	No	Amine Hydroxylation	No	High (Class III)
Reference antimalarial								
Quinine	High	0.55	Yes	-6.23	No	N-Oxidation	No	High (Class III)

Table 3.14: The predicted pharmacokinetic properties of the quinoline-3-carboxamide test compounds screened against *P. falciparum* using SwissADME and Chemicalize web-based software and ToxTree Version 3.1.0-1851. Where GI: Gastro Intestinal ; BBB: Blood Brain Barrier ; Log K_p: Skin Permeability Coefficient ; P-gp: P-Glycoprotein

Compound	Pharmacokinetic predictions					Cytochrome P450 metabolism		Cramer's Rule
	GI absorption	Bioavailability score	BBB permeability	Log Kp-Skin permeation (cm/s)	P-gp substrate	Primary site of metabolism	CYP3A4 Inhibitor	Toxic Hazard
Q3C1	High	0.55	Yes	-5.19	No	Aromatic Hydroxylation	Yes	High (Class III)
Q3C2	High	0.55	Yes	-5.02	No	Aliphatic Hydroxylation	Yes	High (Class III)
Q3C3	High	0.55	Yes	-5.23	No	Aromatic Hydroxylation	Yes	High (Class III)
Q3C4	High	0.55	Yes	-5.23	No	Aromatic Hydroxylation	Yes	High (Class III)
Q3C5	High	0.55	Yes	-4.84	No	Aromatic Hydroxylation	Yes	High (Class III)
Q3C6	High	0.55	Yes	-5.06	No	Aliphatic Hydroxylation	Yes	High (Class III)
Q3C7	High	0.55	Yes	-4.96	No	Aromatic Hydroxylation	Yes	High (Class III)
Q3C8	High	0.55	Yes	-5.06	No	Aliphatic Hydroxylation	Yes	High (Class III)
Q3C9	High	0.55	Yes	-5.00	No	N-Oxidation	Yes	High (Class III)
Q3C10	High	0.55	Yes	-5.06	No	Aliphatic Hydroxylation	Yes	High (Class III)
Q3C11	High	0.55	Yes	-5.00	No	N-Oxidation	Yes	High (Class III)
Q3C12	High	0.55	Yes	-5.27	No	N-Oxidation	Yes	High (Class III)
Reference antimalarial								
Quinine	High	0.55	Yes	-6.23	No	N-Oxidation	No	High (Class III)

Table 3.15: The predicted pKa values and percentage ionisation of the test compounds compared to quinine at physiological pH (7.4) of the human plasma and red blood cell compared to the acidic food vacuole pH (5) of the *P. falciparum* parasite.

Compound	Compound code	pKa	%Ionisation		LogD at pH 5
			pH 7.4	pH 5	
Dihydroquinoline-carbothioamide hybrids	DC1	10.84; 1.17	0.04	0.01	1.00
	DC2	11.07; 1.25	0.02	0.02	1.51
	DC3	10.8; 0.94	0.04	0.01	1.77
	DC4	10.81; 051	0.04	0.00	1.61
	DC5	11.02; 0.51	0.02	0.00	1.15
	DC6	10.79; 1.22	0.04	0.02	1.23
	DC7	11; 1.3	0.03	0.02	1.74
	DC8	10.76; 1	0.04	0.01	1.99
	DC9	10.77; 0.59	0.04	0.00	1.83
	DC10	10.95; 0.6	0.03	0.00	1.37
	DC11	10.78; 1.12	0.04	0.01	3.25
	DC12	10.97; 1.18	0.03	0.02	3.76
	DC13	10.74; 0.94	0.05	0.01	4.01
	DC14	10.75; 0.61	0.04	0.00	3.51
	DC15	10.93; 0.62	0.03	0.00	3.39
Phenyl-hydrazono hybrids	PHYD1	15.73	0.00	0.00	3.65
	PHYD2	15.73	0.00	0.00	4.16
	PHYD3	15.72	0.00	0.00	4.42
	PHYD4	15.72	0.00	0.00	4.25
	PHYD5	15.72	0.00	0.00	3.79
	PHYD6	13.61	0.00	0.00	3.79
	PHYD7	13.62; -1.86	0.00	0.00	4.31
	PHYD8	13.61	0.00	0.00	4.56
	PHYD9	13.6	0.00	0.00	4.4
	PHYD10	13.6; -1.85	0.00	0.00	3.93
	PHYD11	15.79	0.00	0.00	3.79
	PHYD12	15.8; -1.86	0.00	0.00	4.31
	PHYD13	15.78	0.00	0.00	4.56
	PHYD14	15.78	0.00	0.00	4.4
	PHYD15	15.78	0.00	0.00	3.93
Quinoline-3-carboxamide hybrids	Q3C1	14.91; -0.25	0.00	0.00	4.05
	Q3C2	14.98; -0.25	0.00	0.00	4.56
	Q3C3	14.71; -0.25	0.00	0.00	4.19
	Q3C4	14.39; -1.12	0.00	0.00	4.19
	Q3C5	15.03; -0.1	0.00	0.00	5.07
	Q3C6	14.77; -0.1	0.00	0.00	4.7
	Q3C7	14.57; -1.17	0.00	0.00	4.65
	Q3C8	14.46; -1.12	0.00	0.00	4.70
	Q3C9	14.38; -1.17	0.00	0.00	4.79
	Q3C10	14.77; -0.1	0.00	0.00	4.7
	Q3C11	14.38; -1.17	0.00	0.00	4.79
	Q3C12	14.2; -1.12	0.00	0.00	4.33
Control	Quinine	13.89; 8.55	6.61	99.97	-0.80

CHAPTER 4 – DISCUSSION

The emergence of resistance to artemisinin and partner drugs poses a significant risk to global efforts to reduce the burden of malaria. The rapid and effective treatment of malaria is a key component in the fight against the disease and this has warranted the design and development of novel compounds (WHO, 2023a). In addition to parasite resistance to some of the current malaria medicines available, mosquito resistance to insecticides is also a threat towards the eradication of the disease. Since 2021, insecticide resistance data has been reported to the WHO and there have been confirmed cases of malaria vector species resistant to insecticides across all WHO regions to varying extents (WHO, 2023a).

In this study, the *in vitro* antimalarial, larvicidal and ovicidal activity of forty-two heterocyclic quinoline derivatives were assessed and their preliminary toxicological profile elucidated. These forty-two derivatives were grouped into three groups of test compounds. Namely the dihydroquinoline-carbothioamide, phenyl-hydrazono and quinoline-3-carboxamide group test compounds.

The development of hybrid compounds allows for the potential benefit of higher efficacy than that of the parent compound. The working idea of hybridisation was to decrease drug resistance, escalate the binding affinity and biological activity of combination therapy into monotherapy and in the process offer a single molecular agent with one pharmacokinetic profile (Alkhzem *et al.*, 2022). Based on the activity of the hybrid, this could then be further investigated or combined with the current recommended antimalarials or insecticides to combat the threat of drug or insecticide resistance in accordance with the WHO's guidelines.

The three sets of test compounds in this study were based on the quinoline pharmacophore structure which has been used to generate antimalarial drugs such as chloroquine, mefloquine and quinine as reviewed by Foley and Tilley (1997). The quinoline pharmacophore structure can therefore be used as a scaffold upon which hybrid heterocyclic compounds be developed. Given the relatively good safety profile of the quinoline pharmacophore, the core structure was retained and additional side chains added to produce single agent compounds with the possibility of a dual action towards the malaria parasite and *Anopheles* vector. The chemical

group attached to points R1 and R2 on the base structures synthesised varied for each compound (Tables 2.1, 2.2 and 2.3). This variation elicited chemical-structural activity effects associated with the type of group substituted into various positions. Importantly all compounds complied with Lipinski's *Rule of five* and thus deemed to be "drug-like" and orally bioactive in humans as potential oral drug candidates (Table 3.11) (Lipinski *et al*., 1997). *In silico* analysis of all of the test compounds indicated that they had a good bioavailability score, high GI absorption and low skin permeation, (Table3.12-3.14), which warranted further pharmacological investigations.

4.1.1 Phenyl-hydrazono derivatives

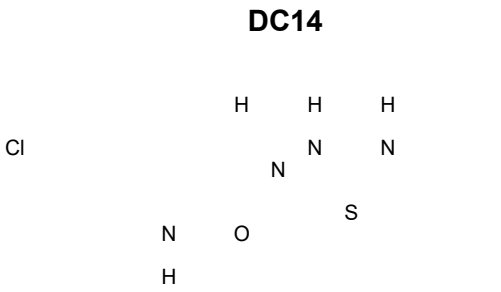
When evaluating a new compound series, the inhibitory activity needs to be directed to the malaria parasite itself and not affect the membrane integrity of the red blood cell. This was found to be the case for all forty-two compounds across all three groups of derivatives in this study (Section 3.5.1). With preliminary haematological safety obtained, the effect on the intra-erythrocytic parasite was assessed. The phenyl-hydrazono group derivatives inhibited the growth of NF54 strain of *P. falciparum* in a dose-dependent manner but were significantly less active than the **DC** and **Q3C1** compounds (Table 3.1). Of the fifteen derivatives in the **PHYD** group, only compounds **PHYD1**, **PHYD2**, **PHYD3** and **PHYD9** had IC_{50} values that ranged between 127.75 and 160.4 µM (Table 3.1); which can be regarded to have very poor to no specific inhibitory activity towards the *Plasmodium* parasites. Notably the substitution of the R1 group with a hydrogen or a methyl group in preference to a chloro-, bromo- or fluoro-halogen group resulted slightly better antimalarial activity; but overall, these compounds did not display significant antimalarial activity targeting the malaria parasite. While the presence of a halogen instead of hydrogen/methyl group has overall been reported to improve the biological activity of potential antimalarial drugs (Metrangolo & Resnati, 2008), this was not the trend observed with this group of test compounds. Amengor *et al*. (2024) found that a series of phenylhydrazone derivatives with different substituents on the aromatic ring tested against a chloroquine-sensitive (3D7) and -resistant (DD2) *P. falciparum* did in fact kill the ring stages of the parasite within an IC_{50} range of 1.29 to 34.89 µM. Thus showing there is potential for phenylhydrazone derivatives, however the current set in this study do not warrant any

further research as antimalarials (Table 3.1) or as larvicides (Table 3.3) due to low activity and high toxicity against the *Artemia* nauplii (Table 3.9).

4.1.2 Dihydroquinoline-carbothioamide derivatives

Overall, the dihydroquinoline-carbothioamide derivatives displayed promising to no activity with the IC_{50} values ranged between 7.23 and 157.15 µM (Table 3.1) against the NF54 strain of *P. falciparum*. All fifteen **DC** test compounds displayed more than 50% parasite growth inhibition in a concentration dependent manner. The IC_{50} value of three of the DC compounds, namely **DC5**, **DC7** and **DC10** could not be determined after multiple experimental repeats (n=5) with high standard deviations between repeats. This could be due to compound instability in solution, or other undetermined physico-chemical effects related to the structure of the test compound. The limited quantity of test compound synthesised and provided also prevented further repeat analyses to determine the IC_{50} values for these three compounds.

From the **DC** group of test compounds, the most active compounds against the NF54 *P. falciparum* parasite determined using the *p*LDH assay were compounds **DC14** (IC_{50}: 7.23 ± 1.17 µM)(Figure 4.1), **DC12** (IC_{50}: 13.5 ± 2.55 µM) and **DC11** (IC_{50}: 14.56 ± 0.28 µM); which all shared a phenylthiosemicarbazone group at the R2 position (Table 2.1). Compound **DC14** had a chloro- group at the R1 position, which contributed to reduced IC_{50} values. Inam *et al.,* (2014) determined that the presence of a chloro- group in the *ortho* position improved the antimalarial properties of most compounds where their lead compounds exhibited a sub-micromolar IC_{50} value (0.78 ± 0.05 µM) against the chloroquine-, quinine-resistant W2 strain of *P. falciparum*. Compound **DC14** possessed a chloro- moiety at the R1 group and this is consistent with the latter study's findings. However, the IC_{50} value of compound **DC14** represented an 80.3-fold lower activity than the standard antimalarial drug, quinine (0.09 ± 0.005 µM) indicating that compound **DC14** would need further derivatisation to improve its antimalarial properties (Table 3.1). In contrast, the addition of a bromine or fluorine group at the R1 position led to a significant decrease in antimalarial activity of all three set of **DC** derivatives (Table 3.1). Halogenation of the dihydroquinoline-carbothioamide test compounds at the R1 group slightly improved the antimalarial activity of those test compounds with a chloro- moiety at the *ortho* position in preference to the addition of bromine and fluorine.



(2*E*)-2-[(6-chloro-2-oxo-1,2-dihydroquinolin-3-yl)methylidene]-*N*-phenylhydrazine-1-carbothioamide

Antimalarial properties

Plasmodium Growth Inhibited	Combination Interaction; ΣFIC	Larvicidal (Mortality)	Ovicidal (Mortality)
100% at 50 µM IC_{50}: 7.23 ± 1.17 µM *ns (P = 0.9993)	Synergistic with quinine ΣFIC = 0.58	6.67% ± 11.55 at 0.5 µM	16.25% ± 13.75 at 0.5 µM

Antioxidant, iron chelating properties

DPPH• Free Radical Scavenging	Ferrous Ion Chelation
15.3% ± 2.06	0.1% ± 0.10

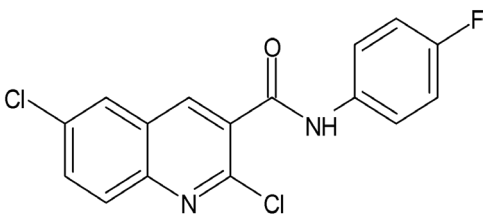
Toxicity properties

K562 Cells (% cellular viability)	HEK293 Cells (% cellular viability)	Selectivity Index (HEK 293 vs NF54)	Haemolysis	*Artemia* lethality (Mortality)
52.94% at 50 µM IC_{50}: 57.35 ± 5.23 µM *ns (P = 0.1995)	61.53% at 50 µM IC_{50}: n.d	11.13	0.1 ± 0.01% at 50 µM	96.86% ± 1.08 at 0.5µM LC_{50} = 2.68 µM Yes (P <0.0001)

Toxic Hazard class	Cytochrome P450 (CYP3A4 inhibition)	BBB	LogD (pH 5)	P-glycoprotein substrate
High (Class III)	Yes	Yes	3.506	No

Figure 4.1: The summary of the activity for test compound **DC14.** The activity of **DC14** across this study divided into its antimalarial, antioxidant and iron chelating, and toxicity properties

Q3C11



2,6-dichloro-*N*-(4-fluorophenyl)-quinoline-3-carboxamide

Antimalarial properties

Plasmodium Growth Inhibited	Combination Interaction; ΣFIC	Larvicidal (Mortality)	Ovicidal (Mortality)
89.15% at 50 µM IC_{50}: 7.99 ± 0.31 µM *ns (P = 0.9992)	Additive with quinine ΣFIC = 0.91	11.67% ± 20.21 at 0.5 µM	8.125% ± 8.00 at 0.5 µM

Antioxidant, iron chelating properties

DPPH• Free Radical Scavenging	Ferrous Ion Chelation
6.88% ± 11.10	13.38% ± 6.22

Toxicity properties

K562 Cells (% cellular viability)	HEK293 Cells (% cellular viability)	Selectivity Index (HEK 293 vs NF54)	Haemolysis	*Artemia* lethality (Mortality)
48.91% at 50 µM IC_{50}: 31.16 ± 1.79 µM Yes (P <0.0001)	81.84% at 50 µM IC_{50}: n.d	7.55	0.1% ± 0.01 at 50 µM	87.5% ± 5.91 at 0.5 µM LC_{50} = 7.83 µM Yes (P <0.0001)

Toxic Hazard class	Cytochrome P450 (CYP3A4 inhibition)	BBB	LogD (pH 5)	P-glycoprotein substrate
High (Class III)	Yes	Yes	4,7938	No

Figure 4.2: The summary of the activity for test compound **Q3C11**. The activity of **Q3C11** across this study divided into its antimalarial, antioxidant and iron chelating, and toxicity properties.

The addition of a methyl or hydrogen at position R1 with the phenylthiosemicarbazone group at the R2 position resulted in compound **DC12** and **DC11**, respectively, possessing a two-fold lower antimalarial activity than compound **D14** (Table 3.1). The addition of a methyl group to a 4-aminoquinoline pharmacophore favourably contributed to the antimalarial activity of this group of derivatives with an IC_{50} values (<0.5 µM) against both the chloroquine-sensitive (3D7) and chloroquine-resistant (K1) strain of *P. falciparum* (Tiwari *et al.*, 2021). Compound **DC12**'s IC_{50} value was statistically different to standard antimalarial quinine, with a 150-fold difference to quinine.

4.1.3 Quinoline-3-carboxamide derivatives

The quinoline-3-carboxamide derivatives had widely variable antimalarial activity with seven of the twelve compounds inhibiting more than 50% parasite growth in a dose dependant manner. The IC_{50} values of the **Q3C** compounds ranged between 7.99 and 160.09 µM (Table 3.1) indicating promising to no antimalarial activity. Compounds **Q3C3**, **QC3C7** and **Q3C11** were the most active but were not as potent as quinine. Carboxamide-based derivatives have previously shown antimalarial efficacy (IC_{50}: <2 µM) (Singh *et al.,* 2021), although the efficacy of the latter set were more potent than those in the present study (Table 3.1).

Compound **Q3C11** was the most active compound and possessed a halogen moiety on both the R1 (chloro-) and R2 (fluoro-) group which likely increased the activity of the compound. Compound **Q3C7** which had a chloro- group at the R1 position and a methyl group at the R2 position displayed 2.1-fold less activity than **Q3C11**, however in comparison with compound **Q3C3** which only had a chloro- group at the R1 position, it was 1.2-fold more active indicating that methylation at the R2 position increased its antimalarial activity slightly. The quinoline-3-carboxamide derivatives displayed a trend where the R1 groups that possessed a chloro- moiety were far more active than the compounds where the R1 group featured a hydrogen, methyl or fluorine group.

4.1.4 Lead Compounds DC14 and Q3C11

Compound **DC14** ((E)-2-((6-chloro-2-oxo-1,2-dihydroquinolin-3-yl)methylene)-N-phenylhydrazine-1-carbothioamide) and **Q3C11** (2-chloro-6-fluoro-N-p-tolylquinoline-3-

carboxamide) were overall the most active of the antimalarial compounds and investigated in more detail. In trying to elucidate at which stage the compounds targeted the malaria parasite, the parasite morphological and stage specific effects of compound **DC14** and **Q3C11**, it can be proposed that their mechanisms of action was similar to that of quinine with the trophozoite stage being affected, resulting in a subsequent decrease in total parasitaemia and second generation of rings after 48 hours of treatment. The synergistic and additive effects of compounds **DC14** and **Q3C11** could be due to the test compounds targeting similar pathways as quinine such as haemozoin formation, falcipain cysteine proteases or the generation of reactive oxidative species inducing lipid peroxidation and inhibiting parasite growth due to structural activity relationships (Zhou *et al.,* 2020; Singh *et al.,* 2021).

It was noted that both compounds **DC14** and **Q3C11** affected parasite growth slightly differently to quinine with gametocytes developing later which could be indicative of the parasites differentiating for survival under stressful environmental conditions or an internal trigger by the drugs themselves (Table 3.2) (Omorou *et al.,* 2022). Additionally, the activity of compounds **DC14** and **Q3C11** were several fold lower than that of quinine as evidenced by higher total parasitaemia for each specific stage of the parasite life cycle in comparison to quinine (Figure 3.5); which was unexpected as the IC_{50} values of all compounds were compared, but indicative that different pathways were affected by compounds **DC14** and **Q3C11** compared to quinine. This is ideal when considering combining compounds to overcome resistance or to improve on the efficacy of current monotherapy drugs.

In accordance with the WHO's guidelines and recommendations for malaria treatment (WHO, 2023b), malaria treatment should involve combination therapy rather than monotherapies to combat the emergence of resistance by rapidly clearing the parasite from the human host. A hybrid compound therefore has the added advantage of combining two pharmacophores into a singular compound, which can then be further added to an existing treatment regimen resulting in a more effective treatment if the test compound displays a synergistic or additive effect. The results from the combination studies showed that compound **DC14** displayed an overall synergistic effect in combination with standard antimalarial drug quinine (Figure 3.3. A/C). Whilst an additive effect was observed with compound **Q3C11** combined with quinine (Figure 3.3. B/D). These favourable interactions indicated that in combination with quinine,

the test compounds were more effective in inhibiting NF54 *P. falciparum* parasite growth and would be more beneficial in combination than used individually.

4.1.5 Possible mechanism of action of the quinoline heterocyclic derivatives

Quinoline was used as the base pharmacophore to generate a range of derivatives with altered side chains and substituted R1 and R2 groups featuring hydrogen, methyl or halogen groups (Table 2.1, Table 2.2 and Table 2.3). The exact mechanism of action of quinoline is not clearly understood however, various mechanisms have been proposed. Sullivan *et al.,* (1996) demonstrated that quinolines act by incorporating a drug-haem complex into haemozoin, a product of haemoglobin digestion in the malaria parasite's digestive food vacuole (DV) formed within an infected erythrocyte. This then prevents the further addition or sequestration of haem to the haemozoin polymer resulting in the toxic accumulation of haem and the eventual death of the malaria parasite within the erythrocyte (Figure 4.3). Kapishnikov *et al.* (2019) reported that quinoline-family drugs are believed to damage the parasite by capping the growing haemozoin crystals thus inhibiting deposition of haem onto the crystalline surface and complexing with free haem in the digestive vacuole. However, the latter process of complexing with free haem should be secondary in terms of inhibiting haemozoin crystal growth (Kapishnikov *et al.,* 2019).

Foley and Tilley (1997) stated that chloroquine, a quinoline based antimalarial that is a diprotic weak base, can traverse the membranes of the parasitised erythrocyte and move down the pH gradient to accumulate in the acidic food vacuole (pH = 5). The host erythrocyte haemoglobin degrades within the food vacuole leading to the release of toxic products. Iron (II) protoporphyrin IX (also known as ferriprotoporphyrin IX) is automatically oxidised to toxic iron (III) protoporphyrin IX or haematin but the malaria parasite detoxifies this to a dimerized non-toxic crystal haemozoin form. Chloroquine (and other quinoline-based compounds) interfere with this detoxification process causing the accumulation of toxic free haematin resulting in the catalysis of oxidative stress, inhibition of cysteine proteases, the dissolution of the cell membrane and the death of the parasite (Herraiz *et al.,* 2019; Zhou *et al.,* 2020). Additionally, the peroxidation of parasite lipid membranes, inhibition of lactate dehydrogenase and tyrosine kinase, oxidation of proteins, and damage to DNA also contribute

to the viability of the parasites (Zhou *et al.,* 2020) within the human host. Chloroquine can insert itself into the DNA double helix structure of *Plasmodium* (Zhou *et al.,* 2020) forming a stable DNA-CQ complex. This complex affects the DNA replication and RNA transcription process inhibiting growth and reproduction; however, the exact mechanism of action is still unknown (Kaur *et al.,* 2010; Lee *et al.,* 2014; Zhou *et al.,* 2020). Oxidation promoted by chloroquine is inhibited by antioxidants and peroxidase inhibitors, while the inhibition of proteolysis is blocked by glutathione, therefore the antioxidant system of the parasite could contribute to quinoline drug resistance (Herraiz *et al.,* 2019).

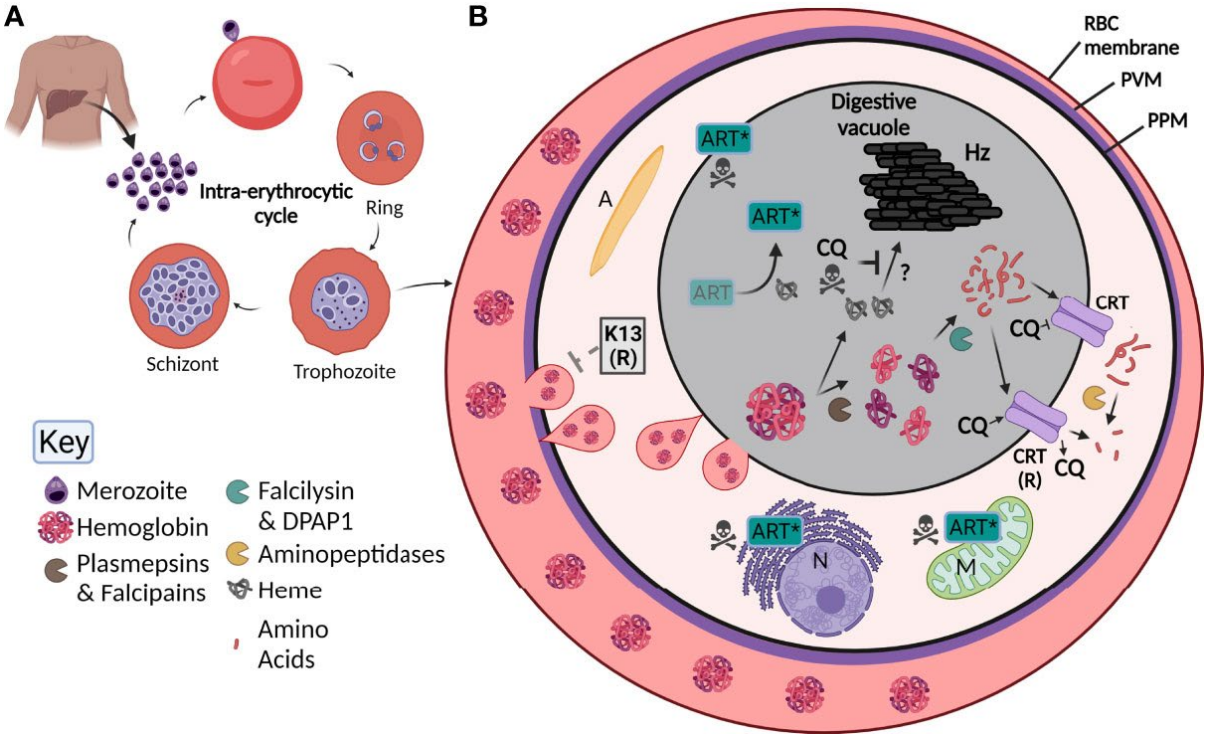


Figure 4.3: Overview of the effect of antimalarials, chloroquine (CQ) and artemisinin (ART) on the haemozoin pathway in the digestive vacuole (DV) of *P. falciparum* lifecycle. (A) The intra-erythrocytic life cycle of the *Plasmodium* parasite. (B) During the trophozoite stage, the digestive food vacuole (grey) is visible, and haemoglobin is taken up into it for digestion by enzymes. Chloroquine Resistant Transporter (CRT) takes up small peptides and these transported through it for further break down into free amino acids by aminopeptidases. Haem (grey chains) are toxic to the parasite and are crystalised into haemozoin (Hz) by unknown mechanisms. Chloroquine (CQ) blocks the formation of Hz and causes parasite death, but mutated forms of CRT are able to transport CQ out of the DV in resistant *Plasmodium* species. Artemisinin (ART) is activated by haem (ART*) and causes free radical damage to many organelles including the parasite nucleus (N) and mitochondria (M). Kelch-13 protein

(K13) is a resistance (R) mechanism to ART involved in endocytosis of haemoglobin and its transport to the DV (Edgar *et al.,* 2022).

Quinoline and chloroquine primarily act on the trophozoite stage of the parasite's development (Figure 4.4; Table 3.2 (16-24 hours)) and can prevent further invasion and replication of *Plasmodium* in the red blood cells of the human host by causing parasite death at this life cycle stage. The exact mechanism of action as to how quinoline based drugs target haem to inhibit haemozoin formation *in vivo* (Figure 4.5) is not known nor is it understood whether various quinoline antimalarials inhibit haemozoin via similar or different pathways (Jones et al., 2015; Zhou *et al.,* 2020).

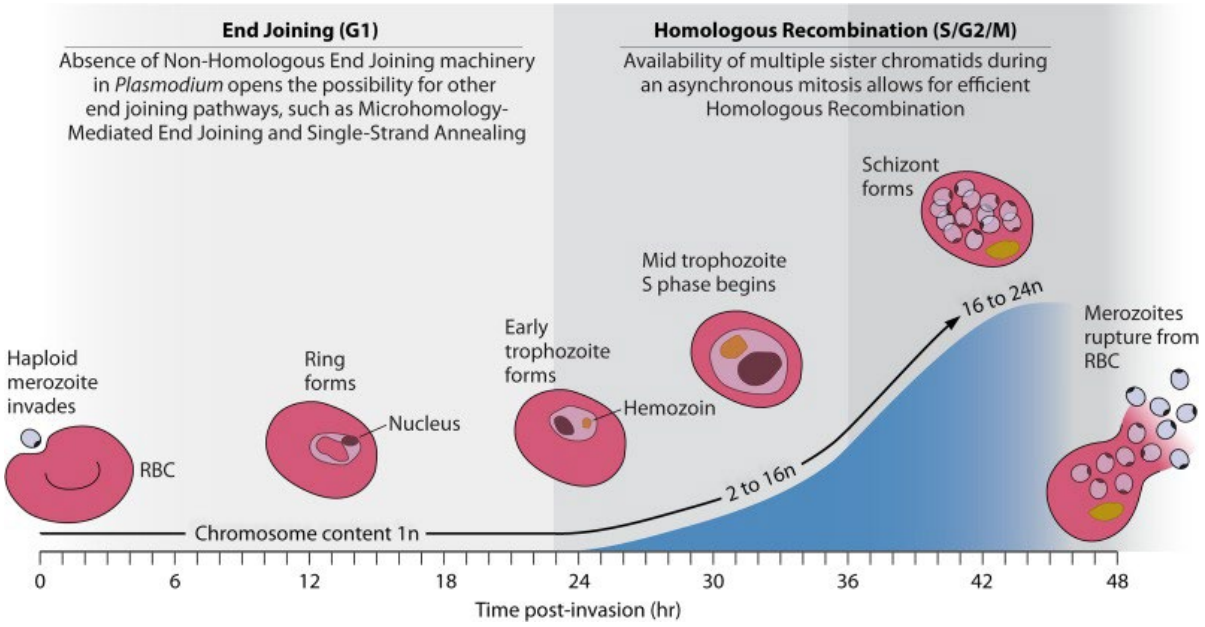


Figure 4.4: The *Plasmodium* asexual intraerythrocytic cycle. A haploid (1n) merozoite invades a red blood cell (RBC) and forms a ring from 0 to 22 hours post invasion. This corresponds to the G1 phase of the cell cycle. As the parasite transitions from the ring stage to the trophozoite stage, its metabolic activity increases in preparation for DNA replication. A food vacuole begins to form as haemoglobin is broken down and toxic haem is packaged into haemozoin. DNA replication produces multiple copies of the parasite genome in an intact nucleus that does not undergo membrane degradation, providing homologous templates for homologous recombination (G2). *Plasmodium* DNA replication is asynchronous and can produce a range of sister chromatids, up to about 24n. Nearing the end of the 48 hour cycle, each genome is packaged into separate daughter merozoites, which then rupture from the RBC and go on to invade new RBCs (Lee *et al.,* 2014).

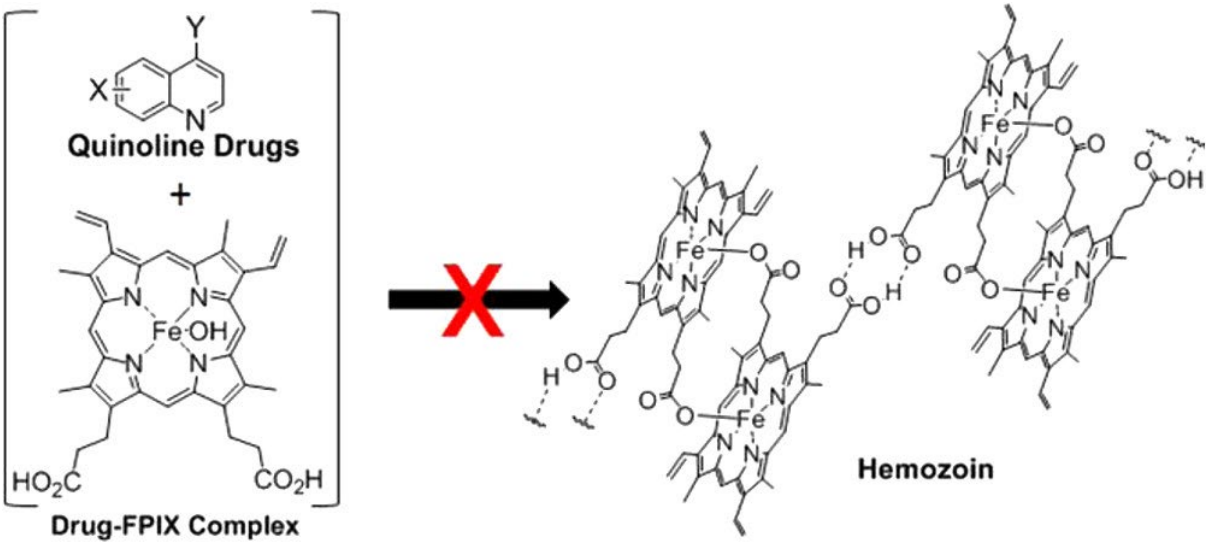


Figure 4.5: Quinoline drugs complex with ferriprotoporphyrin IX (FPIX) and form a complex which inhibits further sequestration of free haem into the haemozoin crystalline polymer (Gorka *et al.,* 2013).

In this study, all three groups of heterocyclic derivatives were based upon the quinoline pharmacophore and as such, their mechanism of action is assumed to be similar to that of known quinoline drugs such as chloroquine or quinine. The two most active compounds against the NF54 *P. falciparum* parasite, compound **DC14** (Figure 4.1) and compound **Q3C11** (Figure 4.2) were investigated for their morphological activity on the parasites *in vitro* as reported in Section 3.3. From the morphological assessment and observations of the infected RBCs, it was noted that gametocytes started to develop alongside trophozoites. This is an indicative of stressful environmental conditions (Omorou *et al.,* 2022) which could have been caused by the compounds altering the pH or other physico-chemical properties of the infected RBCs in the parasite culture. Additionally, the lag phase between the untreated control and the test compound treated parasites could also be indicative of a mechanism of action whereby the test compounds inhibited parasite haemoglobin digestion or interfered with the sequestration of free haem into haemozoin crystals (Figure 4.5). The observation that the total parasitaemia decreased and the lack of new rings at the 48-hour interval also indicate that parasite replication was altered. This could be due to a similar mechanism of action to chloroquine, whereby the DNA replication process was hindered by compounds **DC14** and

Q3C11s' quinoline pharmacophore and the presence of the chloro- group at the R1 position in both compounds possibly causing structural activity related effects or intercalating with *Plasmodium* DNA.

Quinoline carboxamide derivatives have displayed antimalarial activity during the trophozoite stage of parasite growth (Singh *et al.,* 2021) with *Plasmodium* falcipain-2 being the drug target. Falcipain-2 and falcipain-3 are papain-family cysteine proteases or the erythrocytic stage of *P. falciparum* that localise to the food vacuole and readily hydrolyse haemoglobin and are necessary for haemoglobin degradation and denaturation. Inhibition of falcipain-2 leads to a breakdown in this process causing parasite stress in the acidic food vacuole which may inhibit its development (Shenai *et al.,* 2000). Rosenthal (2020) stated that "In summary, available results suggest that falcipains are food vacuole haemoglobinases, that falcipain-3 plays an essential role in erythrocytic parasites, that falcipain-2 participates in haemoglobin hydrolysis directly and by activating plasmepsins, but that falcipain-1 and falcipain-2 are not essential in erythrocytic stage parasites". Cysteine protease inhibitors and falcipain inhibitors, however, remain potential targets for new antimalarials (Rosenthal, 2020). The test compounds in this study could therefore have falcipain activity, though further study would be required to determine if this was a potential mechanism of action in inhibiting parasite growth.

In this study, the two most active compounds, **DC14** and **Q3C11** both contained a quinoline pharmacophore and based on their lipophilicity and good bioavailability (Table 3.11; 3.12), their increased antimalarial activity could be due to increased diffusion and accumulation into the parasite DV. This is further supported by the *in silico* predictions of the compounds LogP values below 5 indicating their ability to cross membranes and bind to target sites more effectively. (Table 3.11).

Additionally, the weak basic nature of the derivatives could have contributed to their mechanism of action by increasing the pH of the parasite digestive vacuole affecting the functionality of various proteases preventing haemoglobin digestion resulting in parasite death.

When looking at the binding of chloroquine to the iron atom in the haem unit, it is apparent that some chelating interaction is present (Gordeuk *et al.*, 1994). Chloroquine has been shown to chelate ferrous ions (26.19 ± 2.47% at 50 µM), but to a lesser extent compared to EDTA

(72.00 ± 3.60% at 50 µM) (Prof van Zyl, personal communications). In addition, 8-hydroxyquinolines and derivatives are well known iron chelators with IC_{50} values in the micromolar ranges as well as antimalarial properties (Chen, 2015; Mahlangu, 2023). Malaria parasites require iron for vital cell functions and during the asexual stage the parasites acquires iron from the host (Cabantchik *et al.,* 1999). Iron chelators such as desferrioxamine and 2,2'bipyridyl have been shown to inhibit iron-dependant ribonucleotide reductase resulting in parasite death (Cabantchik *et al.,* 1999; Mabeza *et al.,* 1999). Thiosemicarbazones proven to chelate iron have previously been studied for their antimalarial properties in chloroquine-sensitive and -resistant *P. falciparum* with variable inhibitory activity (Walcourt *et al*., 2004; Nqeno, 2021). Although the forty-two quinoline heterocyclic derivatives in this study had variable antimalarial activity, they all had minimal iron chelating activity. With only compound **Q3C5** chelating up to 25.87 ± 5.57% ferrous ion in comparison to the metal chelator, EDTA at 50 µM, which has a high affinity for binding to iron and other divalent metals (Section 3.9.2) (Ferrero, 2016). Both Walcourt *et al*., (2004) and Nqeno (2021) reported poor antimalarial activity with IC_{50} values of ≥5 µM compared to the most active in this study of 7.23 µM (Table 3.1). As such this is not the main mechanism of action of these quinoline heterocyclic derivatives within the malaria parasite and the malaria parasite was not as sensitive to iron chelation as cancer cells (Cabantchik *et al.,* 1999).

4.2 Insecticidal Activity

Upon investigating the effect of the quinoline heterocyclic derivatives on the life cycle of the malaria parasite, the forty-two compounds were found to be directed more towards the malaria parasite than the malaria vector (Table 3.1, Table 3.3). The quinoline pharmacophore has been shown to have potential in the development of insecticides targeted at *Anopheles* species. A range of dichloroquinoline derivatives displayed highly toxic larvicidal effects towards *An. stephensi and Aedes aegypti mosquito species with* LC_{50} values between 5 – 10 µM/mL Murugan *et al.* (2022). The latter derivatives were also highly active against the chloroquine sensitive 3D7 strain of *P. falciparum* with IC_{50} values in the nanomolar range (<10 nM). This gave further credence to the current study's rationale that new novel test

compounds should be evaluated for both their antimalarial and insecticidal properties in accordance with the WHO's guidelines and recommendations (WHO, 2023a).

Of all the test compounds, the **DC** group of compounds with a thiosemicarbazone pharmacophore were overall more active than the **PHYD** and **Q3C** series (Table 3.3). A very similar group of thiosemicarbazone derivatives investigated for cholinesterase inhibitory properties as a potential treatment for Alzheimer's disease, were found to be selective towards acetylcholinesterase in the range of 0.12 – 60.9 µM. Where the lead inhibitor with an IC_{50} value of 0.12 ± 0.02 µM, had a 5-fold higher potency than the standard drug (galantamine; IC_{50} = 0.62 ± 0.01 µM) (Zaib *et al.,* 2021). Acetylcholinesterase is a key hydrolase enzyme in regulating synaptic levels of the neurotransmitter acetylcholine in both vertebrates and invertebrates and has been a target for insecticides for decades (Pang, 2014). The emergence of insecticide resistance has necessitated the investigation of new compounds, preferably non-pyrethroid, for their insecticidal properties as recommended by the WHO (WHO, 2023a).

However, none of the compounds across all three derivative groups in this study caused more than 20% larval mortality after 72 hours (Table 3.3) in comparison with DDT which caused 100% mortality. The **DC** group of test compounds showed slightly more larval mortality than the **PHYD** and **Q3C** group compounds and this may have been a result of the thiosemicarbazone pharmacophore's acetylcholinesterase inhibitory properties. Although further enzymatic studies would be required to confirm this on the *Anopheles* acetylcholinesterase compared to the human enzyme. Additionally, there was a notable morphological change in the few larvae exposed to compound **DC3** that died after 72 hours. The thoracic segment of the larvae was enlarged, and the palmate hairs were not visible indicating that compound **DC3** may have had a toxic developmental effect on the larvae during exposure to the test compound in the assay. The other **DC** compounds however did not cause any abnormalities or aberrations nor did the **PHYD** or **Q3C** compounds. This lack of larvicidal activity of the test compounds could be attributed to the differences in their chemical structure in comparison to known insecticides currently in use (Kathrada, 2017) or due to their resistance profile (Mouatcho *et al.,* 2009). The observed effects of the most active compounds were different to that of DDT (Table 3.4). The highly effective insecticide, DDT is a known organochlorine that has a mechanism of action whereby sodium ion channels are prevented

from deactivating, stabilising the open state and prolonging their opening leading to hyperexcitability and eventual death (Silver *et al.,* 2014).

Since the compounds were ineffective against the larvae it was proposed that they may have a mutagenic effect or inhibit egg development thereby preventing hatching. However, when the activity of the forty-two compounds were evaluated against the *An. arabiensis* eggs, none exhibited high ovicidal toxicity in comparison to formalin that prevented 100% of the eggs from hatching after 72 hours (Section 3.4.3). The eggs also showed moderate tolerance to DDT treatment at 0.5 µM with a 60% hatch rate after 72 hours of exposure. The larvae that emerged from the DDT treated eggs subsequently died within 24 hours of hatching due to the presence of DDT at a lethal concentration within the wells. None of the test compounds in this study caused any morphological changes to the *An. arabiensis* eggs. The ovicidal activity of the test compounds was dependent on their ability to act on the embryo inside the eggshell (Grosscurt, 1977). As such the ability of the compounds to penetrate the chorion of the egg, potentially be converted to an active inhibitor, or be detoxified, would be dependent on the exposure time and dose of the compound (Ramar *et al.,* 2014.).

4.3 Toxicity profile

The concept of drug safety is an integrated science and the benefit/risk balance of medication needs to be considered (Alshammari, 2016). As such in-depth toxicological assessment of new compounds in the drug development pipeline needs to be undertaken and *Artemia* serves as a suitable species for use in ecotoxicology experiments (Nunes *et al*., 2006). The activity of the forty-two novel test compounds in this study were evaluated against *Ar. franciscana* for potential toxicity to humans and aquatic organisms and it was found that the test compounds displayed moderate to high activity in comparison to positive control potassium dichromate in a time dependent manner (Table 3.8). Compounds **DC14** and **Q3C11**, which were the two most active compounds against the NF54 *P. falciparum* malaria parasite were notably highly toxic towards *Artemia* (Table 3.9). Consequently, careful consideration of their toxicological profile from this study should be evaluated for further studies involving these compounds, despite the fact that they were deemed less cytotoxic towards the human HEK293 cell line and did not induce haemolysis. This is further emphasised by the morphological assessment

of the *Artemia* displaying detrimental physical changes to the normal morphology of the organism (Table 3.10). However, Ignoto *et al.* (2022) reported on how *Artemia* displayed acute toxicity and morphological changes at 40 μg/mL for the widely used antihistamine, promethazine, which indicates that a nuanced and careful interpretation of results is required in assessing a potential compound's safety based on a single *in vivo* assay. Further extensive tests therefore should be considered to ascertain the safety profile of the active compounds in this study.

In doing so, cytotoxicity studies of the forty-two novel test compounds against the human embryonic kidney epithelial cell line were undertaken (Table 3.5). The purpose of this was to determine whether the test compounds selectively targeted the malaria parasite or if they caused cellular damage to the human host. All three groups of test compounds exhibited low cytotoxicity towards the human HEK293 cell line with selectivity index scores indicating that they were selective towards the NF54 *P. falciparum* parasite in preference to the human cell (Table 3.7). Compound **DC14** had a selectivity index value of 11.13, whereas compound **Q3C11** had a value of 7.55. In comparison to clinically used quinine with a SI value of 11.98, that was similar to **DC14** indicating high selectivity towards the parasite rather than to the human cell, which is favourable when considering drugs to add to the drug discovery pipeline.

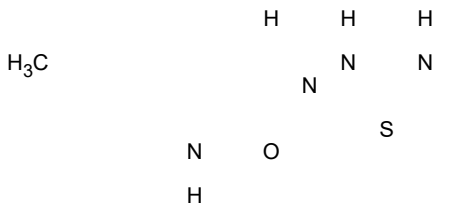
Based on the *in silico* prediction of the test compounds, their respective toxicity class were determined along with their pharmacokinetic properties (Table 3.12-3.14). All of the test compounds were determined to be highly (Class III) toxic according to the revised Cramer's decision tree method (Table 3.12-3.14) (EFSA Scientific Committee *et al.,* 2019), which indicated that further studies are deemed necessary to properly assess the in-depth toxicological profile of the test compounds. It should be noted however that the standard antimalarial drug quinine is also ranked as highly (Class III) toxic – a well-known fact with the narrow therapeutic range of this drug increasing the risk of adverse side effects (Achan *et al.,* 2011; Djimde and Taylor, 2023). As such, a comprehensive approach is needed when assessing a compound's toxicity profile and its pharmacokinetics, pharmacodynamics and additional factors such as patient comorbidities necessary in drug safety, should all be taken into account when deciding on its toxicity category.

The compounds' ability to cross the blood brain barrier, as well as their primary cytochrome P450 metabolic site of metabolism and their ability to inhibit cytochrome P450 3A4 (CYP4A4)

were determined via an *in silico* predictive tool (Table 3.12-3.14). The inhibition of CYP3A4 is associated with a large number of possible drug-drug interactions and increased toxic side effects as CYP4A4 is known to be the main enzyme involved in the metabolism of more than 50% of drugs and most other xenobiotics (Sevrioukova & Poulos, 2013). The two most active antimalarial compounds both inhibit CYP34A. Whilst their primary site of metabolism is via aromatic hydroxylation and N-oxidation for compound **DC14** and **Q3C11**, respectively (Table 3.12, Table 3.14). In comparison, the primary site of metabolism of quinine is via N-oxidation, however does not inhibit CYP3A4 (Djimde and Taylor, 2023). The compounds' ability to inhibit CYP3A4 may lead to increased drug interactions depending on their elimination half-life within the body and careful consideration of their pharmacokinetics needs to be assessed in future work.

Antimalarial drugs such as primaquine and chloroquine have an increased risk of inducing oxidative stress in patient with reduced antioxidant defences such as patients with G6PD deficiency (Percário *et al.,* 2012; Ashley *et al.,* 2014). On the flip side some compounds can be used as antioxidants to assist with the increase in free radical generation in a malaria infected patient. Thus, the antioxidant activity of a test compound can be beneficial to the malaria parasite protecting it from reactive oxidative species and associated damage; while also protecting the sensitive membranes and enzymes in the host that are related to cell differentiation and proliferation (Ye *et al.,* 2015). In this study, all forty-two novel test compounds were evaluated for their antioxidant free radical scavenging activity and were determined to have minimal activity indicating that antioxidant mechanisms of action were not a major component of their activity profile against the NF54 *P. falciparum* parasite. Compound **DC15** displayed the highest activity with 28.75% ± 0.01 free radical scavenging activity (Section 3.9.1) but was not comparable to that of the positive control ascorbic acid.

DC12



(2*E*)-2-[(6-methyl-2-oxo-1,2-dihydroquinolin-3-yl)methylidene]-*N*-phenylhydrazine-1-carbothioamide

Antimalarial properties

Plasmodium Growth Inhibited	Combination Interaction; ΣFIC	Larvicidal (Mortality)	Ovicidal (Mortality)
100% at 50µM IC_{50}: 13.5 ± 2.55 *ns (P = 0.9880)	Synergistic with cisplatin ΣFIC = 0.59	16.67% ± 5.77 at 0.5 µM	0% ± 0.00 at 0.5 µM

Antioxidant, iron chelating properties

DPPH• Free Radical Scavenging	Ferrous Ion Chelation
15.25% ± 1.62	0.10% ± 0.10

Toxicity properties

K562 Cells (% cellular viability)	HEK293 Cells (% cellular viability)	Selectivity Index (HEK 293 vs NF54)	Haemolysis	*Artemia* lethality (Mortality)
49.01% at 50µM IC_{50}: 8.86 ± 1.15 µM Yes (P <0.0001)	80.65% at 50µM IC_{50}: n.d	1.96	0.10% ± 0.01 at 50µM	86.48% ± 4.78 at 0.5µM LC_{50} = 7.95 µM Yes (P <0.0001)

Toxic Hazard class	Cytochrome P450 (CYP3A4 inhibition)	BBB	LogD (pH 5)	P-glycoprotein substrate
High (Class III)	Yes	No	3.75	No

Figure 4.6: The summary of the activity for test compound **DC12**. The activity of **DC12** across this study divided into its antimalarial, antioxidant and iron chelating, and toxicity properties.

All forty-two of the novel test compounds were also evaluated for their toxicity towards the chronic myelogenous leukaemia cell line, where overall the test compounds were moderately cytotoxic to the leukaemia cell line (Table3.5, 3.6). In contrast to the HEK293 cells, the compounds were far more toxic towards the K562 cell line indicating possible mechanisms of action specific to rapidly proliferating cells (Table 3.1, Table 3.7). Quinolone heterocyclic derivatives have been shown to inhibit topoisomerase I in A549 lung cancer cells leading to cytotoxic effects (Ge *et al.,* 2016). Quinoline derivatives were also shown to be potent kinase inhibitors in the treatment of colorectal cancer (Zhou *et al.,* 2020b). The quinoline pharmacophore scaffold plays an important role in anticancer drug development as their derivatives have shown excellent results through a diverse range of mechanisms of action such as growth inhibitors by cell cycle arrest, apoptosis, inhibition of angiogenesis, disruption of cell migration, and modulation of nuclear receptor responsiveness (Afzal *et al*., 2015). Cisplatin's mechanism of action involves the generation of reactive oxidative species and binding to purine bases which ultimately cause DNA damage, block cell division and result in apoptosis through a range of interconnected pathways (Dasari and Bernard Tchounwou, 2014); however, drug resistance and relapse may occur in some forms of cancer.

Combining new compounds with cisplatin may help to overcome drug resistance. In the current study, the combination of compounds **DC12** or **Q3C8** with known anticancer drug, cisplatin yielded a favourable synergistic interaction indicating potential for a combination therapy (Figure 3.9). In addition, all of the test compounds were predicted via an *in silico* tool to not be p-glycoprotein substrates (Table 3.12-3.14) indicating reduced drug efflux of the test compounds is a possibility; which would be beneficial in reversing drug resistance in resistant cells using this mechanism of resistance (Ahmed Juvale *et al.,* 2022). However, due to the scope of this study primarily being focused on antimalarial investigations, further research into the compounds more specific cytotoxic effects, mechanisms of action and their effect against different cell lines would be needed to determine their potential as anticancer treatments.

Chapter 5 - Conclusions, Limitations and Recommendations for further research

5.1 Conclusions

As the burden of malaria continues to increase and with the global emergence of resistance to antimalarial drugs and insecticides, there is an increased need for the development of new compounds with antimalarial and/or insecticidal properties in accordance with the WHO recommendations (WHO, 2023a).

As such, forty-two novel test compound derivatives based on the quinoline pharmacophore scaffold, with the potential for antimalarial and/or insecticidal activity were successfully synthesised, purified and structures verified by NMR before being evaluated. The novel test compounds were evaluated against the NF54 chloroquine-sensitive strain of *P. falciparum* and the *An. arabiensis* KWAG vector for their *in vitro* antimalarial and insecticidal activity, as well as their preliminary toxicological profile.

The quinoline pharmacophore structure was used as a scaffold upon which hybrid heterocyclic compounds were developed to form the three sets of compounds, namely the dihydroquinoline-carbothioamide, phenyl-hydrazono and quinoline-3-carboxamide derivatives. The latter derivatives showed widely variable activity towards the NF54 *P. falciparum* malaria parasite with activities ranging from promising to no antimalarial activity.

From the three groups of test compounds, two compounds were identified based on their promising antimalarial activity, one from the dihydroquinoline-carbothioamide group and the other from the quinoline-3-carboxamide group. Compounds **DC14** and **Q3C11** were identified as lead compounds; however, despite their favourable antimalarial activity they were 80-fold less active than the standard antimalarial, quinine (Table 3.1). Compounds **DC14** and **Q3C11** both showed parasite morphological and stage specific effects similar to that of quinine with the trophozoite parasite stage being affected (Figure 3.5, Table 3.2), resulting in a decrease in total

parasitaemia and the subsequent decrease in the second generation of rings after 48 hours of treatment (Table 3.2). In accordance with the WHO's guidelines on malaria treatment (WHO, 2023b), combination therapies are recommended to overcome the challenges presented by drug resistance and both compound **DC14** and **Q3C11** showed synergistic and additive effects respectively in combination with standard antimalarial drug quinine (Figure 3.3). This could be due to inhibition of similar targets as the quinolines such as the inhibition of haemozoin formation and/or falcipain cysteine proteases or the generation of reactive oxidative species. Further studies to deduce the mechanism of action, such as lipid peroxidation, are therefore recommended.

Although both test compounds had a more favourable selectivity index (Table 3.7) than the other derivatives, only compound **DC14** had a selectivity index greater than 10 indicating that the parasite was a more selective target compared to human cells (Table 3.5, Table 3.7). Further structural modifications to the test compounds may increase the antimalarial activities, while maintaining their safety profiles. Compounds **DC14** and **Q3C11** showed moderate activity towards the rapidly proliferating chronic myelogenous leukemic K562 cell line (Table 3.6). Additionally, both compounds lacked insecticidal properties (Table 3.3) and do not warrant further research as they were also found to be toxic to the aquatic *Ar. franciscana* nauplii indicating a potential hazard to humans and are potentially ecologically toxic if high concentrations are used for a prolonged period (Table 3.8-3.10).

The favourable drug-like properties and *in silico* predicted pharmacokinetic properties of the two lead compounds also indicated potential as therapeutic agents with good bioavailability and absorption with Log P and Log D values <5 indicating an ideal balance between hydrophilicity and lipophilicity as oral drugs (Gao *et al.,* 2017). Compound **Q3C11** was predicted to be able to cross the blood brain barrier and may have potential in the treatment of cerebral malaria much like standard antimalarial drug quinine, however further evaluation would be needed to confirm this. Both lead compounds were predicted to be CYP3A4 inhibitors indicating an increased potential for drug interactions (Table 3.12, Table 3.14).

Overall compound **DC14** had the more favourable activity, safety and pharmacokinetic profile and warrants further research as an antimalarial lead molecule.

5.2. Limitations and Future study recommendations

In summary, the following limitations of the study were identified and need to be taken into consideration for similar studies in the future.

- This study was limited to determining the antimalarial activity of the forty-two novel quinoline heterocyclic derivative test compounds against the chloroquine sensitive NF54 strain of *P. falciparum* and did not determine the effect of the compounds against other drug-resistant strains of *P. falciparum* such as the FCR3 or K1 strain. This would provide valuable information to compare resistance sensitivities.
- Compounds **DC12** and **Q3C8** demonstrated very favourable cytotoxic properties against the human chronic myelogenous leukaemia K562 cell line, as such they should be tested against other cancer cell lines and evaluate the mechanism of action.
- The toxic effects of the test compounds against *Artemia franciscana* and other aquatic organisms should be further explored for ecotoxic considerations.
- Active quinolines inhibit haemozoin and increase free hemin which in the presence of H_2O_2 in the parasite digestive vacuole catalyzes peroxidative reactions and the inhibition of cysteine proteases. As such, the lipid peroxidase activity of the test compounds should be further investigated as a potential mechanism of action towards causing parasite death within the infected red blood cells.
- The effect of the test compounds against the gametocyte stages of the malaria parasite were not determined. Inhibition of the sexual stages of the parasite would decrease the malaria transmission burden and should be further investigated.
- The β-haematin assay was not carried out on the test compounds to determine their haemozoin inhibitory effect due to the assay not working as intended as a result of multiple supplier problems with reagent inactivity that was out of the control of the research group.
- Further structure activity relationships with regards to the stereo-electric chemistry and coordination bond chemistry of the test compounds should be elucidated with *in silico* molecular modelling and target docking software.

REFERENCES

Abhishek, K., Jennifer, F., Pankaj, K. (2014) Synthesis, antimicrobial and anti-inflammatory studies of some novel Schiff base derivatives. *International Journal of Drug Development & Research*, 6(2), 165-171.

Achan, J., Talisuna, A. O., Erhart, A., Yeka, A., Tibenderana, J. K., Baliraine, F. N., Rosenthal, P. J., & D'Alessandro, U. (2011). Quinine, an old anti-malarial drug in a modern world: Role in the treatment of malaria. *Malaria Journal*, *10*(1), 144. https://doi.org/10.1186/1475-2875-10-144

Ackerman, H. C., Beaudry, S. D., & Fairhurst, R. M. (2009). Antioxidant therapy: reducing malaria severity?. *Critical Care Medicine*, *37*(2), 758–760. https://doi.org/10.1097/CCM.0b013e318194d5de

Afzal, O., Kumar, S., Haider, M. R., Ali, M. R., Kumar, R., Jaggi, M., & Bawa, S. (2015). A review on anticancer potential of bioactive heterocycle quinoline. *European Journal of Medicinal Chemistry*, *97*, 871–910. https://doi.org/10.1016/j.ejmech.2014.07.044

Agumba, S., Gimnig, J. E., Ogonda, L., Ombok, M., Kosgei, J., Munga, S., Guyah, B., Omondi, S., & Ochomo, E. (2019). Diagnostic dose determination and efficacy of chlorfenapyr and clothianidin insecticides against *Anopheles* malaria vector populations of western Kenya. *Malaria Journal*, *18*(1), 243. https://doi.org/10.1186/s12936-019-2858-z

Ahmed Juvale, I. I., Abdul Hamid, A. A., Abd Halim, K. B., & Che Has, A. T. (2022). P-glycoprotein: New insights into structure, physiological function, regulation and alterations in disease. *Heliyon*, *8*(6), e09777. https://doi.org/10.1016/j.heliyon.2022.e09777

Alam, M., Abser, M. N., Kumer, A., Bhuiyan, M. M. H., Akter, P., Hossain, M. E., & Chakma, U. (2023). Synthesis, characterization, antibacterial activity of thiosemicarbazones derivatives and their computational approaches: Quantum calculation, molecular docking, molecular

dynamic, ADMET, QSAR. *Heliyon*, *9*(6), e16222. https://doi.org/10.1016/j.heliyon.2023.e16222

Alkhzem, A. H., Woodman, T. J., & Blagbrough, I. S. (2022). Design and synthesis of hybrid compounds as novel drugs and medicines. *RSC Advances*, *12*(30), 19470–19484. https://doi.org/10.1039/D2RA03281C

Alshammari, T. M. (2016). Drug safety: The concept, inception and its importance in patients' health. *Saudi Pharmaceutical Journal*, *24*(4), 405–412. https://doi.org/10.1016/j.jsps.2014.04.008

Amengor, C. D. K., Biniyam, P. D., Brobbey, A. A., Kekessie, F. K., Zoiku, F. K., Hamidu, S., Gyan, P., & Abudey, B. M. (2024). N-Substituted Phenylhydrazones Kill the Ring Stage of *Plasmodium falciparum*. *BioMed Research International*, *2024*, 1–13. https://doi.org/10.1155/2024/6697728

American Mosquito Control Association (2022). Available at: http://www.mosquito.org/life-cycle. [Accessed 4 January 2023].

Ashley, E. A., Recht, J., & White, N. J. (2014). Primaquine: The risks and the benefits. *Malaria Journal*, *13*(1), 418. https://doi.org/10.1186/1475-2875-13-418

Autino, B., Corbett, Y., Castelli, F., & Taramelli, D. (2012). Pathogenesis of malaria in tissues and blood. *Mediterranean Journal of Hematology and Infectious Diseases*, *4*(1), e2012061. https://doi.org/10.4084/MJHID.2012.061

Berenbaum M. C. (1978). A method for testing for synergy with any number of agents. *The Journal of infectious diseases*, *137*(2), 122–130. https://doi.org/10.1093/infdis/137.2.122

Bhal, S. K., Kassam, K., Peirson, I. G., & Pearl, G. M. (2007). The Rule of Five Revisited: Applying Log D in Place of Log P in Drug-Likeness Filters. *Molecular Pharmaceutics*, *4*(4), 556–560. https://doi.org/10.1021/mp0700209

Bhat, A. R., Athar, F., Van Zyl, R. L., Chen, C. T., & Azam, A. (2008). Synthesis and biological evaluation of novel 4-substituted 1-{[4-(10,15,20-triphenylporphyrin-5-yl)phenyl]methylidene}thiosemicarbazides as new class of potential antiprotozoal agents. *Chemistry & biodiversity*, *5*(5), 764–776. https://doi.org/10.1002/cbdv.200890073

Bingul, M., Tan, O., Gardner, C. R., Sutton, S. K., Arndt, G. M., Marshall, G. M., Cheung, B. B., Kumar, N., & Black, D. S. (2016). Synthesis, Characterization and Anti-Cancer Activity of Hydrazide Derivatives Incorporating a Quinoline Moiety. *Molecules (Basel, Switzerland)*, *21*(7), 916. https://doi.org/10.3390/molecules21070916

Blasco, B., Leroy, D., & Fidock, D. A. (2017). Antimalarial drug resistance: linking *Plasmodium falciparum* parasite biology to the clinic. *Nature Medicine*, *23*(8), 917–928. https://doi.org/10.1038/nm.4381

Blumberg L. H. (2015). Recommendations for the treatment and prevention of malaria: Update for the 2015 season in South Africa. *South African Medical Journal = Suid-Afrikaanse Tydskrif vir Geneeskunde*, *105*(3), 175–178. https://doi.org/10.7196/samj.9407

Braack, L., Bornman, R., Kruger, T., Dahan-Moss, Y., Gilbert, A., Kaiser, M., Oliver, S. V., Cornel, A. J., Lee, Y., Norris, D. E., Coetzee, M., Brooke, B., & De Jager, C. (2020). Malaria Vectors and Vector Surveillance in Limpopo Province (South Africa): 1927 to 2018. *International Journal of Environmental Research and Public Health*, *17*(11), 4125. https://doi.org/10.3390/ijerph17114125

Braga, C. B. E., Martins, A. C., Cayotopa, A. D. E., Klein, W. W., Schlosser, A. R., Silva, A. F. D., Souza, M. N. D., Andrade, B. W. B., Filgueira-Júnior, J. A., Pinto, W. D. J., & Da Silva-Nunes, M. (2015). Side Effects of Chloroquine and Primaquine and Symptom Reduction in Malaria Endemic Area (Mâncio Lima, Acre, Brazil). *Interdisciplinary Perspectives on Infectious Diseases*, *2015*, 1–7. https://doi.org/10.1155/2015/346853

Brooke, B., Koekemoer, L., Kruger, P., Urbach, J., Misiani, E., & Coetzee, M. (2013). Malaria vector control in South Africa. *South African Medical Journal*, *103*(10), Article 10. https://doi.org/10.7196/SAMJ.7447

Burke, A., Dandalo, L., Munhenga, G., Dahan-Moss, Y., Mbokazi, F., Ngxongo, S., Coetzee, M., Koekemoer, L., & Brooke, B. (2017). A new malaria vector mosquito in South Africa. *Scientific Reports*, *7*(1), 43779. https://doi.org/10.1038/srep43779

Burke, A., Dahan-Moss, Y., Duncan, F., Qwabe, B., Coetzee, M., Koekemoer, L., & Brooke, B. (2019). *Anopheles parensis* contributes to residual malaria transmission in South Africa. *Malaria Journal*, *18*(1), 257. https://doi.org/10.1186/s12936-019-2889-5

Cabantchik, Z. I., Moody-Haupt, S., & Gordeuk, V. R. (1999). Iron chelators as anti-infectives; malaria as a paradigm. *FEMS Immunology & Medical Microbiology*, *26*(3–4), 289–298. https://doi.org/10.1111/j.1574-695X.1999.tb01401.x

Camarda, G., Jirawatcharadech, P., Priestley, R. S., Saif, A., March, S., Wong, M. H. L., Leung, S., Miller, A. B., Baker, D. A., Alano, P., Paine, M. J. I., Bhatia, S. N., O'Neill, P. M., Ward, S. A., & Biagini, G. A. (2019). Antimalarial activity of primaquine operates via a two-step biochemical relay. *Nature Communications*, *10*(1), 3226. https://doi.org/10.1038/s41467-019-11239-0

CDC (2022) – Malaria - About Malaria - Biology. Cdc.gov. Available at: https://www.cdc.gov/malaria/about/biology/ [Accessed date: 17 December 2022]

Chen, C.T. (2015). The effect of novel compounds on the growth of *Plasmodium falciparum* and haemozoin formation. University of the Witwatersrand, South Africa. Master of Science in Medicine dissertation. Available at: http://hdl.handle.net/10539/18663 [Accessed date: 17 December 2022]

Corey, V. C., Lukens, A. K., Istvan, E. S., Lee, M. C. S., Franco, V., Magistrado, P., Coburn-Flynn, O., Sakata-Kato, T., Fuchs, O., Gnädig, N. F., Goldgof, G., Linares, M., Gomez-Lorenzo, M. G., De Cózar, C., Lafuente-Monasterio, M. J., Prats, S., Meister, S., Tanaseichuk, O., Wree, M., Zhou,

Y., … Winzeler, E. A. (2016). A broad analysis of resistance development in the malaria parasite. *Nature communications*, *7*, 11901. https://doi.org/10.1038/ncomms11901

Cramer, G. M., Ford, R. A., & Hall, R. L. (1978). Estimation of toxic hazard--a decision tree approach. *Food and Cosmetics Toxicology*, *16*(3), 255–276. https://doi.org/10.1016/s0015-6264(76)80522-6

Cui, L., Mharakurwa, S., Ndiaye, D., Rathod, P. K., & Rosenthal, P. J. (2015). Antimalarial Drug Resistance: Literature Review and Activities and Findings of the ICEMR Network. *The American Journal of Tropical Medicine and Hygiene*, *93*(3 Suppl), 57–68. https://doi.org/10.4269/ajtmh.15-0007

Ćurčić, V., Olszewski, M., Maciejewska, N., Višnjevac, A., Srdić-Rajić, T., Dobričić, V., García-Sosa, A. T., Kokanov, S. B., Araškov, J. B., Silvestri, R., Schüle, R., Jung, M., Nikolić, M., & Filipović, N. R. (2024). Quinoline-based thiazolyl-hydrazones target cancer cells through autophagy inhibition. *Archiv Der Pharmazie*, *357*(2), 2300426. https://doi.org/10.1002/ardp.202300426

Dandalo, L. C., Brooke, B. D., Munhenga, G., Lobb, L. N., Zikhali, J., Ngxongo, S. P., Zikhali, P. M., Msimang, S., Wood, O. R., Mofokeng, M., Misiani, E., Chirwa, T., & Koekemoer, L. L. (2017). Population Dynamics and *Plasmodium falciparum* (Haemosporida: Plasmodiidae) Infectivity Rates for the Malaria Vector *Anopheles arabiensis* (Diptera: Culicidae) at Mamfene, KwaZulu-Natal, South Africa. *Journal of Medical Entomology*, *54*(6), 1758–1766. https://doi.org/10.1093/jme/tjx169

Dasari, S., & Bernard Tchounwou, P. (2014). Cisplatin in cancer therapy: Molecular mechanisms of action. *European Journal of Pharmacology*, *740*, 364–378. https://doi.org/10.1016/j.ejphar.2014.07.025

Dinis, T. C., Maderia, V. M., & Almeida, L. M. (1994). Action of phenolic derivatives (acetaminophen, salicylate, and 5-aminosalicylate) as inhibitors of membrane lipid peroxidation and as peroxyl radical scavengers. *Archives of Biochemistry and Biophysics*, *315*(1), 161–169. https://doi.org/10.1006/abbi.1994.1485

Djimde, A. A., & Taylor, S. M. (2023). Chemotherapy of Malaria. In L. L. Brunton & B. C. Knollmann (Eds.), *Goodman & Gilman's: The Pharmacological Basis of Therapeutics, 14th Edition* (Book 1, Section VII). McGraw-Hill Education. accesspharmacy.mhmedical.com/content.aspx?aid=1193241007

Edgar, R. C. S., Counihan, N. A., McGowan, S., & De Koning-Ward, T. F. (2022). Methods Used to Investigate the *Plasmodium falciparum* Digestive Vacuole. *Frontiers in Cellular and Infection Microbiology*, *11*, 829823. https://doi.org/10.3389/fcimb.2021.829823

EFSA Scientific Committee, More, S. J., Bampidis, V., Benford, D., Bragard, C., Halldorsson, T. I., Hernández-Jerez, A. F., Hougaard Bennekou, S., Koutsoumanis, K. P., Machera, K., Naegeli, H., Nielsen, S. S., Schlatter, J. R., Schrenk, D., Silano, V., Turck, D., Younes, M., Gundert-Remy, U., Kass, G. E. N., … Wallace, H. M. (2019). Guidance on the use of the Threshold of Toxicological Concern approach in food safety assessment. *EFSA Journal*, *17*(6). https://doi.org/10.2903/j.efsa.2019.5708

Fereda, D. E. (2022). Mating Behavior and Gonotrophic Cycle in *Anopheles gambiae* Complex and their Significance in Vector Competence and Malaria Vector Control. *Journal of Biomedical Research & Environmental Sciences*, *3*(1), 031–043. https://doi.org/10.37871/jbres1398

Ferrero, M. E. (2016). Rationale for the Successful Management of EDTA Chelation Therapy in Human Burden by Toxic Metals. *BioMed Research International*, *2016*, 1–13. https://doi.org/10.1155/2016/8274504

Foley, M., & Tilley, L. (1997). Quinoline antimalarials: Mechanisms of action and resistance. *International Journal for Parasitology*, *27*(2), 231–240. https://doi.org/10.1016/S0020-7519(96)00152-X

Fransén Pettersson, N., Deronic, A., Nilsson, J., Hannibal, T. D., Hansen, L., Schmidt-Christensen, A., Ivars, F., & Holmberg, D. (2018). The immunomodulatory quinoline-3-carboxamide paquinimod reverses established fibrosis in a novel mouse model for liver fibrosis. *PLOS ONE*, *13*(9), e0203228. https://doi.org/10.1371/journal.pone.0203228

Freese, J.A., Sharp, B.L., Ridl, F.C. and Markus, M.B. (1988). In vitro cultivation of southern African strains of Plasmodium falciparum and gametocytogenesis. *South African Medical Journal,* 73 (12), pp.720-722

Finney, D.J. (1971): Probit analysis. 3rd edn. Cambridge University Press. Cambridge, UK, Pp. 333.

Gao, Y., Gesenberg, C., & Zheng, W. (2017). Chapter 17—Oral Formulations for Preclinical Studies: Principle, Design, and Development Considerations. In Y. Qiu, Y. Chen, G. G. Z. Zhang, L. Yu, & R. V. Mantri (Eds.), *Developing Solid Oral Dosage Forms (Second Edition)* (pp. 455–495). Academic Press. https://doi.org/10.1016/B978-0-12-802447-8.00017-0

Ge, R., Zhao, Q., Xie, Z., Lu, L., Guo, Q., Li, Z., & Zhao, L. (2016). Synthesis and biological evaluation of 6-fluoro-3-phenyl-7-piperazinyl quinolone derivatives as potential topoisomerase I inhibitors. *European Journal of Medicinal Chemistry*, *122*, 465–474. https://doi.org/10.1016/j.ejmech.2016.06.054

Gillies MT, Coetzee M. A Supplement to the Anophelinae of Africa South of the Sahara. South African Institute for Medical Research; Johannesburg: 1987. pp. 1–143.

Gillies MT, De Meillon B. The Anophelinae of Africa South of the Sahara (Ethiopian Zoogeographical Region) 2nd. South African Institute for Medical Research; Johannesburg: 1968. pp. 1–343.

Gordeuk, V. R., Thuma, P. E., & Brittenham, G. M. (1994). Iron Chelation Therapy for Malaria. In C. Hershko, A. M. Konijn, & P. Aisen (Eds.), *Progress in Iron Research* (pp. 371–383). Springer US. https://doi.org/10.1007/978-1-4615-2554-7_39

Gorka, A. P., De Dios, A., & Roepe, P. D. (2013). Quinoline Drug–Heme Interactions and Implications for Antimalarial Cytostatic versus Cytocidal Activities. *Journal of Medicinal Chemistry*, *56*(13), 5231–5246. https://doi.org/10.1021/jm400282d

Govender, H (2018), Synthesis and Bioactivity of Quinoline Derivatives, Doctor of Philosophy Thesis, University of KwaZulu-Natal. Available at: https://researchspace.ukzn.ac.za/handle/10413/22457 [Accessed date: 17 March 2023]

Govender, H., Mocktar, C., & Koorbanally, N. A. (2018). Synthesis and Bioactivity of Quinoline-3-carboxamide Derivatives. *Journal of Heterocyclic Chemistry*, *55*(4), 1002–1009. https://doi.org/10.1002/jhet.3132

Govender, H., Mocktar, C., Kumalo, H. M., & Koorbanally, N. A. (2019). Synthesis, antibacterial activity and docking studies of substituted quinolone thiosemicarbazones. *Phosphorus, Sulfur, and Silicon and the Related Elements*, *194*(11), 1074–1081. https://doi.org/10.1080/10426507.2019.1618298

Grosscurt, A. C. (1978). Diflubenzuron: Some aspects of its ovicidal and larvicidal mode of action and an evaluation of its practical possibilities. *Pesticide Science*, *9*(5), 373–386. https://doi.org/10.1002/ps.2780090502

Gülçin, I., Küfrevioglu, O. I., Oktay, M., & Büyükokuroglu, M. E. (2004). Antioxidant, antimicrobial, antiulcer and analgesic activities of nettle (Urtica dioica L.). *Journal of ethnopharmacology*, *90*(2-3), 205–215. https://doi.org/10.1016/j.jep.2003.09.028

Hasselbalch, K. A. (1917). "Die Berechnung der Wasserstoffzahl des Blutes aus der freien und gebundenen Kohlensäure desselben, und die Sauerstoffbindung des Blutes als Funktion der Wasserstoffzahl". Biochemische Zeitschrift. ***78****: 112–144.*

Hayat, F., Moseley, E., Salahuddin, A., Van Zyl, R.L. & Azam, A. (2011). Antiprotozoal activity of chloroquinoline based chalcones. *European Journal of Medicinal Chemistry*, 46 (5), 1897-1905.

Henderson, L. J. (1908). The Theory Of Neutrality Regulation In The Animal Organism. *American Journal of Physiology-Legacy Content*, *21*(4), 427–448. https://doi.org/10.1152/ajplegacy.1908.21.4.427

Herraiz, T., Guillén, H., González-Peña, D., & Arán, V. J. (2019). Antimalarial Quinoline Drugs Inhibit β-Hematin and Increase Free Hemin Catalyzing Peroxidative Reactions and Inhibition of Cysteine Proteases. *Scientific Reports*, *9*(1), 15398. https://doi.org/10.1038/s41598-019-51604-z

Hill, S.M. & Crampton, J.M. (1994). DNA-based methods for the identification of insect vectors. *Annals of Tropical Medicine and Parasitology*. Jun;88(3):227-50. doi: 10.1080/00034983.1994.11812864. PMID: 7944669.

Hu, Y.-Q., Gao, C., Zhang, S., Xu, L., Xu, Z., Feng, L.-S., Wu, X., & Zhao, F. (2017). Quinoline hybrids and their antiplasmodial and antimalarial activities. *European Journal of Medicinal Chemistry*, *139*, 22–47. https://doi.org/10.1016/j.ejmech.2017.07.061

Huang, D., Ou, B. & Prior, R.L. (2005) The chemistry behind antioxidant capacity assays. *The Journal of Agricultural and Food Chemistry. 53*(6):1841-1856

Hunsaker, D. B., Schenk, G. H. (1983) The determination of thiols with diphenylpicrylhydrazyl as a spectrophotometric reagent. *Talanta. 30*(7):475-80.

Hunt, R. H., Brooke, B. D., Pillay, C., Koekemoer, L. L., & Coetzee, M. (2005). Laboratory selection for and characteristics of pyrethroid resistance in the malaria vector *Anopheles funestus*. *Medical and Veterinary Entomology*, *19*(3), 271–275. https://doi.org/10.1111/j.1365-2915.2005.00574.x

Ignoto, S., Pecoraro, R., Scalisi, E. M., Buttigè, S. E., Contino, M., Ferruggia, G., Salvaggio, A., & Brundo, M. V. (2022). Acute Toxicity of a Marine Emerging Pollutant (Promethazine Hydrochloride) on *Artemia* sp. *ACS Omega*, *7*(44), 39619–39623. https://doi.org/10.1021/acsomega.2c00856

Jones, R. A., Panda, S. S., & Hall, C. D. (2015). Quinine conjugates and quinine analogues as potential antimalarial agents. *European Journal of Medicinal Chemistry*, *97*, 335–355. https://doi.org/10.1016/j.ejmech.2015.02.002

Kapishnikov, S., Staalsø, T., Yang, Y., Lee, J., Pérez-Berná, A. J., Pereiro, E., Yang, Y., Werner, S., Guttmann, P., Leiserowitz, L., & Als-Nielsen, J. (2019). Mode of action of quinoline antimalarial drugs in red blood cells infected by *Plasmodium falciparum* revealed in vivo. *Proceedings of the National Academy of Sciences*, *116*(46), 22946–22952. https://doi.org/10.1073/pnas.1910123116

Kathrada, F. (2017). The effect of 7-chloroquinoline derivatives of the life cycle of the malaria parasite. University of the Witwatersrand, South Africa. Master of Science in Medicine dissertation. Available at: https://hdl.handle.net/10539/25350 [Accessed date: 17 December 2022]

Kaur, K., Jain, M., Reddy, R. P., & Jain, R. (2010). Quinolines and structurally related heterocycles as antimalarials. *European Journal of Medicinal Chemistry*, *45*(8), 3245–3264. https://doi.org/10.1016/j.ejmech.2010.04.011

Khan, M.A., Akhtar, S., Shahid, K. (2014) Synthesis, characterization and in-vitro biological assays of triphenyltin derivatives of phenylhydrazones. *International Journal of Pharmaceutical Sciences Review and Research*, 28(1), 147-151

Klein E. Y. (2013). Antimalarial drug resistance: a review of the biology and strategies to delay emergence and spread. *International Journal of Antimicrobial Agents*, *41*(4), 311–317. https://doi.org/10.1016/j.ijantimicag.2012.12.007

Kumar, S., Bawa, S., & Gupta, H. (2009). Biological activities of quinoline derivatives. *Mini Reviews in Medicinal Chemistry*, *9*(14), 1648–1654. https://doi.org/10.2174/138955709791012247

Kumar, G., Sathe, A., Krishna, V. S., Sriram, D., & Jachak, S. M. (2018). Synthesis and biological evaluation of dihydroquinoline carboxamide derivatives as anti-tubercular agents. *European Journal of Medicinal Chemistry*, *157*, 1–13. https://doi.org/10.1016/j.ejmech.2018.07.046

Lalloo DG, Shingadia D, Bell DJ, Beeching NJ, Whitty CJM, Chiodini PL. (2016). UK malaria treatment guidelines. *Journal of Infection*; 72:635-649.

Lambros, C., & Vanderberg, J. P. (1979). Synchronization of Plasmodium falciparum Erythrocytic Stages in Culture. *The Journal of Parasitology*, *65*(3), 418–420. https://doi.org/10.2307/3280287

Laurens, M. B. (2020). RTS,S/AS01 vaccine (Mosquirix™): An overview. *Human Vaccines & Immunotherapeutics*, *16*(3), 480–489. https://doi.org/10.1080/21645515.2019.1669415

Lee, A. H., Symington, L. S., & Fidock, D. A. (2014). DNA Repair Mechanisms and Their Biological Roles in the Malaria Parasite *Plasmodium falciparum*. *Microbiology and Molecular Biology Reviews*, *78*(3), 469–486. https://doi.org/10.1128/MMBR.00059-13

Leroy D. (2017). How to tackle antimalarial resistance? *EMBO Molecular Medicine*, *9*(2), 133–134. https://doi.org/10.15252/emmm.201607295

Li, L., Keating, M. J., Plunkett, W., & Yang, L. Y. (1997). Fludarabine-mediated repair inhibition of cisplatin-induced DNA lesions in human chronic myelogenous leukemia-blast crisis K562 cells: induction of synergistic cytotoxicity independent of reversal of apoptosis resistance. *Molecular Pharmacology*, *52*(5), 798–806. https://doi.org/10.1124/mol.52.5.798

Li, W. Y., Xiong, X. Q., Zhao, D. M., Shi, Y. F., Yang, Z. H., Yu, C., Fan, P. W., Cheng, M. S., & Shen, J. K. (2012). Quinoline-3-carboxamide derivatives as potential cholesteryl ester transfer protein inhibitors. *Molecules (Basel, Switzerland)*, *17*(5), 5497–5507. https://doi.org/10.3390/molecules17055497

Liang, N., & Kitts, D. (2014). Antioxidant Property of Coffee Components: Assessment of Methods that Define Mechanisms of Action. *Molecules*, *19*(11), 19180–19208. https://doi.org/10.3390/molecules191119180

Lipinski, C. A., Lombardo, F., Dominy, B. W., & Feeney, P. J. (1997). Experimental and computational approaches to estimate solubility and permeability in drug discovery and development settings. *In Vitro Models for Selection of Development Candidates*, *23*(1), 3–25. https://doi.org/10.1016/S0169-409X(96)00423-1

Lobo, V., Patil, A., Phatak, A., & Chandra, N. (2010). Free radicals, antioxidants and functional foods: Impact on human health. *Pharmacognosy Reviews*, *4*(8), 118–126. https://doi.org/10.4103/0973-7847.70902

Mabeza, G. F., Loyevsky, M., Gordeuk, V. R., & Weiss, G. (1999). Iron chelation therapy for malaria: a review. *Pharmacology & Therapeutics*, *81*(1), 53–75. https://doi.org/10.1016/s0163-7258(98)00037-0

Maharaj, R., Seocharan, I., Lakan, V., Nyawo, Z., Mkhabela, M., & Balakrishna, Y. (2024). Field evaluation of the residual efficacy of new generation insecticides for potential use in indoor residual spray programmes in South Africa. *Malaria Journal*, *23*(1), 127. https://doi.org/10.1186/s12936-024-04963-6

Mahlangu, J. (2023) The Inhibitory Effects of Quinoline-, Pyrimidine-Phenyl Hybrid- and Quinazolin-4(3H)-One Derivatives Against the Life Cycle of *Plasmodium* and *Anopheles*. University of the Witwatersrand, Master of Science in Medicine dissertation.

Makler, M. T., Ries, J. M., Williams, J. A., Bancroft, J. E., Piper, R. C., Gibbins, B. L., & Hinrichs, D. J. (1993). Parasite lactate dehydrogenase as an assay for *Plasmodium falciparum* drug sensitivity. *The American Journal of Tropical Medicine and Hygiene*, *48*(6), 739–741. https://doi.org/10.4269/ajtmh.1993.48.739

Marella, A., Tanwar, O. P., Saha, R., Ali, M. R., Srivastava, S., Akhter, M., Shaquiquzzaman, M., & Alam, M. M. (2013). Quinoline: A versatile heterocyclic. *Saudi Pharmaceutical Journal*, *21*(1), 1–12. https://doi.org/10.1016/j.jsps.2012.03.002

Markwalter, C. F., Davis, K. M., & Wright, D. W. (2016). Immunomagnetic capture and colorimetric detection of malarial biomarker *Plasmodium falciparum* lactate dehydrogenase. *Analytical biochemistry*, *493*, 30–34. https://doi.org/10.1016/j.ab.2015.10.003

Metrangolo, P., & Resnati, G. (2008). Halogen Versus Hydrogen. *Science*, *321*(5891), 918–919. https://doi.org/10.1126/science.1162215

Michael, A. S., Thompson, C. G., & Abramovitz, M. (1956). Artemia salina as a Test Organism for Bioassay. *Science (New York, N.Y.)*, *123*(3194), 464. https://doi.org/10.1126/science.123.3194.464

MMV (2022) MMV Annual Report 2022. Geneva. Available at: https://www.mmv.org/sites/default/files/content/document/MMV_AnnualReport_2022_0.pdf [Accessed date: 5 December 2023].

Modarresi Chahardehi, A., Arsad, H., & Lim, V. (2020). Zebrafish as a Successful Animal Model for Screening Toxicity of Medicinal Plants. *Plants*, *9*(10), 1345. https://doi.org/10.3390/plants9101345

Moiseeva, A. A., Artyushin, O. I., Anikina, L. V., & Brel, V. K. (2019). Synthesis and antitumor activity of daunorubicin conjugates with of 3,4-methylendioxybenzaldehyde. *Bioorganic & Medicinal Chemistry Letters*, *29*(19), 126617. https://doi.org/10.1016/j.bmcl.2019.08.021

Moseley, E.J. (2012). The antimalarial properties of thiosemicarbazone, chalcone and nucleoside phosphonate derivatives. University of the Witwatersrand, South Africa. Master of Science in Medicine dissertation. Available at: http://hdl.handle.net/10539/12482 [Accessed date: 5 December 2023].

Mosmann T. (1983). Rapid colorimetric assay for cellular growth and survival: application to proliferation and cytotoxicity assays. *Journal of immunological methods*, *65*(1-2), 55–63. https://doi.org/10.1016/0022-1759(83)90303-4

Mouatcho, J. C., Munhenga, G., Hargreaves, K., Brooke, B. D., Coetzee, M., & Koekemoer, L. L. (2009). Pyrethroid resistance in a major African malaria vector *Anopheles* arabiensis from Mamfene, northern KwaZulu-Natal, South Africa. *South African Journal of Science*, *105*(3/4), 127. https://doi.org/10.4102/sajs.v105i3/4.63

Maret, W., & Wedd, A. (Eds.). (2014). *Binding, Transport and Storage of Metal Ions in Biological Cells*. The Royal Society of Chemistry. https://doi.org/10.1039/9781849739979

MR4 (2014). Anopheles Laboratory Biology and Culture. Methods in *Anopheles* research. 4th ed. Atlanta: Centers for Disease Control and Prevention; p. 1–8.

Murugan, K., Panneerselvam, C., Subramaniam, J., Paulpandi, M., Rajaganesh, R., Vasanthakumaran, M., Madhavan, J., Shafi, S. S., Roni, M., Portilla-Pulido, J. S., Mendez, S. C., Duque, J. E., Wang, L., Aziz, A. T., Chandramohan, B., Dinesh, D., Piramanayagam, S., & Hwang, J.-S. (2022). Synthesis of new series of quinoline derivatives with insecticidal effects on larval vectors of malaria and dengue diseases. *Scientific Reports*, *12*(1), 4765. https://doi.org/10.1038/s41598-022-08397-5

National Center for Biotechnology Information (2024a). PubChem Compound Summary for CID 7047, Quinoline. Available at: https://pubchem.ncbi.nlm.nih.gov/compound/Quinoline. [Accessed date: 25 March 2024].

National Center for Biotechnology Information (2024b). PubChem Compound Summary for CID 54670067, Ascorbic Acid. Available at: https://pubchem.ncbi.nlm.nih.gov/compound/Ascorbic-Acid. [Accessed date: 25 March 2024].

National Center for Biotechnology Information (2024c). PubChem Compound Summary for CID 24360, Camptothecin. Available at: https://pubchem.ncbi.nlm.nih.gov/compound/Camptothecin. [Accessed date: 25 March 2024].

National Center for Biotechnology Information (2024d). PubChem Compound Summary for CID 64927, Chloroquine Phosphate. Available at: https://pubchem.ncbi.nlm.nih.gov/compound/Chloroquine-Phosphate. [Accessed date: 25 March 2024].

National Center for Biotechnology Information (2024e). PubChem Compound Summary for CID 5702198, azane;dichloroplatinum. Available at: https://pubchem.ncbi.nlm.nih.gov/compound/Cisplatin. [Accessed date: 25 March 2024].

National Center for Biotechnology Information (2024f). PubChem Compound Summary for CID 3036, Clofenotane. Available at: https://pubchem.ncbi.nlm.nih.gov/compound/dichlorodiphenyltrichloroethane [Accessed date: 25 March 2024].

National Center for Biotechnology Information (2024g). PubChem Compound Summary for CID 3000518, Dihydroartemisinin. Available at: https://pubchem.ncbi.nlm.nih.gov/compound/Dihydroartemisinin. [Accessed date: 25 March 2024].

National Center for Biotechnology Information (2024h). PubChem Compound Summary for CID 6049, Edetic Acid. Available at: https://pubchem.ncbi.nlm.nih.gov/compound/Edetic-Acid. [Accessed date: 25 March 2024].

National Center for Biotechnology Information (2024i). PubChem Compound Summary for CID 712, Formaldehyde. Available at: https://pubchem.ncbi.nlm.nih.gov/compound/Formaldehyde. [Accessed date: 25 March 2024].

National Center for Biotechnology Information (2024j). PubChem Compound Summary for CID 24502, Potassium Dichromate. Available at: https://pubchem.ncbi.nlm.nih.gov/compound/Potassium-Dichromate. [Accessed date: 25 March 2024].

National Center for Biotechnology Information (2024k). PubChem Compound Summary for CID 16211283, Quinine hydrochloride dihydrate. Available at: https://pubchem.ncbi.nlm.nih.gov/compound/Quinine-hydrochloride-dihydrate. [Accessed date: 25 March 2024].

National Center for Biotechnology Information (2024l). PubChem Compound Summary for CID 5590, Triton X-100. Available at: https://pubchem.ncbi.nlm.nih.gov/compound/ Triton-X-100. [Accessed date: 25 March 2024].

Nayyer, A., Jain, R. (2008) Synthesis and anti-tubercular activity of 2,4-disubstitued quinolines. *Indian Journal of Chemistry*, 47B, 117-128.

Niles, J. C. (2012). Malarial Parasites Accumulate Labile Zinc Pools. *Chemistry & Biology*, *19*(6), 660–661. https://doi.org/10.1016/j.chembiol.2012.06.003

Ngeno, L. (2021) Antimalarial activity of quinoline thiosemicarbazones: synthesis and antiplasmodial evaluation. Rhodes University, Grahamstown, South Africa. Master of Science in Chemistry. Available at: http://hdl.handle.net/10962/291292 [Accessed date: 20 March 2024].

Ngou, O., Nzoumbou-Boko, R., Bakamba, P., & Boum, Y. (2024). R21/Matrix-M malaria vaccine: A vital tool in the arsenal against malaria, not a silver bullet. *The Lancet Infectious Diseases*, S1473309924000100. https://doi.org/10.1016/S1473-3099(24)00010-0

Omorou, R., Bin Sa'id, I., Delves, M., Severini, C., Kouakou, Y. I., Bienvenu, A.-L., & Picot, S. (2022). Protocols for *Plasmodium* gametocyte production *in vitro*: An integrative review and analysis. *Parasites & Vectors*, *15*(1), 451. https://doi.org/10.1186/s13071-022-05566-3

Ott, M., Avendaño-Guzmán, E., Ullrich, E., Dreyer, C., Strauss, J., Harden, M., Schön, M., Schön, M. P., Bernhardt, G., Stadelmann, C., Wegner, C., Brück, W., & Nessler, S. (2019). Laquinimod, a prototypic quinoline-3-carboxamide and aryl hydrocarbon receptor agonist, utilizes a CD155-mediated natural killer/dendritic cell interaction to suppress CNS autoimmunity. *Journal of Neuroinflammation*, *16*(1), 49. https://doi.org/10.1186/s12974-019-1437-0

Parhizgar, A. R., & Tahghighi, A. (2017). Introducing New Antimalarial Analogues of Chloroquine and Amodiaquine: A Narrative Review. *Iranian Journal of Medical Sciences*, *42*(2), 115–128.

Percário, S., Moreira, D. R., Gomes, B. A., Ferreira, M. E., Gonçalves, A. C., Laurindo, P. S., Vilhena, T. C., Dolabela, M. F., & Green, M. D. (2012). Oxidative stress in malaria. *International Journal of Molecular Sciences*, *13*(12), 16346–16372. https://doi.org/10.3390/ijms131216346

Pham-Huy, L. A., He, H., & Pham-Huy, C. (2008). Free radicals, antioxidants in disease and health. *International Journal of Biomedical Science*; *4*(2), 89–96.

Pink R, Hudson A, Mouriès MA. & Bendig, M. (2005). Opportunities and challenges in antiparasitic drug discovery. *Nature Reviews Drug Discovery*;4(9):727-40.

Pokrovskaya, V., Belakhov, V., Hainrichson, M., Yaron, S., & Baasov, T. (2009). Design, Synthesis, and Evaluation of Novel Fluoroquinolone−Aminoglycoside Hybrid Antibiotics. *Journal of Medicinal Chemistry*, *52*(8), 2243–2254. https://doi.org/10.1021/jm900028n

Priyadarshini, G.S., Namitha, R., Mageswari, D., Selvi, G. (2016) Synthesis characterization and antioxidant activity of Ni (II) and Co (II) quinoline-Schiff base. *International Journal of Innovative Research in Science, Engineering and Technology*, *5*(1), 101-106.

Ramar, M., Ignacimuthu, S., & Paulraj, M. G. (2014). Ovicidal and oviposition response activities of plant volatile oils against Culex quinquefasciatus say. *Journal of Entomology and Zoology Studies*; s 2014; 2 (4): 82-86

Rants'o, T. A., van Greunen, D. G., van der Westhuizen, C. J., Riley, D. L., Panayides, J. L., Koekemoer, L. L., & van Zyl, R. L. (2022). The *in silico* and *in vitro* analysis of donepezil derivatives for *Anopheles* acetylcholinesterase inhibition. *PloS one*, *17*(11), e0277363. https://doi.org/10.1371/journal.pone.0277363

Riss TL, Moravec RA, Niles AL, *et al,.* Cell Viability Assays. (2016). In: Markossian S, Grossman A, Brimacombe K, *et al.,* editors. Assay Guidance Manual [Internet]. Bethesda (MD): Eli Lilly & Company and the National Center for Advancing Translational Sciences. Available at: https://www.ncbi.nlm.nih.gov/books/NBK144065/ [Accessed 4 Jan. 2019]

Rollas, S., & Küçükgüzel, S. (2007). Biological Activities of Hydrazone Derivatives. *Molecules*, *12*(8), 1910–1939. https://doi.org/10.3390/12081910

Rosenthal, P. J. (2020). Falcipain cysteine proteases of malaria parasites: An update. *Biochimica et Biophysica Acta (BBA) - Proteins and Proteomics*, *1868*(3), 140362. https://doi.org/10.1016/j.bbapap.2020.140362

Rosenthal P.J. Antiprotozoal drugs. Vanderah T.W.(Ed.), (2023) *Katzung's Basic & Clinical Pharmacology, 16th Edition*. McGraw-Hill. https://accessmedicine.mhmedical.com/content.aspx?bookid=3382&sectionid=28175591 [Accessed date: 15 March 2023]

Rossiter, D. and Blockman, M. (eds) (2020) South African Medicines Formulary (SAMF). 13th edn. Cape Town: South African Medical Association

Ruebhart, D. R., Wickramasinghe, W., & Cock, I. E. (2009). Protective efficacy of the antioxidants vitamin E and Trolox against *Microcystis aeruginosa* and microcystin-LR in *Artemia franciscana* nauplii. *Journal of Toxicology and Environmental Health. Part A*, *72*(24), 1567–1575. https://doi.org/10.1080/15287390903232459

Rueda, L. (2004). Pictorial keys for the identification of mosquitoes (Diptera: Culicidae) associated with Dengue Virus Transmission**.** *Zootaxa, 589*(1), 1–60. doi: http://dx.doi.org/10.11646/zootaxa.589.1.1

Sæbø, I. P., Bjørås, M., Franzyk, H., Helgesen, E., & Booth, J. A. (2023). Optimization of the Hemolysis Assay for the Assessment of Cytotoxicity. *International Journal of Molecular Sciences*, *24*(3), 2914. https://doi.org/10.3390/ijms24032914

Samuels, A. M., Ansong, D., Kariuki, S. K., Adjei, S., Bollaerts, A., Ockenhouse, C., Westercamp, N., Lee, C. K., Schuerman, L., Bii, D. K., Osei-Tutu, L., Oneko, M., Lievens, M., Attobrah Sarfo, M. A., Atieno, C., Morelle, D., Bakari, A., Sang, T., Jongert, E., Kotoh-Mortty, M. F., … RTS,S study group (2022). Efficacy of RTS,S/AS01$_E$ malaria vaccine administered according to different full, fractional, and delayed third or early fourth dose regimens in children aged 5-17 months in Ghana and Kenya: an open-label, phase 2b, randomised controlled trial. *The Lancet. Infectious Diseases*, *22*(9), 1329–1342. https://doi.org/10.1016/S1473-3099(22)00273-0

Savini, L., Chiasserini, L., Gaeta, A., Pelleran, C. (2002) Synthesis and anti-tubercular evaluation of 4-quinolylhydrazones. *Bioorganic & Medicinal Chemistry*, *10,* 2193–2198.

Sevrioukova, I. F., & Poulos, T. L. (2013). Understanding the mechanism of cytochrome P450 3A4: Recent advances and remaining problems. *Dalton Transactions*, *42*(9), 3116–3126. https://doi.org/10.1039/C2DT31833D

Shenai, B. R., Sijwali, P. S., Singh, A., & Rosenthal, P. J. (2000). Characterization of Native and Recombinant Falcipain-2, a Principal Trophozoite Cysteine Protease and Essential Hemoglobinase of *Plasmodium falciparum*. *Journal of Biological Chemistry*, *275*(37), 29000–29010. https://doi.org/10.1074/jbc.M004459200

Sidhu, A. B. S., Verdier-Pinard, D., & Fidock, D. A. (2002). Chloroquine Resistance in *Plasmodium falciparum* Malaria Parasites Conferred by *pfcrt* Mutations. *Science*, *298*(5591), 210–213. https://doi.org/10.1126/science.1074045

Silver, K. S., Du, Y., Nomura, Y., Oliveira, E. E., Salgado, V. L., Zhorov, B. S., & Dong, K. (2014). Voltage-Gated Sodium Channels as Insecticide Targets. *Advances in Insect Physiology; 46*, 389–433). https://doi.org/10.1016/B978-0-12-417010-0.00005-7

Singh, A., Kalamuddin, M., Maqbool, M., Mohmmed, A., Malhotra, P., & Hoda, N. (2021). Quinoline carboxamide core moiety-based compounds inhibit *P. falciparum* falcipain-2: Design, synthesis and antimalarial efficacy studies. *Bioorganic Chemistry*, *108*, 104514. https://doi.org/10.1016/j.bioorg.2020.104514

Sinka, M. E., Bangs, M. J., Manguin, S., Coetzee, M., Mbogo, C. M., Hemingway, J., Patil, A. P., Temperley, W. H., Gething, P. W., Kabaria, C. W., Okara, R. M., Van Boeckel, T., Godfray, H. C., Harbach, R. E., & Hay, S. I. (2010). The dominant *Anopheles* vectors of human malaria in Africa, Europe and the Middle East: occurrence data, distribution maps and bionomic précis. *Parasites & vectors*, *3*, 117. https://doi.org/10.1186/1756-3305-3-117

South African National Department of Health (SA-DOH). (2019a). National guidelines for the treatment of malaria, South Africa 2019. National Department of Health. Available at:

https://www.nicd.ac.za/wp-content/uploads/2017/03/National-Guidelines-for-Malaria-Treatment-SEPTEMBER-2019-Update-WITH-FRONT.pdf [Accessed date: 4 October 2023].

South African National Department of Health (SA-DOH). (2019b). National guidelines for the prevention of malaria, South Africa 2018. National Department of Health. https://www.nicd.ac.za/wp-content/uploads/2019/03/National-Guidelines-for-prevention-of-Malaria_updated-08012019-1.pdf [Accessed date: 4 October 2023]

Strober, W. (1997) Trypan blue exclusion test of cell viability, In: Current Protocols in Immunology, Appendix 3, p. A.3B.1-A.3B.2. doi: 10.1002/0471142735.ima03bs21.

Sullivan, D. J., Gluzman, I. Y., Russell, D. G., & Goldberg, D. E. (1996). On the molecular mechanism of chloroquine's antimalarial action. *Proceedings of the National Academy of Sciences*, *93*(21), 11865–11870. https://doi.org/10.1073/pnas.93.21.11865

Tallarida, R. J., & Raffa, R. B. (2010). The application of drug dose equivalence in the quantitative analysis of receptor occupation and drug combinations. *Pharmacology & Therapeutics*, *127*(2), 165–174. https://doi.org/10.1016/j.pharmthera.2010.04.011

Thermo Fisher (2020), Gibco Cell Culture Basics Handbook, Thermo Fisher Scientific®, UK Available at: https://assets.thermofisher.com/TFS-Assets/BID/Handbooks/gibco-cell-culture-basics-handbook.pdf [Accessed date: 5 November 2022].

Trager, W., & Jensen, J. B. (1976). Human malaria parasites in continuous culture. *Science (New York, N.Y.)*, *193*(4254), 673–675. https://doi.org/10.1126/science.781840

Trampuz, A., Jereb, M., Muzlovic, I., & Prabhu, R. M. (2003). Clinical review: Severe malaria. *Critical care (London, England)*, *7*(4), 315–323. https://doi.org/10.1186/cc2183

Vanhaecke, P., Persoone, G., Claus, C., & Sorgeloos, P. (1981). Proposal for a short-term toxicity test with *Artemia* nauplii. *Ecotoxicology and Environmental Safety*, *5*(3), 382–387. https://doi.org/10.1016/0147-6513(81)90012-9

Van Walbeek, W., Moodie, C. A., Scott, P. M., Harwig, J., & Grice, H. C. (1971). Toxicity and excretion of ochratoxin A in rats intubated with pure ochratoxin A or fed cultures of *Penicillium viridicatum*. *Toxicology and Applied Pharmacology*, *20*(3), 4239–4241.

Van Zyl, R.L., Seatlholo, S.T. and Viljoen, A.M. (2010). Pharmacological interactions of essential oil constituents on the in vitro growth of *Plasmodium falciparum*. South African Journal of Botany, 76 (4), pp.662-667

Van Zyl, R. L. (2016). The Malaria Season Is Upon Us. *South African Family Practice*, *58*(5), 68–72. https://doi.org/10.4102/safp.v58i5.4551

Vector Disease Control International (2018), Life Cycle: Mosquito Biology 101. Vdci.net. Available at: http://www.vdci.net/mosquito-biology-101-life-cycle [Accessed 4 Jan. 2019]

Venter, C. J. (2023) Developing an African Mosquito Model for Malaria Transmission Blocking Studies. University of the Witwatersrand, Master of Science in Medicine dissertation.

Walcourt, A., Loyevsky, M., Lovejoy, D. B., Gordeuk, V. R., & Richardson, D. R. (2004). Novel aroylhydrazone and thiosemicarbazone iron chelators with anti-malarial activity against chloroquine-resistant and -sensitive parasites. *The international Journal of Biochemistry & Cell Biology*, *36*(3), 401–407. https://doi.org/10.1016/s1357-2725(03)00248-6

Wang, J.-J., Si, W.-J., Chen, M., Lu, A.-M., Zhang, W.-H., & Yang, C.-L. (2017). Synthesis and fungicidal activity of phenylhydrazone derivatives containing two carbonic acid ester groups. *Journal of Pesticide Science*, *42*(3), 84–92. https://doi.org/10.1584/jpestics.D16-105

Wei, Y., To, K. K. W., & Au-Yeung, S. C. F. (2015). Synergistic cytotoxicity from combination of imatinib and platinum-based anticancer drugs specifically in Bcr-Abl positive leukemia cells. *Journal of Pharmacological Sciences*, *129*(4), 210–215. https://doi.org/10.1016/j.jphs.2015.10.008

WHO (2005) Guidelines for laboratory and field testing of mosquito larvicides. Geneva. Available at: http://apps.who.int/iris/bitstream/10665/69101/1/WHO_CDS_WHOPES_GCDPP_2005.13.pdf. [Accessed date: 15 May 2017].

WHO (2013) Malaria Entomology and Vector Control – Guide for Participants. Geneva. Available at: http://apps.who.int/iris/handle/10665/85890 [Accessed date: 14 April 2017].

WHO (2015) World Malaria Report 2015. Geneva. Available at: https://www.who.int/publications/i/item/9789241565158 [Accessed date: 4 January 2023].

WHO (2019) World Malaria Report 2019. Geneva. Available at: https://www.who.int/publications/i/item/9789241565721 [Accessed date: 4 January 2023].

WHO (2023a) World Malaria Report 2023. Geneva. Available at: https://www.who.int/publications/i/item/9789240086173 [Accessed date: 5 December 2023].

WHO (2023b) Guidelines for malaria, 14 March 2023. Geneva. Available at: https://iris.who.int/bitstream/handle/10665/373339/WHO-UCN-GMP-2023.01-Rev.1-eng.pdf?sequence=1 [Accessed date: 5 December 2023].

Williams J, Pinto J, Pan American Health Organization (PAHO) (2012), WHO. Training manual on malaria entomology: for entomology and vector control technicians (basic level). https://www.paho.org/hq/dmdocuments/2012/2012-Training-manual-malaria-entomology.pdf. [Accessed date: 5 December 2023].

Yadav, P., & Shah, K. (2021). Quinolines, a perpetual, multipurpose scaffold in medicinal chemistry. *Bioorganic Chemistry*, *109*, 104639. https://doi.org/10.1016/j.bioorg.2021.104639

Yang, Z.-B., Hu, D.-Y., Zeng, S., & Song, B.-A. (2016). Novel hydrazone derivatives containing pyridine amide moiety: Design, synthesis, and insecticidal activity. *Bioorganic & Medicinal Chemistry Letters*, *26*(4), 1161–1164. https://doi.org/10.1016/j.bmcl.2016.01.047

Yao, X., Sun, X., Jin, S., Yang, L., Xu, H., & Rao, Y. (2019). Discovery of 4-Aminoquinoline-3-carboxamide Derivatives as Potent Reversible Bruton's Tyrosine Kinase Inhibitors for the Treatment of Rheumatoid Arthritis. *Journal of Medicinal Chemistry*, *62*(14), 6561–6574. https://doi.org/10.1021/acs.jmedchem.9b00329

Ye, Z.-W., Zhang, J., Townsend, D. M., & Tew, K. D. (2015). Oxidative stress, redox regulation and diseases of cellular differentiation. *Biochimica et Biophysica Acta (BBA) - General Subjects*, *1850*(8), 1607–1621. https://doi.org/10.1016/j.bbagen.2014.11.010

Yin, Z., Deng, Z., Zhao, W., & Cao, Z. (2018). Searching Synergistic Dose Combinations for Anticancer Drugs. *Frontiers in Pharmacology*, *9*, 535. https://doi.org/10.3389/fphar.2018.00535

Yu, J., & Lu, Y. (2018). Artemia spp. Model—A Well-Established Method for Rapidly Assessing the Toxicity on an Environmental Perspective. *Medical Research Archives*, *6*(2). https://doi.org/10.18103/mra.v6i2.1700

Zaib, S., Munir, R., Younas, M. T., Kausar, N., Ibrar, A., Aqsa, S., Shahid, N., Asif, T. T., Alsaab, H. O., & Khan, I. (2021). Hybrid Quinoline-Thiosemicarbazone Therapeutics as a New Treatment Opportunity for Alzheimer's Disease–Synthesis, *In Vitro* Cholinesterase Inhibitory Potential and Computational Modeling Analysis. *Molecules*, *26*(21), 6573. https://doi.org/10.3390/molecules26216573

Zhang, Y., Guiguemde, W. A., Sigal, M., Zhu, F., Connelly, M. C., Nwaka, S., & Guy, R. K. (2010). Synthesis and structure–activity relationships of antimalarial 4-oxo-3-carboxyl quinolones. *Bioorganic & Medicinal Chemistry*, *18*(7), 2756–2766. https://doi.org/10.1016/j.bmc.2010.02.013

Zhou, W., Wang, H., Yang, Y., Chen, Z.-S., Zou, C., & Zhang, J. (2020a). Chloroquine against malaria, cancers and viral diseases. *Drug Discovery Today*, *25*(11), 2012–2022. https://doi.org/10.1016/j.drudis.2020.09.010

Zhou, Y., Xu, X., Wang, F., He, H., Gong, G., Xiong, L., & Qi, B. (2020b). Identification of novel quinoline analogues bearing thiazolidinones as potent kinase inhibitors for the treatment of colorectal cancer. *European Journal of Medicinal Chemistry*, *204*, 112643. https://doi.org/10.1016/j.ejmech.2020.112643

Zou, B.-Q., Lu, X., Qin, Q.-P., Bai, Y.-X., Zhang, Y., Wang, M., Liu, Y.-C., Chen, Z.-F., & Liang, H. (2017). Three novel transition metal complexes of 6-methyl-2-oxo-quinoline-3-carbaldehyde thiosemicarbazone: Synthesis, crystal structure, cytotoxicity, and mechanism of action. *RSC Advances*, *7*(29), 17923–17933. https://doi.org/10.1039/C7RA00826K

Appendix A: Ethics Documents

UNIVERSITY OF THE WITWATERSRAND, JOHANNESBURG	HUMAN RESEARCH ETHICS COMMITTEE (MEDICAL)

Office of the Deputy Vice-Chancellor (Research & Innovation)

TO: Mr S Lala
School: Therapeutic Sciences
Department: Pharmacy and Pharmacology
Division: Pharmacology
University

E-mail: Sahil.Lala@wits.ac.za

CC: Supervisor: Professor R van Zyl <Robyn.vanZyl@wits.ac.za>
and <HREC-Medical.ResearchOffice@wits.ac.za>

FROM: Mr Iain Burns
Human Research Ethics Committee (Medical)
Tel: 011 717 1252

E-mail: Iain.Burns@wits.ac.za

DATE: 07/11/2022

REF: *R14/49*

PROTOCOL NO: W-CBP-221107-01 (This is your ethics application study reference number. Please quote this reference number in all correspondence relating to this study)

PROJECT TITLE: *The effect of novel quinoline heterocyclic derivatives on the malaria parasite and Anopheles vector*

Please find attached the Ethics Waiver Certificate for the above project. I hope it goes well and that an article in a recognized publication comes out of it. This will reflect well on your professional standing and contribute to the Government funding of the University.

MSWorks2000/Iain0007/ClearScanWaiver.wps

UNIVERSITY OF THE WITWATERSRAND, JOHANNESBURG	HUMAN RESEARCH ETHICS COMMITTEE (MEDICAL)

Office of the Deputy Vice-Chancellor (Research & Innovation)

07/11/2022

Ref: W-CBP-221107-01

TO WHOM IT MAY CONCERN

Waiver: This certifies that the following research does not require clearance from the Human Research Ethics Committee (Medical)

Investigator: Mr S Lala
Student No. (if appropriate): 358351
Staff No. (if appropriate):

Supervisor: Professor R van Zyl

School: Therapeutic Sciences
Department: Pharmacy and Pharmacology
Pharmacology
University

Project title: *The effect of novel quinoline heterocyclic derivatives on the malaria parasite and Anopheles vector*

Reason: In vitro laboratory study
No human participants will be involved in the study

Dr N Naran
Co-Chairperson: Human Research Ethics Committee (Medical)

Research Office Secretariat:
Third Floor, Phillip Tobias Building, corner of St Andrews and York Roads, Parktown, Johannesburg 2193
Postal address: Private Bag 3, Wits 2050
Tel Nos: +27 (0)11 717 1234/1252/2656/2700
Office E-mail: HREC-Medical.ResearchOffice@wits.ac.za
Website:
https://www.wits.ac.za/research/researcher-support/research-ethics/ethics-committees/

UNIVERSITY OF THE WITWATERSRAND, JOHANNESBURG

ANIMAL RESEARCH ETHICS COMMITTEE (AREC)

Registration number: AREC0101210-002

Solomon Mahlangu House
10th Floor, Room 10004
Jorissen Street
Braamfontein, Johannesburg

24 November 2017

To whom it may concern,

Re: Professor R van Zyl Waiver (for MSc students) from Animal Research Ethics Committee of the University of the Witwatersrand

This letter serves to confirm that Associate Professor Robyn van Zyl (Department of Pharmacy and Pharmacology, School of Therapeutic Sciences, University of the Witwatersrand) does not require full animal ethics clearance for her studies undertaken by the students detailed below. She has previously been granted a waiver for the studies as detailed in the documents referenced *R van Zyl (Artemia) 07-11-2017-O and R van Zyl-Anopheles waiver 07-11-2017-O*. The students and studies covered by the waiver letters:

1. Ms Fatima Kathrada [0602240N]: The effect of 7-chloroquinoline derivatives on the life cycle of the malaria parasite.

2. Mr Sahil Lala [358351]: The effect of quinolone heterocyclic derivatives on the malaria parasite and Anopheles vector.

3. Ms Teboho Malimabe [152675]: The effect of novel quinoxaline derivatives on the life cycle of malaria parasite and vector.

4. Ms Natasha Jansen van Vuuren [071867W]: The effect of novel compounds on copper homeostasis in *Plasmodium falciparum* and neuroblastoma cells.

5. Mr Thulani Mahlangu [667999]: The chemotherapeutic properties of novel quinazolines and bis-hydrazones compounds.

6. Ms Puleng Thabana [609529: The effect of novel oxo-1, 6 dihydropyrimidine and 2-(quinolone-8-yloyxy) acetohydrazone derivatives on the life cycle of the malaria parasite.

7. Ms W Ramashia [572354]: Transcription analysis of an immune factor in a main Africa malaria vector *Anopheles funestus*.

Conditions: All previously requisite biosafety and biosecurity SOPs should be adhered to.

Should you require any further information, do not hesitate to contact me.

Yours sincerely,



Kennedy Erlwanger

(Chairman: Animal Research Ethics Committee, University of the Witwatersrand)

Reference: R van Zyl –Anopheles & Artemia PGrad students Waiver 07-11-2017-O

Assoc Prof Kennedy H. Erlwanger
School of Physiology
Faculty of Health Sciences, University of the Witwatersrand
7 York Road, Parktown, 2193
SOUTH AFRICA
Tel: +27 (0)11 717 2454
Email: Kennedy.Erlwanger@wits.ac.za

UNIVERSITY OF THE WITWATERSRAND JOHANNESBURG	HUMAN RESEARCH ETHICS COMMITTEE (MEDICAL)

Office of the Deputy Vice-Chancellor (Research & Post Graduate Affairs)

TO: Professor R van Zyl
School of Therapeutic Sciences
Department of Pharmacy and Pharmacology
Medical School
University

E-mail: Robyn.vanzyl@wits.ac.za

CC: Supervisor: Not applicable <>
and <HREC-Medical ResearchOffice@wits.ac.za>

FROM: Iain Burns
Human Research Ethics Committee (Medical)
Tel: 011 717 1252

E-mail: Iain.Burns@wits.ac.za

DATE: 2019/06/10

REF: *R14/49*

PROTOCOL NO: **M190579** *(This is your ethics application study reference number. Please quote this reference number in all correspondence relating to this study)*

PROJECT TITLE: *The chemotherapeutic properties of novel synthetic and natural compounds*

Please find attached the Clearance Certificate for the above project. I hope it goes well and that an article in a recognized publication comes out of it. This will reflect well on your professional standing and contribute to the Government funding of the University.

MSWorks2000/Iain0007/Clearscan.wps

UNIVERSITY OF THE WITWATERSRAND JOHANNESBURG

R14/49 Professor R van Zyl

HUMAN RESEARCH ETHICS COMMITTEE (MEDICAL)
CLEARANCE CERTIFICATE NO. M190579

NAME: (Principal Investigator)	Professor R van Zyl
DEPARTMENT:	School of Therapeutic Sciences Department of Pharmacy and Pharmacology Medical School University
PROJECT TITLE:	The chemotherapeutic properties of novel synthetic and natural compounds
DATE CONSIDERED:	Ad hoc
DECISION:	Approved unconditionally
CONDITIONS:	Renewal of M140669
SUPERVISOR:	Not applicable
APPROVED BY:	Dr CB Penny, Chairperson, HREC (Medical)
DATE OF APPROVAL:	2019/06/10

This clearance certificate is valid for 5 years from date of approval. Extension may be applied for.

DECLARATION OF INVESTIGATORS

To be completed in duplicate and **ONE COPY** returned to the Research Office Secretary on the 3rd Floor, Phillip Tobias Building, Parktown, University of the Witwatersrand, Johannesburg.

I/we fully understand the conditions under which I am/we are authorized to carry out the above-mentioned research and I/we undertake to ensure compliance with these conditions. Should any departure be contemplated, from the research protocol as approved, I/we undertake to submit details to the Committee. **I agree to submit a yearly progress report.** When a funder requires annual re-certification, the application date will be one year after the date when the study was initially reviewed. In this case, the study was initially reviewed in **May** and will therefore reports and re-certification will be due early in the month of **May** each year. Unreported changes to the application may invalidate the clearance given by the HREC (Medical).

Principal Investigator Signature

01/07/2019
Date

PLEASE QUOTE THE CLEARANCE CERTIFICATE NUMBER IN ALL ENQUIRIES

Appendix B: Antimalarial Activity

Table B1: The percentage parasite viability for each of the test compounds in comparison with positive control Quinine at 50 µM.

Compound	% Malaria Parasite viability @ 50 µM	Compound	% Malaria Parasite viability @ 50 µM	Compound	% Malaria Parasite viability @ 50 µM
DC1	33.12 ± 4.79	**PHYD1**	24.07 ± 12.89	**Q3C1**	59.11 ± 13.46
DC2	41.58 ± 17.42	**PHYD2**	20.92 ± 2.44	**Q3C2**	68.34 ± 27.21
DC3	20.48 ± 5.02	**PHYD3**	25.23 ± 5.41	**Q3C3**	27.49 ± 21.09
DC4	10.33 ± 11.97	**PHYD4**	65.12 ± 14.86	**Q3C4**	89.62 ± 7.96
DC5	33.60 ± 1.60	**PHYD5**	58.70 ± 30.05	**Q3C5**	84.93 ± 1.70
DC6	14.52 ± 22.24	**PHYD6**	76.98 ± 5.11	**Q3C6**	55.67 ± 20.98
DC7	38.72 ± 14.79	**PHYD7**	75.27 ± 22.63	**Q3C7**	10.10 ± 21.37
DC8	10.57 ± 4.07	**PHYD8**	79.76 ± 20.35	**Q3C8**	59.32 ± 39.38
DC9	8.67 ± 14.76	**PHYD9**	50.04 ± 24.78	**Q3C9**	55.53 ± 17.34
DC10	18.38 ± 32.93	**PHYD10**	60.96 ± 5.41	**Q3C10**	50.66 ± 6.62
DC11	16.70 ± 22.57	**PHYD11**	79.44 ± 20.77	**Q3C11**	10.85 ± 9.23
DC12	0.01 ± 13.33	**PHYD12**	76.53 ± 20.26	**Q3C12**	38.69 ± 2.02
DC13	13.23 ± 7.05	**PHYD13**	77.12 ± 20.54		
DC14	0.01 ± 6.64	**PHYD14**	72.95 ± 28.52	**Quinine**	7.29 ± 5.18
DC15	0.01 ± 10.04	**PHYD15**	66.85 ± 16.18		

Table B2: Ordinary one-way ANOVA statistical analysis multiple comparisons table for the pLDH assay IC_{50} values obtained

Tukey's multiple comparisons test	Summary	Adjusted P Value	DF	q	Tukey's multiple comparisons test	Summary	Adjusted P Value	DF	q
DC1 vs. Quinine	****	<0,0001	28	32,11	DC14 vs. DC9	****	<0,0001	28	16,09
DC2 vs. Quinine	****	<0,0001	28	14,85	DC15 vs. DC9	**	0,0083	28	6,777
DC3 vs. Quinine	****	<0,0001	28	13,62	PHYD1 vs. DC9	*	0,0159	28	6,401
DC4 vs. Quinine	***	0,0007	28	8,17	PHYD2 vs. DC9	****	<0,0001	28	9,977
DC6 vs. Quinine	****	<0,0001	28	15,56	PHYD3 vs. DC9	****	<0,0001	28	11,56
DC8 vs. Quinine	****	<0,0001	28	30,16	PHYD9 vs. DC9	****	<0,0001	28	12,49
DC9 vs. Quinine	****	<0,0001	28	19,09	Q3C3 vs. DC9	****	<0,0001	28	13,47
DC11 vs. Quinine	ns	0,8972	28	2,958	Q3C7 vs. DC9	****	<0,0001	28	14,2
DC12 vs. Quinine	ns	0,9451	28	2,742	Q3C8 vs. DC9	ns	>0,9999	28	1,543
DC13 vs. Quinine	****	<0,0001	28	21,48	Q3C9 vs. DC9	****	<0,0001	28	12,44
DC14 vs. Quinine	ns	>0,9999	28	1,46	Q3C10 vs. DC9	ns	0,5884	28	3,746
DC15 vs. Quinine	****	<0,0001	28	11,66	Q3C11 vs. DC9	****	<0,0001	28	15,95
PHYD1 vs. Quinine	****	<0,0001	28	26,1	Q3C12 vs. DC9	****	<0,0001	28	12,59
PHYD2 vs. Quinine	****	<0,0001	28	32,49	Chloroquine vs. DC9	****	<0,0001	28	19,1
PHYD3 vs. Quinine	****	<0,0001	28	31,75	DC12 vs. DC11	ns	>0,9999	28	0,1978
PHYD9 vs. Quinine	****	<0,0001	28	32,77	DC13 vs. DC11	****	<0,0001	28	16,91
Q3C3 vs. Quinine	ns	0,3371	28	4,33	DC14 vs. DC11	ns	>0,9999	28	1,368
Q3C7 vs. Quinine	ns	0,6881	28	3,527	DC15 vs. DC11	**	0,001	28	7,947
Q3C8 vs. Quinine	****	<0,0001	28	17,4	PHYD1 vs. DC11	****	<0,0001	28	21,12
Q3C9 vs. Quinine	****	<0,0001	28	32,71	PHYD2 vs. DC11	****	<0,0001	28	26,11
Q3C10 vs. Quinine	****	<0,0001	28	14,98	PHYD3 vs. DC11	****	<0,0001	28	26,29
Q3C11 vs. Quinine	ns	>0,9999	28	1,615	PHYD9 vs. DC11	****	<0,0001	28	27,22
Q3C12 vs. Quinine	****	<0,0001	28	32,88	Q3C3 vs. DC11	ns	>0,9999	28	1,252
Chloroquine vs. Quinine	ns	>0,9999	28	0,01827	Q3C7 vs. DC11	ns	>0,9999	28	0,5188
DC2 vs. DC1	****	<0,0001	28	15,76	Q3C8 vs. DC11	****	<0,0001	28	13,18
DC3 vs. DC1	****	<0,0001	28	16,88	Q3C9 vs. DC11	****	<0,0001	28	27,16
DC4 vs. DC1	****	<0,0001	28	21,85	Q3C10 vs. DC11	****	<0,0001	28	10,98
DC6 vs. DC1	****	<0,0001	28	15,1	Q3C11 vs. DC11	ns	>0,9999	28	1,226
DC8 vs. DC1	ns	0,9997	28	1,782	Q3C12 vs. DC11	****	<0,0001	28	27,31
DC9 vs. DC1	****	<0,0001	28	11,89	Chloroquine vs. DC11	ns	0,8928	28	2,975
DC11 vs. DC1	****	<0,0001	28	26,61	DC13 vs. DC12	****	<0,0001	28	17,11
DC12 vs. DC1	****	<0,0001	28	26,81	DC14 vs. DC12	ns	>0,9999	28	1,17
DC13 vs. DC1	****	<0,0001	28	9,699	DC15 vs. DC12	***	0,0007	28	8,145
DC14 vs. DC1	****	<0,0001	28	27,98	PHYD1 vs. DC12	****	<0,0001	28	21,32
DC15 vs. DC1	****	<0,0001	28	18,66	PHYD2 vs. DC12	****	<0,0001	28	26,32

PHYD1 vs. DC1	ns	0,0709	28	5,487	PHYD3 vs. DC12	****	<0,0001	28	26,48
PHYD2 vs. DC1	ns	0,8723	28	3,046	PHYD9 vs. DC12	****	<0,0001	28	27,42
PHYD3 vs. DC1	ns	>0,9999	28	0,3266	Q3C3 vs. DC12	ns	>0,9999	28	1,45
PHYD9 vs. DC1	ns	>0,9999	28	0,6065	Q3C7 vs. DC12	ns	>0,9999	28	0,7167
Q3C3 vs. DC1	****	<0,0001	28	25,36	Q3C8 vs. DC12	****	<0,0001	28	13,38
Q3C7 vs. DC1	****	<0,0001	28	26,09	Q3C9 vs. DC12	****	<0,0001	28	27,36
Q3C8 vs. DC1	****	<0,0001	28	13,43	Q3C10 vs. DC12	****	<0,0001	28	11,18
Q3C9 vs. DC1	ns	>0,9999	28	0,5506	Q3C11 vs. DC12	ns	>0,9999	28	1,028
Q3C10 vs. DC1	****	<0,0001	28	15,63	Q3C12 vs. DC12	****	<0,0001	28	27,51
Q3C11 vs. DC1	****	<0,0001	28	27,84	Chloroquine vs. DC12	ns	0,9421	28	2,758
Q3C12 vs. DC1	ns	>0,9999	28	0,6999	DC14 vs. DC13	****	<0,0001	28	18,28
Chloroquine vs. DC1	****	<0,0001	28	32,13	DC15 vs. DC13	***	0,0002	28	8,966
DC3 vs. DC2	ns	>0,9999	28	1,122	PHYD1 vs. DC13	ns	0,3829	28	4,212
DC4 vs. DC2	*	0,0267	28	6,095	PHYD2 vs. DC13	**	0,002	28	7,579
DC6 vs. DC2	ns	>0,9999	28	0,6551	PHYD3 vs. DC13	****	<0,0001	28	9,373
DC8 vs. DC2	****	<0,0001	28	13,98	PHYD9 vs. DC13	****	<0,0001	28	10,31
DC9 vs. DC2	ns	0,5309	28	3,871	Q3C3 vs. DC13	****	<0,0001	28	15,66
DC11 vs. DC2	****	<0,0001	28	10,85	Q3C7 vs. DC13	****	<0,0001	28	16,39
DC12 vs. DC2	****	<0,0001	28	11,05	Q3C8 vs. DC13	ns	0,5944	28	3,733
DC13 vs. DC2	*	0,0283	28	6,06	Q3C9 vs. DC13	****	<0,0001	28	10,25
DC14 vs. DC2	****	<0,0001	28	12,22	Q3C10 vs. DC13	*	0,0348	28	5,935
DC15 vs. DC2	ns	0,9106	28	2,906	Q3C11 vs. DC13	****	<0,0001	28	18,14
PHYD1 vs. DC2	****	<0,0001	28	10,27	Q3C12 vs. DC13	****	<0,0001	28	10,4
PHYD2 vs. DC2	****	<0,0001	28	14,22	Chloroquine vs. DC13	****	<0,0001	28	21,5
PHYD3 vs. DC2	****	<0,0001	28	15,43	DC15 vs. DC14	****	<0,0001	28	9,315
PHYD9 vs. DC2	****	<0,0001	28	16,37	PHYD1 vs. DC14	****	<0,0001	28	22,49
Q3C3 vs. DC2	****	<0,0001	28	9,6	PHYD2 vs. DC14	****	<0,0001	28	27,6
Q3C7 vs. DC2	****	<0,0001	28	10,33	PHYD3 vs. DC14	****	<0,0001	28	27,65
Q3C8 vs. DC2	ns	0,9895	28	2,327	PHYD9 vs. DC14	****	<0,0001	28	28,59
Q3C9 vs. DC2	****	<0,0001	28	16,31	Q3C3 vs. DC14	ns	0,9637	28	2,62
Q3C10 vs. DC2	ns	>0,9999	28	0,125	Q3C7 vs. DC14	ns	0,9993	28	1,887
Q3C11 vs. DC2	****	<0,0001	28	12,08	Q3C8 vs. DC14	****	<0,0001	28	14,55
Q3C12 vs. DC2	****	<0,0001	28	16,46	Q3C9 vs. DC14	****	<0,0001	28	28,53
Chloroquine vs. DC2	****	<0,0001	28	14,86	Q3C10 vs. DC14	****	<0,0001	28	12,35
DC4 vs. DC3	ns	0,1504	28	4,974	Q3C11 vs. DC14	ns	>0,9999	28	0,1418
DC6 vs. DC3	ns	0,9997	28	1,777	Q3C12 vs. DC14	****	<0,0001	28	28,68
DC8 vs. DC3	****	<0,0001	28	15,1	Chloroquine vs. DC14	ns	>0,9999	28	1,476
DC9 vs. DC3	ns	0,1465	28	4,992	PHYD1 vs. DC15	****	<0,0001	28	13,18
DC11 vs. DC3	****	<0,0001	28	9,731	PHYD2 vs. DC15	****	<0,0001	28	17,4
DC12 vs. DC3	****	<0,0001	28	9,929	PHYD3 vs. DC15	****	<0,0001	28	18,34
DC13 vs. DC3	**	0,0041	28	7,182	PHYD9 vs. DC15	****	<0,0001	28	19,27

DC14 vs. DC3	****	<0,0001	28	11,1	Q3C3 vs. DC15	**	0,0096	28	6,694
DC15 vs. DC3	ns	0,9997	28	1,784	Q3C7 vs. DC15	**	0,0026	28	7,428
PHYD1 vs. DC3	****	<0,0001	28	11,39	Q3C8 vs. DC15	ns	0,1039	28	5,233
PHYD2 vs. DC3	****	<0,0001	28	15,45	Q3C9 vs. DC15	****	<0,0001	28	19,22
PHYD3 vs. DC3	****	<0,0001	28	16,55	Q3C10 vs. DC15	ns	0,8769	28	3,031
PHYD9 vs. DC3	****	<0,0001	28	17,49	Q3C11 vs. DC15	***	0,0001	28	9,173
Q3C3 vs. DC3	***	0,0004	28	8,479	Q3C12 vs. DC15	****	<0,0001	28	19,36
Q3C7 vs. DC3	***	0,0001	28	9,212	Chloroquine vs. DC15	****	<0,0001	28	11,68
Q3C8 vs. DC3	ns	0,7221	28	3,449	PHYD2 vs. PHYD1	ns	0,8956	28	2,964
Q3C9 vs. DC3	****	<0,0001	28	17,43	PHYD3 vs. PHYD1	ns	0,1155	28	5,16
Q3C10 vs. DC3	ns	>0,9999	28	1,247	PHYD9 vs. PHYD1	*	0,0268	28	6,093
Q3C11 vs. DC3	****	<0,0001	28	10,96	Q3C3 vs. PHYD1	****	<0,0001	28	19,87
Q3C12 vs. DC3	****	<0,0001	28	17,58	Q3C7 vs. PHYD1	****	<0,0001	28	20,61
Chloroquine vs. DC3	****	<0,0001	28	13,63	Q3C8 vs. PHYD1	**	0,001	28	7,945
DC6 vs. DC4	**	0,0087	28	6,75	Q3C9 vs. PHYD1	*	0,0294	28	6,037
DC8 vs. DC4	****	<0,0001	28	20,07	Q3C10 vs. PHYD1	****	<0,0001	28	10,15
DC9 vs. DC4	****	<0,0001	28	9,966	Q3C11 vs. PHYD1	****	<0,0001	28	22,35
DC11 vs. DC4	ns	0,2011	28	4,757	Q3C12 vs. PHYD1	*	0,0229	28	6,187
DC12 vs. DC4	ns	0,1543	28	4,955	Chloroquine vs. PHYD1	****	<0,0001	28	26,12
DC13 vs. DC4	****	<0,0001	28	12,16	PHYD3 vs. PHYD2	ns	0,9539	28	2,688
DC14 vs. DC4	*	0,0254	28	6,125	PHYD9 vs. PHYD2	ns	0,6045	28	3,711
DC15 vs. DC4	ns	0,825	28	3,19	Q3C3 vs. PHYD2	****	<0,0001	28	24,73
PHYD1 vs. DC4	****	<0,0001	28	16,37	Q3C7 vs. PHYD2	****	<0,0001	28	25,54
PHYD2 vs. DC4	****	<0,0001	28	20,89	Q3C8 vs. PHYD2	****	<0,0001	28	11,67
PHYD3 vs. DC4	****	<0,0001	28	21,53	Q3C9 vs. PHYD2	ns	0,6327	28	3,649
PHYD9 vs. DC4	****	<0,0001	28	22,46	Q3C10 vs. PHYD2	****	<0,0001	28	14,08
Q3C3 vs. DC4	ns	0,6977	28	3,505	Q3C11 vs. PHYD2	****	<0,0001	28	27,45
Q3C7 vs. DC4	ns	0,3725	28	4,238	Q3C12 vs. PHYD2	ns	0,5574	28	3,813
Q3C8 vs. DC4	***	0,0004	28	8,423	Chloroquine vs. PHYD2	****	<0,0001	28	32,51
Q3C9 vs. DC4	****	<0,0001	28	22,4	PHYD9 vs. PHYD3	ns	>0,9999	28	0,9332
Q3C10 vs. DC4	*	0,0217	28	6,22	Q3C3 vs. PHYD3	****	<0,0001	28	25,03
Q3C11 vs. DC4	*	0,0321	28	5,983	Q3C7 vs. PHYD3	****	<0,0001	28	25,77
Q3C12 vs. DC4	****	<0,0001	28	22,55	Q3C8 vs. PHYD3	****	<0,0001	28	13,11
Chloroquine vs. DC4	***	0,0007	28	8,186	Q3C9 vs. PHYD3	ns	>0,9999	28	0,8772
DC8 vs. DC6	****	<0,0001	28	13,32	Q3C10 vs. PHYD3	****	<0,0001	28	15,31
DC9 vs. DC6	ns	0,8156	28	3,216	Q3C11 vs. PHYD3	****	<0,0001	28	27,51
DC11 vs. DC6	****	<0,0001	28	11,51	Q3C12 vs. PHYD3	ns	>0,9999	28	1,026
DC12 vs. DC6	****	<0,0001	28	11,71	Chloroquine vs. PHYD3	****	<0,0001	28	31,77
DC13 vs. DC6	ns	0,0804	28	5,405	Q3C3 vs. PHYD9	****	<0,0001	28	25,97
DC14 vs. DC6	****	<0,0001	28	12,88	Q3C7 vs. PHYD9	****	<0,0001	28	26,7
DC15 vs. DC6	ns	0,6728	28	3,561	Q3C8 vs. PHYD9	****	<0,0001	28	14,04

PHYD1 vs. DC6	****	<0,0001	28	9,617	Q3C9 vs. PHYD9	ns	>0,9999	28	0,05599
PHYD2 vs. DC6	****	<0,0001	28	13,5	Q3C10 vs. PHYD9	****	<0,0001	28	16,24
PHYD3 vs. DC6	****	<0,0001	28	14,78	Q3C11 vs. PHYD9	****	<0,0001	28	28,44
PHYD9 vs. DC6	****	<0,0001	28	15,71	Q3C12 vs. PHYD9	ns	>0,9999	28	0,09332
Q3C3 vs. DC6	****	<0,0001	28	10,26	Chloroquine vs. PHYD9	****	<0,0001	28	32,79
Q3C7 vs. DC6	****	<0,0001	28	10,99	Q3C7 vs. Q3C3	ns	>0,9999	28	0,7335
Q3C8 vs. DC6	ns	0,9999	28	1,672	Q3C8 vs. Q3C3	****	<0,0001	28	11,93
Q3C9 vs. DC6	****	<0,0001	28	15,65	Q3C9 vs. Q3C3	****	<0,0001	28	25,91
Q3C10 vs. DC6	ns	>0,9999	28	0,53	Q3C10 vs. Q3C3	****	<0,0001	28	9,725
Q3C11 vs. DC6	****	<0,0001	28	12,73	Q3C11 vs. Q3C3	ns	0,9792	28	2,478
Q3C12 vs. DC6	****	<0,0001	28	15,8	Q3C12 vs. Q3C3	****	<0,0001	28	26,06
Chloroquine vs. DC6	****	<0,0001	28	15,58	Chloroquine vs. Q3C3	ns	0,331	28	4,346
DC9 vs. DC8	****	<0,0001	28	10,11	Q3C8 vs. Q3C7	****	<0,0001	28	12,66
DC11 vs. DC8	****	<0,0001	28	24,83	Q3C9 vs. Q3C7	****	<0,0001	28	26,64
DC12 vs. DC8	****	<0,0001	28	25,03	Q3C10 vs. Q3C7	****	<0,0001	28	10,46
DC13 vs. DC8	**	0,0011	28	7,917	Q3C11 vs. Q3C7	ns	0,9998	28	1,745
DC14 vs. DC8	****	<0,0001	28	26,2	Q3C12 vs. Q3C7	****	<0,0001	28	26,79
DC15 vs. DC8	****	<0,0001	28	16,88	Chloroquine vs. Q3C7	ns	0,6808	28	3,543
PHYD1 vs. DC8	ns	0,6073	28	3,705	Q3C9 vs. Q3C8	****	<0,0001	28	13,98
PHYD2 vs. DC8	ns	>0,9999	28	1,094	Q3C10 vs. Q3C8	ns	0,9945	28	2,202
PHYD3 vs. DC8	ns	>0,9999	28	1,456	Q3C11 vs. Q3C8	****	<0,0001	28	14,41
PHYD9 vs. DC8	ns	0,9859	28	2,389	Q3C12 vs. Q3C8	****	<0,0001	28	14,13
Q3C3 vs. DC8	****	<0,0001	28	23,58	Chloroquine vs. Q3C8	****	<0,0001	28	17,41
Q3C7 vs. DC8	****	<0,0001	28	24,31	Q3C10 vs. Q3C9	****	<0,0001	28	16,18
Q3C8 vs. DC8	****	<0,0001	28	11,65	Q3C11 vs. Q3C9	****	<0,0001	28	28,39
Q3C9 vs. DC8	ns	0,9892	28	2,333	Q3C12 vs. Q3C9	ns	>0,9999	28	0,1493
Q3C10 vs. DC8	****	<0,0001	28	13,85	Chloroquine vs. Q3C9	****	<0,0001	28	32,73
Q3C11 vs. DC8	****	<0,0001	28	26,06	Q3C11 vs. Q3C10	****	<0,0001	28	12,2
Q3C12 vs. DC8	ns	0,9788	28	2,482	Q3C12 vs. Q3C10	****	<0,0001	28	16,33
Chloroquine vs. DC8	****	<0,0001	28	30,17	Chloroquine vs. Q3C10	****	<0,0001	28	15
DC11 vs. DC9	****	<0,0001	28	14,72	Q3C12 vs. Q3C11	****	<0,0001	28	28,54
DC12 vs. DC9	****	<0,0001	28	14,92	Chloroquine vs. Q3C11	ns	>0,9999	28	1,631
DC13 vs. DC9	ns	0,9949	28	2,189	Chloroquine vs. Q3C12	****	<0,0001	28	32,89

Appendix C: Larvicidal Activity

Table C1: The percentage larval mortality at 24 hours for each of the test compounds in comparison with positive control DDT at 0.5 µM.

Compound	% Larval Mortality at 24 hours	Compound	% Larval Mortality at 24 hours	Compound	% Larval Mortality at 24 hours
DC1	0,00	**PHYD1**	3,33	**Q3C1**	0,00
DC2	1,67	**PHYD2**	0,00	**Q3C2**	1,67
DC3	0,00	**PHYD3**	5,00	**Q3C3**	0,00
DC4	0,00	**PHYD4**	1,67	**Q3C4**	0,00
DC5	0,00	**PHYD5**	0,00	**Q3C5**	0,00
DC6	0,00	**PHYD6**	0,00	**Q3C6**	0,00
DC7	1,67	**PHYD7**	1,67	**Q3C7**	0,00
DC8	1,67	**PHYD8**	0,00	**Q3C8**	0,00
DC9	0,00	**PHYD9**	3,33	**Q3C9**	3,33
DC10	0,00	**PHYD10**	3,33	**Q3C10**	0,00
DC11	3,33	**PHYD11**	1,67	**Q3C11**	0,00
DC12	0,00	**PHYD12**	1,67	**Q3C12**	1,67
DC13	0,00	**PHYD13**	0,00		
DC14	1,67	**PHYD14**	0,00	**DDT**	100.00
DC15	3,33	**PHYD15**	0,00		

Table C2: The percentage larval mortality at 48 hours for each of the test compounds in comparison with positive control DDT at 0.5 µM.

Compound	% Larval Mortality at 48 hours	Compound	% Larval Mortality at 48 hours	Compound	% Larval Mortality at 48 hours
DC1	1,67	**PHYD1**	3,33	**Q3C1**	5,00
DC2	5,00	**PHYD2**	1,67	**Q3C2**	1,67
DC3	0,00	**PHYD3**	5,00	**Q3C3**	1,67
DC4	5,00	**PHYD4**	3,33	**Q3C4**	1,67
DC5	0,00	**PHYD5**	0,00	**Q3C5**	5,00
DC6	0,00	**PHYD6**	0,00	**Q3C6**	3,33
DC7	1,67	**PHYD7**	3,33	**Q3C7**	3,33
DC8	5,00	**PHYD8**	1,67	**Q3C8**	5,00
DC9	3,33	**PHYD9**	3,33	**Q3C9**	5,00
DC10	1,67	**PHYD10**	5,00	**Q3C10**	3,33
DC11	3,33	**PHYD11**	5,00	**Q3C11**	3,33
DC12	0,00	**PHYD12**	5,00	**Q3C12**	5,00
DC13	0,00	**PHYD13**	1,67		
DC14	1,67	**PHYD14**	1,67	**DDT**	100.00
DC15	3,33	**PHYD15**	0,00		

Data Tables
Data 1
New Data Table...
Info
Project info 1
New Info...
Results
Transform of Data 1
Nonlin fit of Transform of Data 1
New Analysis...

	Nonlin fit Table of results	S DDT Larvae 24 hours	T DDT Larvae 48 hours	U DDT Larvae 72 hours	V DDT Larvae 24 Hours 2	W DDT Larvae 48 hours 2	X DDT Larvae 72 hours 2
1	**Sigmoidal dose-response (variable slope)**	Interrupted	Interrupted	Interrupted	Interrupted	Interrupted	Interrupted
2	**Best-fit values**						
3	Bottom	-3.604e-012	-8.683e-010	-1.042e-009	-1.389e-024	-2.682e-161	-1.030e-009
4	Top	100.0	87.00	54.25	100.0	80.00	61.34
5	LogEC50	-0.4202	-1.318	-2.242	-0.9182	-1.301	-2.241
6	HillSlope	-11.59	-10.23	-10.65	-40.92	-161.9	-10.72
7	EC50	0.3801	0.04810	0.005733	0.1207	0.05000	0.005742

Figure C1: Larvicidal DDT EC50 Analysis Screenshot

Table C3: The percentage pupae formation at 24, 48 and 72 hours for each of the test compounds in comparison with positive control DDT at 0.5 µM.

	% Larval pupation				% Larval pupation				% Larval pupation		
Compound	**24 hours**	**48 hours**	**72 hours**	**Compound**	**24 hours**	**48 hours**	**72 hours**	**Compound**	**24 hours**	**48 hours**	**72 hours**
DC1	0	0	0	**PHYD1**	0	0	0	**Q3C1**	0	0	2.5
DC2	0	2.5	2.5	**PHYD2**	0	0	0	**Q3C2**	0	0	0
DC3	0	0	0	**PHYD3**	0	0	2.5	**Q3C3**	0	0	0
DC4	0	0	0	**PHYD4**	0	0	2.5	**Q3C4**	0	0	5
DC5	0	5	7.5	**PHYD5**	0	0	5	**Q3C5**	0	0	0
DC6	0	2.5	5	**PHYD6**	0	0	0	**Q3C6**	0	0	0
DC7	2.5	0	2.5	**PHYD7**	0	0	2.5	**Q3C7**	0	0	5
DC8	2.5	5	10	**PHYD8**	0	0	0	**Q3C8**	0	0	2.5
DC9	0	0	2.5	**PHYD9**	0	0	7.5	**Q3C9**	0	0	0
DC10	0	10	12.5	**PHYD10**	0	0	2.5	**Q3C10**	0	0	2.5
DC11	2.5	2.5	2.5	**PHYD11**	0	0	0	**Q3C11**	0	0	7.5
DC12	5	2.5	2.5	**PHYD12**	0	0	2.5	**Q3C12**	0	0	5
DC13	0	0	0	**PHYD13**	0	0	0				
DC14	0	0	5	**PHYD14**	0	0	2.5	**DDT**	0	0	0
DC15	0	0	0	**PHYD15**	0	0	5	**Untreated**	0	0	7

Appendix D: Ovicidal Activity

Table D1: The percentage of unhatched eggs after being exposed to the test compounds at 0.5 µM for 72 hours in comparison with positive control formalin (1% v/v).

Compound	% Unhatched Eggs @ 0.5 µM	Compound	% Unhatched Eggs @ 0.5 µM	Compound	% Unhatched Eggs @ 0.5 µM
DC1	5 ± 5	**PHYD1**	6.25 ± 1.25	**Q3C1**	13.12 ± 3.12
DC2	6.25 ± 1.25	**PHYD2**	0 ± 0	**Q3C2**	2.5 ± 2.5
DC3	1.25 ± 1.25	**PHYD3**	11.25 ± 11.25	**Q3C3**	13.12 ± 3.12
DC4	2.5 ± 2.5	**PHYD4**	0 ± 0	**Q3C4**	8.75 ± 8.75
DC5	3.75 ± 3.75	**PHYD5**	5 ± 5	**Q3C5**	3.34 ± 2.09
DC6	5 ± 5	**PHYD6**	0 ± 0	**Q3C6**	18.12 ± 8.12
DC7	0 ± 0	**PHYD7**	0 ± 0	**Q3C7**	8.12 ± 3.12
DC8	0 ± 0	**PHYD8**	3.12 ± 1.87	**Q3C8**	10.62 ± 5.62
DC9	0 ± 0	**PHYD9**	15.62 ± 15.62	**Q3C9**	18.12 ± 8.12
DC10	0 ± 0	**PHYD10**	0.62 ± 0.62	**Q3C10**	8.12 ± 8.12
DC11	10 ± 10	**PHYD11**	10.62 ± 10.62	**Q3C11**	8.12 ± 8.12
DC12	0 ± 0	**PHYD12**	28.7 ± 3.7	**Q3C12**	15 ± 15
DC13	7.5 ± 7.5	**PHYD13**	10.62 ± 0.62		
DC14	16.25 ± 13.75	**PHYD14**	23.89 ± 23.89	**Formalin (1% v/v)**	100 ± 0
DC15	0 ± 0	**PHYD15**	8.12 ± 8.12		

Table D2: Ordinary one-way ANOVA statistical analysis multiple comparisons table for the most active ovicidal test compounds obtained at 0.5 µM after 72 hours of exposure.

Tukey's multiple comparisons test	Summary	Adjusted P Value	DF	q
DC15 vs. DC14	ns	0,8496	8	1,933
PHYD12 vs. DC14	ns	0,9521	8	1,481
PHYD14 vs. DC14	ns	0,9967	8	0,909
Q3C6 vs. DC14	ns	>0,9999	8	0,2225
Q3C9 vs. DC14	ns	>0,9999	8	0,2225
Q3C12 vs. DC14	ns	>0,9999	8	0,1487
Formalin vs. DC14	**	0,0016	8	9,964
PHYD12 vs. DC15	ns	0,3439	8	3,415
PHYD14 vs. DC15	ns	0,5273	8	2,842
Q3C6 vs. DC15	ns	0,7784	8	2,156
Q3C9 vs. DC15	ns	0,7784	8	2,156
Q3C12 vs. DC15	ns	0,8903	8	1,785
Formalin vs. DC15	***	0,0005	8	11,9
PHYD14 vs. PHYD12	ns	0,9998	8	0,5723
Q3C6 vs. PHYD12	ns	0,9789	8	1,259
Q3C9 vs. PHYD12	ns	0,9789	8	1,259
Q3C12 vs. PHYD12	ns	0,9256	8	1,63
Formalin vs. PHYD12	**	0,0045	8	8,483
Q3C6 vs. PHYD14	ns	0,9994	8	0,6865
Q3C9 vs. PHYD14	ns	0,9994	8	0,6865
Q3C12 vs. PHYD14	ns	0,9919	8	1,058
Formalin vs. PHYD14	**	0,003	8	9,055
Q3C9 vs. Q3C6	ns	>0,9999	8	0
Q3C12 vs. Q3C6	ns	>0,9999	8	0,3712
Formalin vs. Q3C6	**	0,0018	8	9,742
Q3C12 vs. Q3C9	ns	>0,9999	8	0,3712
Formalin vs. Q3C9	**	0,0018	8	9,742
Formalin vs. Q3C12	**	0,0014	8	10,11

Appendix E: Haemolysis Statistical Analysis

Table E1: Ordinary one-way ANOVA statistical analysis multiple comparisons table for the Haemolysis values obtained at 50 µM

Tukey's multiple comparisons test	Summary	Adjusted P Value	DF	q
DC3 vs. Quinine	ns	>0,9999	27	1,072
DC4 vs. Quinine	ns	0,9933	27	1,683
DC6 vs. Quinine	ns	>0,9999	27	0,8887
DC10 vs. Quinine	ns	0,9903	27	1,754
DC11 vs. Quinine	ns	>0,9999	27	0,9539
DC13 vs. Quinine	ns	>0,9999	27	0,0237
PHYD2 vs. Quinine	ns	>0,9999	27	0,7939
PHYD3 vs. Quinine	ns	>0,9999	27	0,3259
PHYD10 vs. Quinine	ns	>0,9999	27	0,1659
Q3C2 vs. Quinine	ns	>0,9999	27	0,5628
Q3C9 vs. Quinine	ns	>0,9999	27	0,09479
Chloroquine vs. Quinine	ns	0,9977	27	1,495
Triton-X vs. Quinine	****	<0,0001	27	58,98
DC4 vs. DC3	ns	>0,9999	27	0,6823
DC6 vs. DC3	ns	>0,9999	27	0,2053
DC10 vs. DC3	ns	>0,9999	27	0,7617
DC11 vs. DC3	ns	>0,9999	27	0,1325
DC13 vs. DC3	ns	0,9998	27	1,172
PHYD2 vs. DC3	ns	>0,9999	27	0,3113
PHYD3 vs. DC3	ns	>0,9999	27	0,8346
PHYD10 vs. DC3	ns	0,9989	27	1,384
Q3C2 vs. DC3	ns	>0,9999	27	0,5697
Q3C9 vs. DC3	ns	0,9994	27	1,305
Chloroquine vs. DC3	ns	>0,9999	27	0,4729
Triton-X vs. DC3	****	<0,0001	27	64,74
DC6 vs. DC4	ns	>0,9999	27	0,8876
DC10 vs. DC4	ns	>0,9999	27	0,07949
DC11 vs. DC4	ns	>0,9999	27	0,8147
DC13 vs. DC4	ns	0,9845	27	1,855
PHYD2 vs. DC4	ns	>0,9999	27	0,9936
PHYD3 vs. DC4	ns	0,9974	27	1,517
PHYD10 vs. DC4	ns	0,9637	27	2,067
Q3C2 vs. DC4	ns	0,9996	27	1,252
Q3C9 vs. DC4	ns	0,973	27	1,987
Chloroquine vs. DC4	ns	>0,9999	27	0,2093

Triton-X vs. DC4	****	<0,0001	27	64,06
DC10 vs. DC6	ns	>0,9999	27	0,9671
DC11 vs. DC6	ns	>0,9999	27	0,07286
DC13 vs. DC6	ns	>0,9999	27	0,9671
PHYD2 vs. DC6	ns	>0,9999	27	0,106
PHYD3 vs. DC6	ns	>0,9999	27	0,6293
PHYD10 vs. DC6	ns	0,9998	27	1,179
Q3C2 vs. DC6	ns	>0,9999	27	0,3643
Q3C9 vs. DC6	ns	>0,9999	27	1,1
Chloroquine vs. DC6	ns	>0,9999	27	0,6783
Triton-X vs. DC6	****	<0,0001	27	64,95
DC11 vs. DC10	ns	>0,9999	27	0,8942
DC13 vs. DC10	ns	0,9782	27	1,934
PHYD2 vs. DC10	ns	>0,9999	27	1,073
PHYD3 vs. DC10	ns	0,9958	27	1,596
PHYD10 vs. DC10	ns	0,9523	27	2,146
Q3C2 vs. DC10	ns	0,9993	27	1,331
Q3C9 vs. DC10	ns	0,9637	27	2,067
Chloroquine vs. DC10	ns	>0,9999	27	0,2888
Triton-X vs. DC10	****	<0,0001	27	63,98
DC13 vs. DC11	ns	>0,9999	27	1,04
PHYD2 vs. DC11	ns	>0,9999	27	0,1788
PHYD3 vs. DC11	ns	>0,9999	27	0,7021
PHYD10 vs. DC11	ns	0,9996	27	1,252
Q3C2 vs. DC11	ns	>0,9999	27	0,4372
Q3C9 vs. DC11	ns	0,9998	27	1,172
Chloroquine vs. DC11	ns	>0,9999	27	0,6054
Triton-X vs. DC11	****	<0,0001	27	64,87
PHYD2 vs. DC13	ns	>0,9999	27	0,8611
PHYD3 vs. DC13	ns	>0,9999	27	0,3378
PHYD10 vs. DC13	ns	>0,9999	27	0,212
Q3C2 vs. DC13	ns	>0,9999	27	0,6028
Q3C9 vs. DC13	ns	>0,9999	27	0,1325
Chloroquine vs. DC13	ns	0,9945	27	1,645
Triton-X vs. DC13	****	<0,0001	27	65,91
PHYD3 vs. PHYD2	ns	>0,9999	27	0,5233
PHYD10 vs. PHYD2	ns	>0,9999	27	1,073
Q3C2 vs. PHYD2	ns	>0,9999	27	0,2583
Q3C9 vs. PHYD2	ns	>0,9999	27	0,9936
Chloroquine vs. PHYD2	ns	>0,9999	27	0,7843
Triton-X vs. PHYD2	****	<0,0001	27	65,05

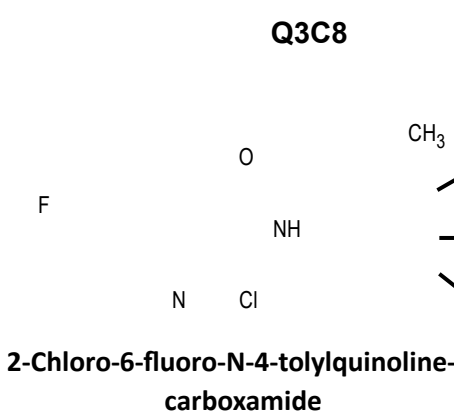
PHYD10 vs. PHYD3	ns	>0,9999	27	0,5498
Q3C2 vs. PHYD3	ns	>0,9999	27	0,265
Q3C9 vs. PHYD3	ns	>0,9999	27	0,4703
Chloroquine vs. PHYD3	ns	0,9994	27	1,308
Triton-X vs. PHYD3	****	<0,0001	27	65,58
Q3C2 vs. PHYD10	ns	>0,9999	27	0,8147
Q3C9 vs. PHYD10	ns	>0,9999	27	0,07949
Chloroquine vs. PHYD10	ns	0,9843	27	1,857
Triton-X vs. PHYD10	****	<0,0001	27	66,13
Q3C9 vs. Q3C2	ns	>0,9999	27	0,7352
Chloroquine vs. Q3C2	ns	>0,9999	27	1,043
Triton-X vs. Q3C2	****	<0,0001	27	65,31
Chloroquine vs. Q3C9	ns	0,9891	27	1,778
Triton-X vs. Q3C9	****	<0,0001	27	66,05
Triton-X vs. Chloroquine	****	<0,0001	27	64,27

Appendix F: 24 hour nauplii mortality

Table F1: The percentage *Ar. franciscana* nauplii mortality at 24 hours for each of the test compounds (0.5 µM) in comparison with positive control potassium dichromate at 50 µM.

Compound	% Nauplii Mortality at 24 hours	Compound	% Nauplii Mortality at 24 hours	Compound	% Nauplii Mortality at 24 hours
DC1	0.00	**PHYD1**	3.33	**Q3C1**	0.00
DC2	1.67	**PHYD2**	0.00	**Q3C2**	1.67
DC3	0.00	**PHYD3**	5.00	**Q3C3**	0.00
DC4	0.00	**PHYD4**	1.67	**Q3C4**	0.00
DC5	0.00	**PHYD5**	0.00	**Q3C5**	0.00
DC6	0.00	**PHYD6**	0.00	**Q3C6**	0.00
DC7	1.67	**PHYD7**	1.67	**Q3C7**	0.00
DC8	1.67	**PHYD8**	0.00	**Q3C8**	0.00
DC9	0.00	**PHYD9**	3.33	**Q3C9**	3.33
DC10	0.00	**PHYD10**	3.33	**Q3C10**	0.00
DC11	3.33	**PHYD11**	1.67	**Q3C11**	0.00
DC12	0.00	**PHYD12**	1.67	**Q3C12**	1.67
DC13	0.00	**PHYD13**	0.00	**K2Cr2O7 (0.5µM)**	0.91
DC14	1.67	**PHYD14**	0.00	**K2Cr2O7 (50µM)**	1.97
DC15	3.33	**PHYD15**	0.00	**DDT**	0.21

Appendix G: The summary of the activity for test compound Q3C8.



Antimalarial properties

Plasmodium Growth Inhibited	Combination Interaction; ΣFIC	Larvicidal (Mortality)	Ovicidal (Mortality)
40.68% at 50 µM IC_{50}: 85.18 ± 12.73 Yes (P <0.0001)	Synergistic with cisplatin ΣFIC = 0.53	7.50% ± 3.54 at 0.5 µM	10.63% ± 5.63 at 0.5 µM

Antioxidant, iron chelating properties

DPPH• Free Radical Scavenging	Ferrous Ion Chelation
0% ± 0.01	8.50% ± 7.47

Toxicity properties

K562 Cells (% cellular viability)	HEK293 Cells (% cellular viability)	Selectivity Index (HEK 293 vs NF54)	Haemolysis	*Artemia* lethality (Mortality)
32.75% at 50 µM IC_{50}: 3.58 ± 0.42 µM Yes (P <0.0001)	62.24% at 50 µM IC_{50}: n.d	1.05	0.1% ± 0.01 at 50 µM	25.00% ± 5.43 at 0.5 µM LC_{50} = n.d

Toxic Hazard class	Cytochrome P450 (CYP3A4 inhibition)	BBB	LogD (pH 5)	P-glycoprotein substrate
High (Class III)	Yes	Yes	4.70	No

Figure G1: The summary of the activity for test compound **Q3C8**. The activity of **Q3C8** across this study divided into its antimalarial, antioxidant and iron chelating, and toxicity properties.